Development of *In Vitro* Models and Analytical Methods to Assess the *In Vivo* Stability of Therapeutic Proteins

Inauguraldissertation

zur

Erlangung der Würde eines Doktors der Philosophie

vorgelegt der

Philosophisch-Naturwissenschaftlichen Fakultät

der Universität Basel

von

Joachim Schuster

Basel, 2021

Genehmigt von der Philosophisch-Naturwissenschaftlichen Fakultät

auf Antrag von

Prof. Dr. Hanns-Christian Mahler

Prof. Dr. Jörg Huwyler

Prof. Dr. Oliver Germershaus

Basel, den 30. März 2021

Prof. Dr. Marcel Mayor (Dean)

Table of contents

Abbreviations 4
Acknowledgement 6
Introduction 1
Protein Stability 1
Physical Stability 1
Denaturation 2
Aggregation and Precipitation 2
Surface Adsorption 5
Chemical Stability 5
Deamidation 5
Oxidation 6
Fragmentation 6
In Vivo Protein Stability 7
Aim of the Thesis 9
Results 10
In Vivo Stability of Therapeutic Proteins 11
Analytical Challenges Assessing Aggregation and Fragmentation of Therapeutic Proteins in Biological Fluids 29
Particle Analysis of Biotherapeutics in Human Serum using Machine Learning 38
Tracking the Physical Stability of Fluorescent-Labeled mAbs under Physiologic *In Vitro* Conditions in Human Serum and PBS 53
Assessing Particle Formation of Biotherapeutics in Biological Fluids 68
Stability of Monoclonal Antibodies after Simulated Subcutaneous Administration 75
Discussion 87
Analytical Challenges Assessing the *In Vivo* Protein Stability 87
Development of an *In Vitro* Intravenous Model 87
Development of an *In Vitro* Subcutaneous Model 91
Outlook 93
Selection of a Biological Fluid 93
Advanced *In Vitro* Models 94
Conclusion 96
References 97
Appendix 103
Publications Included in This Thesis 103
Additional Publications Written During the Research Period (not included in this thesis) 104

Abbreviations

ADC	antibody-drug conjugate
AF488	Alexa Fluor 488
AF	artificial fluid
AF+HA	artificial fluid + hyaluronan
AF4	asymmetrical flow field-flow fractionation
AU	absorbance unit
AUC	analytical ultracentrifugation
BF	brightfield
CDR	complementarity-determining region
CE-MS	capillary electrophoresis-mass spectrometry
CE-SDS	capillary electrophoresis - sodium dodecyl sulfate
cIEF	capillary isoelectric focusing
CLSM	confocal laser scanning microscopy
CMC	chemistry, manufacturing, and controls
CO_2	carbon dioxide
CPP	critical process parameter
CQA	critical quality attribute
CSF	cerebrospinal fluid
CV	coefficient of variation
DP	drug product
DS	Drug substance
DSC	differential scanning calorimetry
EU	emission units
FAL	Float-A-Lyzer
FCM	flow cytometry
FI	flow imaging
FSC	forward scatter
fSPT	fluorescence single particle tracking
HA	hyaluronan
HC	heavy chain
HMW	high-molecular weight
HMWS	high-molecular weight species
HP-SEC	high-performance-size-exclusion chromatography
HP-SEC-FLD	high-performance-size-exclusion chromatography-fluorescence detection
IEX	ion-exchange chromatography
IFC	imaging flow cytometry
IgG	immunoglobulin G
IgG:AF	IgG labeled with AF
IgG:BODIPY	IgG labeled with BODIPY
ISF	interstitial fluid
IT	intrathecal
IV	intravenous
IVT	intravitreal
LC	light chain
LC-MS/MS	liquid chromatography-tandem mass spectrometry
LMW	low-molecular weight
LMWS	low-molecular weight species
LO	light obscuration
mAb	monoclonal antibody
MFI	Micro flow imaging

ML	machine learning
MMP	matrix metalloproteinase
MWCO	molecular weight cut-off
NTA	nanoparticle tracking analysis
NTU	nephelometric turbidity units
PBS	phosphate-buffered saline
pI	isoelectric point
PK/PD	pharmacokinetic/pharmacodynamic
rH	relative humidity
RM	reference material
SAL	Slide-A-Lyzer
SbVP	subvisible particle
SC	subcutaneous
SCISF	subcutaneous interstitial fluid
SD	standard deviation
SDS-PAGE	sodium dodecyl sulfate-polyacrylamide gel electrophoresis
SEC	size-exclusion chromatography
SEC-FLD	size-exclusion chromatography with fluorescence detection
Ser	human serum without the therapeutic IgG
Ser+IgG	human serum spiked with the therapeutic IgG
SPR	surface plasmon resonance
SSC	side scatter
VH	vitreous humor

Acknowledgement

First of all I want to thank Prof. Hanns-Christian Mahler for giving me the opportunity to study for a PhD at Lonza DPS. The work atmosphere at DPS has been unique and I cannot stress enough how much I value being part of this great work atmosphere. It has been inspiring to see at which rate the department has been growing. I want to particularly thank him for his scientific guidance and pragmatic approach of "getting things done".

I would also like to thank Prof. Jörg Huwyler for giving me the chance to study for a PhD and being part of his research team. I want to particularly thank him for always taking time and constantly being supportive. Thank you to Prof. Oliver Germershaus for offering to review my thesis, scientific guidance, and being part of the doctoral committee.

I huge thank you to Dr. Roman Mathaes for always supporting me and regardless of the circumstance constantly taking time for personal and scientific guidance. I am extremely grateful for his positive mindset and lifting up my spirit after every meeting. I learned a lot on a personal and professional level and consider myself incredibly fortunate to have him as a mentor. I would like to thank Dr. Susanne Jörg and Dr. Atanas Koulov for their constructive feedback and scientific guidance throughout my studies.

I would like to thank my colleagues and close friends at DPS who made the time in the laboratory and office particularly enjoyable and filled with great memories. A huge thank you to Tim for all the great memories, insightful conversations, and banter we shared as well as teaching me only the finest vocab Britain has to offer. I want to thank Ariane for all our great conversations, especially all our coffee (and rosehip tea) breaks, and how we made even our long working hours enjoyable. I also want to thank Vinay for your incredible support, particularly in the last months of my studies and constantly going above and beyond. It has been amazing to work with you and I am already looking forward to our next paper celebrations. I would also like to especially mention Elise, Severin, Miriam, Sarah, Jasmin, and Sabrina for all the great memories that we have been sharing.

I also want to thank all members of the Pharmaceutical Technology research group at the University of Basel, particularly Pascal for his scientific advice and support. Moreover, I would like to thank Viktoria, Denise, Sandro, and Maryam. The Imaging Core Facility of the University of Basel, particularly, Kai and Niko, are thanked for their instructions with the fluorescence microscope, machine learning model, and data analysis.

I want to thank Neira for encouraging me to pursuing new things and ultimately to go abroad. I will always be very grateful for your support. Despite being far away from Basel I am particularly

grateful that I can always count on Neno (thanks for the virtual G2 meetings), Dalibor, Maura, Tom, Suzanne, and Michaela. Thank you for your support and our (video) conversations we had over the years.

Last but not least, I would like to thank my parents, Nicole, and Christian, for their constant support throughout all these years. I am deeply grateful for all your patience that you have, that I can always count on you, and your constant encouragement.

Introduction

Monoclonal antibodies (mAbs) are an important therapeutic modality for severe diseases such as cancer, neurological, and immunological disorders. In 2019, seven out of ten of the most successful drugs by revenue were mAbs[1]. To date, there are more than 570 mAb-based therapeutics in clinical development and over 70 mAbs commercialized[2]. mAbs are most commonly administered via intravenous (IV) and subcutaneous (SC) routes of administration[3]. Less common, but gaining interest, are intravitreal (IVT) and intrathecal (IT) administrations[4].

Protein Stability

Controlling and monitoring the stability of therapeutic proteins is the cornerstone of successful drug product (DP) development. Owing to the complex structure and size of proteins, macromolecules are more prone to degradation events as compared to small molecules. Any alteration to the native protein structure, physically and/or chemically, can impair the stability of a protein. Insufficient protein stability can, in turn, impact patient safety and/or treatment efficacy. Such degradants impacting the quality of a DP are classified as critical quality attributes (CQAs).

Protein degradation is a complex interplay of physical and chemical degradation. Physical degradation defines non-covalent modifications within or between protein molecules. Physical degradation can be grouped into conformational (unfolding and misfolding), colloidal stability (aggregation and precipitation), and adsorption to surfaces. Chemical degradation refers to covalent changes in a protein's structure. Although both degradation pathways are distinctly defined, and for the purpose of explanation discussed separately, it is important to note that these pathways are interrelated[5]. Certain chemical degradation pathways are affected by physical instabilities and *vice versa*. For example, deamidation and/or oxidation can cause aggregation[5-7] or conformational changes[8]. Likewise, conformational changes can increase solvent exposure of certain amino acids susceptible to chemical modifications and thus accelerate chemical degradation[5]. To optimize shelf-life stability of a DP, several stability aspects from physical and chemical perspective have to be considered during formulation development. Falconer *et al.* reported a pH range of 5.3 to 6.1 of 22 commercialized mAbs[9].

Physical Stability

At a protein's isoelectric point (pI), i.e., the pH at which a protein has zero net charge; the conformational stability is at its highest, whereas colloidal stability is at its lowest. As the solution pH and a protein's pI deviate from each other, the number of charged groups on a protein and thus charge repulsion increases[7]. This destabilizes the folded protein. At solution pH values close

to a protein's pI, the protein exhibits both positively and negatively charged groups, thus, increasing the likelihood of dipole–dipole interactions and potentially causing protein aggregation. Physical protein stability is therefore a compromise between colloidal and conformational stability.

Denaturation

The native state of a protein refers to its biological active form, which is conformationally stable. Contrary, in a denatured protein the three-dimensional structure is impaired by unfolding of the secondary and/or tertiary structure. Unfolding can result in exposure of hydrophobic patches and thus compromise colloidal stability by impairing a protein's ability to resist aggregation[10]. Thermal denaturation is typically irreversible due to rapid formation of aggregates of the unfolded protein[5]. Melting temperatures of many proteins range from 40 to 80°C[11]; including mAbs, which typically do not show complete unfolding below 50°C[12]. Therapeutic proteins exhibiting melting temperature close to 40°C or lower are particularly concerning due as they may unfold at human body temperature. Chemical denaturation refers to the addition of chaotropes such as urea and guanidinium hydrochloride. Chaotropes bind to the protein and have been reported to change the pKa of amino acid side chains[13], which in turn, can affect the conformational stability of a protein.

Aggregation and Precipitation

Protein aggregation and precipitation is an obligatory CQA and has been extensively reviewed elsewhere[14-16]. Protein aggregates are defined as any protein assembly larger than the desired active unit of a protein (e.g., monomer of mAb)[17]. Protein aggregates are heterogeneous species and can be classified by a variety of categories (Table 1). Precipitation refers to protein aggregates forming macroscopic ensembles due to reduced solubility[18].

The original concern of particles in parenteral preparations arose due to possible occlusion of blood capillaries after administration of particles ≥10 μm[19] and potential safety concerns in patients. Eventually due to the concern of an embolism, health authorities established harmonized pharmacopoeial chapters (USP <788>, Ph. Eur. 2.9.19, JP 6.07) to monitor particles ≥10 μm and ≥25 μm. To date, the main concern of particles, especially proteinaceous particles, is due to aggregates causing an immune response in patients[15]. Pharmacopoeias limit requirements for the SbVP count are 6000 particles/container ≥10 μm and 600 particles/container ≥25 μm. In recent years, smaller SbVPs, i.e., particles ≥2 μm and ≥5 μm received increasing attention from regulatory authorities and the scientific community although there is no evidence that these SbVPs are more immunogenic than larger SbVPs[16].

Owing to the complexity of protein aggregates, several analytical methods are typically required[14]. A variety of stress factors such as temperature, pH, freezing/thawing, mechanical stress (shaking/stirring), formulation, and air-liquid/solid-liquid interfaces can cause aggregation[14]. For

example, temperature can directly impact a protein's higher order structure (secondary or higher); induce unfolding and consequently cause protein aggregation. Temperature also accelerates chemical degradation such as deamidation and oxidation, which can also lead to increased protein aggregation. Protein concentration also needs to be considered as the aggregation is concentration-depending[11].

Table 1: Classification of protein aggregates. Adapted from[14,17,20].

Protein aggregate categories	
Conformation / structure	• Native • partially denatured • denatured

Size	• soluble aggregates (<0.1 μm): dimer, trimer, or oligomer
	• insoluble aggregates
	  ○ visible particles (≥100 μm)
	  ○ subvisible particles (0.1 to 100 μm)

Reversibility	• reversible (e.g., caused by self-assembly of protein molecules) • irreversible • dissociable

Type of bond	• covalent
	  ○ disulfide mediated (through free thiols)
	  ○ non-mediated (e.g., dityrosine formation)
	• non-covalent
	  ○ Van der Waals interactions
	  ○ hydrogen bonding
	  ○ hydrophobic interactions
	  ○ electrostatic interactions

Morphology	• spherical/non-spherical • translucent • homogeneous/heterogeneous • amorphous/fibrillar

Surface Adsorption

Protein surface adsorption is a concern during various pharmaceutical processes involving glass, plastics, and stainless steel. Protein adsorption to a surface is largely influenced by the protein, surface material, surface area, solution, and forces counteracting adsorption (e.g., electrostatic repulsion)[21]. A protein's structure, hydrophilicity/hydrophobicity, and its net charge are key intrinsic factors affecting protein adsorption. Particularly, when dealing with very low protein concentrations, adsorption and consequential loss in protein content is concerning due to insufficient dose with adverse impact on efficacy. Protein adsorption may also cause a protein to aggregate[22] or trigger changes in a protein's secondary structure[23]. Protein adsorption is generally regarded as irreversible[24] or partially reversible[25].

Chemical Stability

Therapeutic proteins can undergo a variety of chemical degradation pathways with over 100 post-translational modifications being reported to date[26]. Common modifications include reactions such as protein deamidation, oxidation, fragmentation, and glycation[27]. Solution pH is one key determining factor for many chemical degradation pathways. Modifications like c-terminal lysine degradation, aspartic acid transpeptidation, methionine oxidation, and peptide cleavage are predominantly occurring at acidic pH[10]. Whereas deamidation, β-elimination, various oxidation reactions, and disulfide shuffling are mainly occurring under basic conditions.

The main focus of this thesis was to assess physical stability, common chemical degradation events are discussed briefly for the purpose of explanation, however, with the exception of fragmentation were not analyzed in this thesis. Several comprehensive review articles on chemical protein degradation are available[5,7,11,14,18,28,29].

Deamidation

Deamidation is widely regarded as the most common modification for peptides and proteins. Deamidation introduces changes in a protein by increasing its molecular weight by 1 Da as well as lowers pI and hydrophobicity. Deamidation typically involves the hydrolysis of asparagine to aspartic acid. The reaction is largely driven by external factors such as pH, temperature, and ionic strength. Asparagine deamidation reaction rate is at its lowest between pH 3 and 6. At pH values>6 deamidation includes an irreversible nucleophilic attack forming a succinimide intermediate due to the loss of ammonia. Succinimide readily hydrolyzes to form aspartic acid and isoaspartic acid[5]. Deamidation can also refer to hydrolyzes of glutamine to glutamic acid, however, this reaction is less common as it requires pH values <3 and involves a less stable six-membered intermediate form[5]. Particularly susceptible to deamidation are motifs in which asparagine is followed by an

amino acid with a smaller side chain (e.g., asparagine-glycine), as it has been argued to be sterically favorable to form succinimide. Another important aspect of amino acids following asparagine is their capability to function as a hydrogen bond donor, as this may accelerate deamidation[5].

Oxidation

Oxidation can occur through metal-catalyzed oxidation, photooxidation, and free radical cascades. Methionine, histidine, cysteine, tyrosine, and tryptophan are prone to oxidation. Methionine is particularly susceptible leading to the formation of methionine sulfoxide. Metal-catalyzed oxidation is typically occurring on glycine, aspartic acid, histidine, and cysteine, whereas photooxidation often involves tryptophan, tyrosine, and phenylalanine. Contrary to the general correlation between protein oxidation rate and pH, methionine oxidation occurs almost independently of pH. Moreover, methionine oxidation may also not follow Arrhenius behavior, as oxygen solubility increases inversely with solution temperature. Controlling protein oxidation is generally difficult as sources of free radicals can be encountered during several stages of DP development due to their presence in excipients, primary packaging, etc.

Another critical aspect is the solvent exposure of residues and the conformational stability of a protein. For example, methionine252 and methionine428 (EU number system[30]), located in the CH_2-CH_3 interface (i.e., the binding site for protein A and the neonatal Fc receptor) are highly solvent-exposed and known to be susceptible to oxidation[31]. Contrary, Met358 and Met397, located in the CH_3-CH_3 interface of the constant region of IgG2, are buried inside a protein and thus less susceptible to oxidation. Oxidation can have an impact on a protein's pharmacokinetics as it impacts binding to the neonatal Fc receptor[32] and Fcγ receptors[33], potentially decreasing its biological activity[31].

Fragmentation

Protein fragmentation is a complex process as it involves several factors such as solvent and solvent conditions like pH as well as temperature[5]. Moreover, intrinsic protein factors such as sequence motifs contribute largely to their fragmentation susceptibility[34]. Protein fragmentation can be categorized into enzymatic and non-enzymatic hydrolysis or β-elimination[34,35].

Proteolytic (enzymatic) hydrolysis is often abbreviated as proteolysis or hydrolysis. Due to intermolecular cyclization of aspartic acid, peptide bonds located before or after aspartic acid are particularly susceptible to hydrolysis (e.g., aspartic acid - proline)[10]. Likewise, certain amino acids succeeding aspartic acid, particularly, glycine, serine, proline, and valine are susceptible to hydrolysis[5,36,37]. Besides aspartic acid, hydrolysis may also occur on the side chain of tryptophan. Tryptophan hydrolysis forms kynurenine, a degradation product occurring from tryptophan oxidation[5]. Another amino acid prone to fragmentation is asparagine. Asparagine residues have

been shown to form new C-terminal succinimide residues in peptides and proteins under physiologic conditions[10]. In addition to amino acid side chains, protein regions exhibiting higher flexibility are concerning. For example, the hinge region, CH_2-CH_3 domain interface of mAbs, or local protein regions may also undergo hydrolysis[38-41]. Furthermore, disulfide bonds are susceptible to modifications and fragmentation due to their fairly low dissociation energy[39]. The reaction rate of fragmentation is at its lowest at pH 6, and increases linearly above pH 6[42].

β-elimination refers to a reaction that readily occurs in proteins, mostly at high temperatures[5]. Cysteine is particularly susceptible, however, the reaction may also involve serine, threonine, phenylalanine, or lysine[18]. From a chemical point of view, β-elimination refers to the deprotonation of the hydrogen atom on the α-carbon[5]. Due to rearrangement of a carbanion, a double bond between the α- and β-carbon atom forms, which is defined as β-elimination.

In Vivo Protein Stability

The stability of therapeutic proteins is tightly monitored and controlled during various stages of manufacturing, storage and shipping, as well as preparation for clinical use. Maintaining the stability of therapeutic proteins ensures patient safety and/or treatment efficacy. Once a therapeutic protein is administered to patients, the physiologic conditions (e.g., 37°C; pH 7.4) substantially differ from those in the DP. These conditions can be regarded as unfavorable as they may cause protein degradation, potentially even at faster rates than in the DP[43,44]. Thus, an increasing number of studies emerged, which simulated the physiologic environment under *in vitro* conditions to evaluate the *in vivo* protein stability. Such models typically include spiking the protein of interest in the desired biological fluid (e.g., human SC tissue to simulate SC administration).

While IgGs are naturally circulating in human biological fluids, due to their variable region, each IgG exhibits unique biophysical properties and thus the *in vivo* stability of each molecule may differ[27]. Biophysical properties of therapeutic IgGs such as charge and pI are frequently modulated to improve pharmacokinetic properties and as such may alter their *in vivo* stability[27,45]. Solely based on sequence hotspots, pI, and hydrophobicity their susceptibility to *in vivo* degradation may vary. Specifically pI and hydrophobicity of therapeutic proteins have been argued to cause protein aggregation *in vivo*. Further studies are strongly needed to understand which physiologic factors and protein properties (e.g., pI, charge, hydrophobicity), impact the *in vivo* stability.

In vivo degradation of many proteins, including IgGs, has been reported[46,47]. For example, (i) oxidation of methionine[48] in the constant domain of a mAb may decrease binding affinity to the Fcγ receptors[33] or neonatal Fc receptor and thus decrease its half-life[32], (ii) aspartic acid deamidation[49-51] in the CDR can lower its antigen binding affinity[50], (iii) aspartic acid

isomerization[52], may decrease potency[47], (iv) glycation of lysine located in the CDR may affect antigen binding and potency due to loss of its positive charge[53,54], (v) aggregation/precipitation[55-57] may cause an immune response, (vi) fragmentation may lower bioavailability[58].

Aim of the Thesis

The aim of this PhD thesis was to develop *in vitro* models and analytical methods, which enable to evaluate the *in vivo* stability of therapeutic proteins under simulated physiologic conditions. While the stability analyzed *in vitro* may not translate to results observed in a clinical setting, early stage evaluation of the *in vivo* stability can be a valuable screening tool to assess protein liabilities. These *in vitro* models are particularly appealing during pre-clinical stages of development as they can support the selection of molecules, preferably prior to clinical lead candidate selection.

Milestones of this thesis were defined as follows:

Evaluation of physiologic stress factors potentially impacting the *in vivo* stability of therapeutic proteins.

- Which physiologic factors are known to impact protein stability?
- Which human physiologic conditions and constituents of biological fluids should be simulated using *in vitro*/*ex vivo* models.

Comparison of different analytical strategies to investigate *in vivo* protein stability.

- What are advantages and limitations of each analytical strategy?
- Which analytical strategies are applicable to investigate *in vivo* protein aggregation and fragmentation?

Development of fluorescence methods to assess protein stability in biological fluids.

- Are fluorescence methods suitable to assess the *in vivo* stability of proteins directly in biological fluids, i.e., enable distinct detection of the protein of interest in human serum?
- How stable are biological fluids under *in vitro*/*ex vivo* conditions (e.g., particle formation)?

Development of *in vitro* models to assess the stability of therapeutic proteins without labeling or purification techniques.

- How applicable is PBS to assess the *in vivo* protein stability?
- How applicable are protein-free artificial fluids (bicarbonate buffer) to assess *in vivo* protein stability?

Results

Chapter I:

In Vivo Stability of Therapeutic Proteins

Chapter II:

Analytical Challenges Assessing Aggregation and Fragmentation of Therapeutic Proteins in Biological Fluids

Chapter III:

Particle Analysis of Biotherapeutics in Human Serum using Machine Learning

Chapter IV:

Tracking the Physical Stability of Fluorescent-Labeled mAbs under Physiologic *In Vitro* Conditions in Human Serum and PBS

Chapter V:

Assessing Particle Formation of Biotherapeutics in Biological Fluids

Chapter VI:

Stability of Monoclonal Antibodies after Simulated Subcutaneous Administration

In Vivo Stability of Therapeutic Proteins

The following chapter has been published as review article in the Pharmaceutical Research journal.

Joachim Schuster, Atanas Koulov, Hanns-Christian Mahler, Pascal Detampel, Joerg Huwyler, Satish Singh, and Roman Mathaes
In Vivo Stability of Therapeutic Proteins
Pharm Res. 2020, 37(2), 1-17
doi: 10.1007/s11095-019-2689-1

Pharm Res (2020) 37:23
https://doi.org/10.1007/s11095-019-2689-1

EXPERT REVIEW

In Vivo Stability of Therapeutic Proteins

Joachim Schuster[1,2] • Atanas Koulov[1] • Hanns-Christian Mahler[1] • Pascal Detampel[2] • Joerg Huwyler[2] • Satish Singh[1] • Roman Mathaes[1]

Received: 7 May 2019 / Accepted: 16 August 2019 / Published online: 3 January 2020

ABSTRACT Significant efforts are made to characterize molecular liabilities and degradation of the drug substance (DS) and drug product (DP) during various product life-cycle stages. The *in vivo* fate of a therapeutic protein is usually only considered in terms of pharmacokinetics (PKs) and pharmacodynamics (PDs). However, the environment in the human body differs substantially from that of the matrix (formulation) of the DP and may impact on the stability of an injected therapeutic protein. Stabilizing excipients used in protein formulations are expected to undergo more rapid distribution and dissociation *in vivo,* compared to a protein as a highly charged macromolecule. Thus, *in vivo* stability may significantly differ from shelf-life stability. *In vivo* degradation of a therapeutic protein may alter efficacy and/or safety characteristics such as immunogenicity. Studying the stability of a therapeutic protein in the intended body compartment can de-risk drug development in early stages of development by improving the selection of better clinical lead molecules. This review assesses the considerations when aiming to evaluate the *in vivo* fate of a therapeutic protein by comparing the physiology of relevant human body compartments and assessing their potential implications on the stability of a therapeutic protein. Moreover, we discuss the limitations of current experimental approaches mimicking physiologic conditions, depending on the desired route of administration, such as intravenous (IV), subcutaneous (SC), intravitreal (IVT), or intrathecal (IT) administration(s). New models more closely mimicking the relevant physiologic environment and updated analytical methods are required to understand the *in vivo* fate of therapeutic proteins.

✉ Roman Mathaes
roman.mathaes@lonza.com

[1] Lonza AG, Drug Product Services, Basel, Switzerland

[2] Division of Pharmaceutical Technology, University of Basel, Basel, Switzerland

KEY WORDS developability · human body fluids · *in vitro* model · *in vivo* protein stability · therapeutic protein

ABBREVIATIONS

ADC	Antibody-drug conjugate
AF4	Asymmetric flow field-flow fractionation
AUC	Analytical ultracentrifugation
CE-MS	Capillary electrophoresis-mass spectrometry
CE-SDS	Capillary electrophoresis sodium dodecyl sulfate
cIEF	Capillary isoelectric focusing
CLSM	Confocal laser scanning microscopy
CMC	Chemistry, manufacturing, and controls
CPP	Critical process parameter
CQA	Critical quality attribute
CSF	Cerebrospinal fluid
DS	Drug substance
DSC	Differential scanning calorimetry
DP	Drug product
FCM	Flow cytometry
fSPT	Fluorescence single particle tracking
IEX	Ion-exchange chromatography
IgG	Immunoglobulin G
ISF	Interstitial fluid
IT	Intrathecal
IV	Intravenous
IVT	Intravitreal
LC-MS/MS	Liquid chromatography-tandem mass spectrometry
LO	Light obscuration
mAb	Monoclonal antibody
MFI	Micro flow imaging
MMP	Matrix metalloproteinase
NTA	Nanoparticle tracking analysis
PBS	Phosphate-buffered saline
pI	Isoelectric point
PK/PD	Pharmacokinetic/pharmacodynamic

Published online: 03 January 2020

SC	Subcutaneous
SCISF	Subcutaneous interstitial fluid
SEC	Size exclusion chromatography
SPR	Surface plasmon resonance
VH	Vitreous humor

INTRODUCTION

Biopharmaceuticals, such as recombinant proteins, monoclonal antibodies (mAbs), and antibody-drug conjugates (ADCs), are therapeutic modalities to treat many severe diseases such as immunological disorders and various cancers.

Protein stability is generally a major challenge during biopharmaceutical product development. In contrast to traditional small molecules, biotherapeutics possess complex degradation pathways, mainly due to their large size and structure. The variant heterogeneity of proteins can be categorized in (a) process-related variants (e.g. sequence variants) and (b) product-related variants (e.g. degradation products). Any alteration to the native protein structure - either chemical or physical - may affect its therapeutic efficacy and/or patient safety. Degradation products from proteins can have different pharmacokinetics (PKs) and/or pharmacodynamics (PDs), and/or may lead to different adverse effects, e.g. undesired immune response (1). Degradation products should be categorized as either critical quality attributes (CQAs) or non-CQAs, depending on whether or not product efficacy (e.g. potency, PK) and/or safety are potentially impaired (2). Thus, protein degradation products and pathways require sufficient understanding and characterization during product development. These assessments aim to reveal which degradation product is a CQA and to what extent degradants may form in the drug substance (DS) and drug product (DP). This is typically assessed as a function of critical process parameters (CPP) or various stresses. Stress conditions that support CQA and CPP assessments include temperature, shipping simulations, interfacial stresses (e.g. freezing, shaking), and changes in formulation parameters such as pH. Moreover, process characterization studies such as downscale models of manufacturing unit operations can provide additional support for these assessments. Interestingly, CQA assessments typically do not directly consider *in vivo* changes that a given attribute may undergo, but may detect them only indirectly, e.g. via PK studies.

IN VIVO STABILITY OF THERAPEUTIC PROTEINS

To date, the *in vivo* stability of therapeutic proteins or their excipients after administration has received limited attention beyond PK/PD considerations. PK/PD studies do not typically aim at evaluating possible degradation pathways (3). However, after administration of therapeutic proteins in humans, several modifications (e.g. deamidation) may continue (or begin) due to changes in temperature and/or pH, for example (4–10). Conversely, the blood matrix may also reverse certain modifications, such as reforming open disulfide bonds (11) or reversing trisulfide to disulfide bonds (12,13).

After administration of therapeutic proteins, excipients may lose their stabilizing effect due to dilution or separation from the therapeutic protein. The latter may occur due to rapid tissue distribution and elimination at the injection site or in the blood stream (8,14). Thus, administered therapeutic proteins are exposed to human body compartments, in the absence of stabilizers (Fig. 1). This may affect the stability of the administered protein. As an example, if a protein aggregated or precipitated *in vivo* as a result of specific physiologic conditions such as pH or ionic strength the protein may exhibit altered levels of immunogenicity, reduced efficacy, and/or increased potency (4,15). Recently, Kinderman *et al* observed *in vivo* precipitation after SC injection of a fully human IgG2 (16). The authors concluded that this specific type of particle formation did not lead to an enhanced immune response. Furthermore, binding activity and epitope recognition may be impaired by *in vivo* post-administration modifications such as deamidation (17) or glycation (18).

In recent years, there has been an increasing focus on benchmarking lead candidate molecules from a PK/PD or CMC standpoint but also in terms of *in vivo* stability liabilities. Identification of potential degradation hot spots or sequence liabilities and subsequent sequence optimization during lead candidate selection increase the chance of successful drug development. Assessing various molecular variants in studies simulating the actual physiologic exposure (*in vivo* stability) at an early stage of development may further strengthen the selection of a clinical candidate and mitigate the risks associated with potential liabilities during preclinical and clinical development. Thus, investigating protein degradation in the intended human body environment allows to identify critical attributes and providing insight into interactions with matrix constituents (e.g. antigen) (10,19).

PHYSIOLOGY AND COMPOSITION OF HUMAN BODY FLUIDS

Parenteral routes of administration include intravenously (IV), intraarterially (IA), intramuscularly (IM), interdermally (ID), subcutaneously (SC), intravitreally (IVT), or intrathecally (IT). Besides the traditional IV and SC route IVT and IT injections of therapeutic proteins are receiving increasing attention (20). Tables I and II summarize the chemical and physical parameters as well as concentrations of selected electrolytes and other components of human body fluids/compartments. The fluid dynamics and composition of these four body

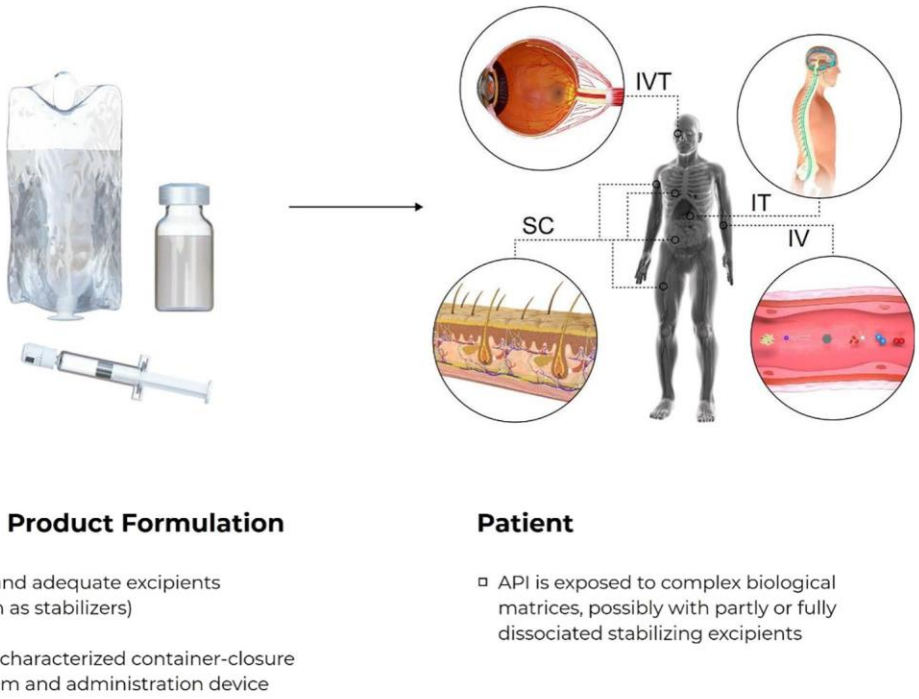

Fig. 1. From the drug product (DP) to the patient. After injection or infusion of a DP, the PK of excipients may show for instance shorter half-lives due to their physicochemical properties. This may expose therapeutic proteins to complex biological matrices without or with less stabilizing excipients present.

compartments feature significant differences and may lead to specific profiles of excipient degradation.

Blood

Human blood contains lipids, proteins, cells, sugars, electrolytes, etc. Overall, 22 proteins make up 99% of the total human serum protein content, which includes the family of blood proteins: albumin (60%), globulins (35%), and fibrinogen (4%). Several hundred different signaling proteins (e.g. hormones) make up the majority of the remaining 1 %. The pH of around 7.4 in extracellular human body fluids, i.e. in blood but also in the subctuaneous interstitial fluid (SCISF), vitreous humor, and CSF is primarily maintained by continous adjustment of carbon dioxide and bicarbonate concentrations (38). Moreover, hemoglobin present in red blood cells, additional proteins, and phosphate contribute to the buffering capacity of blood.

The Subcutaneous Tissue

The human subcutaneous (SC) tissue (hypodermis) comprises a highly vascularized adipose tissue and the interstitium (interstitial space), containing interstitial fluid (ISF) and extracellular matrix (ECM) components. The ECM consists mainly of a collagen fiber network (mostly type I collagen), glycosaminoglycans (e.g. hyaluronan), elastin, and cell adhesion proteins (31). The compositon of the ISF is comparable to that of blood but contains significantly less protein (23). Moreover, due to the Gibbs-Donnan effect, Na^+ and K^+ concentrations in the SC tissue are lower, whereas the Cl^- concentration is higher than that in plasma (38,83).

Within the SC tissue, alternating regions of low and high negative charge densities are hypothesized to exist (84). Conversely, it has been proposed that the majority of ISF is entrapped in the SC tissue gel resulting in exceedingly small volumes of free flowing fluid (38,85). The overall charge of the SC tissue remains also controversial as overall positive or negative charges have been proposed (31). The buffering capacity of the SC tissue is lower compared to that of blood due to lower endogenous protein concentration (23,86).

Vitreous Humor

Human vitreous humor (VH) is a liquid/gel-like substance occupying a total volume of approx. 3.9 mL per eye, comprising water (98–99.7%), electrolytes (0.9%), and polysaccharides as well as proteins (0.1%) (39,55). The network between collagen fibrils (mostly type II collagen) and hyaluronan provides the gel state of the VH. In human VH proteome analysis, several hundred proteins not related to plasma were detected (87). The majority of those proteins were classified as enzymes, binding proteins, and signaling proteins. Although hyaluronan has been argued to stabilize the pH in the VH, its overall buffering capacity is also assumed to be lower than that of blood (65).

Cerebrospinal Fluid

To bypass the blood-brain barrier therapeutic proteins are most commonly administered into the CSF via IT lumbar

Table I Chemical and Physical Parameters of Human Body Fluids/Compartments: Whole Blood, SCISF, VH, and CSF

	Whole blood, Plasma, or Serum	SC Interstitial Fluid (ISF) / SC Tissue	Vitreous Humor (VH)	Cerebrospinal Fluid (CSF)
Total protein concentration (mg/mL)	Serum: 55–80 (21) Plasma contains 3–5 mg/mL more protein than serum (22)	21.6–32.9[ac]* 14.0–22.6[bc]* (23)	0.5–1 (22)	0.15–0.45 (24) Lumbar concentration is slightly higher than cisternal (25)
Total IgG content (mg/mL)	Serum: 6.14–12.95 (21)	4.70–8.30 (26)[ad]	0.0305–0.0365 (27)	0.003–0.030 (28)
High-molecular weight components	Enzymes (29) Cells: e.g. erythrocytes, leukocytes, and thrombocytes	Enzymes: e.g. MMPs (30) Cells: e.g. adipocytes, fibroblasts, dendritic cells, and macrophages (31,32)	Enzymes: e.g. MMPs (33), Cells: hyalocytes, fibrocytes, retinal pigment epithelial cells, astrocytes, macrophages, myofibroblast-like cells, and white blood cells (22,34)	Enzymes: e.g. MMPs (35) Cells: mainly lymphocytes and monocytes,also segmented non-degenerate neutrophils, erythrocytes, plexus cells, and ependymal cells (36,37)
Low-molecular weight components	Lipids, sugars, lactate, urea, etc.	Expected to be similar due to the continuous exchange between blood and ISF (38). E.g. higher Cl^- concentration than that in plasma due to Gibbs-Donnan effect.	Different composition due to the metabolic activity in the VH and adjacent tissues (39,40). E.g. higher lactate, Na^+, and Cl^-, concentrations than that in plasma (41).	Different composition: CSF is a secretion and not an ultrafiltrate of plasma (42). E.g. higher Na^+ and Cl^- concentrations than that in plasma (43).
pO_2 (mmHg)	Venous: 35–40 Arterial: 80–100 (44)	21-49[f] (45)	Mid-cavity: 20.9–46.5 (46)	Basilar cisterns: 38–92 Third ventricle: 81–179 (47)
pCO_2 (mmHg)	Venous: 41–51 Arterial: 35–45 (44)	38-50[f] (45)	19.2–30.4 (48)	30–50 (49)
Colloid osmotic pressure (mmHg)	Serum: 20.6–24.4* (23)	6.1–10.9[ac]* 4.7–7.7[bc]* (23)	Intraocular pressure: 16 (50)	CSF pressure: 7.4–14.7 (42) Intracranial pressure: 5–15 (49)
Volume (mL)	Whole blood: • male: 4490 (plasma: 2460) • female: 3600 (plasma: 2130) (51)	At the injection site: 2.57[g] (52)	Liquid and gel volume: 3.9 (40)	150–160 (total) • subarachnoid CSF: 75% • ventricular CSF: 25% (42)
Water content	Whole blood: 55% by volume Plasma: 92% by volume (53)	92.5%[jk] (54)	98–99.7% (55)	99% (42)
Viscosity (mPa s)	Whole blood: non-newtonian • 3.03–4.01 mPa s Plasma/serum: newtonian • plasma: 1.25–1.43 • serum: 1.15–1.29 Measured at 37°C (56)	Expected to be higher than plasma due to hyaluronan[h] (57) Lymph fluid: 1.8[l] Measured at 37°C (58)	Non-newtonian[h] (59) vitreous gel: 300–2000 Measured at 20–25°C (60,61)	Newtonian: 0.7–1.0 Measured at 37°C (24)
Refractive index	Plasma: 1.3485–1.3513 (51)	interstitial fluid: slightly higher than water adipose tissue: 1.46 (62)	1.3345 (40)	1.3349–1.3351 (51)
Osmolality/osmolarity	Plasma 285–295 mOsm/kg serum water (21)	300.8 mOsm/L H_2O[l] (38)	282.6–296.4 mOsm/kg (41)	281.7–292.7 mOsm/kg (63)
pH	Venous: 7.33–7.43 Arterial: 7.35–7.45 (44)	7.49–7.637.39–7.63 (64)	7.0–7.4 (65)	lumbar: 7.325 cisternal: 7.345 (66)
Temperature (°C)	36–37.5 (38)	33–35 (comfort conditions) (67)	32.05–34.03 (68)	intraventricular cerebrospinal fluid: 36.0–37.4 (males) 36.2–38.8 (females) (69)
Flow rate (mL/min)	40–2000 depending on the vein (70)	Lymphatic flow rate: 0.0043 (71)	Aqueous fluid flow: 0.0015–0.0030 (72) Vitreous outflow: 0.0001[h] (73)	in craniocaudal direction: 0.304–1.2 (74)

[a] wick fluid

[b] blister fluid

[c] SCISF of human legs

[d] SCISF of human forearm

[e] venous blood

[f] muscle ISF of human forearm

[g] The calculated subcutaneous interstitial space is based on the diameter of a radiolabelled depot of for an IgG immediately following injection in the forearm. The volume distribution was assumed to be spherical

[h] rabbit

[i] mouse

[j] Location of ISF not specified

[k] The water content of the interstitial fluid is expected to be slightly higher (ca. 0.5%) than that of plasma due to a lower protein concentration in the interstitial fluid

[l] SCISF of rats

*Results are expressed as 95% confidence intervals (23)

IgG, Immunoglobulin G

MMP, matrix metalloproteinase

delivery. The CSF is actively secreted by epithelial cells in the choroid plexus (42) and circulates between the subarachnoid space and the spinal CSF spaces (74). The CSF composition differs from that of blood due to the blood-CSF barrier (42). For example, levels of glucose, urea, protein, and K^+ are lower, while those of Cl^- and Mg^{2+} are higher in the CSF than in blood. Likewise, the buffering capacity of the CSF is much lower than that of blood (66). Of note, leaking of blood into the CSF may interfere with the buffering capacity of the CSF.

IN VIVO INTERACTIONS OF A THERAPEUTIC PROTEIN WITH HUMAN BODY COMPARTMENTS

Several factors such as temperature, pH, pressure, interfacial stresses (e.g. agitation, freezing and thawing), salts, and protein concentration, are known to affect protein stability (88). During DP formulation and process development, the process conditions and formulation parameters are carefully adjusted to minimize the impact of such stress factors on product stability and quality. The shelf-life stability of therapeutic proteins is typically ≥3 years at 2–8°C. In comparison, therapeutic proteins need to be stable *in vivo* for days, weeks, or months at 37°C. However, the conditions encountered *in vivo* differ significantly from those during storage. The human body presents a variety of stress factors to the therapeutic protein (Table III) and its excipients (Table IV) (3,4,7,109). After administration, excipients will be significantly diluted, distributed, or degraded, depending on their size and type. Thus, the stabilizing effect on the therapeutic protein may be lost quickly *in vivo*.. Moreover, the therapeutic protein is subjected to a rapid pH increase from the formulation buffer upon administration (for a mAb, typically pH 5.5–6.5 (117)) to the physiologic buffer system (pH: ~7.4). The temperature increases dramatically from the intended storage condition (typically 2–8°C) to body temperature (e.g. blood: ~37°C). Although stress studies such as accelerated storage conditions (e.g. 25°C/60% relative humidity, 40°C/75% relative humidity) are typically performed during DP development, parameters other than temperature may affect DP stability. For example, formulation buffers differ from the bicarbonate buffer system present in the human body. Moreover, the therapeutic protein is exposed to electrolytes (primarily: Na^+, Cl^-, HCO_3^-, and K^+), reducing sugars, enzymes, and other metabolites.

Therefore, *in vivo* stability of a therapeutic protein does not necessarily correlate with accelerated storage stability. - Studies better mimicking the physiologic conditions are needed.

In conclusion, administration of a protein DP may lead to chemical changes of the protein and/or impact a protein higher order structure with potential loss of potency. This may lead to altered PK and more side effects such as immunogenicity.

IN VIVO CHEMICAL DEGRADATION

Protein instability can be categorized as chemical or physical degradation (88). Several *in vivo* chemical degradation mechanisms of recombinant and endogenous Immunoglobulin Gs (IgGs) have been described (5). However, it remains controversial whether and how endogenous modifications modify the pharmacologic performance and side-effect profile of a therapeutic protein (5). The criticality of *in vivo* modifications can be assessed by comparing the rate of *in vivo* conversion and mAb elimination, the function of the modified sequence (e.g. CDR, Fc region), the level of modification, and whether or not the degradation occurs endogenously (5,6).

Table II Concentrations of Selected Electrolytes and Other Components

	Whole blood, Plasma, or Serum (21)	Subcutaneous interstitial fluid (SCISF) (75)	Vitreous Humor (VH) (41)	Cerebrospinal Fluid (CSF) (51)
Sodium	136–145	134.6	143.4–150	137–153
Potassium	3.5–5.0	3.17	4.87–6.59	2.62–3.30
Chloride	98–106	111 (8)	119–124.2	119–131
Calcium	2.2–2.6	1.551	0.61–1.646	1.02–1.34
Magnesium	0.8–1.2	0.666	0.742–1.058	0.55–1.23
Bicarbonate	21–28	31 (8)	22.7–26.9[a] (76)	18.6–25.0
Phosphate	1.0–1.4	0.610	0.8* (77)	0.442–0.694
Glucose	4.2–6.4 (21)	3.1–3.3 (78)	1.99–3.95	2.4–3.6
Hyaluronan	0.01–0.1 μg/g (79)	1% in wet SC tissue[b] (8)	65–400 μg/mL[c] (55)	0.089–0.243 μg/mL (80)
Collagen	–	55% of dry weight SC tissue[b] (8)	300 μg/mL[c] (81)	–

Unless otherwise stated, values are in mmol/L.

Values for the SCISF depend mainly on the body location and method used for the calculation, e.g. "Stewart's approach" which neglects the Gibbs-Donnan effect

[a] measured in the core of rabbit vitreous humor

[b] measured in rat

[c] During liquefaction of the human vitreous humor (increase in liquid volume and decrease in gel volume with age), the concentration changes in liquid and gel volume (82)

*Estimation for living humans based on post-mortem measurements in humans

Deamidation, oxidation, glycation, and disulfide bond scrambling are amongst the most thoroughly investigated *in vivo* chemical degradation mechanisms of therapeutic proteins. Deamidation increases with *in vivo* circulation time and can affect PK. *In vivo* deamidation was described as a so-called 'molecular clock' (118). For instance, N384 (EU numbering) deamidation on recombinant and endogenous mAbs in circulation was used to predict the half-life of the protein (99). Furthermore, Huang *et al.* demonstrated that N55 deamination occurs following IV and SC administration in cynomolgus monkeys (17). N55 is located in the CDR2 of the heavy chain and can decrease antigen binding affinity.

Significant oxidation of the conserved M252 and M428, located at the CH2 and CH3 domain, can decrease the FcRn binding affinity and consequently lower the half-life of human IgG1 and IgG2 (119). Further studies are required to determine to which extent IgG oxidation occurs *in vivo* and how this may alter the fate of a given drug.

Glycation is a non-enzymatic naturally occurring reaction of endogenous and therapeutic IgGs which increases with circulation time (18). In particular, glycation of K located in the framework region or CDR may impair antigen binding (5). In a study characterizing the impact of low glycation abundance of 10% of a K residue located in the CDR, mAb binding was not affected (120).

In addition to deamidation, oxidation, and glycation, endogenous thiols in human body fluids (e.g. 13–20 μM in serum (121)) can substantially alter the secondary structure of mAbs (7) via disulfide shuffling in IgG2 (92–94), stabilization of disulfide bonds in IgG1 (11), and Fab exchange in IgG4 (95). Of note, certain *in vivo* modifications such as oxidative carbonylation are of interest in aging as these modifications mark protein degradation *in vivo* (122). *In Vivo* Physical Degradation.

Protein aggregation and particle formation are generally considered as obligatory CQA and are well studied during pharmaceutical development and manufacturing. Parenteral preparations need to be "practically free" and "essentially free" of visible particles as required by the pharmacopoeias: USP <1>, USP <790> (123) and Ph. Eur. "Parenteral preparations", 2.9.19 and 2.9.20 (124,125). Protein aggregation and proteinaceous particles have been hypothesized to increase immunogenicity (126).

Protein aggregation or precipitation may be triggered, increased, or minimized *in vivo*, compared to degradation observed in DP stability studies.. The difference in physical stability may be explained by changes in pH, ionic strength, and presence of specific compounds *in vivo* that may alter electrostatic interactions. For instance, *in vivo* precipitation due to steric exclusion (8) or *in vivo* fragmentation due to enzymatic proteolysis were reported (127). Additionally, dissociation and distribution of excipients *in vivo* may lead to a loss of excipients present at the protein to protect it from possible interactions. Similarly, therapeutic proteins may be stabilized against aggregation and precipitation due to highly abundant proteins such as albumin in serum.

Table III Potential Stress Factors of Human Body Compartments Affecting Therapeutic Proteins

Factors potentially impacting on protein stability	Details	Theoretical consequences
Macromolecular crowding • Excluded volume • Steric interactions	• mAb occupies reduced volume • Differences in diffusion rate in the SCISF (8)	• Adaptation to a compact structure and/or enhanced antigen interaction (7,19,89) • Faster transport of negatively charged macromolecules in ISF (90) • GAGs can impact the ISF distribution of macromolecules (31)
Endogenous thiols (e.g. albumin, cysteine, glutathione) in blood/tissue (12)	• Stabilizing effect of matrix/tissue • Susceptibility of disulfide bonds to scrambling in the presence of thiols (13) - in particular interchain disulfides due to solvent exposure (12,13)	• Repair/reformation of disulfide bonds with free cysteine of an IgG (11,13) • Michael addition on maleimide ADC-linkers (91) • Reversal of trisulfides to disulfide bonds (12,13) • Disulfide shuffling of IgG2 (92–94) • Fab exchange of IgG4 (95) • Thioether (lanthionine) formation (96) • Trisulfide bond formation (12) • Fragmentation (97)
pH	• Physiologic bicarbonate/CO_2 buffer • Strong buffering capacity in human body compartments maintains physiologic pH after injection • Rapid pH increase, may even include pH shift through the pI of a protein • Salting out effect as a consequence of pH shift	• Carbamylation of proteins may affect its function (98) • Buffering capacity of the VH is sufficient to maintain the physiologic pH (65) • Decreased colloidal stability • Accelerated reaction due to increased pH, e.g. deamidation (10,99) • *In vivo* precipitation (15)
Temperature	• Increase in temperature	• Aggregation or accelerated chemical reactions, e.g. isomerization, deamidation (10)
Flow rate	• Non-uniform mixing due to streaming of infused drug solutions (3)	• DP-blood interface during administration may lead to protein aggregation (3) • Impact of complex fluid dynamics during saccadic eye movement or within blood vessels
Electrolytes/osmolality	• Change in electrolyte composition and osmolality	• Influence of formulation osmolality on diffusion in the interstitium (100) • Precipitation may occur due to salting-out effect (15)
Enzymes	• Accelerated reactions • Degradation	• Fc glycation (mannosidase) (101). • C-terminal lysine clipping (basic carboxypeptidase) (102) • pyroGlu (glutaminyl cyclase) (103) • Large variety of proteolytic enzymes in human blood may degrade, e.g. ester bonds of the therapeutic protein (29) • Fragmentation due to e.g. plasmin (97,104) • Proteolytic activity in SC tissue is expected to be low (8,30)
Interaction with other components of human body compartments	• Lipids • Proteins • Cells • Sugars (e.g. glucose)	• e.g. albumin binds fatty acids • e.g. increased likelihood of IgG-IgG interaction especially for highly concentrated SC formulations (105) • e.g. Potential degradation and elimination by macrophages (106) • Increase of glycation over time (18) • Aggregation (107)
Endogenous degradation products	• Aggregation of endogenous proteins	• e.g. precipitation of therapeutic IgGs triggered by endogenous proteins (108)
Inflammation/metabolic byproducts (e.g. reactive oxygen species)	• Acceleration of reactions under certain disease states due to changes in body fluid composition	• e.g. aggregation (109) • e.g. increase of IgG glycation in diabetic patients with elevated blood glucose levels (18) • Protein citrullination in patients with e.g. rheumatoid arthritis (110) • e.g. oxidation (5)

IgG, Immunoglobulin G

ISF, interstitial fluid

SCISF, subcutaneous interstitial fluid

Additional modifications of endogenous and/or therapeutic IgGs *in vivo* were reviewed elsewhere (5,7,8)

Table IV Potential Interactions Between Excipients and Human Body Compartments. Interactions may Cause a Separation of a Therapeutic Protein and its Excipients and/or Loss of Stabilizing Properties. Dilution/Diffusion of Stabilizing Excipients may have the Strongest Impact on Therapeutic Protein Degradation

Factors potentially impacting excipients	Details	Theoretical consequences
Large volume of body fluid and high flow rate	• Dilution of excipients due to large blood volume and high flow rate • Dilution of excipients due to relatively low IVT injection volumes compared to VH volume	• Blood volume 4490 mL in male, 3600 mL in female (51) • Flow rate of 40–2000 mL/min in veins (70) leads to rapid distribution • e.g. ranibizumab (Lucentis®): ~50 μL into ~3900 μL VH
Increased lymphatic fluid flow	• Increase in ISF volume and pressure upon SC injection increases lymphatic fluid flow and may concentrate excipients (38)	• Rapid removal of water from the SC tissue thus concentrating the excipients (8)
Interaction with other components of human body compartments	• Some excipients may show a higher affinity to matrix components than the therapeutic protein leading to separation (8)	• e.g. hydrophobic interaction with e.g. albumin (111)
Elimination/Half-life	• Excipients follow different route of distribution and elimination, thus can result in different half-lives than the therapeutic protein	• e.g. posterior route of elimination from VH for small and lipophilic molecules (112) • e.g. low PS80 concentrations 1 h after administration (113) may lead to increased interaction with matrix components.
Enzymes	• Enzymatic degradation of excipients • Inhibition of enzymes	• e.g. carboxylesterase present in blood can degrade PS (114) or other esters • Excipients may inhibit protease and/or peptidase activity (115). E.g. PS20 inhibits lipase A activity (116)

PS, polysorbate

VH, vitreous humor

The *in vivo* physical stability of therapeutic proteins may substantially depend on the charge of the protein, charge distribution, and apparent isoelectric point(s) (pI). For example, a pI close to the physiologic pH of 7.4 is expected to result in a net neutrally charged molecule with inferior colloidal stability and potential risk for *in vivo* precipitation, whereas high pI values lead to electric repulsion forces and an increased colloidal stability *in vivo*.

Table V Examples of Innovative *In Vitro/Ex Vivo* Models Mimicking Physiologic Conditions

Author	Degradation		Model		(Simulated) administration	Molecule	Investigation
	Chemical	Physical	*in vitro*[a]/ *ex vivo*[b]	*in vivo*			
Awwad *et al.* (136)	–	–	dialysis membrane, inflow and outflow [a]	–	IVT	e.g. bevacizumab, ranibizumab	*in vitro/in vivo* correlation of PK parameters
Awwad *et al.* (137)	–	–	dialysis membrane, inflow and outflow [a]	–	IVT	Dexamethasone	*in vitro/in vivo* correlation of PK parameters
Bown *et al.* (133)	–	–	dinjection cartridge ("SCISSOR")[a]	–	SC	mAbs	*in vitro/in vivo* correlation of bioavailability
Groell *et al.* (141)	–	–	3D hydrogel-dendritic cells[ab]	–	SC	e.g. interleukin-4	Trigger of immune cells
Kinnunen *et al.* (132,142)	–	–	dialysis cassette ("SCISSOR")[a]	–	SC	insulin and mAbs	Fate of protein (e.g. drug release)
Lobo *et al.* (15)		X	dialysis tubing[a]	rat	SC	rhuMAb anti-CD11a (Raptiva™) and humanized 2H7 (rituximab)	Method and formulation to reduce aggregation
Patel *et al.* (14)		X	intraocular - porcine eye[b]	–	IVT	mAbs and FAb	Model development and formulation influence on stability
Patel *et al.* (135)	X	X	intraocular - porcine eye[b]	–	IVT	Bispecific mAb	Differences in mAb degradation kinetics compared to PBS

Table VI Key Parameters for the Development of an *In Vitro/Ex Vivo* Study/Model (14,132,135)

Parameter	Consideration
Therapeutic protein	PK data of mAbs after administration (e.g. C_{max}, steady-state parameters):
• Concentration of the drug during exposure to the body fluid (spiking concentration)	• e.g. C_{max} after IV administration: 0.5–206 μg/mL (143)
• Duration of exposure of the drug to the body fluid (incubation period)	• $T_{1/2}$ in blood: 12–13 d (144)
	• T_{max} following SC administration: 1.7–13.5 d (145)
	• $T_{1/2}$ in VH: 2.8–6.5 d (146)
	• $T_{1/2}$ in CSF: ventricular: 2.50 d, lumbar: 0.49 d (147)
Body fluid/compartment	
• Composition of different species	• Intra-subject and inter-subject variability e.g.
- osmolality, pH, etc.	- of fluid composition (148)
• Volume	- of SC tissue structure (105,133,149)
	- of human VH liquid/gel volume with age (40,82)
	- pathophysiologic state
	• Physiologically relevant volume
	- Sink conditions (132)
	- Significant dilution of excipients
Innovative model	
• Monitoring and controlling of	
- pH/buffering mechanism	• Use of bicarbonate and carbon dioxide to maintain the physiologic pH and simulate its buffering mechanism (132)
- Temperature	• Simulate the physiologic temperature (132)
- Pressure	• Simulate e.g. ISF pressure (132)
- Flow rate	• Simulate *in vivo* fluid dynamics (136)
• Dialysis membrane	• Separation of drug and excipients
	- e.g. mimic slow diffusion of excipients from the SC injection site (132,133)
	- PS removal by dialysis is likely not possible (150)
	• Removal of degradants to improve body fluid stability (14)
• Material of model	• Avoiding adsorption of proteins to material
• Injection needle	• Selection of an adequate injection needle
	- e.g. 23-27G hypodermic needle (132)
	• Controlling injection force and duration
• Additional parameters/controls	• Avoiding dilution prior to analysis, in particular for physical stability
	• Discrimination of endogenous and therapeutic IgG

C_{max}: Maximum concentration of drug in plasma after administration
CSF, cerebrospinal fluid
ISF, interstitial fluid
IV, intravenous
PS, polysorbate
SC, subcutaneous
$t_{1/2}$: Plasma elimination half-life
t_{max}: Time to reach the maximum plasma concentration
VH, vitreous humor

The pI values of therapeutic IgG vary greatly, ranging from 6.1 to 9.4 (128).

Arvinte *et al.* investigated the physical stability of three mAbs *in vitro* by comparing two diluents for infusion mixed with human plasma to simulate the *in vivo* situation (107). No aggregation of the investigated mAbs occurred when 0.9% sodium chloride solutions of mAbs were mixed with human plasma. Conversely, when mixing bevacizumab (Avastin®) or trastuzumab (Herceptin®) with 5% dextrose solution and human plasma, aggregates

Table VII Examples of Analytical Methods used to Characterize Therapeutic Proteins in Biological Fluids

Degradation pathway	Method	Reference
Physical	AF4	(155)
	AUC	(19)
	CE-SDS/SDS-PAGE	(108,130,135,138)
	DSC	(135)
	FCM	(130)
	fSPT	(130,154)
	Fluorescence microscopy	(16,130)
	Intact LC-MS	(138)
	Light microscopy	(14,107,135)
	LO	(130)
	MFI	(108)
	NTA	(130,154)
	Fluorescence imaging (live imaging)	(16)
	SEC	(10,14,130,135)
	Turbidity	(14)
	Visual Particles	(14)
Chemical	CE-MS	(156)
	cIEF	(138)
	IEX chromatography	(10,17,135)
	LC-MS/MS /	(10,17)
	SPR	(10,107,135)

with a mean diameter of 2 µm and 4 µm occurred. Based on follow-up experiments, the authors hypothesized that certain plasma proteins (pI 5.5–6.7) lose their solubility and triggered co-precipitation of bevacizumab (formulated at pH 6.2) and trastuzumab (pH 6.0) along with abundant plasma proteins (e.g. apolipoprotein) (108). Ultimately, aggregate formation occurs only after diluting a mAb with dextrose and plasma but not when using sodium chloride (107,108), as prescribed in the product leaflets. It is noteworthy that incubation of therapeutic proteins with dextrose (glucose) is expected to lead to potential chemical modifications (Maillard products, glycation) as a function of time and temperature (129), making dextrose solutions often not a preferred diluent for therapeutic proteins.

In conclusion, monitoring *in vivo* post-administration modifications is of high importance, and further studies are necessary to assess the impact of such *in vivo* degradation pathways on protein stability.

IN VITRO/EX VIVO MODELS

Predictability of *In Vitro* Incubation Studies

Studying *in vivo* stability of therapeutic protein lead candidates in human body fluids is not yet routinely done during preclinical development of a DP. Moreover, testing the stability and *in vivo* behavior of multiple clinical candidates in humans and animals is not feasible. Therefore, *in vitro* incubation studies involving incubation of the drug in the intended body fluid (or a possible surrogate) have emerged, trying to mimic and simulate *in vivo* conditions. Human and animal plasma/serum (7,19,107,130), SC tissue/ISF (131–133), lymph (134), and VH (14,135–137) were the most commonly used fluids/compartments. Two studies investigated various modifications of mAbs *in vitro* (phosphate-buffered saline (PBS) and animal serum) and compared the results to those obtained in animal models (rat and mice) (10,138). Yin *et al.* suggested that PBS under-estimated and rat plasma over-estimated protein degradation in comparison to actual *in vivo* conditions in the rat. Contrary, Schmid *et al.* concluded the results obtained in PBS are in agreement with those obtained *in vivo* and thus PBS can be used as surrogate medium to assess the *in vivo* stability of therapeutic proteins. Differences in the reliability of *in vitro* incubation studies may be explained by the chemical nature of the reactions. For instance, deamidation rates of mAbs were successfully predicted by incubation in PBS, indicating and confirming that temperature and pH are the determining factors promoting this reaction. Other *in vivo* degradation pathways (e.g. fragmentation) may be affected or driven by additional components of biological

fluids such as enzymes and thus require exposure to complex fluids such as serum. In summary, *in vitro* studies of therapeutic proteins in a body fluid or body fluid surrogate appear to be valuable tools to aid molecule selections, although findings may not accurately predict the *in vivo* situation in patients.

Limitations of Static *In Vitro* Incubation Studies

Human body fluids themselves show degradation over time. The *in vitro* degradation processes of human body fluids include cell lysis in whole blood (94), alkaline pH shifts when using VH (139) or serum (10), and precipitation of endogenous plasma proteins (138). The stability of body fluids is improved by the addition of sodium azide to prevent bacterial growth (10,101,140), removal of degradants (14), and incubation in a controlled carbon dioxide atmosphere to maintain the physiologic pH (132).

Currently, the majority of *in vitro* studies lack accurate simulation of the complex *in vivo* fluid dynamics (14,135). Arvinte *et al.* reported that during IA or IV administration, the drug solution may form a stream within the blood vessel due to incomplete mixing with blood locally (3,107). This may facilitate aggregation *in vivo*. Roethlisberger *et al.* shed light on the complexity of *in vivo* fluid dynamics and emphasized the rapid dilution of an injected/infused drug solution due the high peripheral blood flow (117). In this context, degradation observed under static *in vitro* conditions (107,108) may not occur *in vivo* or could potentially exist only transiently due to the dynamic environment.

In summary, current discrepancies between *in vitro* studies and the complex homeostatic conditions encountered *in vivo* represent clear limitations in the application of static *in vitro* incubation studies to predict *in vivo* stability of therapeutic proteins. Innovative and more sophisticated *in vitro/ex vivo* models need to be developed and qualified by correlating *in vitro-in vivo* results.

Innovative *In Vitro/Ex Vivo* Model Developments

The limitations of *in vitro* incubation studies of therapeutic proteins led to the development of advanced models (Table V). These advanced models feature a more innovative setup to enable longer incubation periods under defined conditions. Models may include a dialysis membrane and monitoring of parameters such as temperature, pH, pressure, and flow rate. For example, a commercially available model comprises a cartridge filled with hyaluronan and PBS. A surrounding chamber containing electrolytes and a bicarbonate buffer system simulates the physiologic conditions present in the SC tissue. This model aims to mimic the diffusion of a SC injected therapeutic protein from the injection site into blood capillaries and/or lymph capillaries (132). Thus far, promising correlations to human bioavailability data of some mAbs were reported indicative of instability under physiologic conditions (133). Nevertheless, the composition of the SC tissue is more complex containing additional ECM components (e.g. collagen) and blood components (e.g. proteases) which may lead to *in vivo* degradation. Therefore, additional studies of more complex models are required to investigate the *in vivo* stability of therapeutic proteins.

Table VI summarizes key parameters that should be considered in the development of an *in vitro* study/model. In particular, the concentration of the therapeutic protein and its duration of exposure to the biological fluid should be relevant from a PK perspective. Furthermore, the absence of stabilizing excipients *in vivo* should be mimicked *in vitro* by e.g. separating excipients from the therapeutic protein using dialysis. Of note, after SC injection, it has been hypothesized that the concentration of excipients may increase due to removal of excess water from the injection site (8). Therefore, each route of administration and intended body compartment features unique challenges when assessing *in vivo* stability. For instance, volumetric differences between the human vasculature (~4.5 l of blood) and other body compartments require careful extrapolation towards buffering capacity and bioavailability of the DS/excipients.

In Vivo Studies

The physiology and composition of body fluids/compartments in animals differs from those encountered in humans. This is particularly important when selecting relevant animal models and species for specific studies during preclinical development.

In recent years, several animal models were employed in pharmacology and toxicology studies to extrapolate *in vivo* performance and potential safety liabilities to humans. Rodents emerged as the most used model, but they often lack cross reactivity of the target molecules and thus do not accurately simulate the human *in vivo* environment. Theoretically, non-human primates (possibly transgenic) are the most physiologically relevant models to evaluate *in vivo* performance, safety liabilities, and possibly *in vivo* stability of therapeutic proteins (9). However, several studies compared the *in vivo* performance of therapeutic proteins in animals as well as humans and observed significant discrepancies (e.g. bioavailability) (133). One factor contributing to such poor correlations has been linked to the variable SC tissue structure among species. For example, the SC tissue of rodents or cynomolgus monkeys differs markedly from that of humans. This led to the selection of alternative species such as Göttingen minipigs, whose SC tissue may be more representative of that in humans (149).

In vivo performance of a therapeutic protein is a complex interplay of protein bioavailability, chemical/physical

degradation, as well as elimination. Goetze *et al.* reviewed clinical studies and concluded that *in vivo* degradation of a therapeutic protein strongly depends on the mAb conversion and elimination rate (6).

Only a few studies evaluated the biological consequences of physical and chemical degradation of therapeutic proteins *in vivo*. For example, Wang *et al.* assessed the effect of oxidation on serum half-life. Therefore, oxidatively stressed mAbs were injected into human FcRn mice (119). In this study, only highly oxidized mAbs significantly reduced serum half-life. Physical stability of fluorescent-labeled mAbs was recently characterized using live imaging in mice (16). Kinderman *et al.* observed that increased retention at the injection site occurred due to *in vivo* precipitation.

Lastly, the residence time of a therapeutic protein within the SC tissue has been studied by characterizing the behavior after SC administration. For instance, insulin shows non-isotropic spreading as the depot is restricted in vertical direction due to the thickness of the SC tissue (151). Insulin did not spread into the dermis but in regions of lower density, that is the muscle or inhomogenic regions within the adipose tissue. An innovative sampling method by open flow microperfusion allowed continuous sampling in humans and revealed accumulation of secukinumab (Cosentyx®) into the dermal ISF after SC injection (152).

A particular challenge of clinical trials is that systematic evaluation of different therapeutic protein degradations in humans and the impact on patient safety is unethical and not possible. In addition, clinical trials are typically vastly underpowered and only provide limited clarity on degradation induced side effects.

ANALYTICAL CHALLENGES

Characterizing the stability of a therapeutic protein in human body fluids remains challenging due to several reasons. Human body fluids present a highly complex matrix. For instance, the endogenous protein concentration in plasma/serum ranges from 55 to 80 mg/mL (21).

A specific challenge for therapeutic IgG *in vivo* stability studies in human body fluids is the separation and discrimination of therapeutic and endogenous IgGs. For example, detection limitations due to plasma protein interferences were observed when using capSEC and CE-SDS (138). Thus, studies of therapeutic proteins in body fluids require adequate purification or labeling techniques (9). Anti-human Fc antibody or anti-idiotype antibody purification steps were used to discriminate animal or human IgGs (153). Fluorescence labeling (e.g. Alexa Fluor® 488) has been used successfully in several studies to detect macromolecules in complex biological matrices without altering the protein characteristics, e.g. maintaining potency and physicochemical properties (19,130,154). Table VII summarizes the analytical methods to assess therapeutic proteins in biological fluids.

In general, purification techniques are required to isolate the biotherapeutic protein of interest and sample preparation steps often include harsh conditions leading to analytical artifacts (6). In addition, co-purification of a therapeutic IgG with different endogenous IgG subclasses in biological fluids may lead to artifacts in LC-MS analysis (e.g. double oxidation). If applicable, orthogonal methods, adequate controls, a sufficient degree of drug recovery, and minimal exposure to modifying conditions during sample preparation should be employed.

CONCLUSION AND OUTLOOK

Several studies reported significant differences between the shelf-life stability and *in vivo* stability of therapeutic proteins. Although *in vivo* degradation may have a direct impact on the biological performance of therapeutic proteins, robust methods and models to characterize *in vivo* stability remain missing.

IV, SC, IVT, and IT administration are of particular interest to the pharmaceutical industry. Physical and chemical properties of human body compartments differ significantly from those of commonly used DP formulations. These body compartments/fluids feature differences in physiologic properties e.g. flow rate, temperature, macromolecules, metabolites, and endogenous degradation products, which may lead to different physical/chemical degradation profiles. Moreover, significant inter-subject variability of the composition of human body fluids due to factors such as age, gender, and pathophysiologic conditions should be considered with surrogate *in vitro* and *in vivo* studies. Therefore, different body compartments require the development of individual *in vitro* models, each with specific attributes and challenges. Certain attributes have been accurately simulated *in vitro* and may give insight into protein stability and fate of excipients in the human systemic circulation. Nevertheless, robust *in vitro* models do not exist to reliably predict *in vivo* stability of therapeutic proteins in humans.

Similarly, animal studies are required for *in vivo* studies of pharmacological and toxicological properties of therapeutic proteins, but these studies often cannot reliably predict *in vivo* protein stability in humans. The majority of animal studies aimed at predicting PK/PD profiles neglect characterization of physical and chemical degradation.

Overall, accurate assessments of the *in vivo* stability of a therapeutic protein under *in vitro* conditions are difficult to extrapolate. *In vitro* studies will, however, allow to select clinical candidates during development based on their stability in biological fluids. Future studies should aim at the development of innovative *in vitro* models to accurately simulate the *in vivo*

situation in humans. Systematic studies with therapeutic proteins featuring diverse attributes (e.g. pI, hydrophobicity, chemical degradation hot spots, etc.) are required to define critical molecular attributes of the *in vivo* stability of therapeutic proteins.

Acknowledgments and Disclosures. We are very thankful to Dr. Ashutosh Rao from the Laboratory of Applied Biochemistry of the FDA for his comments and valuable suggestions in the manuscript.

REFERENCES

1. Boll B, Bessa J, Folzer E, Rios Quiroz A, Schmidt R, Bulau P, et al. Extensive chemical modifications in the primary protein structure of IgG1 subvisible particles are necessary for breaking immune tolerance. Mol Pharm. 2017;14(4):1292–9.
2. Quality by Design for Biopharmaceuticals: Principles and Case Studies. Hoboken: John Wiley & Sons, Inc; 2009.
3. Arvinte T, Poirier E, Palais C. Prediction of aggregation in vivo by studies of therapeutic proteins in human plasma. In: Rosenberg AS, Demeule B, editors. Biobetters - protein engineering to approach the curative. New York: Springer; 2015. p. 91–104.
4. Jiskoot W, Randolph TW, Volkin DB, Middaugh CR, Schoneich C, Winter G, et al. Protein instability and immunogenicity: roadblocks to clinical application of injectable protein delivery systems for sustained release. J Pharm Sci. 2012;101(3):946–54.
5. Liu H, Ponniah G, Zhang HM, Nowak C, Neill A, Gonzalez-Lopez N, et al. In vitro and in vivo modifications of recombinant and human IgG antibodies. MAbs. 2014;6(5):1145–54.
6. Goetze AM, Schenauer MR, Flynn GC. Assessing monoclonal antibody product quality attribute criticality through clinical studies. MAbs. 2010;2(5):500–7.
7. Correia IR. Stability of IgG isotypes in serum. MAbs. 2010;2(3):221–32.
8. Kinnunen HM, Mrsny RJ. Improving the outcomes of biopharmaceutical delivery via the subcutaneous route by understanding the chemical, physical and physiological properties of the subcutaneous injection site. J Control Release. 2014;182:22–32.
9. Hall MP. Biotransformation and in vivo stability of protein biotherapeutics: impact on candidate selection and pharmacokinetic profiling. Drug Metab Dispos. 2014;42(11):1873–80.
10. Schmid I, Bonnington L, Gerl M, Bomans K, Thaller AL, Wagner K, Schlothauer T, Falkenstein R, Zimmermann B, Kopitz J, Hasmann M, Bauss F, Haberger M, Reusch D, Bulau P. Assessment of susceptible chemical modification sites of trastuzumab and endogenous human immunoglobulins at physiological conditions. Nat Commun Biol. 2018.
11. Ouellette D, Alessandri L, Chin A, Grinnell C, Tarcsa E, Radziejewski C, et al. Studies in serum support rapid formation of disulfide bond between unpaired cysteine residues in the VH domain of an immunoglobulin G1 molecule. Anal Biochem. 2010;397(1):37–47.
12. Gu S, Wen D, Weinreb PH, Sun Y, Zhang L, Foley SF, et al. Characterization of trisulfide modification in antibodies. Anal Biochem. 2010;400(1):89–98.
13. Moritz B, Stracke JO. Assessment of disulfide and hinge modifications in monoclonal antibodies. Electrophoresis. 2017;38(6):769–85.
14. Patel S, Muller G, Stracke JO, Altenburger U, Mahler HC, Jere D. Evaluation of protein drug stability with vitreous humor in a novel ex-vivo intraocular model. Eur J Pharm Biopharm. 2015;95(Pt B):407–17.
15. Lobo B, Lo S, Wang YJ, Wong RL. Method and formulation for reducing aggregation of a macromolecule under physiological conditions. In: Genentech I, editor.: Google Patents. 2014.
16. Kinderman F, Yerby B, Jawa V, Joubert MK, Joh NH, Malella J, Herskovitz J, Xie J, Ferbas J, McBride HJ. Impact of precipitation of antibody therapeutics following subcutaneous injection on pharmacokinetics and immunogenicity. J Pharm Sci. 2019.
17. Huang L, Lu J, Wroblewski VJ, Beals JM, Riggin RM. In vivo deamidation characterization of monoclonal antibody by LC/MS/MS. Anal Chem. 2005;77(5):1432–9.
18. Goetze AM, Liu YD, Arroll T, Chu L, Flynn GC. Rates and impact of human antibody glycation in vivo. Glycobiology. 2012;22(2):221–34.
19. Demeule B, Shire SJ, Liu J. A therapeutic antibody and its antigen form different complexes in serum than in phosphate-buffered saline: a study by analytical ultracentrifugation. Anal Biochem. 2009;388(2):279–87.
20. Hamuro L, Kijanka G, Kinderman F, Kropshofer H, Bu DX, Zepeda M, et al. Perspectives on subcutaneous route of administration as an immunogenicity risk factor for therapeutic proteins. J Pharm Sci. 2017;106(10):2946–54.
21. Kratz A, Ferraro M, Sluss PM, Lewandrowski KB. Case records of the Massachusetts General Hospital. Weekly clinicopathological exercises. Laboratory reference values. N Engl J Med. 2004;351(15):1548–63.
22. Bishop PN. Biochemistry. In: Sebag J, editor. Vitreous in health and disease. New York: Springer; 2014. p. 3–92.
23. Haaverstad R, Romslo I, Larsen S, Myhre HO. Protein concentration of subcutaneous interstitial fluid in the human leg. A comparison between the wick technique and the blister suction technique. Int J Microcirc Clin Exp. 1996;16(3):111–7.
24. Bloomfield IG, Johnston IH, Bilston LE. Effects of proteins, blood cells and glucose on the viscosity of cerebrospinal fluid. Pediatr Neurosurg. 1998;28(5):246–51.
25. Di Terlizzi R, Platt S. The function, composition and analysis of cerebrospinal fluid in companion animals: part I - function and composition. Vet J. 2006;172(3):422–31.
26. Poulsen HL. Interstitial fluid concentrations of albumin and immunoglobulin G in normal men. Scand J Clin Lab Invest. 1974;34(2):119–22.
27. Clausen R, Weller M, Wiedemann P, Heimann K, Hilgers RD, Zilles K. An immunochemical quantitative analysis of the protein pattern in physiologic and pathologic vitreous. Graefes Arch Clin Exp Ophthalmol. 1991;229(2):186–90.
28. Schliep G, Rapic N, Felgenhauer K. Quantitation of high-molecular proteins in cerebrospinal fluid. Z Klin Chem Klin Biochem. 1974;12(8):367–9.
29. Werle M, Bernkop-Schnurch A. Strategies to improve plasma half life time of peptide and protein drugs. Amino Acids. 2006;30(4):351–67.
30. Pizzo SV, Lundblad RL, Willis MS. Proteolysis in the interstitial space. Boca Raton: Taylor & Francis Group; 2017.
31. Wiig H, Swartz MA. Interstitial fluid and lymph formation and transport: physiological regulation and roles in inflammation and cancer. Physiol Rev. 2012;92(3):1005–60.
32. Fung PCW, Kong RKC. The integrative five-fluid circulation system in the human body. Open J Mol Integ Physiol. 2016;6:45–97.
33. Vaughan-Thomas A, Gilbert SJ, Duance VC. Elevated levels of proteolytic enzymes in the aging human vitreous. Invest Ophthalmol Vis Sci. 2000;41(11):3299–304.

34. Narumi M, Nishitsuka K, Yamakawa M, Yamashita H. A survey of vitreous cell components performed using liquid-based cytology. Acta Ophthalmol. 2015;93(5):e386–90.
35. Castellazzi M, Ligi D, Contaldi E, Quartana D, Fonderico M, Borgatti L, et al. Multiplex matrix Metalloproteinases analysis in the cerebrospinal fluid reveals potential specific patterns in multiple sclerosis patients. Front Neurol. 2018;9:1080.
36. Guseo A. Classification of cells in the cerebrospinal fluid. A review. Eur Neurol. 1977;15(3):169–76.
37. Di Terlizzi R, Platt SR. The function, composition and analysis of cerebrospinal fluid in companion animals: part II - analysis. Vet J. 2009;180(1):15–32.
38. Guyton AC, Hall JE. Textbook of medical physiology. Philadelphia: Elsevier Inc.; 2006.
39. Zilg B. Postmortem analyses of vitreous fluid. In. Department of Oncology-Pathology. Stockholm: Karolinska Institutet; 2015. p. 50.
40. Chirila TV, Hong Y. The vitreous humor. In: Murphy W, Black J, Hastings G, editors. Handbook of biomaterial properties. New York: Springer; 2016. p. 125–34.
41. Kokavec J, Min SH, Tan MH, Gilhotra JS, Newland HS, Durkin SR, et al. Biochemical analysis of the living human vitreous. Clin Exp Ophthalmol. 2016;44(7):597–609.
42. Johanson CE, Duncan JA 3rd, Klinge PM, Brinker T, Stopa EG, Silverberg GD. Multiplicity of cerebrospinal fluid functions: new challenges in health and disease. Cerebrospinal Fluid Res. 2008;5:10.
43. Johanson CE. Choroid plexus–cerebrospinal fluid circulatory dynamics: impact on brain growth, metabolism, and repair. In: Conn MP, editor. Neuroscience in Medicine. Totowa: Humana Press; 2008. p. 173–200.
44. Sacks GS. The ABC's of Acid-Base balance. J Pediatr Pharmacol Ther. 2004;9(4):235–42.
45. Hagan RD, Soller BR, Shear M, Walz M, Landry M, Heard S. Comparison of Interstitial Fluid pH, PCO2, PO2 with Venous Blood Values During Repetitive Handgrip Exercise. In.52nd Annual American College of Sports Medicine; 1–4 Jun 2004. Nashville, TN; United States: NASA Johnson Space Center; Houston, TX, United States; 2006.
46. Williamson TH, Grewal J, Gupta B, Mokete B, Lim M, Fry CH. Measurement of PO2 during vitrectomy for central retinal vein occlusion, a pilot study. Graefes Arch Clin Exp Ophthalmol. 2009;247(8):1019–23.
47. Zaharchuk G, Martin AJ, Rosenthal G, Manley GT, Dillon WP. Measurement of cerebrospinal fluid oxygen partial pressure in humans using MRI. Magn Reson Med. 2005;54(1):113–21.
48. Sato Y, Tamai M. pO2, pCO2 and acid-base balance in the human vitreous sample. Nippon Ganka Gakkai Zasshi. 1992;96(10):1295–9.
49. Rodriguez-Boto G, Rivero-Garvia M, Gutierrez-Gonzalez R, Marquez-Rivas J. Basic concepts about brain pathophysiology and intracranial pressure monitoring. Neurologia. 2015;30(1):16–22.
50. Gabelt BT, Kaufman PL. Production and flow of aqueous humor. In: Levin LA, Nilsson SFE, Ver Hoeve J, Wu SM, Alm A, Kaufman PL, editors. Adler's physiology of the eye. Philadelphia: Elsevier; 2011. p. 274–307.
51. Turitto V, Slack SM. Blood and related fluids. In: Murphy W, Black J, Hastings G, editors. Handbook of biomaterial properties. New York: Springer; 2016. p. 115–24.
52. Gill KL, Gardner I, Li L, Jamei M. A bottom-up whole-body physiologically based pharmacokinetic model to mechanistically predict tissue distribution and the rate of subcutaneous absorption of therapeutic proteins. AAPS J. 2016;18(1):156–70.
53. Body fluids. In: McMurry J, Castellion M, Ballantine DS, Hoeger CA, Peterson VE, editors. Fundamentals of General, Organic, and Biological Chemistry. New Jersey: Pearson; 2010. p. 878–901.
54. Cardiovascular Physiology. In: Widmaier EP, Raff H, Strang KT, editors. Vander's Human Physiology - The Mechanisms of Body Function. New York: McGraw-Hill; 2008. p. 359–441.
55. Le Goff MM, Bishop PN. Adult vitreous structure and postnatal changes. Eye (Lond). 2008;22(10):1214–22.
56. Lowe G. Blood rheology in vitro and in vivo. Baillière's Clin Haematol. 1987;1(3):597–636.
57. Zurovsky Y, Mitchell G, Hattingh J. Composition and viscosity of interstitial fluid of rabbits. Exp Physiol. 1995;80(2):203–7.
58. Bouta EM, Wood RW, Brown EB, Rahimi H, Ritchlin CT, Schwarz EM. In vivo quantification of lymph viscosity and pressure in lymphatic vessels and draining lymph nodes of arthritic joints in mice. J Physiol. 2014;592(6):1213–23.
59. Silva AF, Alves MA, Oliveira MSN. Rheological behaviour of vitreous humour. Rheol Acta. 2017;56(4):377–86.
60. Lee B, Litt M, Buchsbaum G. Rheology of the vitreous body. Part I: viscoelasticity of human vitreous. Biorheology. 1992;29(5–6):521–33.
61. Stefansson E. Physiology of vitreous surgery. Graefes Arch Clin Exp Ophthalmol. 2009;247(2):147–63.
62. Barton JK. Dynamic changes in optical properties. In: Welch AJ, van Gemert MJC, editors. Optical-thermal response of laser-irradiated tissue. Dordrecht: Springer; 2011. p. 321–49.
63. Sambrook MA. The relationship between cerebrospinal fluid and plasma electrolytes in patients with meningitis. J Neurol Sci. 1974;23(2):265–73.
64. Wike-Hooley JL, Van der Zee J, van Rhoon GC, Van den Berg AP, Reinhold HS. Human tumour pH changes following hyperthermia and radiation therapy. Eur J Cancer Clin Oncol. 1984;20(5):619–23.
65. Sobolewska B, Heiduschka P, Bartz-Schmidt KU, Ziemssen F. pH of anti-VEGF agents in the human vitreous: low impact of very different formulations. Int J Retina Vitreous. 2017;3:22.
66. Siesjö B. The regulation of cerebrospinal fluid pH. Kidney Int. 1972;1:360–74.
67. Webb P. Temperatures of skin, subcutaneous tissue, muscle and core in resting men in cold, comfortable and hot conditions. Eur J Appl Physiol Occup Physiol. 1992;64(5):471–6.
68. Salcedo-Villanueva G, Kon-Jara V, Harasawa M, Cervantes-Coste G, Ochoa-Contreras D, Morales-Canton V, et al. Vitreous humor thermodynamics during phacoemulsification. Int Ophthalmol. 2015;35(4):557–64.
69. Sumida K, Sato N, Ota M, Sakai K, Nippashi Y, Sone D, et al. Intraventricular cerebrospinal fluid temperature analysis using MR diffusion-weighted imaging thermometry in Parkinson's disease patients, multiple system atrophy patients, and healthy subjects. Brain Behav. 2015;5(6):e00340.
70. Stranz M, Kastango ES. A review of pH and Osmolarity. Int J Pharm Compd. 2002;6(3):216–20.
71. Baxter LT, Zhu H, Mackensen DG, Butler WF, Jain RK. Biodistribution of monoclonal antibodies: scale-up from mouse to human using a physiologically based pharmacokinetic model. Cancer Res. 1995;55(20):4611–22.
72. Goel M, Picciani RG, Lee RK, Bhattacharya SK. Aqueous humor dynamics: a review. Open Ophthalmol J. 2010;4:52–9.
73. Park J, Bungay PM, Lutz RJ, Augsburger JJ, Millard RW, Sinha Roy A, et al. Evaluation of coupled convective-diffusive transport of drugs administered by intravitreal injection and controlled release implant. J Control Release. 2005;105(3):279–95.
74. Brinker T, Stopa E, Morrison J, Klinge P. A new look at cerebrospinal fluid circulation. Fluids Barriers CNS. 2014;11:10.
75. Fogh-Andersen N, Altura BM, Altura BT, Siggaard-Andersen O. Composition of interstitial fluid. Clin Chem. 1995;41(10):1522–5.

76. Green H, Leopold IH, Sawyer JL. Elaboration of bicarbonate ion in intraocular fluids. II. Vitreous humor, normal values. AMA Arch Ophthalmol. 1957;57(1):85–9.
77. Naumann HN. Postmortem chemistry of the vitreous body in man. Arch Ophthalmol. 1959;62:356–63.
78. Schaupp L, Ellmerer M, Brunner GA, Wutte A, Sendlhofer G, Trajanoski Z, et al. Direct access to interstitial fluid in adipose tissue in humans by use of open-flow microperfusion. Am J Phys. 1999;276(2):E401–8.
79. Fraser JR, Laurent TC, Laurent UB. Hyaluronan: its nature, distribution, functions and turnover. J Intern Med. 1997;242(1): 27–33.
80. Laurent UB, Laurent TC, Hellsing LK, Persson L, Hartman M, Lilja K. Hyaluronan in human cerebrospinal fluid. Acta Neurol Scand. 1996;94(3):194–206.
81. Bishop PN. Structural macromolecules and supramolecular organisation of the vitreous gel. Prog Retin Eye Res. 2000;19(3):323–44.
82. Sebag J. Ageing of the vitreous. Eye (Lond). 1987;1(Pt 2):254–62.
83. Gilanyi M, Ikrenyi C, Fekete J, Ikrenyi K, Kovach AG. Ion concentrations in subcutaneous interstitial fluid: measured versus expected values. Am J Phys. 1988;255(3 Pt 2):F513–9.
84. Haljamae H. Anatomy of the interstitial tissue. Lymphology. 1978;11(4):128–32.
85. Brace RA, Guyton AC. Interstitial fluid pressure: capsule, free fluid, gel fluid, and gel absorption pressure in subcutaneous tissue. Microvasc Res. 1979;18(2):217–28.
86. Ellison G, Straumfjord JVJ, Hummel JP. Buffer capacities of human blood and plasma. Clin Chem. 1958;4(6):452–61.
87. Aretz S, Krohne TU, Kammerer K, Warnken U, Hotz-Wagenblatt A, Bergmann M, et al. In-depth mass spectrometric mapping of the human vitreous proteome. Proteome Sci. 2013;11(1):22.
88. Manning MC, Chou DK, Murphy BM, Payne RW, Katayama DS. Stability of protein pharmaceuticals: an update. Pharm Res. 2010;27(4):544–75.
89. Zimmerman SB, Minton AP. Macromolecular crowding: biochemical, biophysical, and physiological consequences. Annu Rev Biophys Biomol Struct. 1993;22:27–65.
90. Reddy ST, Berk DA, Jain RK, Swartz MA. A sensitive in vivo model for quantifying interstitial convective transport of injected macromolecules and nanoparticles. J Appl Physiol (1985). 2006;101(4):1162–9.
91. Ross PL, Wolfe JL. Physical and chemical stability of antibody drug conjugates: current status. J Pharm Sci. 2016;105(2):391–7.
92. Liu YD, Chen X, Enk JZ, Plant M, Dillon TM, Flynn GC. Human IgG2 antibody disulfide rearrangement in vivo. J Biol Chem. 2008;283(43):29266–72.
93. Wypych J, Li M, Guo A, Zhang Z, Martinez T, Allen MJ, et al. Human IgG2 antibodies display disulfide-mediated structural isoforms. J Biol Chem. 2008;283(23):16194–205.
94. Dillon TM, Ricci MS, Vezina C, Flynn GC, Liu YD, Rehder DS, et al. Structural and functional characterization of disulfide isoforms of the human IgG2 subclass. J Biol Chem. 2008;283(23): 16206–15.
95. Labrijn AF, Buijsse AO, van den Bremer ET, Verwilligen AY, Bleeker WK, Thorpe SJ, et al. Therapeutic IgG4 antibodies engage in fab-arm exchange with endogenous human IgG4 in vivo. Nat Biotechnol. 2009;27(8):767–71.
96. Zhang Q, Schenauer MR, McCarter JD, Flynn GC. IgG1 thioether bond formation in vivo. J Biol Chem. 2013;288(23): 16371–82.
97. Vlasak J, Ionescu R. Fragmentation of monoclonal antibodies. MAbs. 2011;3(3):253–63.
98. Linthwaite VL, Janus JM, Brown AP, Wong-Pascua D, O'Donoghue AC, Porter A, et al. The identification of carbon dioxide mediated protein post-translational modifications. Nat Commun. 2018;9(1):3092.
99. Liu YD, van Enk JZ, Flynn GC. Human antibody fc deamidation in vivo. Biologicals. 2009;37(5):313–22.
100. Porter CJ, Edwards GA, Charman SA. Lymphatic transport of proteins after s.c. injection: implications of animal model selection. Adv Drug Deliv Rev. 2001;50(1–2):157–71.
101. Chen X, Liu YD, Flynn GC. The effect of fc glycan forms on human IgG2 antibody clearance in humans. Glycobiology. 2009;19(3):240–9.
102. Cai B, Pan H, Flynn GC. C-terminal lysine processing of human immunoglobulin G2 heavy chain in vivo. Biotechnol Bioeng. 2011;108(2):404–12.
103. Brorson K, Jia AY. Therapeutic monoclonal antibodies and consistent ends: terminal heterogeneity, detection, and impact on quality. Curr Opin Biotechnol. 2014;30:140–6.
104. Diemel RV, ter Hart HG, Derksen GJ, Koenderman AH, Aalberse RC. Characterization of immunoglobulin G fragments in liquid intravenous immunoglobulin products. Transfusion. 2005;45(10):1601–9.
105. Mathaes R, Koulov A, Joerg S, Mahler HC. Subcutaneous injection volume of biopharmaceuticals-pushing the boundaries. J Pharm Sci. 2016;105(8):2255–9.
106. Turner MR, Balu-Iyer SV. Challenges and opportunities for the subcutaneous delivery of therapeutic proteins. J Pharm Sci. 2018;107(5):1247–60.
107. Arvinte T, Palais C, Green-Trexler E, Gregory S, Mach H, Narasimhan C, et al. Aggregation of biopharmaceuticals in human plasma and human serum: implications for drug research and development. MAbs. 2013;5(3):491–500.
108. Luo S, Zhang B. Dextrose-mediated aggregation of therapeutic monoclonal antibodies in human plasma: implication of isoelectric precipitation of complement proteins. MAbs. 2015;7(6):1094–103.
109. Rao VA. Perspectives on engineering biobetter therapeutic proteins with greater stability in Infl ammatory environments. In: Rosenberg AS, Demeule B, editors. Biobetters - protein engineering to approach the curative. New York: Springer; 2015. p. 183–202.
110. Wegner N, Lundberg K, Kinloch A, Fisher B, Malmstrom V, Feldmann M, et al. Autoimmunity to specific citrullinated proteins gives the first clues to the etiology of rheumatoid arthritis. Immunol Rev. 2010;233(1):34–54.
111. Ruiz-Pena M, Oropesa-Nunez R, Pons T, Louro SR, Perez-Gramatges A. Physico-chemical studies of molecular interactions between non-ionic surfactants and bovine serum albumin. Colloids Surf B Biointerfaces. 2010;75(1):282–9.
112. Del Amo EM, Rimpela AK, Heikkinen E, Kari OK, Ramsay E, Lajunen T, et al. Pharmacokinetic aspects of retinal drug delivery. Prog Retin Eye Res. 2017;57:134–85.
113. van Zuylen L, Verweij J, Sparreboom A. Role of formulation vehicles in taxane pharmacology. Investig New Drugs. 2001;19(2):125–41.
114. van Tellingen O, Beijnen JH, Verweij J, Scherrenburg EJ, Nooijen WJ, Sparreboom A. Rapid esterase-sensitive breakdown of polysorbate 80 and its impact on the plasma pharmacokinetics of docetaxel and metabolites in mice. Clin Cancer Res. 1999;5(10):2918–24.
115. Mrsny RJ. Metabolic processes at injection sites affecting pharmacokinetics, pharmacodynamics, and metabolism of protein and peptide therapeutics. In: Mrsny RJ, Daugherty A, editors. Proteins and peptides: pharmacokinetic, Pharmacodynamic, and metabolic outcomes. Bosa Roca: CRC Press; 2009. p. 80–105.
116. Zottig X, Meddeb-Mouelhi F, Beauregard M. Development of a high-throughput liquid state assay for lipase activity using natural substrates and rhodamine B. Anal Biochem. 2016;496:25–9.

117. Roethlisberger D, Mahler HC, Altenburger U, Pappenberger A. If Euhydric and isotonic do not work, what are acceptable pH and osmolality for parenteral drug dosage forms? J Pharm Sci. 2017;106(2):446–56.
118. Robinson NE, Robinson AB. Molecular clocks. Proc Natl Acad Sci U S A. 2001;98(3):944–9.
119. Wang W, Vlasak J, Li Y, Pristatsky P, Fang Y, Pittman T, et al. Impact of methionine oxidation in human IgG1 fc on serum half-life of monoclonal antibodies. Mol Immunol. 2011;48(6–7):860–6.
120. Quan C, Alcala E, Petkovska I, Matthews D, Canova-Davis E, Taticek R, et al. A study in glycation of a therapeutic recombinant humanized monoclonal antibody: where it is, how it got there, and how it affects charge-based behavior. Anal Biochem. 2008;373(2):179–91.
121. Moorthy BS, Xie B, Moussa EM, Iyer LK, Chandrasekhar S, Panchal JP, et al. Effect of hydrolytic degradation on the in vivo properties of monoclonal antibodies. In: Rosenberg AS, Demeule B, editors. Biobetters - protein engineering to approach the curative. New York: Springer; 2015. p. 105–35.
122. Stadtman ER, Levine RL. Protein oxidation. Ann N Y Acad Sci. 2000;899:191–208.
123. United States Pharmacopeial Convention, United States Pharmacopeia. General chapter <790> Visible Particulates in Injections. 2014.
124. European Directorate for the Quality of Medicines & HealthCare (EDQM), European Pharmacopoeia (Ph. Eur.) 9.0, 2.9.19 Particulate contamination: sub-visible particles. 2016.
125. European Directorate for the Quality of Medicines & HealthCare (EDQM), European Pharmacopoeia (Ph. Eur.) 9.0, 2.9.20 Particulate contamination: visible particles. 2016.
126. Carpenter JF, Randolph TW, Jiskoot W, Crommelin DJ, Middaugh CR, Winter G, et al. Overlooking subvisible particles in therapeutic protein products: gaps that may compromise product quality. J Pharm Sci. 2009;98(4):1201–5.
127. Page M, Ling C, Dilger P, Bentley M, Forsey T, Longstaff C, et al. Fragmentation of therapeutic human immunoglobulin preparations. Vox Sang. 1995;69(3):183–94.
128. Goyon A, Excoffier M, Janin-Bussat MC, Bobaly B, Fekete S, Guillarme D, et al. Determination of isoelectric points and relative charge variants of 23 therapeutic monoclonal antibodies. J Chromatogr B Analyt Technol Biomed Life Sci. 2017;1065-1066:119–28.
129. Fischer S, Hoernschemeyer J, Mahler HC. Glycation during storage and administration of monoclonal antibody formulations. Eur J Pharm Biopharm. 2008;70(1):42–50.
130. Filipe V, Poole R, Oladunjoye O, Braeckmans K, Jiskoot W. Detection and characterization of subvisible aggregates of monoclonal IgG in serum. Pharm Res. 2012;29(8):2202–12.
131. Mach H, Gregory SM, Mackiewicz A, Mittal S, Lalloo A, Kirchmeier M, et al. Electrostatic interactions of monoclonal antibodies with subcutaneous tissue. Ther Deliv. 2011;2(6):727–36.
132. Kinnunen HM, Sharma V, Contreras-Rojas LR, Yu Y, Alleman C, Sreedhara A, et al. A novel in vitro method to model the fate of subcutaneously administered biopharmaceuticals and associated formulation components. J Control Release. 2015;214:94–102.
133. Bown HK, Bonn C, Yohe S, Yadav DB, Patapoff TW, Daugherty A, et al. In vitro model for predicting bioavailability of subcutaneously injected monoclonal antibodies. J Control Release. 2018;273:13–20.
134. Wang W, Chen N, Shen X, Cunningham P, Fauty S, Michel K, et al. Lymphatic transport and catabolism of therapeutic proteins after subcutaneous administration to rats and dogs. Drug Metab Dispos. 2012;40(5):952–62.
135. Patel S, Stracke JO, Altenburger U, Mahler HC, Metzger P, Shende P, et al. Prediction of intraocular antibody drug stability using ex-vivo ocular model. Eur J Pharm Biopharm. 2017;112:177–86.
136. Awwad S, Lockwood A, Brocchini S, Khaw PT. The PK-eye: a novel in vitro ocular flow model for use in preclinical drug development. J Pharm Sci. 2015;104(10):3330–42.
137. Awwad S, Day RM, Khaw PT, Brocchini S, Fadda HM. Sustained release ophthalmic dexamethasone: in vitro in vivo correlations derived from the PK-eye. Int J Pharm. 2017;522(1–2):119–27.
138. Yin S, Pastuskovas CV, Khawli LA, Stults JT. Characterization of therapeutic monoclonal antibodies reveals differences between in vitro and in vivo time-course studies. Pharm Res. 2013;30(1):167–78.
139. Lorget F, Parenteau A, Carrier M, Lambert D, Gueorguieva A, Schuetz C, et al. Characterization of the pH and temperature in the rabbit, pig, and monkey eye: key parameters for the development of long-acting delivery ocular strategies. Mol Pharm. 2016;13(9):2891–6.
140. Battersby JE, Mukku VR, Clark RG, Hancock WS. Affinity purification and microcharacterization of recombinant DNA-derived human growth hormone isolated from an in vivo model. Anal Chem. 1995;67(2):447–55.
141. Groell F, Kalia YN, Jordan O, Borchard G. Hydrogels in three-dimensional dendritic cell (MUTZ-3) culture as a scaffold to mimic human immuno competent subcutaneous tissue. Int J Pharm. 2018;544(1):297–303.
142. Mrsny RJ, Kinnunen HM. Methods and apparatus for the in vitro modelling of drug administration. In: Bath Uo, editor.; 2012.
143. Kuester K, Kloft C. Pharmacokinetics of monoclonal antibodies. In: Meibohm B, editor. Pharmacokinetics and pharmacodynamics of biotech drugs: principles and case studies in drug development. Weinheim: WILEY-VCH Verlag GmbH & Co. KGaA; 2006. p. 45–91.
144. Strohl W. Fusion proteins for half-life extension of biologics as a strategy to make biobetters. BioDrugs. 2015;29(4):215–39.
145. Zhao L, Ji P, Li Z, Roy P, Sahajwalla CG. The antibody drug absorption following subcutaneous or intramuscular administration and its mathematical description by coupling physiologically based absorption process with the conventional compartment pharmacokinetic model. J Clin Pharmacol. 2013;53(3):314–25.
146. Lin P, Menda S, de Juan E. Principles and practice of Intravitreal application of drugs. In: Sebag J, editor. Vitreous in health and disease. New York: Springer; 2014. p. 509–21.
147. Bousquet G, Darrouzain F, de Bazelaire C, Ternant D, Barranger E, Winterman S, et al. Intrathecal Trastuzumab halts progression of CNS metastases in breast Cancer. J Clin Oncol. 2016;34(16):e151–5.
148. Powell MF. Peptide stability in aqueous parenteral formulation. In: Cleland JL, Langer R, editors. Formulation and delivery of proteins and peptides. Washington DC: American Chemical Society; 1994. p. 100–17.
149. Zheng Y, Tesar DB, Benincosa L, Birnbock H, Boswell CA, Bumbaca D, et al. Minipig as a potential translatable model for monoclonal antibody pharmacokinetics after intravenous and subcutaneous administration. MAbs. 2012;4(2):243–55.
150. Mahler HC, Printz M, Kopf R, Schuller R, Muller R. Behaviour of polysorbate 20 during dialysis, concentration and filtration using membrane separation techniques. J Pharm Sci. 2008;97(2):764–74.
151. Thomsen M, Poulsen M, Bech M, Velroyen A, Herzen J, Beckmann F, et al. Visualization of subcutaneous insulin injections by x-ray computed tomography. Phys Med Biol. 2012;57(21):7191–203.
152. Dragatin C, Polus F, Bodenlenz M, Calonder C, Aigner B, Tiffner KI, et al. Secukinumab distributes into dermal interstitial fluid of

psoriasis patients as demonstrated by open flow microperfusion. Exp Dermatol. 2016;25(2):157–9.

153. Wei C, Su D, Wang J, Jian W, Zhang D. LC–MS challenges in characterizing and quantifying monoclonal antibodies (mAb) and antibody-drug conjugates (ADC) in biological samples. Curr Pharmacol Rep. 2018;4(1):45–63.
154. Filipe V, Poole R, Kutscher M, Forier K, Braeckmans K, Jiskoot W. Fluorescence single particle tracking for the characterization of submicron protein aggregates in biological fluids and complex formulations. Pharm Res. 2011;28(5):1112–20.
155. Leeman M, Choi J, Hansson S, Storm MU, Nilsson L. Proteins and antibodies in serum, plasma, and whole blood-size characterization using asymmetrical flow field-flow fractionation (AF4). Anal Bioanal Chem. 2018;410(20):4867–73.
156. Han M, Pearson JT, Wang Y, Winters D, Soto M, Rock DA, et al. Immunoaffinity capture coupled with capillary electrophoresis - mass spectrometry to study therapeutic protein stability in vivo. Anal Biochem. 2017;539:118–26.
157. Gullino PM, Grantham FH, Smith SH, Haggerty AC. Modifications of the acid-base status of the internal milieu of tumors. J Natl Cancer Inst. 1965;34(6):857–69.

Analytical Challenges Assessing Aggregation and Fragmentation of Therapeutic Proteins in Biological Fluids

The following chapter has been published as mini-review in the Journal of Pharmaceutical Sciences.

Joachim Schuster, Hanns-Christian Mahler, Susanne Joerg, Joerg Huwyler, and Roman Mathaes
Analytical Challenges Assessing Aggregation and Fragmentation of Therapeutic Proteins in Biological Fluids
J Pharm Sci. 2021, 110(9), 3103-3110
doi: 10.1016/j.xphs.2021.04.014

Journal of Pharmaceutical Sciences 110 (2021) 3103–3110

Contents lists available at ScienceDirect

Journal of Pharmaceutical Sciences

journal homepage: www.jpharmsci.org

Mini Review

Analytical Challenges Assessing Protein Aggregation and Fragmentation Under Physiologic Conditions

Joachim Schuster[a,b], Hanns-Christian Mahler[a], Susanne Joerg[a], Joerg Huwyler[b], Roman Mathaes[a,*]

[a] Lonza Pharma and Biotech, Drug Product Services, Basel, Switzerland
[b] University of Basel, Pharmacenter, Division of Pharmaceutical Technology, Basel, Switzerland

ARTICLE INFO

Article history:
Received 12 November 2020
Revised 1 March 2021
Accepted 9 April 2021
Available online 29 April 2021

Keywords:
Protein aggregation
Stability
In vitro model(s)
Monoclonal antibody(s)
Analytical biochemistry

ABSTRACT

Therapeutic proteins are administered by injection or infusion. After administration, the physiologic environment in the desired body compartment - fluid or tissue - can impact protein stability and lead to changes in the safety and/or efficacy profile. For example, protein aggregation and fragmentation are critical quality attributes of the drug product and can occur after administration to patients. In this context, the *in vivo* stability of therapeutic proteins has gained increasing attention. However, *in vivo* protein aggregation and fragmentation are difficult to assess and have been rarely investigated. This mini-review summarizes analytical approaches to assess the stability of therapeutic proteins using simulated physiologic conditions. Furthermore, we discuss factors potentially causing *in vivo* protein aggregation, precipitation, and fragmentation in complex biological fluids. Different analytical approaches are evaluated with respect to their applicability and possible shortcomings when it comes to these degradation events in biological fluids. Tracking protein stability in biological fluids typically requires purifying or labeling the protein of interest to circumvent matrix interference of biological fluids. Improved analytical methods are strongly needed to gain knowledge on *in vivo* protein aggregation and fragmentation. *In vitro* models can support the selection of lead candidates and accelerate the pre-clinical development of therapeutic proteins.

Introduction

Stability of therapeutic proteins is a complex interplay between chemical and physical degradation, which may compromise the quality of a drug product (DP). Modifications on specific protein attributes have a direct impact on treatment efficacy and/or patient safety. They are therefore considered as critical quality attributes. Examples of such modifications include subvisible particle (SbVP) formation (physical degradation) and protein fragmentation (chemical degradation).

Proteins can undergo degradation during different stages such as manufacturing, storage and shipment,[1] preparation for clinical use (in-use stability),[2] and even after administration (post-administration changes; *in vivo* stability).[3] The latter phenomenon is of special interest since previous studies demonstrated that protein modifications can occur at substantially faster rates in patients than under real-time storage conditions. .[3,7-] Liu et al. pointed out that most modifications occur on endogenous and therapeutic proteins *in vivo* and likely pose a lower safety risk than modifications occurring solely on therapeutic proteins.[8,9] However, naturally occurring modifications such as deamidation have been reported to cause loss of potency during circulation[8,10,11]

Assessing the *in vivo* stability of therapeutic proteins is difficult and typically limited to animal or in rare cases clinical studies.[12] Besides ethical concerns, animals models show poor correlation to clinical results for therapeutic proteins. *In vitro* models are an attractive alternative by simulating physiologic conditions.[13] Such studies typically use an adequately diluted biotherapeutic of interest in isolated fluids from animal/human subjects or a representative surrogate solution to evaluate the criticality of quality attributes in regards to patient exposure.[3,5,12,14-17] *In vitro* studies are based on the notion that evaluating *in vivo* protein stability prior to the selection of clinical lead candidates can mitigate risks during product development.[3] We showed in a recent *in vitro* study that the stability among different monoclonal antibodies (mAbs) varied profoundly in human serum, highlighting the importance of assessing their stability in

Abbreviations: AF4, asymmetrical flow field-flow fractionation; AUC, analytical ultracentrifugation; CE-SDS, capillary electrophoresis-sodium dodecyl sulfate; DP, drug product; IgG, immunoglobulin G; mAbs, monoclonal antibodies; MS, mass spectrometry; PBS, phosphate-buffered saline; SbVP, subvisible particle; SDS-PAGE, sodium dodecyl sulfate-polyacrylamide gel electrophoresis; SEC, Size-exclusion chromatography.

* *Correspondence to:* Roman Mathaes.
E-mail address: roman.mathaes@lonza.com (R. Mathaes).

https://doi.org/10.1016/j.xphs.2021.04.014
0022-3549/

biological fluids.[18] Modelling the human physiology *in vitro* is difficult and *in vitro* models may lack important aspects such as flow rate, concentration changes due to drug elimination, and age-related changes of a biological fluid (e.g., vitreous humor).[3] Despite these shortcomings, previous studies reported a high correlation between an intravenous[12] and subcutaneous[19] human-based *in vitro* models to results obtained in patients.

Monitoring protein stability in biological fluids is; however, substantially more challenging than in the DP formulation due to matrix interference.[14] To date, the majority of studies investigating *in vivo* protein stability focus on chemical modifications such as deamidation, isomerization, glycation, and oxidation.

Contrary to studies investigating these modifications, studies on *in vivo* protein aggregation and fragmentation are scarce, presumably due to analytical challenges. However, both degradation pathways are critical quality attributes and can occur *in vivo*.[3,7,20-22] This mini-review discusses knowledge on physiologic stress factors potentially affecting stability in regards to protein aggregation and fragmentation. Furthermore, we discuss different analytical approaches that were employed to monitor these degradation events in biological fluids.

Table 1
Conditions Encountered by Therapeutic Proteins During Storage and *In Vivo*. Summary of important conditions encountered during storage and after administration (e.g., intravenous injection/infusion), which may impact chemical and physical protein stability. *In vivo* conditions differ depending on the desired route of administration and subsequent exposure to specific body fluids or tissues. .[3]

Conditions	Storage(e.g., mAbs)	*In Vivo*(e.g., blood)[3]
Temperature (°C)	2–8 °C	36.0–37.5
pH	typically: 5.5–6.5	7.35–7.45
Buffer system	E.g., histidine buffer	Bicarbonate buffer
Osmolality (mOsmol/kg)	≥240	285–295
Matrix	▫ Excipients (e.g., polysorbate, sucrose) ▫ Container-closure system ▫ Administration device	▫ Lipids ▫ Proteins ▫ Sugars ▫ Cells ▫ Electrolytes ▫ Thiols ▫ Enzymes
Duration	Shelf-life stability: ≥3 years	Half-life of mAbs: 6–32 days[48]
Interfacial stress	Static and agitational stress during DP development	Dynamic venous blood flow

In Vivo *Aggregation and Precipitation of Therapeutic Proteins*

A therapeutic protein may aggregate after administration to patients.[3,23] Moreover, aggregates present in the DP may revert back to monomers after administration, or, they may persist and continue to circulate *in vivo*.[23] Pre-systemic degradation at the subcutaneous injection site and during lymphatic uptake has been attributed as potential cause for bioavailability losses ranging from 20 to 50% for mAbs.[22] Previous studies have shown that a therapeutic protein can aggregate/precipitate under physiologic conditions[7,20,21] which may cause an immune response.[24]

During administration, the therapeutic protein is subjected to rapid changes in conditions encountered in humans versus those of the DP formulation (Table 1). Particularly, changes in pH, composition, osmolality, and temperature (typically, DP storage at 2 to 8 °C versus 37 °C body temperature) may be key factors contributing to protein aggregation.[25]

Additionally, thousands of different macromolecules present in human body fluids may alter the properties of administered proteins and impact their stability by e.g., heteroaggregation or other interactions such as enzymatic modification or cleavage. Protein-protein interactions between the therapeutic protein and endogenous proteins may cause aggregation/precipitation.[26] In addition, the complexity of intravenous fluid dynamics has been proposed to cause aggregation at the interface of blood and the infused DP.[27] Pathologic conditions such as a pro-inflammatory environment found in some patients may accelerate aggregation, precipitation, and oxidation.[24,28] Methionine (Met) oxidation has been reported to increase the rate of aggregation and lower the thermal stability of mAbs.[29] Yang et al. analyzed clinical samples and showed that Met-oxidation increases *in vivo* over time.[12] For example, oxidation of Met40 increased from 1.9 to 6.2% after 40 days of circulation. Interestingly, a similar oxidation rate was measured *in vitro* in human serum but not when using an *in vitro* phosphate-buffered saline (PBS) model. Lastly, reduced disulfide bonds of circulating immunoglobulin Gs (IgGs) may trigger protein aggregation *in vivo*.[30]

In Vivo *Fragmentation of Therapeutic Proteins*

Protein fragmentation occurs through hydrolysis (enzymatic or non-enzymatic) or β-elimination.[31,32] Particularly prone to hydrolysis are protein regions with higher flexibility such as hinge region and local protein structures.[30,33,34] Hydrolysis may also occur at the C_H2-C_H3 domain interface of mAbs[35] and specific amino acids such as Asp-or Trp.[36] Protein fragmentation is generally caused by a complex interplay of solvent, solvent conditions (e.g., pH, temperature), and the protein sequence.[31] Under physiologic conditions (37 °C; pH 7.4), fragmentation may accelerate as the *in vivo* environment has been regarded as unfavorable.[31]

While the protein backbone is regarded as stable *in vivo*,[30,31] a protein may become susceptible to fragmentation, depending on factors such as protein sequence motifs and flexibility within specific sides. Vlasak *et al.* summarized residues (e.g., Xaa: Gly-and Xaa: Ser, Val, Leu, or Pro), which were involved in fragmentation under simulated physiologic conditions.[31] Numerous enzymes in the human body[37] may cause hydrolysis of Ser, Thr, Cys, Asp, and Glu.[38] Diemel et al. showed that human blood-derived proteases cleave intravenous IgG products under *in vitro* conditions.[39] Human blood and tissues provide a redox system, which has been shown to affect a protein's secondary and tertiary structure. Previous reported modifications include disulfide shuffling,[40-42] fragment antigen-binding exchange,[43] trisulfide bond formation,[44] and thioether formation.[45] Contrary, the redox system can also act as a repair mechanism by reforming disulfide bonds[46] and reversing trisulfide to disulfide bonds.[30,44] Open disulfide bonds can decrease the structural stability of a protein and as such may be more prone to fragmentation *in vivo*.[30] *In vivo* protein fragmentation may lower bioavailability,[22] decrease efficacy,[47] or cause protein aggregation.[31]

Analytical Approaches and Challenges

Biological fluids are highly complex and contain numerous endogenous proteins with concentrations often considerably exceeding those of administered therapeutic proteins (e.g., endogenous vs. therapeutic IgG). Depending on the route of administration, the composition of the associated biological fluid is unique.[3] For example, blood (after intravenous administration) contains a total protein concentration of 55 to 80 mg/mL,[49] whereas cerebrospinal fluid (after intrathecal administration) contains 0.15 to 0.45 mg/mL protein.[50] Cerebrospinal fluid is an actively secreted fluid and markedly differs in its composition from blood.[3] Differences in protein concentration in the biological fluid may have implications for the choice of analytics. For example, substantially lower matrix interference is expected in cerebrospinal fluid which may enable to analyze the protein of

interest without prior sample manipulation. Thus each route of administration and associated body compartment requires careful consideration (e.g., SC tissue).[51,52]

Most characterization methods are unable to detect a specific protein of interest in a biological fluid without prior sample treatment. Typical analytical approaches to enable detection of a therapeutic protein include labeling (e.g., via covalent coupling of a fluorescent dye) or selective purification (e.g., via antigen-specific affinity) of the therapeutic protein. A third analytical approach to circumvent matrix interference is to alter the biological fluid itself (e.g., substituting with an artificial biological fluid/surrogate buffer). Table 2 summarizes advantages and disadvantages of these approaches.

Fluorescence labeling has been successfully used to track the stability of proteins in unaltered biological fluids such as human serum and appeared particularly beneficial for SbVP analysis.[14,18,53-56] While enabling detection of the protein of interest in biological fluids directly, the conjugated fluorophore can potentially impact the native protein. Different approaches have been implemented to successfully control and mitigate the potential risk on a protein's stability. For example, fluorophores with a fairly low molecular weight of ca. 600 Da and hydrophilic properties have been successfully used to assess the *in vivo* protein stability and appeared to have no impact the protein's stability.[14,18,53-56] The hydrophobic nature of some fluorophores[57] may pose a higher risk for protein aggregation. .[58] The degree of labeling[14,59] and charge of a fluorophore are additional aspects to consider.[60] Accelerated stability studies are often employed to ensure that the impact of labeling on stability, biophysical properties, and potency are negligible.[14,53,55]

Most purification techniques do not alter the native structure of a therapeutic protein. However, such procedures often require harsh conditions that can affect pH-sensitive proteins. Moreover, the removal of the protein of interest from the biological fluid and transfer to a new medium may cause dissociation of certain degradants. Modifications occurring in biological fluids can impair binding to the target, thus leaving stressed proteins undetectable.[16] Such examples include methionine (Met) oxidation impairing a protein's binding affinity to protein A/G,[61] Asn deamidation affecting binding affinity to its antigen,[10] or the formation of insoluble aggregates. Depending on the purification selectivity, endogenous proteins of a biological fluid may co-elute with the protein of interest and interfere with subsequent analysis.[62] Sample dilution may cause dissociation of protein aggregates formed in biological fluids.[63]

Reducing the complexity of biological fluids can be achieved by depleting abundant endogenous proteins[64] or by substituting biological fluids with e.g., PBS.[21] However, altering or replacing a biological fluid may compromise its relevance due to the removal of critical biological matrix components.[18] While analysis in PBS is uncomplicated, its composition deviates markedly from that found in human biological fluids in regards to proteins, electrolytes, buffering mechanism, and redox system. The absence of such factors may influence

Table 2
Analytical Approaches to Detect Modifications of Therapeutic Proteins in Biological Fluids. Advantages and disadvantages of selected analytical approaches are summarized.

Approaches	Advantages	Disadvantages
Labeling of the therapeutic protein by		
radionuclides[65]	• Direct analysis in biological fluid • High sensitivity • Radiolabeled protein is chemically identical to native protein	• Potential biohazard • Requires specialized equipment
fluorescence dyes[14,53,56] (e.g., near-infrared[65])	• Direct analysis in biological fluid • Instruments with fluorescence detection are readily available	• Altering the native biotherapeutic • Non-labeled proteins and fragments remain undetected
Purification of the therapeutic protein by		
Protein A/G[4,66]	• High sample throughput	• Low selectivity • Degradation (e.g., Met-oxidation) may impair binding[61] • Co-elution of endogenous proteins[62]
Biotinylation[16,55,67,68]	• High sample throughput • High selectivity	• Altering the native biotherapeutic • Non-biotinylated protein fragments remain undetected • Degradation may impair binding
Anti-human antibody[12,62,67]	• High selectivity	• Requires animal biological fluid • Degradation may impair binding
Target antigen[41,45]	• Highest selectivity	• Low sample throughput • Degradation (e.g., deamidation in CDR) may impair antigen binding[10]
Biological fluid		
Neat human biological fluid[14,53,56]	• Most representative	• Matrix interference • Limited stability of biological fluid *in vitro/ex vivo* • May not be readily accessible (e.g., human subcutaneous interstitial fluid)[69]
Depleting the fluid of abundant endogenous proteins[64]	• Highly representative	• Lower buffering capacity • Certain protein-protein interactions may not be detectable
Diluting biolfluid[21]	• Reduces protein concentration	• Lower buffering capacity • May impact stability of biological fluid • Co-dilution of protein (degradants) of interest
Animal body fluid[4,62]	• Some species have a lower endogenous protein concentration[4]	• Potential matrix interference • Different composition than human subjects
Artificial biological fluid/surrogate buffer[70]	• No matrix interference • Bicarbonate buffer mechanism • High fluid stability	• Limited physiologic-relevance (e.g., absence of proteins)
Alternative buffer with a buffering capacity at pH 7.4[4,12,62]	• No matrix interference • High fluid stability	• Physiologic-relevance limited (e.g., other buffering mechanism)

degradation events such as protein aggregation or fragmentation in a given fluid.

In summary, the selection of an appropriate analytical approach is typically a compromise between the physiologic-relevance of a fluid and analytical applicability to detect the protein of interest.

Analysis of Soluble and Insoluble Protein Aggregates in Biological Fluids

Subvisible particle (SbVP) analysis in biological fluids remains a challenge due to the plethora of matrix components covering a wide size range. For example, whole blood contains molecules covering a size range between 1 and 1000 nm (e.g., proteins, peptides, small molecules, lipids, exosomes),[71,72] 1−5 μm (apoptotic vesicles), and 2−20 μm (platelets and cells).[71,73] Although, the cell-free liquid fraction of blood, i.e., serum or plasma, is typically used as surrogate for whole blood,[74] recent studies showed that particles may still form under *in vitro* conditions, creating a high background of SbVPs.[14,18] Commonly used analytical methods to assess SbVPs in the DP, e.g., light obscuration and flow imaging, are generally unable to discriminate particles originating from a biological fluid from those of the protein of interest.[14,18]

Flow cytometry, enables distinct detection of fluorescent-particles and has been applied to analyze protein SbVPs in biological fluids.[18,53] Depending on the autofluorescence of biological fluid components,[75] fluorescence intensity thresholds need to be defined to separate particles of the biological fluids from pre-labeled protein particles.[18] However, due to an interaction between non-fluorescent and fluorescent-labeled particles,[26,53,56] the fluorescence brightness can be reduced considerably and thus may become undetectable.[54] Comparison of absolute particle counts and size is difficult as the particle size range of flow cytometry (e.g., 0.5 to 10 μm for protein particles)[76] depends on user-defined photomultiplier tube voltages. Moreover, as a non-imaging method, particle size is not directly measured but rather estimated by a calibration using standard beads, and hence it must be assumed that absolute quantification significantly differs from other methods. Beads may not be representative of protein particles due to differences in their refractive index. Likewise, light scattering detection of particles is affected by the refractive index of the core (sample) fluid and sheath fluid.[76] PBS, typically used as sheath fluid for flow cytometry, may also create light scattering artefacts as the refractive index of the sample and PBS sheet fluid may not match. Exchanging the sheath fluid is usually not possible due to specific laser-detector alignments. These limitations and the lack of historic data on particle counts compared to other methods (e.g., light obscuration) are reasons that flow cytometry remains a method for discriminative analysis comparing different molecules and make it less suitable for absolute particle counts and size.

Fluorescence microscopy is another method, which was employed to study SbVPs in serum.[14,18,21,53] Due to high-resolution images (down to ca. 200 nm) microscopy is particularly appealing to monitor changes in particle size and morphology. Filipe et al. detected a reduction of protein particle size after dilution with serum, which was not observed with flow cytometry, presumably due to detection limitations.[53] Fluorescence microscopy is less suitable as a quantitative method as typically only sections of a sample are imaged leading to a high extrapolation factor. Our group recently developed a method by scanning several thousand images to quantify particles in serum samples.[14] However, extrapolation limitations persisted allowing only for semi-quantitative analysis. Other drawbacks of fluorescence microscopy include low sample throughput, sedimentation of particles, and potential evaporation of fluids due to time-consuming analysis.

Soluble protein aggregates in the DP are typically quantified by size-exclusion chromatography (SEC). However, known shortcomings of SEC such as interaction of proteins and protein aggregates with the stationary phase may be particularly challenging with protein-rich biological fluids. SEC was used to evaluate protein stability in biological fluids directly via fluorescence detection[18] or after purification.[4,62] In three studies high-molecular weight species of mAbs increased in biological fluids over time; however, substantial difference in the rate of aggregation were observed.[4,18,62] These differences may be explained due to a protein's propensity to aggregate and different analytical approaches (i.e., labeling vs. purification).[4,18,62]

Fluorescence labeling enables distinct detection of mAbs in biological fluids such as serum. Nevertheless, adequate sample preparation and control samples are required to exclude unspecific binding of excessive fluorescence dye to endogenous proteins (e.g., albumin) and interference of autofluorescence of biological fluid components.[55,75] Moreover, due to biological fluids forming particles *in vitro* over time[3,14,18,26,42,62,77] an interaction between fluorescent-labeled and unlabeled aggregates cannot be excluded.[26,53,56] This may influence the quantification of high-molecular weight species. On the other hand, purification may lead to a loss of aggregated protein or co-purification of abundant endogenous proteins, which requires careful evaluation.[62]

Asymmetrical flow field-flow fractionation (AF4) and analytical ultracentrifugation were used as alternative quantitation methods to SEC. Leeman et al.[78] and Demeule et al.[55] demonstrated the capability of AF4 and analytical ultracentrifugation to detect a fluorescent-labeled mAb in whole blood, plasma, and serum.,These methods are particularly desirable for assessing the stability in biological fluids due to the absence of a stationary phase, minimal sample treatment, and analysis under physiologic-like conditions.[78] For the separation of mAb aggregates by AF4, it was demonstrated that a mobile phase with a high pH value is desirable to improve sample recovery.[79] At high pH values (e.g., 10.5) both a mAb and membrane are negatively charged and thus interactions are markedly reduced.

Another challenge often associated with AF4 is oversaturation of membranes, which is specifically challenging for protein-rich biological fluids. Leeman et al. minimized the protein load on the AF4 channel by removing endogenous serum proteins smaller than 100 kDa.[78] Additionally, the viscosity of whole blood, serum, and plasma was reduced by diluting each biological fluid 100-fold with the carrier solution (PBS). Despite these precautions, it was noted that red blood cells of whole blood stuck to the membrane and routine analysis of biological fluids require meticulous method development. Although not observed by Leeman et al. clogging of flow lines in the autosampler and detector is another concern related to biological fluids.

Visible particles have been rarely investigated under physiologic conditions.[21,77] Kinderman et al. showed that certain mAbs may form a viscous precipitate upon mixing with PBS or diluted human serum at pH 7.4.[21] The study highlighted that PBS and serum differ substantially from typically formulation buffers and sudden changes in pH and osmolality to the protein may cause visible particle formation. Such events may cause injection site reactions or trigger an immune response in patients.

Generally, sample treatment and analysis conditions (e.g., mobile phase) have to carefully evaluated for each method due to the potential impact on the DP and on biological fluids, which generally show limited stability under *in vitro/ex vivo* conditions.[3,14,18,26,42,62,77] Analysis time is especially concerning as the pH of biological fluids increases in absence of carbon dioxide.[18,80] Thus, biological fluids require a controlled carbon dioxide environment to maintain the physiologic pH and avoid incubation under non-physiologic conditions, which may not be representative of events occurring in patients. Endogenous molecules of biological fluids may degrade under non-physiologic conditions, which in turn can trigger degradation of the protein of interest.[26]

Table 3
Selected Studies Investigating Protein Aggregation and Fragmentation in Biological Fluids. Different analytical methods and approaches are summarized. Studies for the analysis of fragmentation of fusion proteins are reviewed elsewhere. .[65]

Author	Method		Therapeutic protein	Experiment and Fluid	Analytical approach
	Aggregation	Fragmentation			
Arvinte *et al.*[88]	Light microscopy	–	adalimumab, cetuximab, bevacizumab, trastuzumab, infliximab	*in vitro*: human plasma and serum, rhesus monkey and mouse wild type and knockout serum	Diluting biological fluid, direct analysis
Demeule *et al.*[55]	AUC	–	IgE	*in vitro*: human serum, human plasma	Alexa Fluor488
Filipe *et al.*[56]	NTA fSPT	–	IgG1, human serum albumin	*in vitro*: human serum, human plasma	Alexa Fluor488 Alexa Fluor546 Alexa Fluor594
Filipe et al.[89]	Fluorescence imaging	–	IgG1	*in vivo*: SKH1 mice	IRDye800CW, IRDye RD680 NHS labeling
Filipe *et al.*[53]	fSPT CLSM Flow cytometry	–	IgG1	*in vitro*: human serum	Alexa Fluor488
Han et al.[67]		Intact CE-MS	Fc fusion protein	*in vitro:* mouse serum *in vivo:* C57BL/6 mice	Neutravidin
Jiskoot *et al.*[7]	SEC SDS-PAGE	SEC SDS-PAGE	IgG1	*in vitro*: Sodium phosphate pH 7.4+ sodium chloride	Direct analysis
Kijanka et al.[90]	Fluorescence imaging	–	IgG1	*in vivo*: SKH1 mice	IRDye800 CW NHS ester
Kinderman *et al.*[21]	Fluorescence imaging Multiphoton imaging and fluorescence microscopy	–	IgG2	*in vitro*: human serum, PBS, *ex vivo/in vivo*: Male CD-1 athymic nude mice and female SKH1-Elite mice	Dilution of biological fluid, Cy5.5 NHS ester labeling
Li *et al*[68]		Intact LC-MS LC-MS/MS	Fc fusion protein	*in vitro:* rat serum *in vivo:* rats	Streptavidin
Liu *et al.*[17]	–	Microchip CE-SDS	F(ab')2	*in vitro*: 200 μM GSH, 20 μM GSSG	Direct analysis
Luo *et al.*[26]	Flow imaging SDS-PAGE LC-MS/MS	–	Bevacizumab Trastuzumab Infliximab	*in vitro*: human plasma+0.9% saline mouse serum	Diluting biological fluid, direct analysis
Luo *et al.*[91]	SDS-PAGE LC-MS/MS	–	IgG1, IgG2, IgG4, Fc fusion protein	*in vitro*: human serum/human plasma+diluent (e.g., 0.9% saline)	Diluting biological fluid, direct analysis
Patel *et al.*[85]	Light microscopy LO SEC CE-SDS	SEC CE-SDS	Bispecific mAb	*in vitro*: porcine vitreous humor	Diluting biological fluid with PBS, direct analysis
Patel *et al.*[77]	SEC Turbidity	SEC	mAb and Fab	*in vitro*: porcine vitreous humor	Diluting biological fluid with PBS, direct analysis
Piparia et al.[86]	Microchip CE-SDS	Microchip CE-SDS	IgG	*in vitro*: Sprague Dawley rat serum *in vivo*: male Sprague-Dawley rats	Pico protein dye
Schmid *et al.*[4]	SEC	SEC	Trastuzumab	*in vitro*: SCID mouse serum, PBS *in vivo*: SCID mouse	Protein A
Schuster *et al.*[14]	LO Flow imaging Fluorescence microscopy	–	IgG1	*in vitro*: human serum	Alexa Fluor488
Schuster *et al.*[18]	LO Flow imaging SEC Flow cytometry Fluorescence microscopy	SEC	IgG1, IgG4	*in vitro*: human serum, PBS	Alexa Fluor488

(*continued on next page*)

Table 3 (*Continued*)

Author	Method		Therapeutic protein	Experiment and Fluid	Analytical approach
	Aggregation	Fragmentation			
Schuster et al.[54]	LO Flow imaging Imaging flow cytometry	–	IgG1, IgG4	*in vitro*: human serum, PBS	Alexa Fluor488
Yang *et al.*[63]	SEC SDS-PAGE Western blot LC-MS/MS	–	IgG1, IgG2	*in vitro*: human serum, human plasma, PBS+20 μM cysteine +250 μM cystine	Fluorescent-labeled streptavidin
Yin *et al.*[62]	capSEC	capSEC CE-SDS intact LC-MS LC-MS/MS	IgG1	*in vitro*: rat plasma, PBS *in vivo*: rat	Anti-human IgG Fc affinity

AUC, analytical ultracentrifugation.
CE-SDS, Capillary electrophoresis-sodium dodecyl sulfate.
CLSM, confocal laser scanning microscopy.
fSPT, fluorescence single particle tracking.
GSH, glutathione.
GSSG, glutathione disulfide.
LC-MS, liquid chromatography-mass spectrometry.
LC-MS/MS, liquid chromatography-mass spectrometry/mass spectrometry.
LO, light obscuration.
NTA, nanoparticle tracking analysis.
SDS-PAGE, sodium dodecyl sulfate-polyacrylamide gel electrophoresis.
SEC, size-exclusion chromatography.

Analysis of Protein Fragmentation in Biological Fluids

Studies investigating fragmentation in biological fluids are largely missing, presumably attributed to the lack of adequate analytical methods. In recent years, significant improvements of mass spectrometry (MS) coupled with capillary electrophoresis[67] or liquid chromatography[62,81] allowed insight on *in vivo* fragmentation of therapeutic proteins, particularly Fc fusion proteins.[65] In this publication, MS methods are only mentioned briefly as challenges to monitor protein stability in biological fluids by MS have been extensively reviewed elsewhere.[65,82-84] CE-SDS is the preferred method to analyze protein fragmentation due to their superior sensitivity compared to SEC.

Yin *et al.* reported that peptide hydrolysis may occur *in vivo* in the upper hinge region of a mAb creating Fab and desFab fragments (a mAb with one Fab domain missing).[62] However, even after anti-human Fc purification of a human mAb from rat plasma, matrix interference from endogenous proteins was reported.[62] Reduced CE-SDS revealed a stronger increase of an incompletely reduced heavy chain-light chain peak. The fragment was identified by intact LC-MS and LC-MS/MS experiments as a thioether-linked fragment of a heavy and light chain peptide. The fragment may have formed through β-elimination of an interchain disulfide bond located close to the upper hinge region.

Patel *et al.* reported fragmentation of a mAb in vitreous humor; however, possible interference from endogenous proteins could not be excluded.[77] In another study, CE-SDS revealed fragments of light chains and non-glycosylated mAb possibility due to disulfide bond hydrolysis occurring in vitreous humor.[85] Schuster *et al.* reported profound differences in protein fragmentation among fluorescent-labeled mAbs subjected to human serum.[18] Fragmentation of mAbs was directly analyzed in the biological fluid using SEC. Certain mAbs showed little or no fragmentation whereas some mAbs fragmented upon mixing with serum, which increased up to ca. 20% over time. Unlabeled fragments of the protein of interest were not distinguishable from serum proteins.

Piparia et al., labeled an IgG1 molecule at a higher degree of labeling with only 0.5% and 2.0% of the heavy and light chain remaining unlabeled.[86] This enabled to track protein fragments and covalent aggregates after intravenous injection to rats. The tested mAb was stable *in vivo*, however, it remains unknown if the mAb would have shown a different stability in its unlabeled form. While pharmacokinetic parameters of the unlabeled and labeled mAb were comparable, the half-life increased from 14 days (unlabeled) to 21 days (labeled).

Table 3 summarizes different analytical techniques investigating *in vivo* protein aggregation and fragmentation. Notably, regardless of the analytical approach, *in vivo* fragmentation remains specifically challenging, as protein fragments formed in biological fluids may not contain the initially conjugated fluorophore nor the desired target-binding site. Thus, these fragments remain undetected in the biological fluid. If an unbiased quantification of fragments is the aim of a study, at least two independent capturing techniques ought to be used.[87]

Conclusion

Assessing the *in vivo* stability of therapeutic proteins has attracted significant interest. Several *in vitro* models are available to evaluate the stability of therapeutic proteins in a pre-clinical setting. However, reliably evaluating the *in vivo* stability under *in vitro/ex vivo* conditions remains difficult due to the complexity of the human physiology, limited stability of biological fluids outside a living organism, and lack of analytical methods under physiologic conditions.

Degradation of biological fluid components can lead to matrix interference (e.g., particle formation of biological fluid components) and make extensive sample treatment of the protein of interest

inevitable (e.g., fluorescence labeling). Substituting biological fluids with surrogate buffers may compromise the physiologic relevance of an *in vitro* model to an extent that it may not allow to monitor protein aggregation and/or fragmentation.

Despite these technical challenges, we strongly suggest to monitor the stability of therapeutic proteins in biological fluids over time. Particularly, critical quality attributes with relevance to clinical efficacy and safety performance of the molecules should be assessed during pre-clinical development, ideally before clinical lead selection. Knowledge on *in vivo* protein stability may help to re-engineer lead molecules and improve their stability and thus efficacy in patients. From a safety perspective, the knowledge of *in vivo* protein fragmentation and aggregation may help to evaluate the immunogenic potential of proteins.[38] Such studies should be an integral part of the preclinical development of therapeutic proteins.

References

1. Krause ME, Sahin E. Chemical and physical instabilities in manufacturing and storage of therapeutic proteins. *Curr Opin Biotechnol*. 2019;60:159–167.
2. Nejadnik MR, Randolph TW, Volkin DB. Postproduction handling and administration of protein pharmaceuticals and potential instability issues. *J Pharm Sci*. 2018;107(8):2013–2019.
3. Schuster J, Koulov A, Mahler HC. Vivo stability of therapeutic proteins. *Pharm Res*. 2020;37:23.
4. Schmid I, Bonnington L, Gerl M. Assessment of susceptible chemical modification sites of trastuzumab and endogenous human immunoglobulins at physiological conditions. *Nature Commun Biol*. 2018;1(28).
5. Li Y, Monine M, Huang Y, Swann P, Nestorov I, Lyubarskaya Y. Quantitation and pharmacokinetic modeling of therapeutic antibody quality attributes in human studies. *MAbs*. 2016;8(6):1079–1087.
6. Liu YD, van Enk JZ, Flynn GC. Human antibody Fc deamidation in vivo. *Biologicals*. 2009;37(5):313–322.
7. Jiskoot W, Beuvery EC, de Koning AA, Herron JN, Crommelin DJ. Analytical approaches to the study of monoclonal antibody stability. *Pharm Res*. 1990;7 (12):1234–1241.
8. Liu H, Nowak C, Patel R. Modifications of recombinant monoclonal antibodies in vivo. *Biologicals*. 2019;59:1–5.
9. Liu H, Ponniah G, Zhang HM. In vitro and in vivo modifications of recombinant and human IgG antibodies. *MAbs*. 2014;6(5):1145–1154.
10. Huang L, Lu J, Wroblewski VJ, Beals JM, Riggin RM. In vivo deamidation characterization of monoclonal antibody by LC/MS/MS. *Anal Chem*. 2005;77(5):1432–1439.
11. Yang X, Xu W, Dukleska S. Developability studies before initiation of process development: improving manufacturability of monoclonal antibodies. *MAbs*. 2013;5 (5):787–794.
12. Yang N, Tang Q, Hu P, Lewis MJ. Use of in vitro systems to model in vivo degradation of therapeutic monoclonal antibodies. *Anal Chem*. 2018;90(13):7896–7902.
13. Awwad S, Henein C, Ibeanu N, Khaw PT, Brocchini S. Preclinical challenges for developing long acting intravitreal medicines. *Eur J Pharm Biopharm*. 2020;153:130–149.
14. Schuster J, Koulov A, Mahler HC. Particle analysis of biotherapeutics in human serum using machine learning. *J Pharm Sci*. 2020;109(5):1827–1832.
15. Goetze AM, Schenauer MR, Flynn GC. Assessing monoclonal antibody product quality attribute criticality through clinical studies. *MAbs*. 2010;2(5):500–507.
16. Doell A, Schmitz OJ, Hollmann M. Shedding light into the subcutis: a mass spectrometry based Immunocapture assay enabling full characterization of therapeutic antibodies after injection in Vivo. *Anal Chem*. 2019;91(15):9490–9499.
17. Liu YD, Chen Y, Tsui G. Predictive in vitro vitreous and serum models and methods to assess thiol-related quality attributes in protein therapeutics. *Anal Chem*. 2020.
18. Schuster J, Mahler HC, Koulov A. Tracking the physical stability of fluorescent-labeled mAbs under physiologic in vitro conditions in human serum and PBS. *Eur J Pharm Biopharm*. 2020;152:193–201.
19. Bown HK, Bonn C, Yohe S. In vitro model for predicting bioavailability of subcutaneously injected monoclonal antibodies. *J Control Release*. 2018;273:13–20.
20. Lobo B, Lo S, Wakankar A, et al. 2010. Method and formulation for reducing aggregation of a macromolecule under physiological conditions. In Genentech I, F. Hoffmann-La Roche Ag, Ed., ed.: Google Patents.
21. Kinderman F, Yerby B, Jawa V. Impact of Precipitation of Antibody Therapeutics following Subcutaneous Injection on Pharmacokinetics and Immunogenicity. *J Pharm Sci*. 2019;108(6):1953–1963.
22. Richter WF, Christianson GJ, Frances N, Grimm HP, Proetzel G, Roopenian DC. Hematopoietic cells as site of first-pass catabolism after subcutaneous dosing and contributors to systemic clearance of a monoclonal antibody in mice. *MAbs*. 2018;10(5):803–813.
23. Wang W, Singh SK, Li N, Toler MR, King KR, Nema S. Immunogenicity of protein aggregates–concerns and realities. *Int J Pharm*. 2012;431(1–2):1–11.
24. Rosenberg AS. Effects of protein aggregates: an immunologic perspective. *AAPS J*. 2006;8(3):E501–E507.
25. Mahler HC, Friess W, Grauschopf U, Kiese S. Protein aggregation: pathways, induction factors and analysis. *J Pharm Sci*. 2009;98(9):2909–2934.
26. Luo S, Zhang B. Dextrose-mediated aggregation of therapeutic monoclonal antibodies in human plasma: implication of isoelectric precipitation of complement proteins. *MAbs*. 2015;7(6):1094–1103.
27. Arvinte T, Poirier E, Palais C. Prediction of aggregation in vivo by studies of therapeutic proteins in human plasma. In: Rosenberg AS, Demeule B, eds. *Biobetters - Protein Engineering to Approach the Curative*. New York: Springer; 2015:91–104.
28. Varkhede N, Bommana R, Schoneich C, Forrest ML. Proteolysis and oxidation of therapeutic proteins after intradermal or subcutaneous administration. *J Pharm Sci*. 2020;109(1):191–205.
29. Liu D, Ren D, Huang H. Structure and stability changes of human IgG1 Fc as a consequence of methionine oxidation. *Biochemistry* . 2008;47(18):5088–5100.
30. Moritz B, Stracke JO. Assessment of disulfide and hinge modifications in monoclonal antibodies. *Electrophoresis* . 2017;38(6):769–785.
31. Vlasak J, Ionescu R. Fragmentation of monoclonal antibodies. *MAbs*. 2011;3 (3):253–263.
32. Mills BJ, Moussa EM, Jameel F. Monoclonal antibodies: structure, physicochemical stability, and protein engineering. In: Jameel F, Skoug JW, Nesbitt RR, eds. *Development of Biopharmaceutical Drug-Device Products*. Cham, Switzerland: Springer International Publishing; 2020:3–26.
33. Cordoba AJ, Shyong BJ, Breen D, Harris RJ. Non-enzymatic hinge region fragmentation of antibodies in solution. *J Chromatogr B Analyt Technol Biomed Life Sci*. 2005;818(2):115–121.
34. Moorthy BS, Xie B, Moussa EM. Effect of hydrolytic degradation on the in vivo properties of monoclonal antibodies. In: Rosenberg AS, Demeule B, eds. *Biobetters - Protein Engineering to Approach the Curative*. New York: Springer; 2015:105–135.
35. Liu H, Gaza-Bulseco G, Sun J. Characterization of the stability of a fully human monoclonal IgG after prolonged incubation at elevated temperature. *J Chromatogr B Analyt Technol Biomed Life Sci*. 2006;837(1–2):35–43.
36. Manning MC, Chou DK, Murphy BM, Payne RW, Katayama DS. Stability of protein pharmaceuticals: an update. *Pharm Res*. 2010;27(4):544–575.
37. Werle M, Bernkop-Schnurch A. Strategies to improve plasma half life time of peptide and protein drugs. *Amino Acids*. 2006;30(4):351–367.
38. Rao VA. Perspectives on engineering biobetter therapeutic proteins with greater stability in infl ammatory environments. In: Rosenberg AS, Demeule B, eds. *Biobetters - Protein Engineering to Approach the Curative*. New York: Springer; 2015:183–202.
39. Diemel RV, ter Hart HG, Derksen GJ, Koenderman AH, Aalberse RC. Characterization of immunoglobulin G fragments in liquid intravenous immunoglobulin products. *Transfusion* . 2005;45(10):1601–1609.
40. Wypych J, Li M, Guo A. Human IgG2 antibodies display disulfide-mediated structural isoforms. *J Biol Chem*. 2008;283(23):16194–16205.
41. Liu YD, Chen X, Enk JZ, Plant M, Dillon TM, Flynn GC. Human IgG2 antibody disulfide rearrangement in vivo. *J Biol Chem*. 2008;283(43):29266–29272.
42. Dillon TM, Ricci MS, Vezina C. Structural and functional characterization of disulfide isoforms of the human IgG2 subclass. *J Biol Chem*. 2008;283 (23):16206–16215.
43. Labrijn AF, Buijsse AO, van den Bremer ET. Therapeutic IgG4 antibodies engage in Fab-arm exchange with endogenous human IgG4 in vivo. *Nat Biotechnol*. 2009;27 (8):767–771.
44. Gu S, Wen D, Weinreb PH. Characterization of trisulfide modification in antibodies. *Anal Biochem*. 2010;400(1):89–98.
45. Zhang Q, Schenauer MR, McCarter JD, Flynn GC. IgG1 thioether bond formation in vivo. *J Biol Chem*. 2013;288(23):16371–16382.
46. Ouellette D, Alessandri L, Chin A. Studies in serum support rapid formation of disulfide bond between unpaired cysteine residues in the VH domain of an immunoglobulin G1 molecule. *Anal Biochem*. 2010;397(1):37–47.
47. Fan X, Brezski RJ, Fa M. A single proteolytic cleavage within the lower hinge of trastuzumab reduces immune effector function and in vivo efficacy. *Breast Cancer Res*. 2012;14(4):R116.
48. Carter PJ, Lazar GA. Next generation antibody drugs: pursuit of the 'high-hanging fruit'. *Nat Rev Drug Discov*. 2018;17(3):197–223.
49. Kratz A, Ferraro M, Sluss PM, Lewandrowski KB. Case records of the Massachusetts general hospital. Weekly clinicopathological exercises. Laboratory reference values. *N Engl J Med*. 2004;351(15):1548–1563.
50. Bloomfield IG, Johnston IH, Bilston LE. Effects of proteins, blood cells and glucose on the viscosity of cerebrospinal fluid. *Pediatr Neurosurg*. 1998;28(5):246–251.
51. Viola M, Sequeira J, Seica R. Subcutaneous delivery of monoclonal antibodies: how do we get there? *J Control Release*. 2018;286:301–314.
52. Kinnunen HM, Mrsny RJ. Improving the outcomes of biopharmaceutical delivery via the subcutaneous route by understanding the chemical, physical and physiological properties of the subcutaneous injection site. *J Control Release*. 2014;182:22–32.
53. Filipe V, Poole R, Oladunjoye O, Braeckmans K, Jiskoot W. Detection and characterization of subvisible aggregates of monoclonal IgG in serum. *Pharm Res*. 2012;29 (8):2202–2212.
54. Schuster J, Probst C, Mahler HC, Joerg S, Huwyler J, Mathaes R. Assessing particle formation of biotherapeutics in biological fluids. *J Pharm Sci*. 2021;110(4):1527–1532.
55. Demeule B, Shire SJ, Liu J. A therapeutic antibody and its antigen form different complexes in serum than in phosphate-buffered saline: a study by analytical ultracentrifugation. *Anal Biochem*. 2009;388(2):279–287.
56. Filipe V, Poole R, Kutscher M, Forier K, Braeckmans K, Jiskoot W. Fluorescence single particle tracking for the characterization of submicron protein aggregates

in biological fluids and complex formulations. *Pharm Res*. 2011;28(5):1112–1120.
57. Zanetti-Domingues LC, Tynan CJ, Rolfe DJ, Clarke DT, Martin-Fernandez M. Hydrophobic fluorescent probes introduce artifacts into single molecule tracking experiments due to non-specific binding. *PLoS ONE*. 2013;8(9):e74200.
58. Chi EY, Krishnan S, Randolph TW, Carpenter JF. Physical stability of proteins in aqueous solution: mechanism and driving forces in nonnative protein aggregation. *Pharm Res*. 2003;20(9):1325–1336.
59. Cilliers C, Nessler I, Christodolu N, Thurber GM. Tracking antibody distribution with near-infrared fluorescent dyes: impact of dye structure and degree of labeling on plasma clearance. *Mol Pharm*. 2017;14(5):1623–1633.
60. Goulet DR, Atkins WM. Considerations for the design of antibody-based therapeutics. *J Pharm Sci*. 2020;109(1):74–103.
61. Gaza-Bulseco G, Faldu S, Hurkmans K, Chumsae C, Liu H. Effect of methionine oxidation of a recombinant monoclonal antibody on the binding affinity to protein A and protein G. *J Chromatogr B Analyt Technol Biomed Life Sci*. 2008;870(1):55–62.
62. Yin S, Pastuskovas CV, Khawli LA, Stults JT. Characterization of therapeutic monoclonal antibodies reveals differences between in vitro and in vivo time-course studies. *Pharm Res*. 2013;30(1):167–178.
63. Yang J, Goetze AM, Flynn GC. Assessment of naturally occurring covalent and total dimer levels in human IgG1 and IgG2. *Mol Immunol*. 2014;58(1):108–115.
64. Wang Q, Han J, Sha C. Novel strategy using tryptic peptide immunoaffinity-based LC-MS/MS to quantify denosumab in monkey serum. *Bioanalysis* . 2017;9(19):1451–1463.
65. Schadt S, Hauri S, Lopes F. Are biotransformation studies of therapeutic proteins needed? Scientific considerations and technical challenges. *Drug Metab Dispos*. 2019;47(12):1443–1456.
66. Liu H, Manuilov AV, Chumsae C, Babineau ML, Tarcsa E. Quantitation of a recombinant monoclonal antibody in monkey serum by liquid chromatography-mass spectrometry. *Anal Biochem*. 2011;414(1):147–153.
67. Han M, Pearson JT, Wang Y. Immunoaffinity capture coupled with capillary electrophoresis - mass spectrometry to study therapeutic protein stability in vivo. *Anal Biochem*. 2017;539:118–126.
68. Li F, Weng Y, Zhang G, Han X, Li D, Neubert H. Characterization and quantification of an Fc-FGF21 fusion protein in rat serum using immunoaffinity LC-MS. *AAPS J*. 2019;21(5):84.
69. Wiig H, Swartz MA. Interstitial fluid and lymph formation and transport: physiological regulation and roles in inflammation and cancer. *Physiol Rev*. 2012;92(3):1005–1060.
70. Kinnunen HM, Sharma V, Contreras-Rojas LR. A novel in vitro method to model the fate of subcutaneously administered biopharmaceuticals and associated formulation components. *J Control Release*. 2015;214:94–102.
71. van der Pol E, Boing AN, Harrison P, Sturk A, Nieuwland R. Classification, functions, and clinical relevance of extracellular vesicles. *Pharmacol Rev*. 2012;64(3):676–705.
72. Wojczynski MK, Glasser SP, Oberman A. High-fat meal effect on LDL, HDL, and VLDL particle size and number in the Genetics of Lipid-Lowering Drugs and Diet Network (GOLDN): an interventional study. *Lipids Health Dis*. 2011;10:181.
73. Turitto V, Slack SM. Blood and related fluids. In: Murphy W, Black J, Hastings G, eds. *Handbook of Biomaterial Properties*. New York: Springer; 2016:115–124.
74. Freisleben A, Brudny-Kloppel M, Mulder H, de Vries R, de Zwart M, Timmerman P. Blood stability testing: european Bioanalysis Forum view on current challenges for regulated bioanalysis. *Bioanalysis* . 2011;3(12):1333–1336.
75. Wolfbeis OS, Leiner M. Mapping of the total fluorescence of human blood serum as a new method for its characterization. *Anal Chim Acta*. 1985;167:203–215.
76. Nishi H, Mathas R, Furst R, Winter G. Label-free flow cytometry analysis of subvisible aggregates in liquid IgG1 antibody formulations. *J Pharm Sci*. 2014;103(1):90–99.
77. Patel S, Muller G, Stracke JO, Altenburger U, Mahler HC, Jere D. Evaluation of protein drug stability with vitreous humor in a novel ex-vivo intraocular model. *Eur J Pharm Biopharm*. 2015;95(Pt B):407–417.
78. Leeman M, Choi J, Hansson S, Storm MU, Nilsson L. Proteins and antibodies in serum, plasma, and whole blood-size characterization using asymmetrical flow field-flow fractionation (AF4). *Anal Bioanal Chem*. 2018;410(20):4867–4873.
79. Boll B, Josse L, Heubach A. Impact of non-ideal analyte behavior on the separation of protein aggregates by asymmetric flow field-flow fractionation. *J Sep Sci*. 2018;41(13):2854–2864.
80. Lorget F, Parenteau A, Carrier M. Characterization of the pH and temperature in the rabbit, pig, and monkey eye: key parameters for the development of long-acting delivery ocular strategies. *Mol Pharm*. 2016;13(9):2891–2896.
81. Zell M, Husser C, Staack RF. In Vivo biotransformation of the fusion protein Tetranectin-Apolipoprotein A1 analyzed by ligand-binding mass spectrometry combined with quantitation by ELISA. *Anal Chem*. 2016;88(23):11670–11677.
82. Kellie JF, Karlinsey MZ. Review of approaches and examples for monitoring biotransformation in protein and peptide therapeutics by MS. *Bioanalysis*. 2018.
83. Wei C, Su D, Wang J, Jian W, Zhang D. LC–MS challenges in characterizing and quantifying monoclonal Antibodies (mAb) and Antibody-Drug Conjugates (ADC) in biological samples. *Curr Pharmacol Rep*. 2018;4(1):45–63.
84. Kellie JF, Tran JC, Jian W. Intact protein mass spectrometry for therapeutic protein quantitation, pharmacokinetics, and biotransformation in preclinical and clinical studies: an industry perspective. *J Am Soc Mass Spectrom*. 2020.
85. Patel S, Stracke JO, Altenburger U. Prediction of intraocular antibody drug stability using ex-vivo ocular model. *Eur J Pharm Biopharm*. 2017;112:177–186.
86. Piparia R, Ouellette D, Stine WB. A high throughput capillary electrophoresis method to obtain pharmacokinetics and quality attributes of a therapeutic molecule in circulation. *MAbs*. 2012;4(4):521–531.
87. Li Y, Huang Y, Ferrant J. Assessing in vivo dynamics of multiple quality attributes from a therapeutic IgG4 monoclonal antibody circulating in cynomolgus monkey. *MAbs*. 2016;8(5):961–968.
88. Arvinte T, Palais C, Green-Trexler E. Aggregation of biopharmaceuticals in human plasma and human serum: implications for drug research and development. *MAbs*. 2013;5(3):491–500.
89. Filipe V, Que I, Carpenter JF, Lowik C, Jiskoot W. In vivo fluorescence imaging of IgG1 aggregates after subcutaneous and intravenous injection in mice. *Pharm Res*. 2014;31(1):216–227.
90. Kijanka G, Bee JS, Bishop SM, Que I, Lowik C, Jiskoot W. Fate of multimeric oligomers, submicron, and micron size aggregates of monoclonal antibodies upon subcutaneous injection in mice. *J Pharm Sci*. 2016;105(5):1693–1704.
91. Luo S, McSweeney KM, Wang T, Bacot SM, Feldman GM, Zhang B. Defining the right diluent for intravenous infusion of therapeutic antibodies. *MAbs*. 2020;12:(1)1685814.

Particle Analysis of Biotherapeutics in Human Serum using Machine Learning

The following chapter has been published as note in the Journal of Pharmaceutical Sciences.

Joachim Schuster, Atanas Koulov, Hanns-Christian Mahler, Susanne Joerg, Joerg Huwyler, Kai Schleicher, Pascal Detampel, and Roman Mathaes.
Particle Analysis of Biotherapeutics in Human Serum using Machine Learning
J Pharm Sci. 2020, 109(5), 1827-1832
doi: 10.1016/j.xphs.2020.02.015

The supplementary data was inserted into this chapter.

Journal of Pharmaceutical Sciences 109 (2020) 1827-1832

Contents lists available at ScienceDirect

Journal of Pharmaceutical Sciences

journal homepage: www.jpharmsci.org

Note

Particle Analysis of Biotherapeutics in Human Serum Using Machine Learning

Joachim Schuster [1, 2], Atanas Koulov [1], Hanns-Christian Mahler [1], Susanne Joerg [1], Joerg Huwyler [2], Kai Schleicher [3], Pascal Detampel [2, *], Roman Mathaes [1, *]

[1] *Lonza AG, Drug Product Services, Basel, Switzerland*
[2] *University of Basel, Pharmacenter, Division of Pharmaceutical Technology, Basel, Switzerland*
[3] *University of Basel, Biozentrum, Imaging Core Facility, Basel, Switzerland*

ARTICLE INFO

Article history:
Received 19 September 2019
Revised 4 February 2020
Accepted 11 February 2020
Available online 27 February 2020

Keywords:
machine learning
imaging method(s)
physical stability
developability
protein aggregation
IgG antibody(s)

ABSTRACT

In recent years, an increasing number of studies assessed the stability of biotherapeutics in biological fluids. Such studies aim to simulate the conditions encountered in the human body and investigate the *in vivo* stability under *in vitro* conditions. However, on account of complexity of biological fluids, standard pharmaceutical methods are poorly suited to assess the stability of biotherapeutics. In this study, a fluorescent-labeled therapeutic immunoglobulin G (IgG) was analyzed for proteinaceous particles after mixing with human serum and after incubation at 37°C for 5 days. Samples were analyzed using standard pharmaceutical methods (light obscuration and dynamic imaging). Moreover, we developed a fluorescence microscopy method allowing to semiquantitatively detect IgG particles in serum. Several hundred IgG particles were detected after exposure to serum. Moreover, particle counts and particle size increased in serum over time. The results showed that an IgG may form particles on mixing with serum and novel methods such as fluorescence microscopy are required to gain insight on the stability of biotherapeutics in biological fluids. Furthermore, we showed distinct advantages of machine learning over traditional threshold-based methods by analyzing microscopy images. Machine learning allowed simplifying particles in regards to count, size, and shape.

Introduction

The stability of biotherapeutics is a primary concern during pharmaceutical product development and can impact product efficacy and patient safety[1] and is monitored during different product life-cycle stages.[2] For example, particulates in parenteral preparations can relate to inadequate product stability and thus be proteinaceous in nature. Assessing subvisible particles (SVPs) in parenteral preparations can be required by light obscuration (LO) or optical microscopy as described in the harmonized pharmacopoeial chapters (USP <788>, Ph. Eur. 2.9.19, and JP 6.07). Although this has traditionally served to monitor particulate contamination, these methods are also suitable to monitor particulates that can stem from inadequate stability.

In recent years, health authorities increasingly suggested to characterize particle formation of biotherapeutics in biological fluids to simulate the stability in patients (*in vivo* stability).[3] After administration to patients, biotherapeutics can undergo changes, which have been described as biotransformation[4] and post-administration modifications.[5] Such changes may impact the stability of biotherapeutics and in turn can affect product efficacy or patient safety, or both.[5] For example, the formation of particulates *in vivo* may be associated to potential safety concerns because proteinaceous particulates have been suggested to be involved in triggering an immune response.[1] To date, such preclinical *in vitro* studies have been carried out by spiking the biotherapeutic into the intended body fluid to simulate the conditions encountered in patients after administration (e.g., serum for intravenous administration).[5]

Abbreviations used: AF, Alexa Fluor 488; DSC, differential scanning calorimetry; IgG, immunoglobulin G; IgG:AF, IgG labeled with AF; IgG:BODIPY, IgG labeled with BODIPY; LO, light obscuration; mAb, monoclonal antibody; ML, machine learning; rH, relative humidity; SEC, size-exclusion chromatography; Ser, human serum without the therapeutic IgG; Ser + IgG, human serum spiked with the therapeutic IgG; SVP, subvisible particle.

The authors Detampel and Mathaes contributed equally.

This article contains supplementary material available from the authors by request or via the Internet at https://doi.org/10.1016/j.xphs.2020.02.015.

* *Correspondence to:* Roman Mathaes (Telephone: +41 79 238 5775) and Pascal Detampel (Telephone: +41 61 207 1687).

E-mail addresses: pascal.detampel@unibas.ch (P. Detampel), roman.mathaes@lonza.com (R. Mathaes).

https://doi.org/10.1016/j.xphs.2020.02.015
0022-3549/

Standard pharmaceutical methods lack the ability to unambiguously detect particles of biotherapeutics in complex matrices such as human serum.[6] Thus, innovative methods such as fluorescence microscopy were recently suggested for this purpose.[7] Fluorescence microscopy allows differentiating between particles of fluorescent-labeled biotherapeutics and those of (unlabeled) endogenous molecules. Moreover, the resolution of fluorescence confocal laser scanning microscopy allows the characterization of sub-1 μm range to some extent.[7] In this work, we developed a method using widefield fluorescence microscopy to assess the stability of a biotherapeutic exposed to human serum. Contrary to previous studies using microscopy, we acquired several thousand images by scanning an entire sample volume of 4 μL allowing for semiquantitative analysis. Particle formation of a therapeutic immunoglobulin G1 (IgG1) labeled with Alexa Fluor 488 (AF) was analyzed after exposure to human serum (t0) and after an incubation at 37°C for 5 days (t1) (Supplemental Fig. 1).

Materials and Methods

Materials

A therapeutic IgG1 formulated in 20 mM histidine-HCl buffer (pH 6.0) was provided by Lonza Biologics plc (Slough, UK). Alexa Fluor 488 NHS succinimidyl ester, sodium azide, and phosphate-buffered saline (PBS) pH 7.4 were purchased from Sigma-Aldrich (Buchs, Switzerland). BODIPY FL NHS succinimidyl ester was purchased from Fisher Scientific (Reinach, Switzerland). PVDF filters (0.22 μm) were used (Merck Millipore, Darmstadt, Germany). Human male AB serum (plasma-derived serum) was purchased from BioIVT (West Sussex, UK).

Labeling and Stability of IgG

Therapeutic IgG was buffer-exchanged to PBS pH 7.4 using Vivaspin 2 with a molecular weight cutoff of 30,000 Da (Sartorius, Goettingen, Germany). Labeling was performed with AF and BODIPY each at a IgG:dye molar ratio of 1:4, 1:1, and 4:1 at 25°C for 2 h. The unbound dye was removed using Princeton pro spin columns (LubioScience, Zurich, Switzerland) using 20 mM Histidine-HCl buffer, pH 6.0. The degree of labeling (Supplemental Fig. 2) was determined by UV-Vis spectroscopy using Lunatic (Unchained Labs, Pleasanton, CA).

To determine which dye and labeling ratio has the smallest impact on the biotherapeutic's stability and will subsequently be used in serum, we performed an accelerated stability study. Unlabeled IgG in PBS and histidine-HCl buffer, IgG labeled with AF (IgG:AF), and IgG labeled with BODIPY (IgG:BODIPY) were each measured after preparation and after an incubation at 40°C and 75% relative humidity (rH) for 2 weeks. Unlabeled IgG, IgG:AF, and IgG:BODIPY were analyzed using LO. Moreover, the unlabeled IgG and IgG:AF were analyzed using size-exclusion chromatography (SEC) after preparation and after an incubation at 40°C and 75% rH for 2 weeks. Differential scanning calorimetry (DSC) of the unlabeled IgG and IgG:AF 1:4 was measured after preparation. All samples were stored at 5°C.

In Vitro *Exposure of IgG:AF to Human Serum*

Human serum was thawed, sterile-filtered (0.22 μm), and mixed with sodium azide to reach a final concentration of 0.1% (w/v). Human serum was adjusted to a pH of 7.3 to 7.5 in a carbon dioxide (CO_2) incubator.

Based on our accelerated stability study, we selected a molar ratio between IgG and AF of 1:4 for spiking experiments in serum. The AF-IgG concentration was 9.1 mg/mL with a degree of labeling of ca. 2 molecules AF per molecule IgG. A total of 40 μL of the AF-IgG sample was spiked to 1.8 mL of human serum (Ser + IgG) to reach a final AF-IgG concentration of 200 μg/mL. Samples were analyzed after exposure to serum (t0) and after incubating for 5 days (t1) in a CO_2 incubator at 37°C and 6.7% CO_2.

Light Obscuration

A HIAC 9703+ equipped with an HRLD-150 detector (Beckman Coulter, Brea, CA) was used to measure SVPs. Four measurements of each 0.2 mL were performed. The first measurement was discarded and the average of the last 3 measurements was reported. A syringe size of 1 mL with a flow rate of 10 mL/min was used. The system was calibrated using COUNT-CAL Count Precision Size Standard (Thermo Fisher Scientific, Waltham, MA).

Size-Exclusion Chromatography

SEC was performed using a TSKgel G3000SWXL column (Tosoh Biosciences, Griesheim, Germany) connected to a Waters Alliance e2695 HPLC equipped with an UV/Vis detector (Waters, Eschborn, Germany). The flow rate was set at 0.5 mL/min. Ten μL of samples at 0.75 mg/mL were injected. The absorbance at 210 nm was measured. Chromatograms were exported from Empower 3 (Waters).

Differential Scanning Calorimetry

DSC was performed using a MicroCal VP-Capillary DSC (Malvern Panalytical, Malvern, UK). Samples were measured at 1 mg/mL and in the temperature range between 15°C to 110°C at 2.5°C/min. The DSC profiles were calculated using Origin 7.0 (OriginLab Corporation, Northampton, MA).

Dynamic Imaging

A FlowCAM VS1 from Fluid Imaging Technologies (Scarborough, ME) equipped with a 10x NA/0.3 UPLFLN objective (Olympus, Tokyo, Japan), 80 μm field-of-view flow cell, and 1.0 mL syringe was used to analyze SVPs. Sample volume was set to 0.3 mL at 0.1 mL/min. The instrument was manually primed with 0.2 mL of sample. Camera focus and particle size were calibrated using 25 μm and 5 μm NIST traceable standards (Thermo Fisher Scientific). Particle count was calibrated using COUNT-CAL Count Precision Size Standards (Thermo Fisher Scientific). Data were acquired using VisualSpreadsheet software 4.2.52 (Fluid Imaging Technologies).

Inverted Widefield Fluorescence Microscopy

Four μL of samples were placed on a 35 mm glass bottom dish (14 mm glass diameter, # 1.5, MatTek Corporation, Ashland, MA) and spread with a 13 mm cover glass (VWR, Dietikon, Switzerland), covering the entire sample volume. During acquisition, the rH was controlled at 60%. Samples were imaged using inverted widefield microscope (FEI "MORE," Munich, Germany) equipped with LED illumination (Lumencore SpectraX) with 470/24 nm excitation and 517/20 nm emission filter, a U Plan S Apo 10× NA 0.4 air objective, and an ORCA flash 4.0 cooled sCMOS camera (Hamamatsu Photonics, Hamamatsu, Japan). Images were acquired with 100 ms exposure time and z-stacks in 3 μm increments covering 30 μm to 50 μm in depth using Live Acquisition 2.5 software (FEI Munich).

Data Processing

All image processing was done in Fiji.[8] Individual tiles were corrected for uneven illumination using BaSiC to calculate and apply flatfield and darkfield correction.[9] Shading correction images were calculated based on 30 central tiles and applied to all images (Supplemental Fig. 7). A maximum intensity z-projection of the corrected tile images was stitched and fused using the Grid/Collection stitching plugin.[10] Large-scale uneven illumination across the entire sample dish was corrected by dividing the fused maximum intensity z-projection by a normalized copy of itself filtered with a strong Gaussian blur.

We analyzed particles by comparing threshold methods (e.g., Shanbhag,[11] RenyiEntropy,[12] and Otsu[13]) to machine learning (ML). To exclude artifacts, particles were analyzed within a central circular area of 103.1 mm^2. The sample volume was calculated according to the analyzed area.

For ML, we used Interactive Learning and Segmentation Toolkit (ilastik version 1.3.2).[14] The ML model was trained on 25 cropped areas of several samples at t0 and t1. Each crop covered several tiles of a sample, with each tile containing specific features such as particles, background, air bubbles, out-of-focus light, and so on. Labels were assigned for particles and background based on pixel features and user annotations (pixel classification). Feature types include color/intensity, edge, and texture. For each feature, sigma values of 10.0 pixel were selected. A Random Forest classifier was trained interactively from the annotations made on the aforementioned crops of samples. After training of the model, a simple segmentation was performed on the serum samples and serum controls each at t0 and t1.

To extrapolate particle counts per images to particle counts per mL, the theoretical volume of the imaged sample was calculated by multiplying the circular area of interest (103.1 mm^2) with the number of z-stacks (10 to 15) and the distance between the z-stacks (3 μm). On average, 11 z-stacks in 3 μm increments scanned the entire depth of a 4 μL sample, matching our observation that the whole liquid was covered in the field of view. During acquisition, an additional margin of ca. 15 μm in depth was used because samples were not leveled. Edges of the sample were excluded in the particle analysis yielding a total sample volume of 3.4 μL. Cumulative counts of particles were extrapolated to 1 mL and grouped for particles ≥2 μm, ≥5 μm, ≥10 μm, and ≥25 μm.

Results

Impact of Labeling

Particle concentration of IgG:BODIPY increased with the degree of labeling and as a function of time (Supplemental Fig. 3). Particle levels of IgG:AF were comparable to those of unlabeled IgG samples (Figs. 1a and 1b). Moreover, the degree of labeling of IgG:AF did not impact the stability of the IgG. On account of the low influence of conjugated AF on mAb aggregation, only IgG:AF was used for further studies.

SEC analysis of IgG:AF and unlabeled control samples showed no significant impact on the stability of the IgG (Supplemental Figs. 4 and 5). The melting temperature was measured at 67.9°C, 71.6°C, and 73.7°C for the unlabeled IgG and at 67.6°C, 70.7°C, and 72.8°C for IgG:AF at a molar ratio of 1:4 (Supplemental Fig. 6). Overall, IgG:AF at a low- (4:1), mid- (1:1), and high- (1:4) degree of labeling did not impact the stability of the therapeutic IgG. Therefore, human serum experiments were performed with IgG:AF at a molar ratio of 1:4.

Particle Analysis in Serum Using Light Obscuration and FlowCAM

Serum samples spiked with IgG:AF at a molar ratio of 1:4 (Ser + IgG) and the control samples of serum without the therapeutic IgG (Ser) were analyzed at t0 and after incubation for 5 days (t1). All samples were analyzed using LO (Fig. 2a) and FlowCAM (Fig. 2b).

Figure 2a shows that already shortly after filtration of serum (t0), several hundred particles were detected in Ser and Ser + IgG. After an incubation period of 5 days (t1), a pronounced increase of SVPs (≥2 μm, ≥5 μm, and ≥10 μm) was measured in Ser + IgG sample. The control samples without the therapeutic IgG also showed an increase in SVPs. However, the increase in SVP counts of the serum control samples was less pronounced when compared to the spiked samples.

Particle Analysis Using Machine Learning

Ser and Ser + IgG samples were imaged at t0 and t1. Using ML, we only detected baseline levels of particles in the control samples. A total of 46 particles were observed in Ser at t0 and 121 particles in Ser at t1 (images not shown). By contrast, in the Ser + IgG samples, we detected 497 particles at t0 (Fig. 3a) and 918 particles at t1 (Fig. 3b). Most IgG-particles were smaller than 10 μm (Fig. 3c).

In addition to serum control samples, we evaluated the instrument variability and variability of sample preparation. A model therapeutic IgG was exposed to serum at 200 μg/mL and measured at t0 and t1. For the instrument variability, the same sample was analyzed 3 times. The variability of sample preparation was evaluated by analyzing 3 independently prepared samples. Supplemental Table 1 shows mean values and coefficient of variation of three 4 μL measurements at t0 and t1.

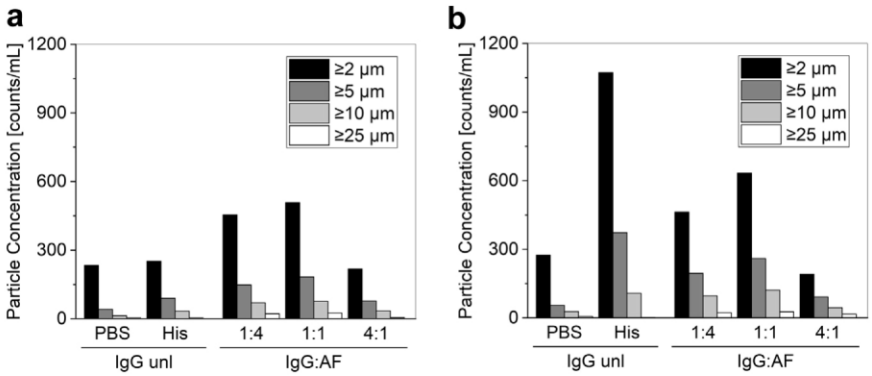

Figure 1. Particle analysis of unlabeled IgG and labeled IgG using LO. Analysis of the unlabeled IgG (IgG unl) in PBS and histidine-HCl buffer (His) as well as AF-labeled IgG (IgG:AF) after preparation (a) and after an incubation at 40°C and 75% rH for 2 weeks (b). IgG was labeled with AF at an IgG:dye molar ratio of 1:4, 1:1, and 4:1. AF, Alexa Fluor 488.

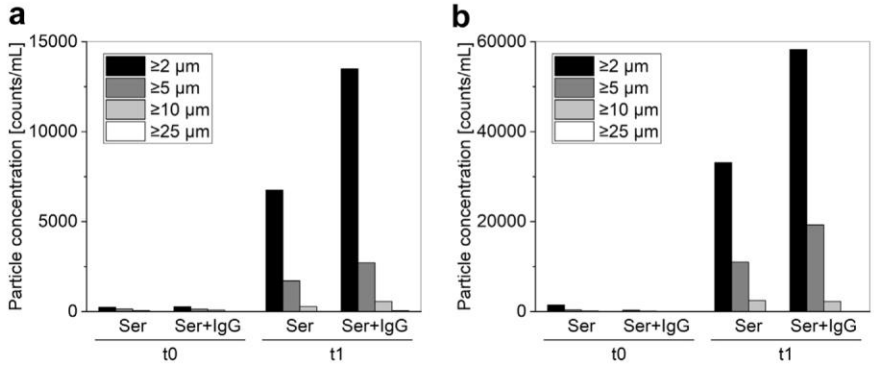

Figure 2. Particle analysis using light obscuration and FlowCAM. Analysis of serum samples at t0 and after an incubation at 37°C for 5 days (t1) using light obscuration (a) and FlowCAM (b). Human serum without the therapeutic IgG, Ser; human serum spiked with the therapeutic IgG, Ser + IgG.

Advantages of Machine Learning Over Traditional Threshold Methods

After background correction of the images acquired, we compared particle analysis using various traditional threshold methods to ML. Threshold methods showed reasonable discrimination of particles and the background within certain regions of the dish, however, performed poorly at detecting particles properly when applied over the entire sample (Supplemental Fig. 8).

Figures 4a, 4d, and 4g show example particles of microscopy images at t0 and t1. The examples were analyzed using 3 different threshold methods, namely Shanbhag (Fig. 4b), RenyiEntropy (Fig. 4e), and Otsu (Fig. 4h). The analysis of those particles was compared to particle analysis using ML (Figs. 4c, 4f, and 4i).

Figure 4b shows that 3 particles were detected using the threshold method Shanbhag. Using ML, 6 particles were detected (Fig. 4c). Moreover, we observed that particle size and particle shape were more accurately analyzed using ML. For example, RenyiEntropy (Fig. 4e) detected several artifact background pixels as particles, whereas ML detected one distinct particle (Fig. 4f). Particularly, bright spots within a particle can lead to significant differences in the detected particle size. As an example, Figure 4h shows the detection of 2 comparatively small particles using the Otsu threshold method due to 2 bright spots within the particle

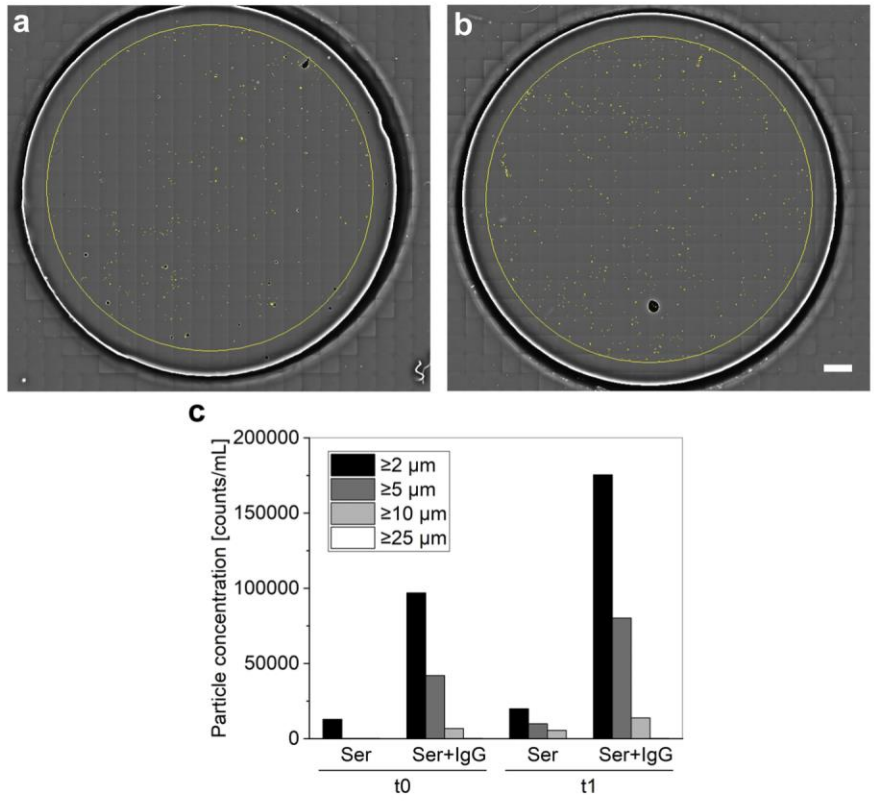

Figure 3. Particle analysis of the IgG exposed to human serum. (a) Analysis of serum samples after exposure to human serum (t0). (b) Analysis of serum samples after incubation at 37°C for 5 days (t1). (c) Cumulative particle counts/mL. Panels a and b show each 483 stitched images with a maximum intensity projection. Human serum without the therapeutic IgG, Ser; human serum spiked with the therapeutic IgG, Ser + IgG. Scale bar length in b: 1 mm.

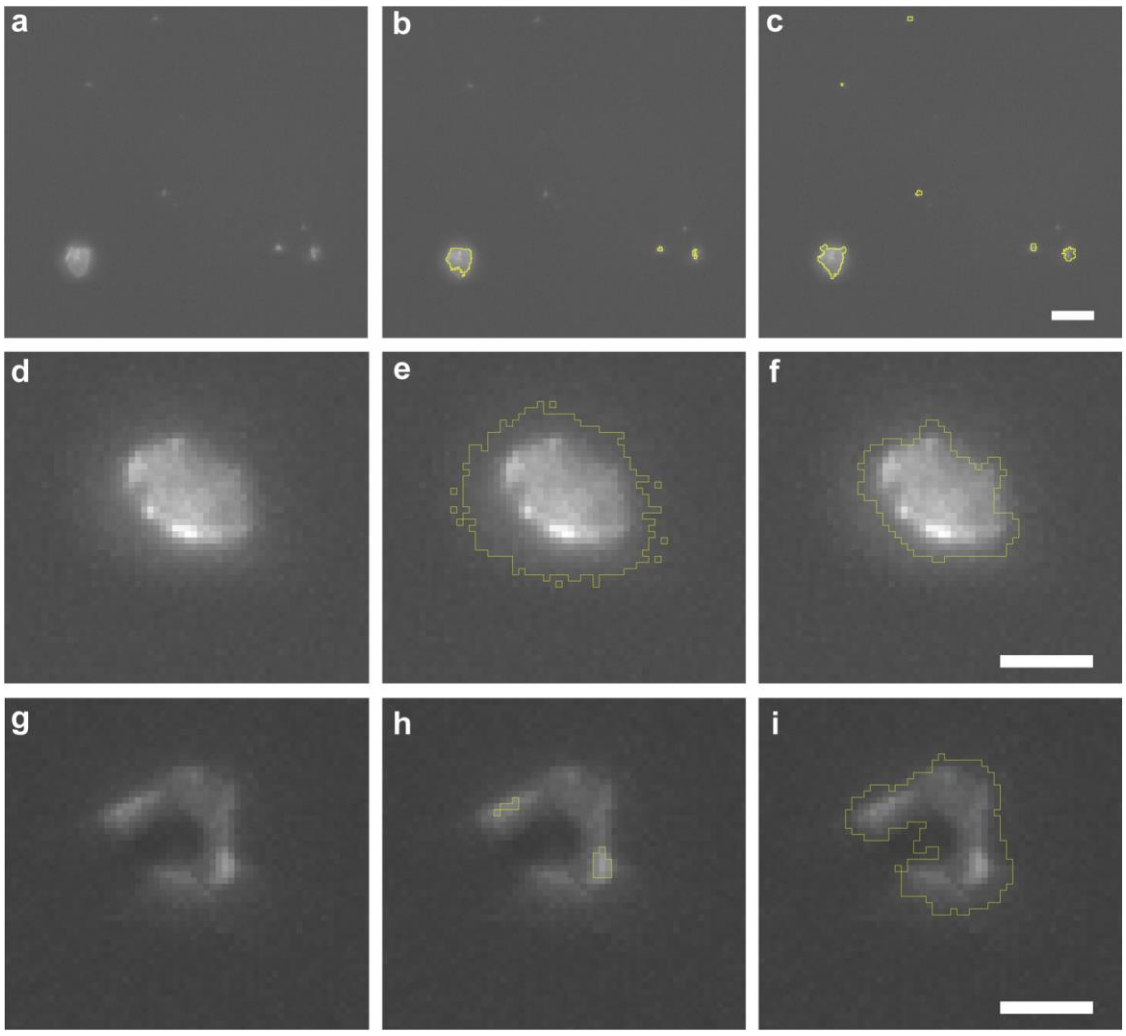
a
b
c
d
e
f
g
h
i

accurate detection of the particle shape and particle size compared to traditional threshold-based analysis. Although traditional threshold methods may also yield similar results, significant efforts of data processing would be required to overcome the challenges encountered. It is of note that other pharmaceutical methods such as dynamic imaging contain a uniform background and thus threshold methods will likely perform better than observed in this study. We believe the capability of ML to extract additional information embedded in the image raw data may also be promising for instruments such as dynamic imaging as previously reported.[17]

Using advanced methods such as deep learning and a larger data set can arguably improve particle analysis further.[17] To date, only a limited number of studies used ML for particle analysis of biotherapeutics. For example, protein particles and silicon particles of FlowCAM images were successfully classified using neural network analysis.[17] Contrary to classic neural network analysis, ilastik allows for interactive particle analysis of large data sets without requiring sophisticated ML expertise. We showed that fluorescence labeling of a biotherapeutic is a reasonable approach to assess its physical stability in biological fluids as a preclinical study. However, labeling may affect the behavior of the biotherapeutic in a complex environment such as serum. Although the stability of the unlabeled and labeled IgG after an accelerated stability study was comparable, the propensity of the IgG to aggregate in serum may be impacted. Generally, knowledge of the clinical relevance of physiologic-like *in vitro* studies simulating the complex *in vivo* homeostasis in patients is limited.[5] For example, the use of serum or plasma as surrogate for whole blood is even debated for clinical samples.[18] Briefly, serum differs from plasma due to the absence of fibrin and fibrin-associated proteins and thus offers a slightly less complex matrix, containing 3 to 5 g/L less protein.[5] Depending on the analysis required, serum or plasma may not be interchangeable surrogates.[18] For example, plasma has been argued as preferred surrogate for clinical sample collection, on account of the avoidance of proteolysis.[4] Contrarily, the addition of an anticoagulant to plasma may interfere with the analysis.[19]

Finally, to resemble the conditions of clinical settings more closely, the mAb spiking concentration in serum used in this study (200 μg/mL) was based on a typical mAb concentration in human serum samples. As an example, after an intravenous infusion of 10 mg/kg mAb in humans, serum mAb concentrations of ca. 280, 260, 180, and 115 μg/mL were measured 1, 24, 72, and 168 h after administration, respectively.[20] Of note, serum mAb concentrations can vary considerably depending on factors such as the administered mAb molecule and dosing regimen. Typical intravenous infusion doses of mAbs range from less than 1 mg/kg to 15 mg/kg.[21] The volumetric ratios used in this study (mixing 40 μL of mAb to 1.8 mL serum) led to a mAb to serum ratio of 1:46 (v/v). In clinical settings, the vast majority of mAbs are diluted in 100 mL or 250 mL of diluent (mostly 0.9% saline) before infusion.[22] Considering an average blood volume of 5 L for a 70 kg male, a mAb to blood ratio of 1:50 (100 mL infusion) and 1:20 (250 mL infusion) will be achieved after infusion.

Conclusion

Traditional SVP methods are poorly suitable to assess *in vivo* stability of biotherapeutics in biological fluids. The developed method can serve as an analytical tool to characterize particle formation of biotherapeutics in biological fluids. The specific IgG used in this study showed particle formation, particularly in the sub-10 μm range, when exposed to human serum, however, did not completely precipitate, thus emphasizing the importance of assessing the stability of biotherapeutics in biological fluids during development.

Finally, we have shown that ML can be a valuable tool for complex particle detection allowing for high-throughput data analysis complementing standard pharmaceutical methods.

Acknowledgments

The authors are thankful to the Imaging Core Facility (Biozentrum, University of Basel) for the valuable technical guidance.

References

1. Rosenberg AS. Effects of protein aggregates: an immunologic perspective. *AAPS J*. 2006;8(3):E501-E507.
2. Mahler HC, Friess W, Grauschopf U, Kiese S. Protein aggregation: pathways, induction factors and analysis. *J Pharm Sci*. 2009;98(9):2909-2934.
3. Wang W, Singh SK, Li N, Toler MR, King KR, Nema S. Immunogenicity of protein aggregates—concerns and realities. *Int J Pharm*. 2012;431(1-2):1-11.
4. Hall MP. Biotransformation and in vivo stability of protein biotherapeutics: impact on candidate selection and pharmacokinetic profiling. *Drug Metab Dispos*. 2014;42(11):1873-1880.
5. Schuster J, Koulov A, Mahler HC, et al. In vivo stability of therapeutic proteins. *Pharm Res*. 2020;37(2):23.
6. Yin S, Pastuskovas CV, Khawli LA, Stults JT. Characterization of therapeutic monoclonal antibodies reveals differences between in vitro and in vivo time-course studies. *Pharm Res*. 2013;30(1):167-178.
7. Filipe V, Poole R, Oladunjoye O, Braeckmans K, Jiskoot W. Detection and characterization of subvisible aggregates of monoclonal IgG in serum. *Pharm Res*. 2012;29(8):2202-2212.
8. Schindelin J, Arganda-Carreras I, Frise E, et al. Fiji: an open-source platform for biological-image analysis. *Nat Methods*. 2012;9(7):676-682.
9. Peng T, Thorn K, Schroeder T, et al. A BaSiC tool for background and shading correction of optical microscopy images. *Nat Commun*. 2017;8:14836.
10. Preibisch S, Saalfeld S, Tomancak P. Globally optimal stitching of tiled 3D microscopic image acquisitions. *Bioinformatics*. 2009;25(11):1463-1465.
11. Shanbhag AG. Utilization of information measure as a means of image thresholding. *ImageJ*. 1994;56(5):414-419. Graph. Models Image Process (Academic Press, Inc.).
12. Kapur JN, Sahoo PK, Wong ACK. A new method for gray-level picture thresholding using the entropy of the histogram. *Graph Models Image Process*. 1985;29(3):273-285.
13. Otsu N. A threshold selection method from gray-level histograms. *IEEE Trans Syst Man Cybern*. 1979;9:62-66.
14. Sommer C, Straehle C, Kothe U, Hamprecht FA. *Ilastik: Interactive Learning and Segmentation Toolkit*. IEEE International Symposium on Biomedical Imaging: From Nano to Macro. 2011.
15. Probst C, Zeng Y, Zhu RR. Characterization of protein particles in therapeutic formulations using imaging flow cytometry. *J Pharm Sci*. 2017;106(8):1952-1960.
16. Rios Quiroz A, Lamerz J, Da Cunha T, et al. Factors governing the precision of subvisible particle measurement methods - a case study with a low-concentration therapeutic protein product in a prefilled syringe. *Pharm Res*. 2016;33(2):450-461.
17. Calderon CP, Daniels AL, Randolph TW. Deep convolutional neural network analysis of flow imaging microscopy data to classify subvisible particles in protein formulations. *J Pharm Sci*. 2018;107(4):999-1008.
18. Lima-Oliveira G, Monneret D, Guerber F, Guidi GC. Sample management for clinical biochemistry assays: are serum and plasma interchangeable specimens? *Crit Rev Clin Lab Sci*. 2018;55(7):480-500.
19. Uges DR. Plasma or serum in therapeutic drug monitoring and clinical toxicology. *Pharm Weekbl Sci*. 1988;10(5):185-188.
20. Yang N, Tang Q, Hu P, Lewis MJ. Use of in vitro systems to model in vivo degradation of therapeutic monoclonal antibodies. *Anal Chem*. 2018;90(13):7896-7902.
21. Kuester K, Kloft C. Pharmacokinetics of monoclonal antibodies. In: Meibohm B, ed. *Pharmacokinetics and Pharmacodynamics of Biotech Drugs: Principles and Case Studies in Drug Development*. Weinheim, Germany: WILEY-VCH; 2006:45-91.
22. Luo S, McSweeney KM, Wang T, Bacot SM, Feldman GM, Zhang B. Defining the right diluent for intravenous infusion of therapeutic antibodies. *MAbs*. 2020;12(1):1685814.

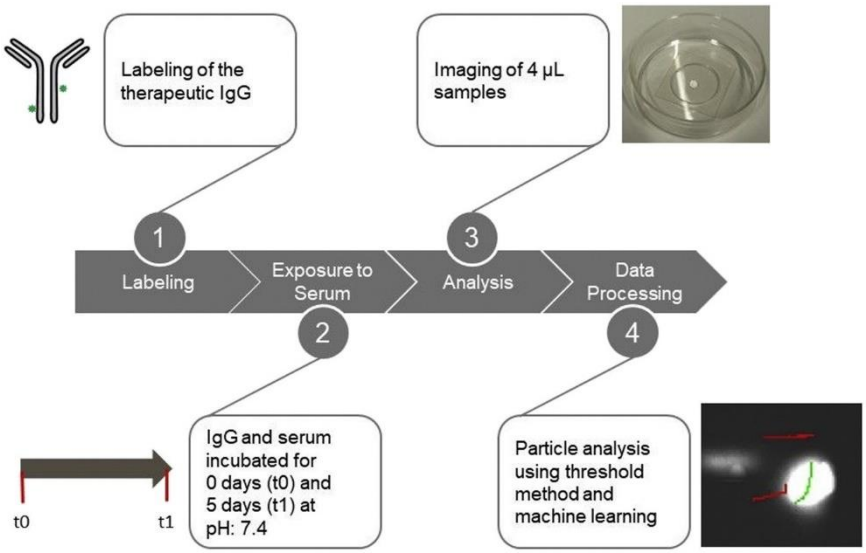

Supplemental Figure 1. Workflow. 1. Labeling of Alexa Fluor 488 (AF) and a therapeutic immunoglobulin (IgG). 2. Exposure of an IgG to serum at physiologic conditions. 3. Inverted widefield fluorescence microscopy of 4 µL samples at t0 and after 5 days of incubation (t1). 4. Particle analysis using machine learning.

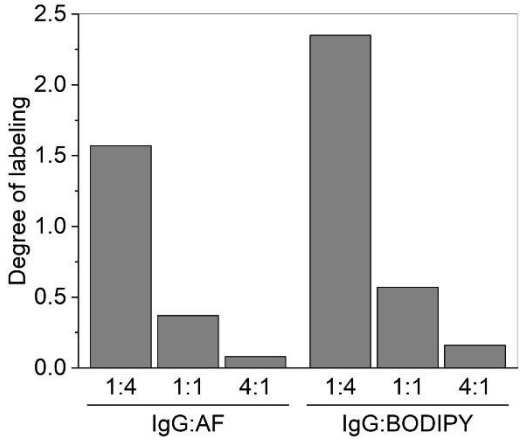

Supplemental Figure 2. Degree of labeling. The IgG was labeled with AF and BODIPY each at a IgG:dye molar ratio of 1:4, 1:1, and 4:1. The degree of labeling was determined by UV-Vis spectroscopy and denotes the number of dyes per molecule of IgG. AF, Alexa Fluor 488.

A **B**

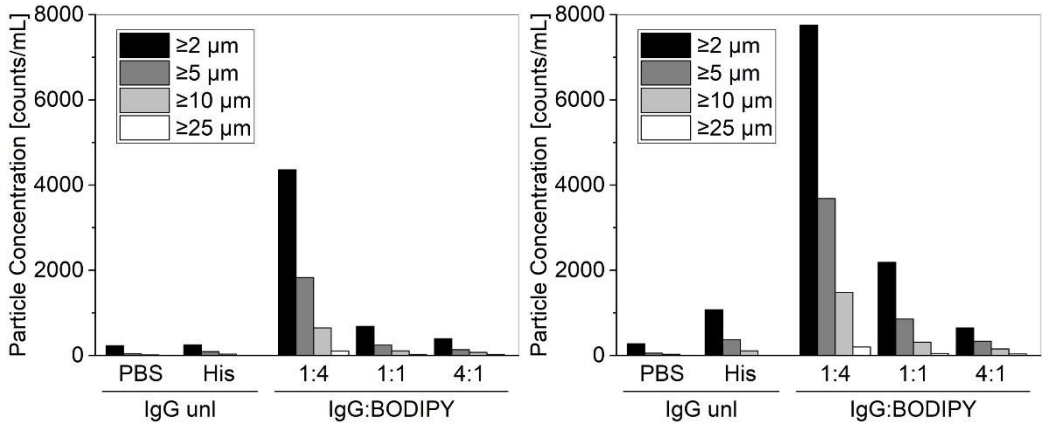

Supplemental Figure 3. Particle analysis of unlabeled IgG and labeled IgG using LO. Analysis of the unlabeled IgG (IgG unl) in PBS and histidine-HCl buffer (His) as well as BODIPY-labeled IgG (IgG:BODIPY) after preparation (a) and after an incubation at 40°C and 75% rH for 2 weeks (b). IgG was labeled with BODIPY at an IgG:dye molar ratio of 1:4, 1:1, and 4:1.

A

B

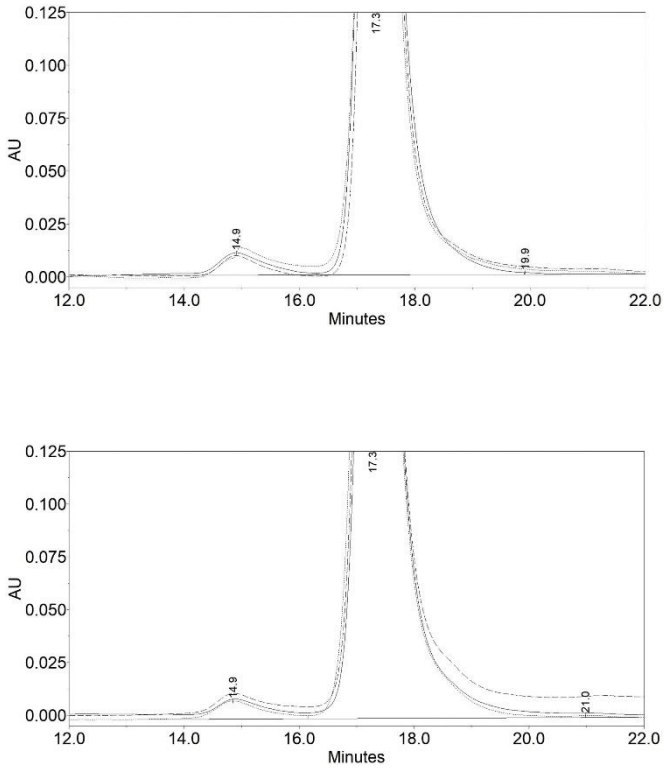

Supplemental Figure 4. Chromatogram of SEC of unlabeled and labeled IgG. Analysis of unlabeled IgG in histidine-HCl buffer (solid line), unlabeled IgG in PBS (dashed line), and IgG labeled with AF at 1:4 (dotted line) after preparation (a) and after an incubation at 40°C and 75% rH for 2 weeks (b).

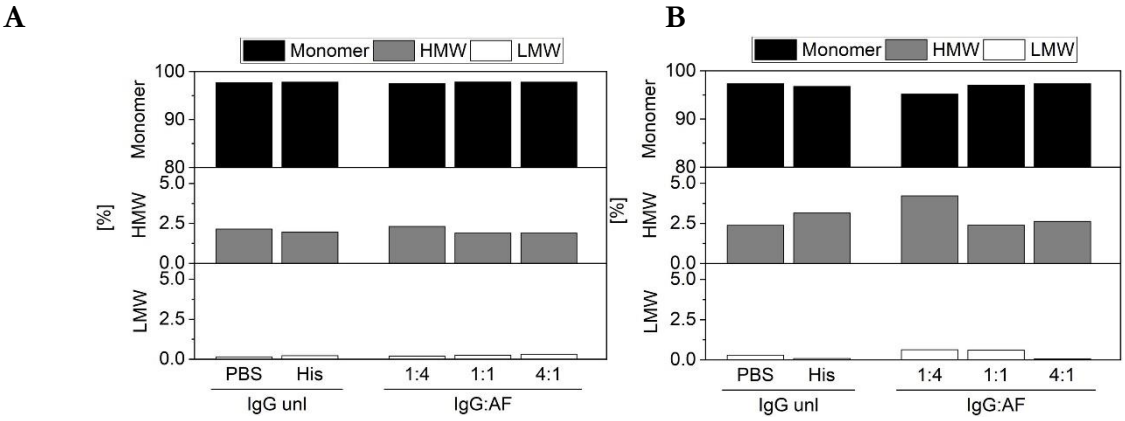

Supplemental Figure 5. Size-exclusion chromatography. Analysis of the unlabeled IgG in PBS and histidine-HCl buffer (IgG unl) and IgG labeled with AF (IgG:AF) at 3 degrees of labeling after preparation (a) and after an incubation at 40°C and 75% rH for 2 weeks (b).

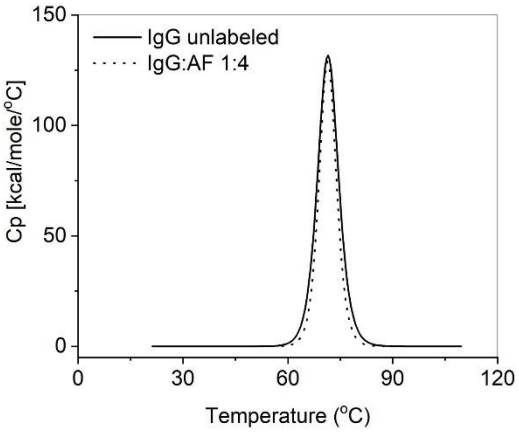

Supplemental Figure 6. Temperature-induced unfolding of the therapeutic IgG. IgG unlabeled (solid line), IgG:AF labeled 1:4 (dotted line). The melting temperature was measured at 67.9°C, 71.6°C, and 73.7°C for the unlabeled IgG and 67.6°C, 70.7°C, and 72.8°C for IgG:AF 1:4. Samples were formulated in 20 mM histidine-HCl buffer (pH 6.0).

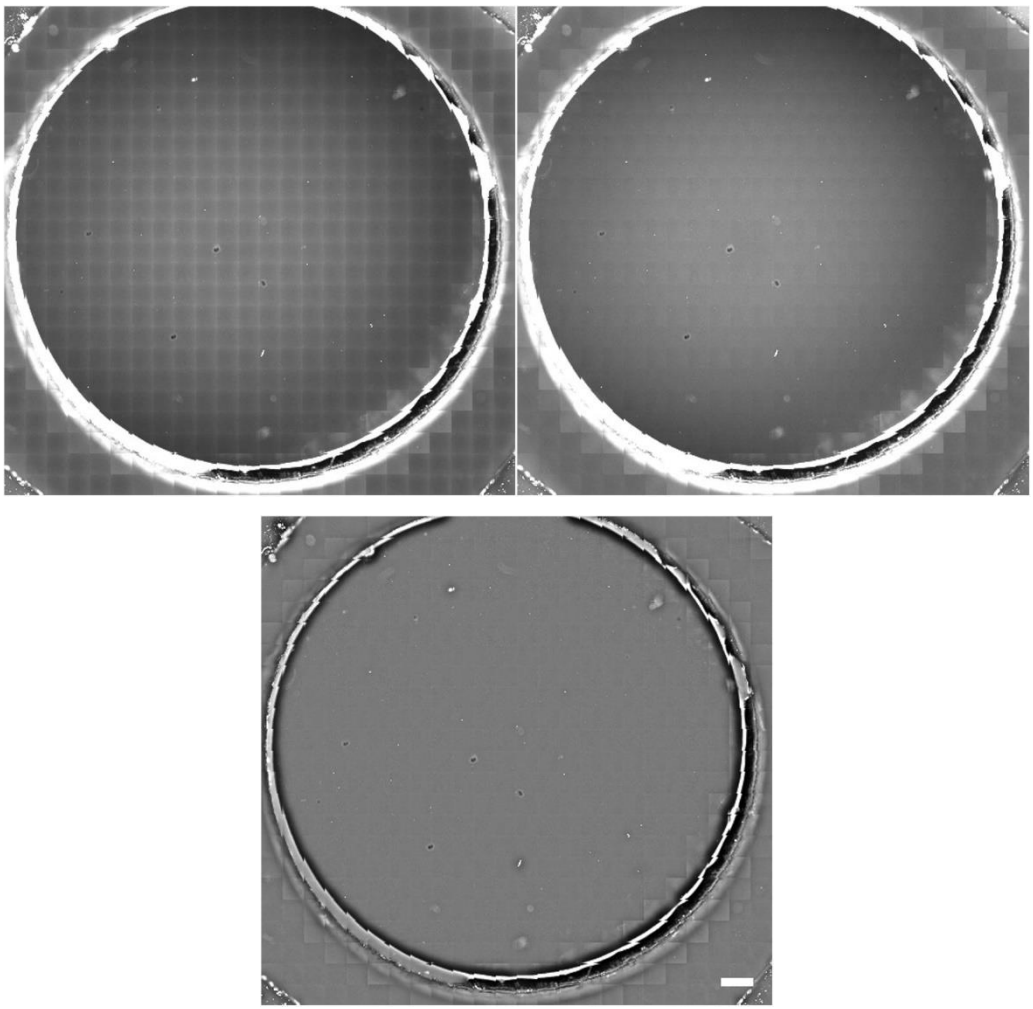

Supplemental Figure 7. Shading correction and background correction. (a) Fused and stitched images. (b) After applying a shading correction. (c) After applying a shading correction and background correction. Panels a, b, and c show each 483 stitched images with a maximum intensity projection of 24 z-stacks. Scale bar length: 1 mm.

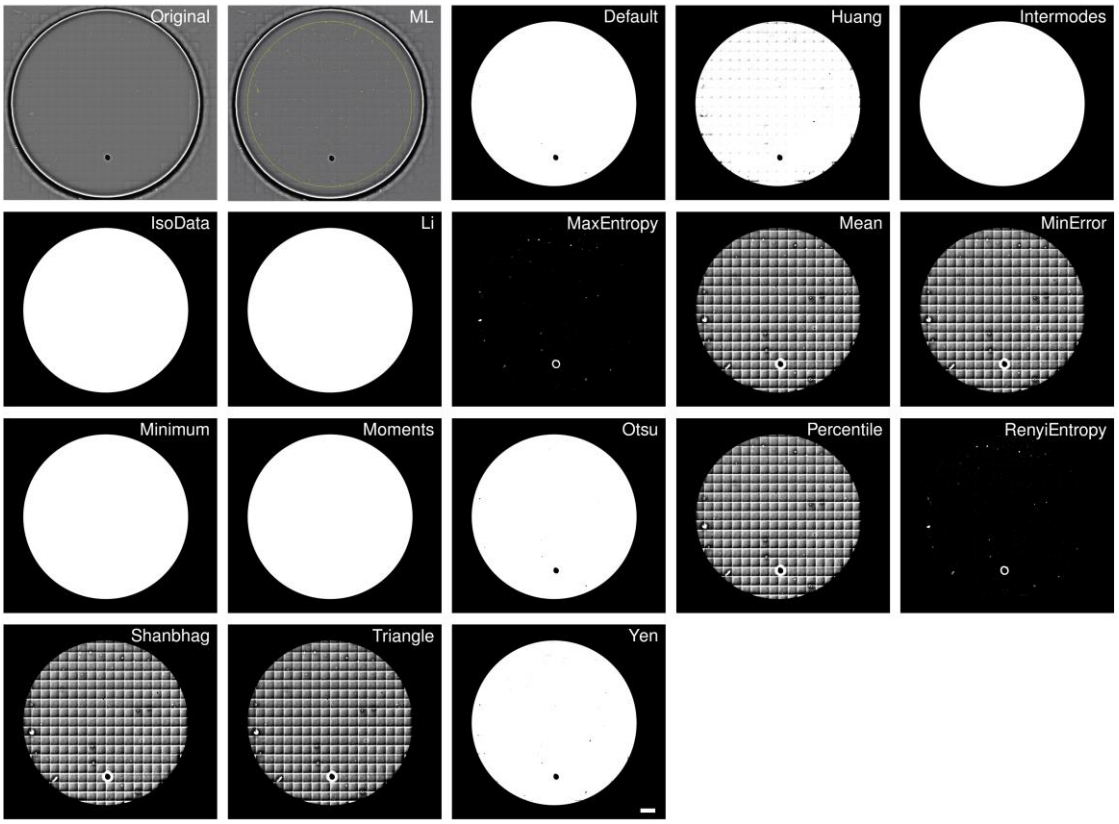

Supplemental Figure 8. Particle detection by machine learning and auto threshold methods. Detection of particles in serum samples at t1. Scale bar length: 1000 µm.

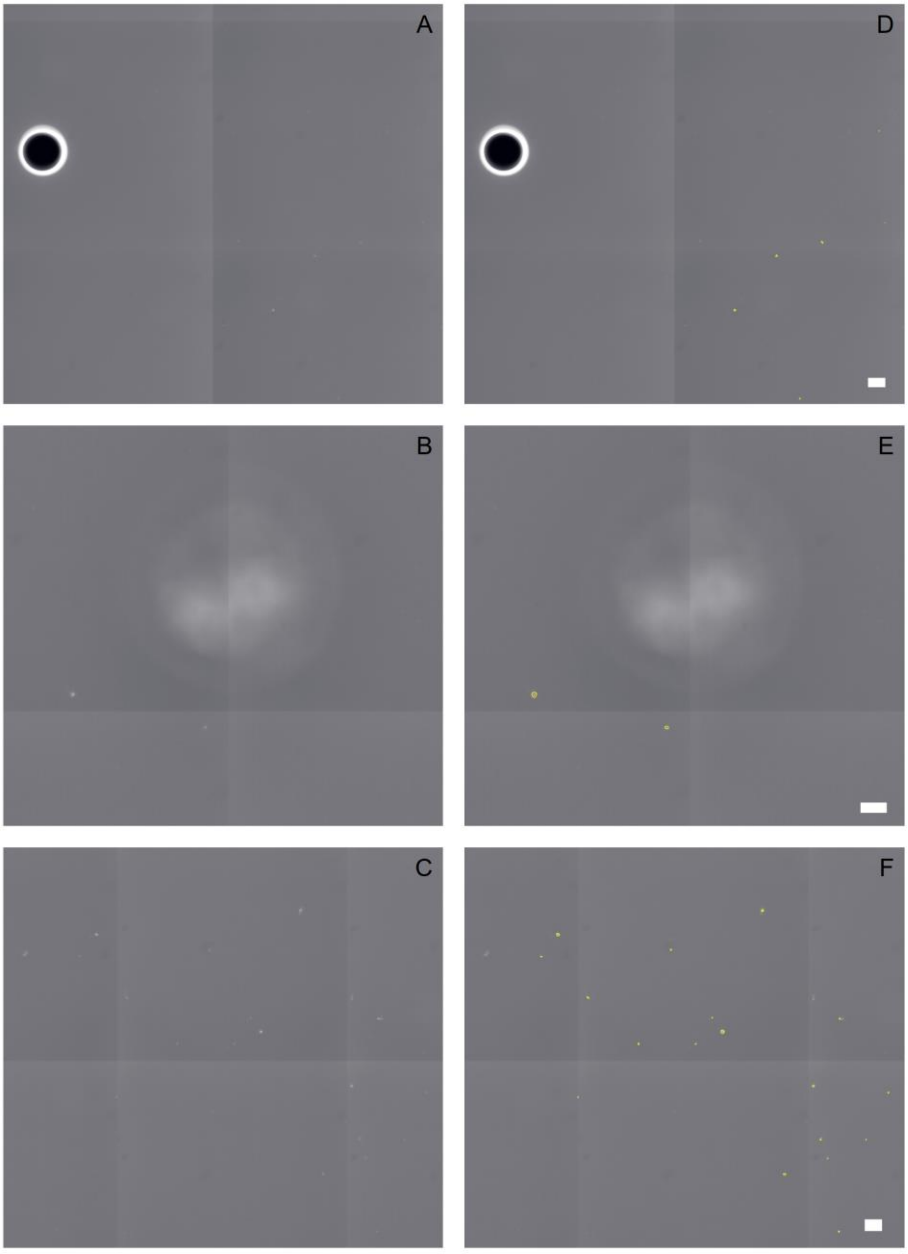

Supplemental Figure 9. Example of particle detection using machine learning. Particle detection by machine learning in exemplary sample crops containing air bubbles (a), out-of-focus light (b), and different background brightness at the tiling border (c). Panels a, b, and c depict original sample crops. Panels d, e, and f are the identical crops depicting particle detection by machine learning. Scale bar length: 50 µm.

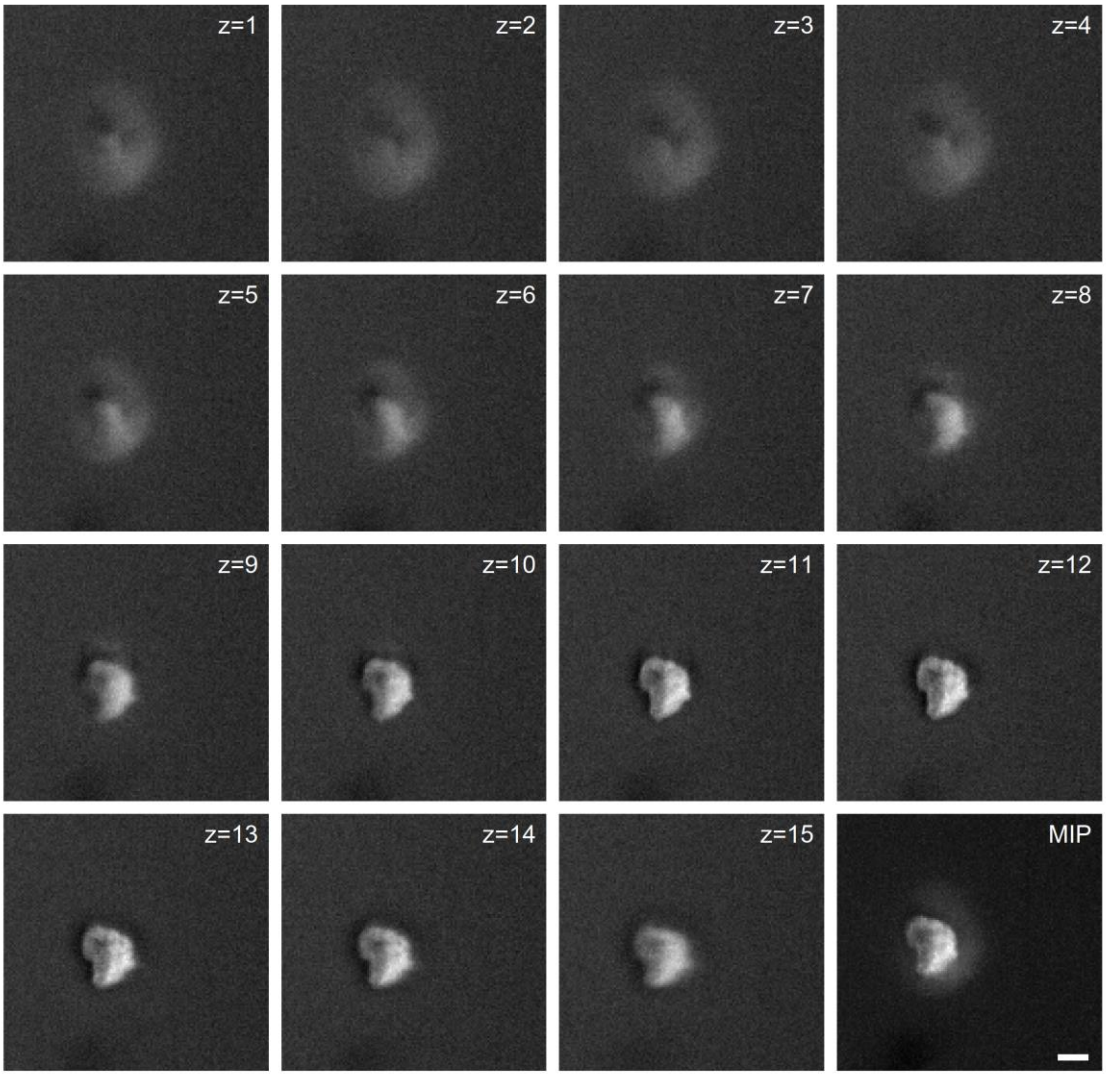

Supplemental Figure 10. Image stack and MIP of an exemplary crop. Z-stacks (z = 1 to z = 15) and the maximum intensity projection (MIP) of the same example crop are shown. Of note, halos surrounding the particles as seen in the MIP may be falsely detected as particles using traditional threshold methods. Scale bar length: 10 µm.

Suppl. Tab. 1: Repeated measurements of particle analysis using machine learning. Particle analysis of a model IgG exposed to human serum at t0 and t1. Instrument variability was defined by consecutive triplicate measurements of identically prepared samples at t0 and t1. The variability of sample preparation was measured by the analysis of 3 independelty prepared samples at t0 and t1. Each sample was analyzed once. Mean cumulative particle counts of 4 µL samples. n=3.

	instrument variability				sample preparation			
Particle size	IgG t0		IgG t1		IgG t0		IgG t1	
	Mean	CV [%]	Mean	CV [%]	Mean	CV [%]	Mean	CV [%]
≥2	131.7	5.1	329.7	77.2	245.0	44.5	263.7	42.9
≥5	69.7	17.3	168.0	75.9	121.0	35.7	126.7	23.9
≥10	13.3	49.9	75.7	104.7	41.0	20.8	43.0	22.2
≥25	0.3	-*	4.3	-*	0.3	-*	0.67	-*

*Only a few particles ≥25 µm were analyzed in one of the three samples at t0 and t1. Therefore, CV calculations were not of practical relevance.

Tracking the Physical Stability of Fluorescent-Labeled mAbs under Physiologic *In Vitro* Conditions in Human Serum and PBS

The following chapter has been published as research article in the European Journal of Pharmaceutics and Biopharmaceutics.

Joachim Schuster, Hanns-Christian Mahler, Atanas Koulov, Susanne Joerg, Andy Racher, Joerg Huwyler, Pascal Detampel, and Roman Mathaes.
Tracking the Physical Stability of Fluorescent-Labeled mAbs under Physiologic In Vitro Conditions in Human Serum and PBS
Eur J Pharm Biopharm. 2020, 152: 193-201
doi: 10.1016/j.ejpb.2020.04.014

The supplementary data was inserted into this chapter.

European Journal of Pharmaceutics and Biopharmaceutics 152 (2020) 193–201

Contents lists available at ScienceDirect

European Journal of Pharmaceutics and Biopharmaceutics

journal homepage: www.elsevier.com/locate/ejpb

Tracking the physical stability of fluorescent-labeled mAbs under physiologic in vitro conditions in human serum and PBS

Joachim Schuster[a,b], Hanns-Christian Mahler[a], Atanas Koulov[a], Susanne Joerg[a], Andy Racher[c], Joerg Huwyler[b], Pascal Detampel[b], Roman Mathaes[a,*]

[a] Lonza Pharma and Biotech, Drug Product Services, Basel, Switzerland
[b] University of Basel, Pharmacenter, Division of Pharmaceutical Technology, Basel, Switzerland
[c] Lonza Biologics plc, Slough, Berkshire, United Kingdom

ARTICLE INFO

Keywords:
In vivo stability
Developability
Serum stability
Protein aggregation
Post-administration modification
In vitro model

ABSTRACT

In recent years, the stability of biotherapeutics *in vivo* has received increasing attention. Assessing the stability of biotherapeutics in serum may support the selection of adequate molecule candidates. In our study, we compared the physical stability of 8 different monoclonal antibodies (mAbs) in phosphate-buffered saline (PBS) and human serum. mAbs were Alexa Fluor 488-labeled and characterized with respect to fragmentation, aggregation, and proteinaceous particle formation. Samples were analyzed using size-exclusion chromatography, light obscuration, and flow imaging. In addition, novel methods such as flow cytometry and fluorescence microscopy were applied. mAbs were selected based on their hydrophobicity and isoelectric point. All mAbs studied were inherently less stable in human serum as compared to PBS. Particle size and particle counts increased in serum over time. Interestingly, certain mAbs showed significant levels of fragmentation in serum but not in PBS. We conclude that PBS cannot replicate the physical stability measured in serum. The stability of labeled mAbs in human serum did not correlate with their hydrophobicity and isoelectric point . Serum stability significantly differed amongst the tested mAbs.

1. Introduction

The stability of biotherapeutics is monitored during various product-life cycle stages to ensure patient safety and product efficacy. Critical quality attributes in parenteral preparations in general, but especially for biologics, include aggregation, visible particles, subvisible particles (SbVPs), and other attributes that may affect product safety of efficacy. In addition to instability of biotherapeutics during production, storage (shelf-life stability), and administration (in-use stability), the stability of biotherapeutics may also be impaired in the human body, i.e. after administration (*in vivo* stability) [1]. Modifications occurring *in vivo* have been described as biotransformation [2] and post-administration modifications [1]. Previous studies have shown that the physiologic pH of 7.4 and a temperature of 37 °C can impair the physical [3] and chemical stability [4] of biotherapeutics such as monoclonal antibodies (mAbs). Moreover, numerous matrix components of human body fluids/compartments (e.g. electrolytes, enzymes, and reducing sugars) may affect protein stability [1]. Knowledge on the fate of biotherapeutics after administration, particularly their physical stability, is however limited. To date, physical *in vivo* destabilization events of administered biotherapeutics have been hypothesized to be caused by steric exclusion (*in vivo* aggregation/precipitation) [5], salting-out effect as a consequence to the pH shift [6], enzymatic degradation (*in vivo* fragmentation) [7–9], co-precipitation due to aggregation of endogenous proteins [10], and the complex interplay between an infused biotherapeutic and *in vivo* fluid dynamics [11]. Due to the variety of factors in the human body that may create stresses for proteins, *in vivo* degradation of a biotherapeutic may significantly differ from degradation events in the drug substance and drug product. Thus, *in vivo* stability of biotherapeutics should be analyzed under conditions most adequately simulating the human body. Such studies can be carried out *in vitro* by spiking the

Abbreviations: AF, Alexa Fluor 488; AU, absorbance unit; CV, coefficient of variation; EU, emission unit; FSC, forward scatter; HMW, high-molecular weight; IgG, immunoglobulin G; LMW, low-molecular weight; LO, light obscuration; mAb, monoclonal antibody; PBS, phosphate-buffered saline; pI, isoelectric point; SD, standard deviation; SEC, size-exclusion chromatography; SEC-FLD, size-exclusion chromatography with fluorescence detection; SSC, side scatter; SbVP, subvisible particle

* Corresponding author.
E-mail address: roman.mathaes@lonza.com (R. Mathaes).

https://doi.org/10.1016/j.ejpb.2020.04.014
Received 13 January 2020; Received in revised form 18 April 2020; Accepted 22 April 2020
Available online 01 May 2020
0939-6411/

biotherapeutic of interest into animal or human body fluids.

Due to the complexity of biological fluids and the lack of established analytical methods, assessing the *in vivo* stability of biotherapeutics is challenging [2]. For example, human serum contains a total protein concentration of 55–80 mg/mL [12]. Therefore, typical analytical methods have limited suitability to assess the stability of a biotherapeutic in biological fluids as they often lack specificity, i.e. the ability to differentiate between endogenous immunoglobulins G (IgGs) and the therapeutic IgG. This led to the development of novel methods to assess the *in vivo* stability of biotherapeutics [13,14]. Alternatively, previous studies used protein-free fluids, such as phosphate-buffered saline (PBS) under physiologic conditions, as substitution medium for plasma/serum [15–20].

In this study, we (i) evaluated the ability of typical analytical methods and novel developed methods to assess aggregation, fragmentation, and particulate formation of fluorescently labeled mAbs in biological fluids, (ii) compared the stability of biotherapeutics in human serum versus PBS, and (iii) assessed if certain molecular properties of the protein (i.e. hydrophobicity, isoelectric point (pI)) correlate to *in vivo* protein stability.

We used 8 mAbs differing in their molecular properties. In order to enable detectability in the serum matrix, we labelled the mAbs with Alexa Fluor 488 (AF) and characterized degradation after exposure to PBS (P0) and human serum (S0), as well as after an incubation in PBS (P1) and human serum (S1) at pH 7.4 and 37 °C for 5 days. As a prerequisite, we evaluated if labelling would impact biophysical properties of the mAbs, in order to ensure that the simulated *in vivo* stability results are not altered. Results obtained in serum and PBS were also compared to control samples of AF-labeled mAbs stored in histidine-HCl buffer, pH 6.0 (H0). All samples were analyzed with light obscuration (LO), flow imaging, size-exclusion chromatography with fluorescence detection (SEC-FLD), flow cytometry, and fluorescence microscopy.

2. Materials and methods

2.1. Material

Eight mAbs, formulated in 20 mM histidine-HCl, pH 6.0, were provided by Lonza Biologics plc (Slough, UK). Alexa Fluor 488 NHS succinimidyl ester, sodium azide, and PBS pH 7.4 were purchased from Sigma-Aldrich (Buchs, Switzerland). Human male AB serum was purchased from BioIVT (West Sussex, UK). Hydrophilic PVDF filters with a mesh-size of 0.22 µm were purchased from Merck Millipore (Darmstadt, Germany).

2.2. Labeling and exposure to fluids

mAbs were labeled with Alexa Fluor 488 (AF) at a molar mAb:dye ratio of 1:4 as described by the manufacturer. AF-labeled mAbs were purified of excessive dye using Princeton pro spin columns (LubioScience, Zurich, Switzerland). Princeton pro spin columns were hydrated with 20 mM histidine-HCl (pH 6.0) to buffer-exchange back to the initial formulation buffer. Moreover, AF is an amine-specific fluorescent dye (succinimidyl ester) and thus may react with histidine. All fluids and mAbs were prepared under sterile conditions and 0.22 µm filtered before mixing. Then, 0.2 mg/mL AF-labeled mAbs were spiked into 20 mM histidine-HCl (pH 6.0), PBS (pH 7.4), and human serum (pH 7.4) (Fig. 1). mAbs were directly analyzed after exposure to histidine-HCl (H0), PBS (P0), and serum (S0) as well as after an incubation at 37 °C for 5 days in PBS (P1) and serum (S1). As control samples, all 3 fluids (histidine-HCl, PBS, and human serum) were measured without spiking of AF-labeled mAbs (His, PBS, and Serum) and after spiking of AF without a mAb (His + AF, PBS + AF, Serum + AF). The initial pH of serum at 8.0 was adjusted and maintained at 7.4 using 6.7% CO2 and 37 °C in an incubator to closely resemble the conditions encountered in patients. A final concentration of 0.1% (w/v) sodium azide was added to all fluids to improve the stability of serum (Suppl. Fig. 1A and B). Previous studies stated the prevention of bacterial growth using 0.0065% [21], 0.02% [22], or 0.1% [15,18] sodium azide in serum/plasma.

2.3. Light obscuration

The measurement follows in the assay as described in the pharmacoepeia (Ph Eur 2.9.19), however, with modified sample volume. SbVPs were measured using a HIAC 9703 + equipped with a HRLD-150 detector (Beckman Coulter, Brea, CA). Samples were analyzed using 4 runs with each 0.2 mL. The first run was discarded and the average of the remaining runs was reported. The system was set up with a 1 mL syringe and a flow rate of 10 mL/min. System suitability test was performed using 5 µm COUNT-CAL Count Precision Size Standard beads (Thermo Fisher Scientific, Waltham, MA).

2.4. Flow imaging

A FlowCAM VS1 (Fluid Imaging Technologies, Scarborough, ME) equipped with an 80 µm field of view flow cell, 1 mL syringe, and a 10x NA/0.3 UPLFLN objective (Olympus, Tokyo, Japan) was used. A sample volume of 0.3 mL was analyzed at a flow rate of 0.1 mL/min. System suitability involved the analysis of 5 µm NIST traceable standards (Thermo Fisher Scientific) for particle size and COUNT-CAL Count Precision Size Standards (Thermo Fisher Scientific) to verify particle count. VisualSpreadsheet software 4.2.52 (Fluid Imaging Technologies) was used to acquire and process data.

2.5. Size-exclusion chromatography with fluorescence-detection

SEC-FLD was performed using a TSKgel SWXL type guard column and a TSKgel G3000SWXL column (Tosoh Biosiences, Griesheim, Germany) connected to a Waters Alliance e2695 HPLC system equipped with an UV/Vis and fluorescence detector (Waters, Eschborn, Germany). The column temperature was maintained at 25 °C. The mobile phase was 0.2 M sodium phosphate pH 7.0 at a flow rate of 0.5 mL/min. An injection volume of 5 µL at 0.2 mg/mL labeled-mAb was used. Absorbance was measured at 210 nm, whereas fluorescence was set to excitation of 495 nm and emission of 519 nm. Chromatograms were processed and exported from Empower 3 (Waters, Milford, MA).

2.6. Flow cytometry

A LSR Fortessa Analyzer (BD Bioscience, Franklin Lakes, NJ) equipped with a 488 nm laser and bandpass filters at 512/25 nm and 542/27 nm was used for flow cytometry analysis. Detector gains were optimized using silica beads with diameters of 2 µm, 5 µm, and 10 µm (Thermo Fisher Scientific) to allow detection of protein particles ≤ 10 µm. Forward scatter (FSC) was set to 265 V, side scatter (SSC) to 240 V, AF to 390 V, and Ex488 to 471 V. For each detector the integral (area) of the pulse was collected. Data was collected at a flow rate of 18.5 ± 0.1 µL/min for 2 min for each sample. Data was collected using the BD FACSDiva 8.0.1 software and analyzed with the FlowJo 10.5.3 software (FlowJo LLC, Ashland, OR).Widefield fluorescence microscopyAn inverted widefield microscope (FEI “MORE”, Munich, Germany) was used for fluorescence imaging based on a previously described method [23]. Briefly, an entire volume of 4 µL of each mAb at H0, P0, S0, P1, and S1 as well as control samples was imaged. The microscope was equipped with an ORCA flash 4.0 cooled sCMOS camera (Hamamatsu Photonics, Hamamatsu, Japan), U Plan S Apo 10x NA 0.4 air objective, and LED illumination (Lumencore SpectraX) at 470/24 nm (excitation) and 517/20 nm (emission). Samples were put on a 35 mm glass bottom dish (14 mm glass diameter, # 1.5, MatTek

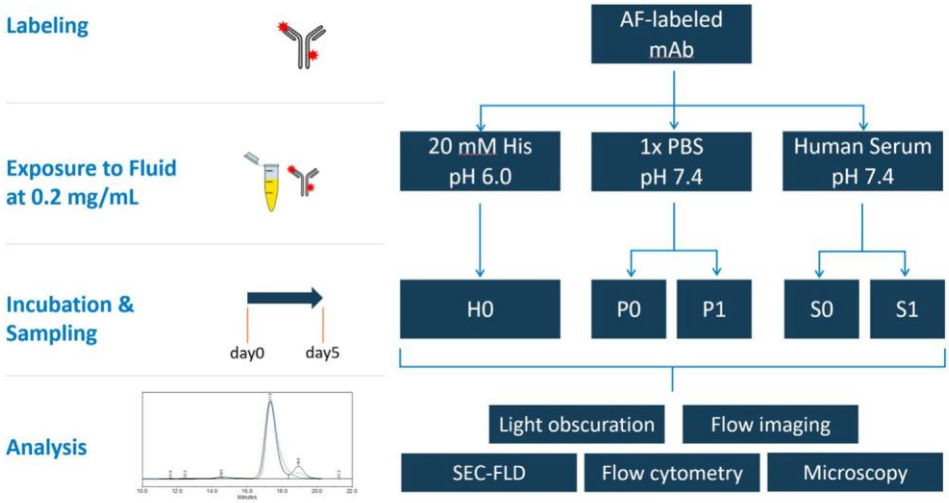

Fig. 1. Experimental workflow. Labeling of mAbs with Alexa Fluor 488 (AF). Exposure of labeled mAbs to 3 different fluids (histidine-HCl, PBS, and human serum). Control samples in histidine-HCl were measured after exposure (H0). Samples were measured after exposure to PBS (P0) and human serum (S0) and after incubation at pH 7.4 and 37 °C for 5 days (P1 and S1). Samples were characterized by light obscuration, flow imaging, size-exclusion chromatography with fluorescence detection (SEC-FLD), flow cytometry, and fluorescence microscopy.

Corporation, Ashland, MA) and covered with a 13 mm cover glass (VWR, Dietikon, Switzerland). The sample volume was covered using 21 × and 21 y tile scans as well as 10 to 15 z-stacks depending on the depth of the sample. z-stacks were acquired in 3 µm increments. Exposure time was set at 100 ms. Several thousand images were processed for each sample. Images were processed using Fiji [24]. Uneven illumination of individual tiles were corrected using BaSiC [25]. A maximum intensity z-projection was applied to all tiles which were stitched and fused with the Grid/Collection stitching plugin [26]. The background was further corrected by applying a strong Gaussian-blur. Particles size and particle shape were detected by machine learning using Interactive Learning and Segmentation Toolkit (ilastik version 1.3.2) [27]. A model was trained using 25 cropped areas (each containing 6 to 9 tiles) of different samples.

2.7. Repeatability experiments

Flow cytometry and fluorescence microscopy method performance was assessed by preparing 1 model mAb sample which was measured 3 times at S0 and S1. The impact of sample preparation was assessed by preparing a triplicate of the same model mAb. Each preparation was measured once at S0 and S1. Data was plotted using Origin 9.6 (OriginLab, Northhampton, MA).

3. Results

The composition of the fluids used in this study differs substantially. PBS is a protein-free, non-bicarbonate buffer, containing only 4 electrolytes present in serum. Moreover, the electrolyte concentration and thus osmolality differs from that in serum (Table 1). Eight different mAbs were selected based on their differences in pI and hydrophobicity to cover a broad range of different physicochemical properties. mAb1 to mAb4 showed pI values < 7.4, close to 7.4, and > 7.4 while their hydrophobicity values were in a narrow range of 13.4 to –16.9 min (Table 2). mAb5 to mAb8 showed low (12.9 min), mid-range (17.7 min), and high hydrophobicity values (24.0 and 33.2 min) with a similar pI. Moreover, all mAbs showed a similar degree of labeling. Each fluid was spiked with AF-labeled mAbs (Fig. 1).

3.1. Particle analysis using light obscuration and flow imaging

Particle analysis using LO and flow imaging showed that SbVP levels at S0 appeared to be consistently greater than those at H0, P0, and P1 (Fig. 2 and Suppl. Fig. 3). All samples at S1 (2 serum controls and 8 serum samples containing a mAb) showed significant levels of SbVPs. mAb4 and mAb5 showed the highest particle counts at S1 using LO and

Table 1
Experimental conditions and nominal composition of the fluids used in this study.

	20 mM histidine-HCl (control samples)	PBS	Human Serum
Experimental conditions			
Temperature (°C)	25	37 °C	37 °C
pH	6.0	7.4	adjusted to 7.4 original: 8.0
AF-labeled mAb (mg/mL)	0.2	0.2	0.2
Incubation period (days)	0	0 and 5	0 and 5
Nominal composition			
Osmolality (mOsm/kg)	–	293[a]	317
Sodium (mM)	–	157.0[a]	164.0
Chloride (mM)	–	154.0[a]	113.0
Potassium (mM)	–	1.1[a]	3.7
Phosphorus (mM)	–	4.0[a]	1.0
Bicarbonate (mM)	–	–	21–28[b]
Magnesium (mM)	–	–	0.8–1.2[b]
Calcium (mM)	–	–	> 3.75
Glucose (mM)	–	–	5.1
Uric acid (mg/mL)	–	–	0.04
Blood urea nitrogen (mg/mL)	–	–	0.12
Albumin (mg/mL)	–	–	32
Endogenous protein, total (mg/mL)	–	–	51

Unless otherwise stated, values were provided by the vendor.
Serum was collected from healthy male donors of the AB serotype.
[a] Theoretical calculation of weighed portion.
[b] Laboratory reference values [12].

Table 2
Properties of monoclonal antibodies.

Molecule name	Isotype	pI[a]	HIC (min)[b]	Degree of Labeling[c]
mAb1	IgG1λ	6.8	13.4	1.5
mAb2	IgG4κ	7.5	16.4	1.7
mAb3	IgG1λ	7.8	16.9	1.9
mAb4	IgG1λ	9.5	15.3	2.1
mAb5	IgG1κ	9.2	12.9	1.9
mAb6	IgG1κ	9.1	17.7	1.9
mAb7	IgG1κ	9.1	24.0	2.0
mAb8	IgG1κ	9.3	33.2	2.0

All mAbs were stored in 20 mM histidine-HCl buffer, pH 6.0.
[a] Isoelectric point (pI). Theoretical calculation.
[b] Measured by hydrophobic interaction chromatography (HIC).
[c] Measured by UV–Vis spectroscopy and expressed as number of molecules dye per molecule mAb.

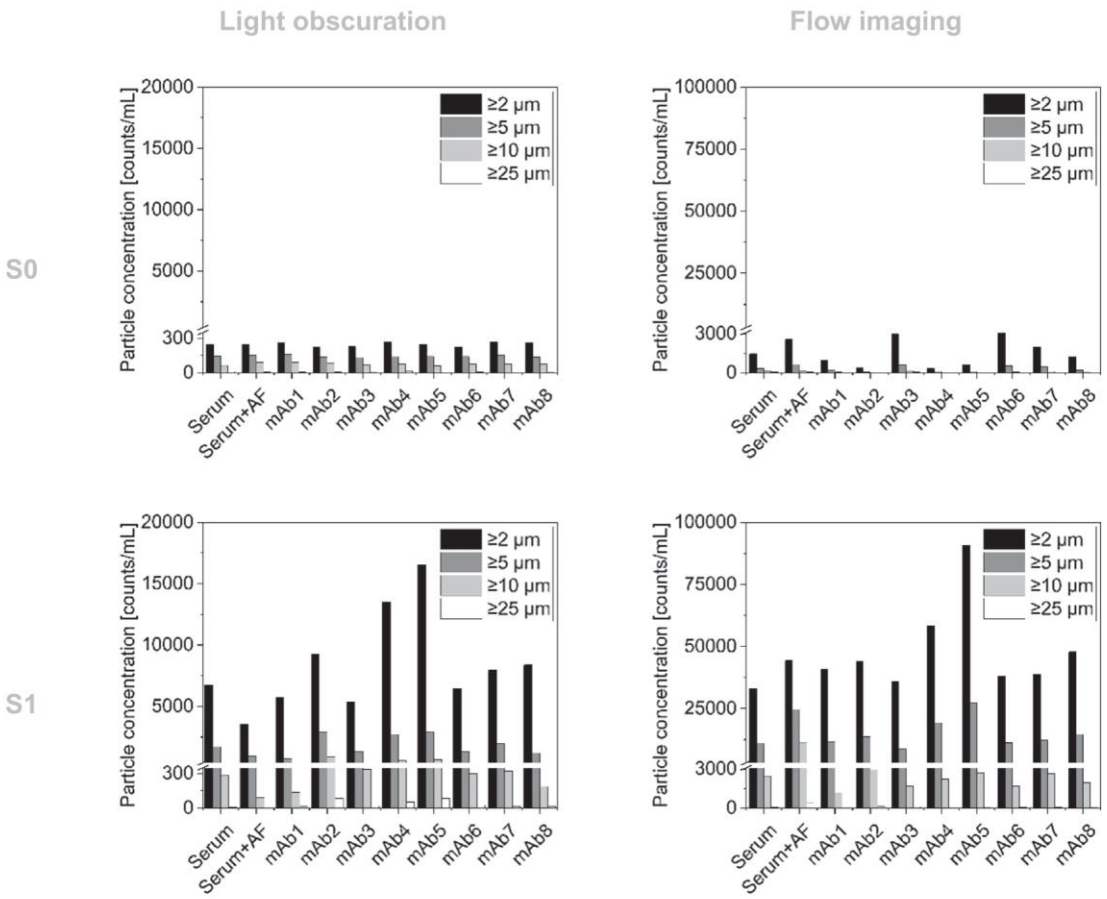

Fig. 2. Subvisible particles. (A) Analysis of human serum samples after preparation (S0) and after incubation at 37 °C for 5 days (S1) using light obscuration (left column) and flow imaging (right column row). Control sample without AF-labeled mAb, Serum, control sample spiked with AF, Serum + AF. n = 1.

flow imaging. As expected, the results obtained with LO and flow imaging show similar trends of particle levels, however both methods did not allow differentiating between particles of serum-related protein molecules and those of labeled-mAbs. Moreover, assessment of particle morphology of flow imaging data using image analysis algorithms did not allow differentiating between endogenous serum particles and those of the therapeutic mAb (data not shown).

3.2. Size-exclusion chromatography

The developed SEC-FLD method enabled discriminating between AF-labeled mAbs and endogenous serum proteins. One particular concern during incubation in serum at pH 7.4 was binding of excessive fluorescent dye (stemming from the labeling process) to highly abundant endogenous serum proteins (e.g. 35–55 mg/mL albumin and 6–13 mg/mL IgGs [12]). Suppl. Fig. 4 shows a comparison of mAb2, mAb3, and the serum control sample spiked with AF, each at S1.The signal intensity in the serum control sample is negligible in comparison to that of the AF-labeled mAbs. Moreover, despite mAb2 containing the highest concentration of unbound AF (retention time: 25 min) no fragmentation was observed in serum, which further confirms that no unspecific binding of AF to serum proteins was observed.

Fig. 3B shows that mAb7 contained fragments in S0 and S1 but not in H0. HMW species of all 8 mAbs increased from H0 to S0, i.e. aggregation occurred within 16 h of exposure to serum (Fig. 3B). Moreover, the majority of mAbs showed an increase of HMW species in serum over time (S0 to S1). Five mAbs (mAb1, mAb4, mAb5, mAb6, and mAb7) showed quite pronounced fragmentation in serum. Particularly, mAb6 and mAb7 showed already high levels of fragmentation at S0, which increased as a function of time in serum (S0 to S1). LMW species of mAb7 increased from 0.08% at H0 to 12.81% at S0 and 21.13% at S1. Interestingly, LMW species of mAb7 were not detectable in PBS. LMWs species of 0.03% and 0.22% were measured at P0 and P1. mAb2, mAb3, and mAb8 showed < 0.15% and < 0.6% of LMW species at S0 and S1.. All mAbs were stable in PBS showing comparable values of LMW species and HMW species at P0 and P1 compared to H0 (Fig. 3C). We believe the decrease of HMW species from H0 to P0 and P1 for most mAbs was within the method variability. However, certain mAbs (e.g., mAb7) showed unexpectedly low values in PBS, which cannot be explained.

3.3. Flow cytometry

Autofluorescence of endogenous serum particles, which formed in control samples (Serum and Serum + AF) at S1 increased by particle size. Endogenous serum particles showed significantly lower fluorescence intensity than particles of AF-labeled mAbs at S0 and S1 (Fig. 4A). Adjusting the AF:SSC gate accordingly enabled discriminating between endogenous serum particle (autofluorescence) and particles of AF-labeled mAbs. The same method was applied for all samples at H0, P0, P1, and S0.

The majority of AF-labeled mAb particles were < 2 µm. SSC showed better separation of silica beads with a diameter of 2 µm, 5 µm, and 10 µm than FSC. Therefore, particle size was determined by SSC due to a higher sensitivity at this size range than FSC as previously reported [13]. Additionally, we analyzed all samples with the FSC and confirmed the same trend observed with the SSC (data not shown).

Fig. 4B summarizes the flow cytometry counts measured within the AF:SSC gate of samples spiked with mAbs and control samples without a mAb at S0 and S1. All mAbs were stable at P0 and P1 and showed no

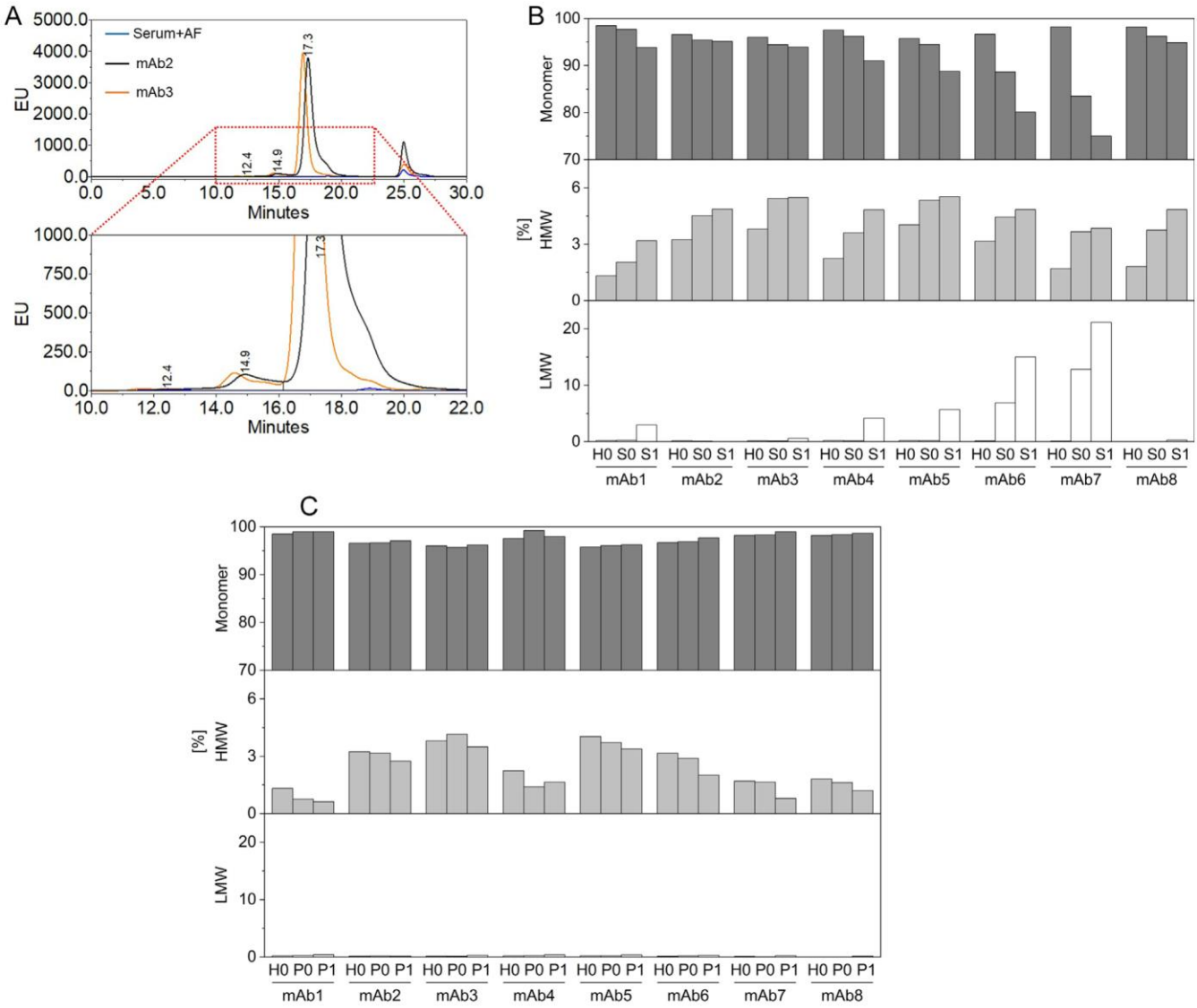

Fig. 3. Analysis of mAbs using SEC. (A) AF-labeled mAb7 (exemplary) measured in H0 (blue), in S0 (orange) and S1 (black). (B) Analysis of mAbs at H0, S0, and S1. (C) Analysis of mAbs at H0, P0, and P1. Fluorescence was measured at 495/519 nm. Emission units, EU; High-molecular weight, HMW; Low-molecular weight, LMW. (For interpretation of the references to colour in this figure legend, the reader is referred to the web version of this article.)

significant increase of counts to those obtained at H0 (Suppl. Fig. 5). Whereas an increase of counts was measured at S0, which increased over time (S1). mAb2, mAb4, mAb6, and mAb8 showed the highest level of counts at S1. Fig. 4C shows the mean intensity of SSC measured within the AF:SSC gate and thus relates to particle size at S0 and S1. With the exception of mAb1, particle size increased in serum over time. While lower counts were measured for mAb3 and mAb5, the mean SSC intensity of these mAbs were the highest, suggesting a larger particle size.

3.4. Fluorescence microscopy

Fig. 5 shows that both serum control samples (S and S + AF) contain lower particle counts than the serum samples containing the AF-labeled mAb at S0 and S1. The results confirmed the increase of particle counts and particle size in serum over time as observed with all other methods. In line with our previous observations, SbVP levels at H0, P0, and P1 were substantially lower than at S0 (data not shown).

3.5. Repeatability experiments

Three measurements of the same sample using flow cytometry resulted in a coefficient of variation (CV) of 4.9% and 4.4% at S0 and S1 (Table 3). The CV for fluorescence microscopy was measured at 7.6% and 81.1% at S0 and S1.

The variability of sample preparation resulted in a CV of 17.0% and 6.5% at S0 and S1 using flow cytometry. Using fluorescence microscopy a CV of 39.4% and 34.5% at S0 and S1 was measured. Total particle counts were used for CV calculations.

To verify serum results observed by SEC, we measured three independently prepared samples of mAb2 and mAb6, which showed substantial differences in their serum stability (Table 4). Triplicate measurements confirmed that mAb2 showed no fragmentation in serum at S0 and S1, whereas mAb6 showed fragmentation in all samples prepared. Variability measured for HMW and LMW species of the same mAb, particularly at S0, may be explained due to slightly varying time spans between exposure to serum and analysis time (< 16 h). Furthermore, we confirmed that the physiologic pH of serum (7.4) did not increase above 7.6 (Suppl. Fig. 1C), thus, confirming that all analyses were done under physiologic-like conditions.

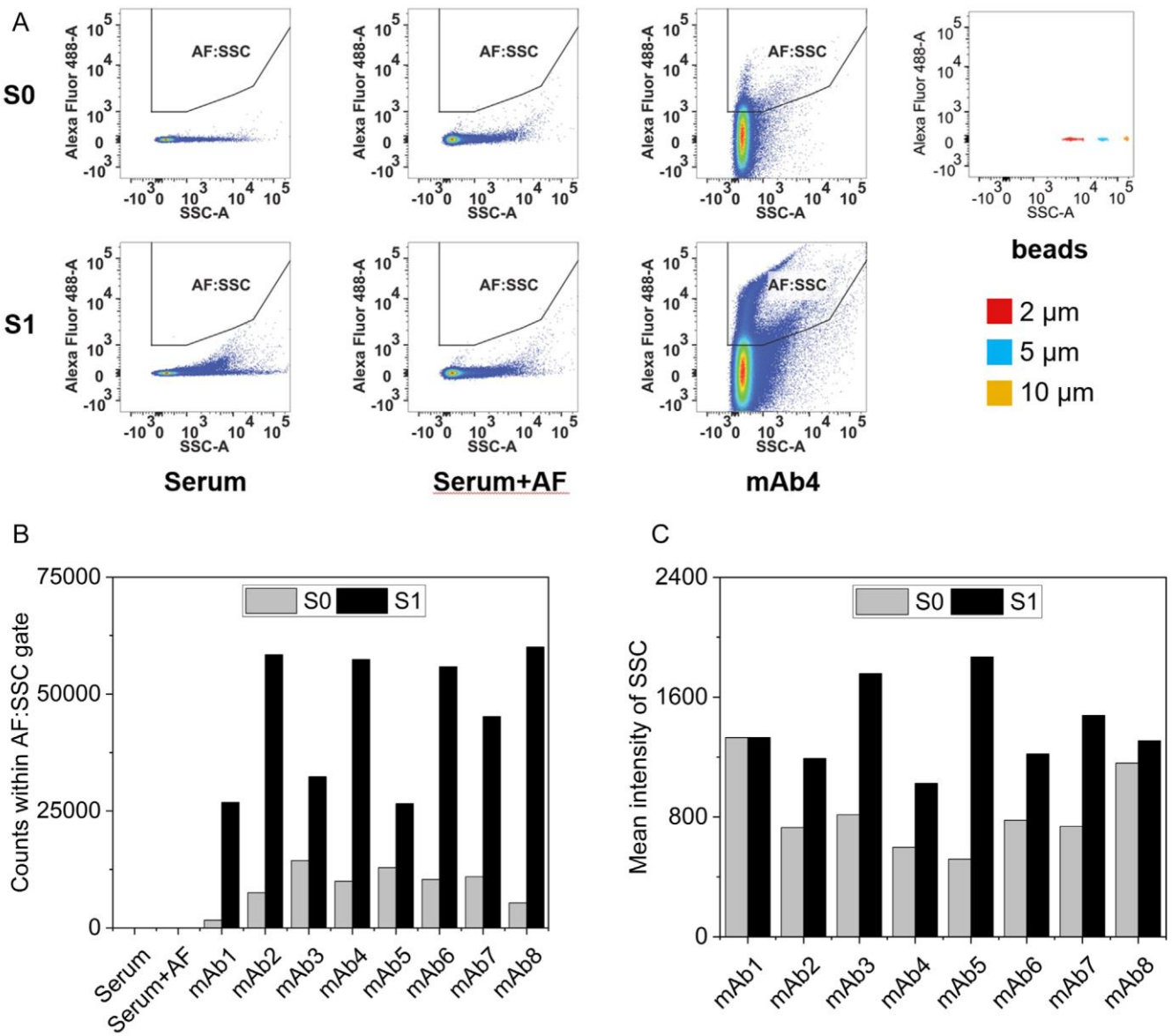

Fig. 4. Flow cytometry of mAbs in human serum. (A) Analysis of serum samples after preparation (S0; upper row) and after incubation at 37 °C for 5 days (S1; lower row). mAb4 is shown as a representative example. Event densities in 'logicle' plot are depicted from low (blue) to very high (red). (B) Total counts measured within the AF:SSC gate at S0 and S1. (C) Mean intensity of SSC measured within AF:SSC gate at S0 and S1. Serum sample without AF-labeled mAb, Serum; serum sample spiked with AF, Serum + AF. Signal intensity of Alexa Fluor 488-area, Alexa Fluor A488-A; side scatter, SSC. (For interpretation of the references to colour in this figure legend, the reader is referred to the web version of this article.)

3.6. Impact of labeling

The stability of unlabeled and AF-labeled mAbs each in histidine-HCl buffer were assessed by SEC (Fig. 6). The majority of mAbs showed little impact on HMW and LMW species. Most mAbs showed a decrease of LMW species upon labeling. Moreover, retention times of the monomeric peak of an unlabeled mAb at H0, AF-labeled mAb at H0, and AF-labeled mAb at S0 were compared by SEC-FLD (Suppl. Fig. 2). An earlier elution time of ca. 0.1 min for AF-labeled mAbs compared to its unlabeled counterpart can be attributed to the small increase in molecular weight (643.4 Da per molecule AF).

4. Discussion

Analytical methods generally used for biotherapeutic drug products (SEC, LO, and flow imaging) were used to assess aggregation, fragmentation, and particle formation of biotherapeutics in serum. However, LO and flow imaging were unable to discriminate between endogenous serum proteins and the spiked AF-labeled mAb. This was expected due to the lack of fluorescence detection and the low concentration of the spiked AF-labeled mAb (0.2 mg/mL) compared to the total serum protein concentration (51 mg/mL). The concentration of the spiked mAb in serum was based on clinical human serum concentration following intravenous administration [28]. Previous *in vitro* studies spiked mAb concentrations of 0.02–2 mg/mL [13,17].

PBS has been frequently used as substitution medium for plasma/serum due to its buffering capacity at the physiologic pH, osmolality, and protein-free composition [15–20]. The latter circumvents analytical challenges encountered with protein-rich body fluids such as serum. Spiking a biotherapeutic into PBS *in vitro* successfully predicted the rate of certain chemical modifications occurring in humans after administration (post-administration modifications) [1,15–18,28]. Contrary, PBS spiking studies have been rarely used to predict the physical stability of biotherapeutics *in vivo* [18]. In general, the predictability of

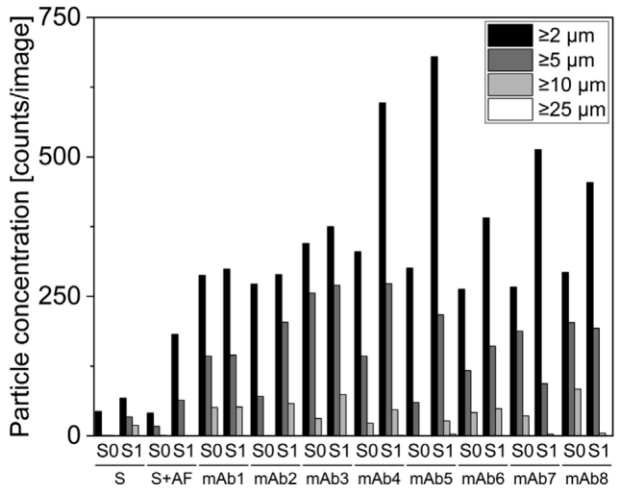

Fig. 5. Fluorescence microscopy of serum samples at S0 and S1. A total of 4 µL of each sample was imaged by widefield fluorescence microscopy after exposure to serum (S0) and after incubation at 37 °C and at a pH of 7.4 for 5 days (S1). Each sample scan comprised several thousand stitched and fused images to cover the sample volume of 4 µL. Particles were detected using machine learning. Serum sample without AF-labeled mAb, S; serum sample spiked with AF, S + AF.

Table 3
Instrument variability and variability of sample preparation.

			Flow cytometry [Counts within AF:SSC gate]	Fluorescence microscopy [Counts per image]
Instrument variability	S0	Mean ± SD	4947.0 ± 244.3	215.0 ± 16.4
		CV [%]	4.9	7.6
	S1	Mean ± SD	51339.7 ± 2262.7	577.7 ± 468.7
		CV [%]	4.4	81.1
Sample preparation	S0	Mean ± SD	6761.3 ± 1146.8	407.3 ± 160.5
		CV [%]	17.0	39.4
	S1	Mean ± SD	44720.0 ± 2887.9	434.0 ± 149.9
		CV [%]	6.5	34.5

n = 3; coefficient of variation, CV; standard deviation, SD. Volume analyzed using flow cytometry: 37 µL; volume analyzed using fluorescence microscopy: 4 µL.

Table 4
Variability of sample preparation. SEC of serum samples at S0 and S1.

		mAb2		mAb6	
		Mean ± SD [%]	CV [%]	Mean ± SD [%]	CV [%]
S0	Monomer	95.4 ± 0.4	0.4	88.7 ± 2.2	2.5
	HMW	4.5 ± 0.4	9.9	4.5 ± 0.7	15.7
	LMW	0.1 ± 0.1	105.4*	6.9 ± 1.7	24.0
S1	Monomer	95.1 ± 0.6	0.6	80.1 ± 0.9	1.1
	HMW	4.9 ± 0.6	11.4	4.8 ± 0.4	9.0
	LMW	0.0 ± 0.0	0.0	15.0 ± 0.7	4.9

* Only low values measured in one of the three samples. Thus, CV calculations were not of relevance. n = 3; coefficient of variation, CV; standard deviation, SD.

in vitro spiking studies in PBS is debated [1,15,18,28].

In our study, we observed that all mAbs were inherently less stable in human serum compared to PBS. For example, mAbs showed substantially higher counts of particles in serum than in PBS. Moreover, several mAbs fragmented after exposure to human serum but not after exposure to PBS. This indicates that other factors than temperature, pH, and osmolality impact on the physical *in vivo* stability of biotherapeutics. Interestingly, LMW and HMW species in all 8 mAbs were higher after exposure to serum (S0) than after incubation in PBS for 5 days (P1). Likewise, particle counts measured by flow cytometry were higher at S0 compared to P1.

To investigate the size of AF-labeled particles, i.e. mAb particles, we used flow cytometry allowing to detect protein particles down to ca. 500 to 1000 nm [29]. Our results suggested that the majority of mAb particles in serum were in the sub-µm range. Similarly, the majority of particles measured by fluorescence microscopy were < 5 µm. All 5 methods showed high particle counts/aggregates for all spiked mAbs in serum, which increased over time (S0 to S1), confirming the stability indicating properties of the methods. Particle images obtained by flow imaging and fluorescence microscopy confirmed a wide variety of particle morphology. Particles differed in terms of size, shape, and intensity (Suppl. Fig. 6).

We demonstrated that all 3 methods using fluorescence detection (SEC-FLD, flow cytometry, and fluorescence microscopy) were able to detect the AF-labeled mAbs and discriminate from serum control samples. Neither the autofluorescence of serum (e.g. due to bilirubin [30]), nor excessive AF stemming from the labeling procedure, interfered with the analysis.

Furthermore, we assessed the method performance and the impact of sample preparation. We measured an instrument variability for independent experiments (sample preparations and measurements) of ≤5% CV for flow cytometry, whereas a CV of 8% and 81% at S0 and S1 were measured by fluorescence microscopy. Although machine learning was used to simplify particle detection and avoid counting artifacts such as out-of-focus light, such challenges may still persist and can contribute to the instrument variability [23]. Moreover, the analysis volume of 4 µL is small compared to the other SbVP methods used, namely, LO (600 µL), flow imaging (300 µL), and flow cytometry (37 µL). Similar CVs were found when the method performance of LO and micro-flow imaging were assessed [31]. The variability of sample preparation was < 20% CV and < 40% CV using flow cytometry and fluorescence microscopy. While comparing absolute particle counts by different methods is generally challenging [31,32], we observed a 30- to 90-fold increase of particles counts from S0 to S1 by LO and flow imaging, whereas fluorescence microscopy showed only a twofold increase from S0 to S1. This may be explained as LO and flow imaging detect both endogenous and fluorescence particles whereas microscopy solely detected fluorescence particles.

While the reaction rate of post-administration modifications *in vitro* may differ from that in humans, degradation events observed in this study are conceivable due to the conditions encountered in the human body. Knowledge on *in vivo* fragmentation is limited. Vlasak et al reported several hot spots, which may lead to fragmentation under physiologic conditions, i.e. 37 °C and pH 7.4 [8]. We found no correlation between motifs (e.g. Asp-Gly, Asn-Ser, or Asn-Pro) and serum stability of mAbs used in this study. *In vivo* fragmentation has been argued to be caused by human serum enzymes [9] such as plasmin, neutrophil elastase, Factor XI, and kallikrein [7]. Although the redox conditions in blood are also regarded as a repair system, fragmentation may also occur at flexible regions such as the hinge region of mAbs [1,35]. Further *in vitro* studies simulating the *in vivo* conditions may help to identify which components or properties of the serum matrix lead to protein degradation. For example, exposing different mAb molecules to relevant human body fluids (e.g. serum, subcutaneous interstitial fluid) may allow comparing their *in vivo* stability and hence further strengthen the selection of lead candidates during the preclinical development phase beyond pharmacological (e.g. pharmacokinetic), safety (e.g. immunological), and binding/potency studies.

We intentionally chose 8 mAbs for this study, that closely relate (mostly IgG1), yet have wide differences in their biophysical properties (i.e. pI and hydrophobicity), to evaluate if and to what extent these properties would affect the physical *in vivo* stability. pI and hydrophobicity are often assumed to be relevant for different aggregation and particle-formation tendencies of proteins [33,34]. If the solution pH is

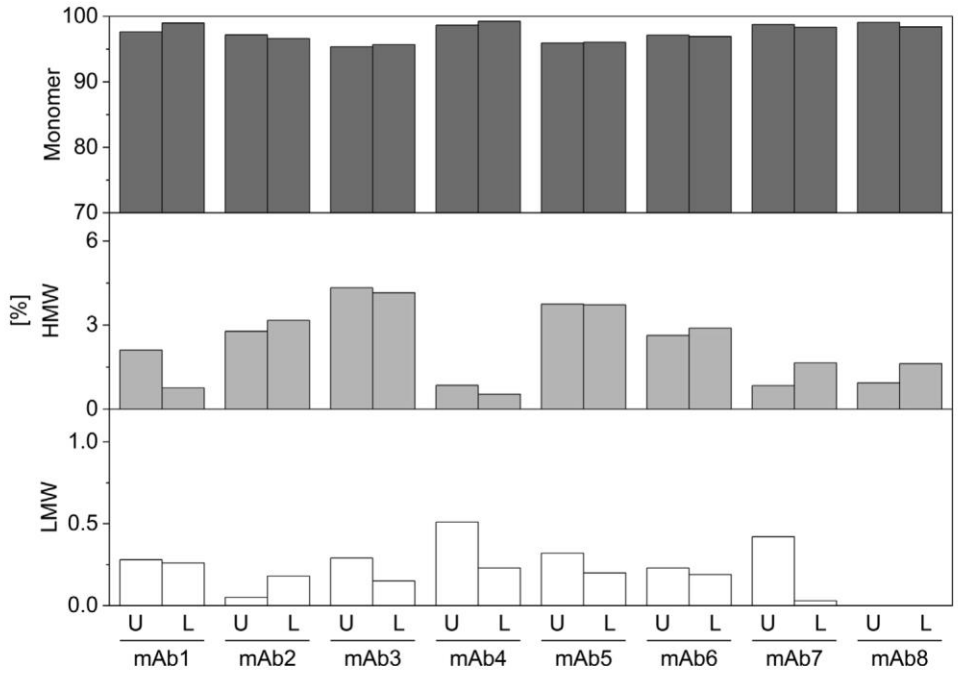

Fig. 6. Comparison of unlabeled mAbs and labeled mAbs using SEC. Analysis of unlabeled mAbs (U) and labeled mAbs (L). Absorbance units at 210 nm were measured for labeled and unlabeled mAbs. All samples were stored in 20 mM histidine-HCl buffer, pH 6.0.

close to a protein's pI, dipole–dipole interactions are likely to occur and likely cause protein precipitation and/or aggregation [33]. mAb2 and mAb3 had pI values close to the physiologic pH of 7.4 and should therefore show limited colloidal stability *in vivo*. Interestingly, no correlation between biotherapeutic properties and their stability in human serum was observed in our study. A drawback of studies assessing the physical stability of mAbs in biological fluids is related to the potential impact of a fluorescent dye on a protein's structure and properties. AF is negatively charged and may change the physicochemical properties of mAbs. Thus, it is of note that the physicochemical properties of unlabeled mAbs and the stability of the labeled mAbs in serum were correlated. Accelerated stability studies and analytical characterization of labeled and unlabeled biotherapeutics may help to determine the impact of labeling. We recently showed that the specific mAb used did not show differences in stability between its AF-labeled and unlabeled counterpart when assessed by LO, SEC, and differential scanning calorimetry [23].

While our SEC data did not show differences between labeled and unlabeled mAbs in this study, an impact of labeling on the structural stability and ultimately the behavior in serum cannot be excluded and should always be carefully considered and characterized.

5. Conclusion

Assessing the stability of biotherapeutics in human body fluids remains challenging. PBS showed pronounced differences in mAb stability compared to the results obtained in human serum and hence is considered poorly suitable. Thus, physical *in vivo* stability of biotherapeutics should be assessed in the intended human body fluid/compartment containing specific matrix components (e.g. enzymes [7,9]) and specific physiologic conditions (e.g. bicarbonate buffer [36]). However, the assessment of the protein analyte in the complex biological matrix provides various challenges. When using typical analytical methods, due to their lack of specificity, the protein analyte (mAb) cannot be detected in the background of endogenous proteins. We demonstrated that SEC-FLD, flow cytometry, and fluorescence microscopy are suitable methods to analyze the *in vivo* stability of biotherapeutics. All 3 fluorescence methods used in this study were stability indicating and allowed unambiguous detection of the biotherapeutic in serum. In particular, we were able to measure aggregation and fragmentation using SEC-FLD, while flow cytometry allowed insight into the microparticle formation of mAbs. Moreover, method performance of the developed methods (flow cytometry and fluorescence microscopy) was characterized and found to be suitable for the intended use. Although we did not identify biophysical properties of mAbs which predicted the physical *in vivo* stability, our data confirmed that different mAbs might show profound differences in their *in vivo* stability (e.g. fragmentation). Thus, the *in vivo* stability of mAbs should be considered and assessed during early pharmaceutical development stages, i.e. the lead candidate selection of biotherapeutics.

Declaration of Competing Interest

The authors declare that they have no known competing financial interests or personal relationships that could have appeared to influence the work reported in this paper.

Acknowledgments

The authors gratefully acknowledge the financial support as this work was partly funded by the UK Government Advanced Manufacturing Supply Chain Initiative (AMSCI) as part of the BioStreamline Project. We thank Dr. Olga Obrezanova from Lonza Biologics in Cambridge for the calculation of the isoelectric point of all mAbs. We would also like to thank Janine Boegli and Stella Stefanova from the FACS Core Facility (University of Basel) for their technical support on flow cytometry. Lastly, we thank the team of the Imaging Core Facility (University of Basel), in particular, Dr. Kai Schleicher for the technical support for fluorescence microscopy analysis and data processing.

Appendix A. Supplementary material

Supplementary data to this article can be found online at https://doi.org/10.1016/j.ejpb.2020.04.014.

References

[1] J. Schuster, A. Koulov, H.C. Mahler, P. Detampel, J. Huwyler, S. Singh, R. Mathaes, In vivo stability of therapeutic proteins, Pharm. Res. 37 (23) (2020).

[2] M.P. Hall, Biotransformation and in vivo stability of protein biotherapeutics: impact on candidate selection and pharmacokinetic profiling, Drug Metab. Dispos. 42 (2014) 1873–1880.

[3] W. Jiskoot, E.C. Beuvery, A.A. de Koning, J.N. Herron, D.J. Crommelin, Analytical approaches to the study of monoclonal antibody stability, Pharm. Res. 7 (1990) 1234–1241.

[4] L. Huang, J. Lu, V.J. Wroblewski, J.M. Beals, R.M. Riggin, In vivo deamidation characterization of monoclonal antibody by LC/MS/MS, Anal. Chem. 77 (2005) 1432–1439.

[5] H.M. Kinnunen, R.J. Mrsny, Improving the outcomes of biopharmaceutical delivery via the subcutaneous route by understanding the chemical, physical and physiological properties of the subcutaneous injection site, J. Control. Release 182 (2014) 22–32.

[6] Lobo, B., Lo S., Wang Y.J., Wong R.L., Method and formulation for reducing aggregation of a macromolecule under physiological conditions. US Patent 20140093493A1 (2014).

[7] R.V. Diemel, H.G. ter Hart, G.J. Derksen, A.H. Koenderman, R.C. Aalberse, Characterization of immunoglobulin G fragments in liquid intravenous immunoglobulin products, Transfusion 45 (2005) 1601–1609.

[8] J. Vlasak, R. Ionescu, Fragmentation of monoclonal antibodies, MAbs 3 (2011) 253–263.

[9] M. Werle, A. Bernkop-Schnurch, Strategies to improve plasma half life time of peptide and protein drugs, Amino Acids 30 (2006) 351–367.

[10] S. Luo, B. Zhang, Dextrose-mediated aggregation of therapeutic monoclonal antibodies in human plasma: implication of isoelectric precipitation of complement proteins, MAbs 7 (2015) 1094–1103.

[11] T. Arvinte, E. Poirier, C. Palais, Prediction of aggregation in vivo by studies of therapeutic proteins in human plasma, in: A.S. Rosenberg, B. Demeule (Eds.), Biobetters - Protein Engineering to Approach the Curative, Springer, New York, 2015, pp. 91–104.

[12] A. Kratz, M. Ferraro, P.M. Sluss, K.B. Lewandrowski, Case records of the Massachusetts General Hospital. Weekly clinicopathological exercises. Laboratory reference values, N. Engl. J. Med. 351 (2004) 1548–1563.

[13] V. Filipe, R. Poole, O. Oladunjoye, K. Braeckmans, W. Jiskoot, Detection and characterization of subvisible aggregates of monoclonal IgG in serum, Pharm. Res. 29 (2012) 2202–2212.

[14] H. Mach, T. Arvinte, Addressing new analytical challenges in protein formulation development, Eur. J. Pharm. Biopharm. 78 (2011) 196–207.

[15] S. Yin, C.V. Pastuskovas, L.A. Khawli, J.T. Stults, Characterization of therapeutic monoclonal antibodies reveals differences between in vitro and in vivo time-course studies, Pharm. Res. 30 (2013) 167–178.

[16] Y.D. Liu, A.M. Goetze, R.B. Bass, G.C. Flynn, N-terminal glutamate to pyroglutamate conversion in vivo for human IgG2 antibodies, J. Biol. Chem. 286 (2011) 11211–11217.

[17] Y.D. Liu, J.Z. van Enk, G.C. Flynn, Human antibody Fc deamidation in vivo, Biologicals 37 (2009) 313–322.

[18] I. Schmid, L. Bonnington, M. Gerl, K. Bomans, A.L. Thaller, K. Wagner, T. Schlothauer, R. Falkenstein, B. Zimmermann, J. Kopitz, M. Hasmann, F. Bauss, M. Haberger, D. Reusch, P. Bulau, Assessment of susceptible chemical modification sites of trastuzumab and endogenous human immunoglobulins at physiological conditions, Nat. Commun. Biol. 1 (28) (2018).

[19] A.M. Goetze, Y.D. Liu, T. Arroll, L. Chu, G.C. Flynn, Rates and impact of human antibody glycation in vivo, Glycobiology 22 (2012) 221–234.

[20] Q. Zhang, M.R. Schenauer, J.D. McCarter, G.C. Flynn, IgG1 thioether bond formation in vivo, J. Biol. Chem. 288 (2013) 16371–16382.

[21] X. Chen, Y.D. Liu, G.C. Flynn, The effect of Fc glycan forms on human IgG2 antibody clearance in humans, Glycobiology 19 (2009) 240–249.

[22] J.E. Battersby, V.R. Mukku, R.G. Clark, W.S. Hancock, Affinity purification and microcharacterization of recombinant DNA-derived human growth hormone isolated from an in vivo model, Anal. Chem. 67 (1995) 447–455.

[23] J. Schuster, A. Koulov, H.C. Mahler, S. Joerg, J. Huwyler, K. Schleicher, P. Detampel, R. Mathaes, Particle analysis of biotherapeutics in human serum using machine learning, J. Pharm. Sci. 109 (5) (2020) 1827–1832.

[24] J. Schindelin, I. Arganda-Carreras, E. Frise, V. Kaynig, M. Longair, T. Pietzsch, S. Preibisch, C. Rueden, S. Saalfeld, B. Schmid, J.Y. Tinevez, D.J. White, V. Hartenstein, K. Eliceiri, P. Tomancak, A. Cardona, Fiji: an open-source platform for biological-image analysis, Nat. Methods 9 (2012) 676–682.

[25] T. Peng, K. Thorn, T. Schroeder, L. Wang, F.J. Theis, C. Marr, N. Navab, A BaSiC tool for background and shading correction of optical microscopy images, Nat. Commun. 8 (2017) 14836.

[26] S. Preibisch, S. Saalfeld, P. Tomancak, Globally optimal stitching of tiled 3D microscopic image acquisitions, Bioinformatics 25 (2009) 1463–1465.

[27] C. Sommer, C. Straehle, U. Kothe, F.A. Hamprecht, ilastik: interactive learning and segmentation toolkit, in: IEEE International Symposium on Biomedical Imaging: From Nano to Macro, 2011.

[28] N. Yang, Q. Tang, P. Hu, M.J. Lewis, Use of in vitro systems to model in vivo degradation of therapeutic monoclonal antibodies, Anal. Chem. 90 (2018) 7896–7902.

[29] H. Nishi, R. Mathas, R. Furst, G. Winter, Label-free flow cytometry analysis of subvisible aggregates in liquid IgG1 antibody formulations, J. Pharm. Sci. 103 (2014) 90–99.

[30] O.S. Wolfbeis, M. Leiner, Mapping of the total fluorescence of human blood serum as a new method for its characterization, Anal. Chim. Acta 167 (1985) 203–215.

[31] A. Rios Quiroz, J. Lamerz, T. Da Cunha, A. Boillon, M. Adler, C. Finkler, J. Huwyler, R. Schmidt, H.C. Mahler, A.V. Koulov, Factors governing the precision of subvisible particle measurement methods - a case study with a low-concentration therapeutic protein product in a prefilled syringe, Pharm. Res. 33 (2016) 450–461.

[32] K. Wuchner, J. Buchler, R. Spycher, P. Dalmonte, D.B. Volkin, Development of a microflow digital imaging assay to characterize protein particulates during storage of a high concentration IgG1 monoclonal antibody formulation, J. Pharm. Sci. 99 (2010) 3343–3361.

[33] E.Y. Chi, S. Krishnan, T.W. Randolph, J.F. Carpenter, Physical stability of proteins in aqueous solution: mechanism and driving forces in nonnative protein aggregation, Pharm. Res. 20 (2003) 1325–1336.

[34] S. Salgın, U. Salgın, S. Bahadır, Zeta potentials and isoelectric points of biomolecules: the effects of ion types and ionic strengths, Int. J. Electrochem. Sci. 7 (2012) 12404–12414.

[35] B. Moritz, J.O. Stracke, Assessment of disulfide and hinge modifications in monoclonal antibodies, Electrophoresis 38 (2017) 769–785.

[36] V.L. Linthwaite, J.M. Janus, A.P. Brown, D. Wong-Pascua, A.C. O'Donoghue, A. Porter, A. Treumann, D.R.W. Hodgson, M.J. Cann, The identification of carbon dioxide mediated protein post-translational modifications, Nat. Commun. 9 (2018) 3092.

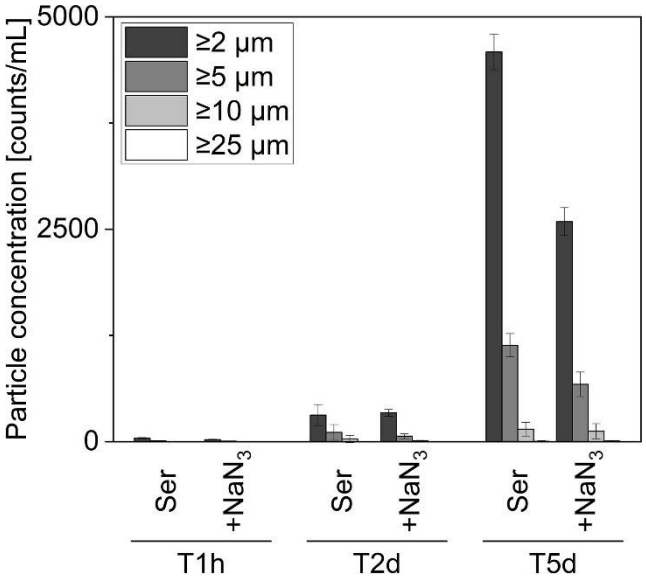

Supplementary Fig. 1A. Stability of human serum. A: Light obscuration of serum (Ser) vs. serum containing 0.1% (w/v) sodium azide (+NaN3). B: Turbidity of Ser vs. +NaN3. Measurements were done 1 h (T1h), 2 days (T2d), and 5 days (T5d) after preparation at 37°C and pH 7.4. C: pH measurement of serum. pH was measured in a closed and open vial outside a carbon dioxide incubator. Values are expressed as mean±standard deviation. n=3.

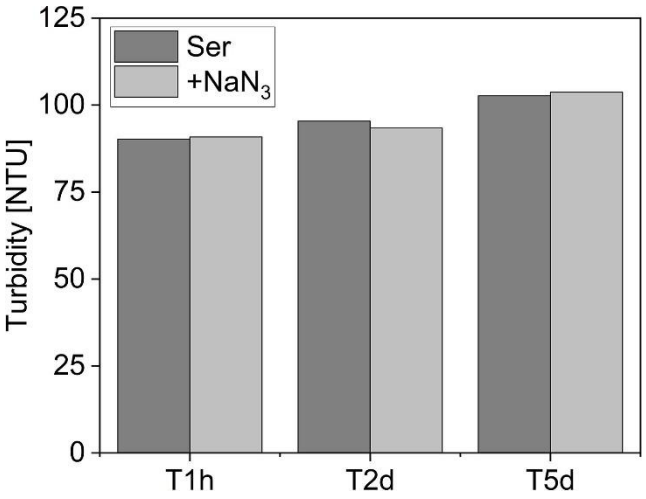

Supplementary Fig. 1B. Stability of human serum. B: Turbidity of Ser vs. +NaN3. Measurements were done 1 h (T1h), 2 days (T2d), and 5 days (T5d) after preparation at 37°C and pH 7.4.

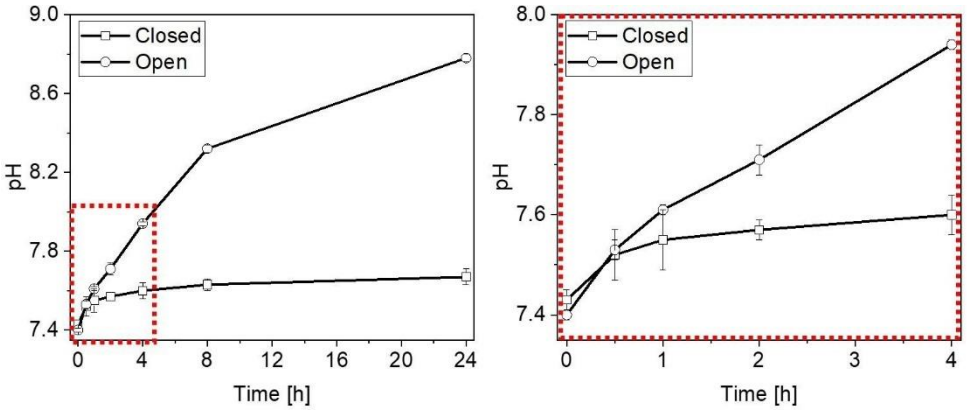

Supplementary Fig. 1C. Stability of human serum. C: pH measurement of serum. pH was measured in a closed and open vial outside a carbon dioxide incubator. Values are expressed as mean±standard deviation. n=3

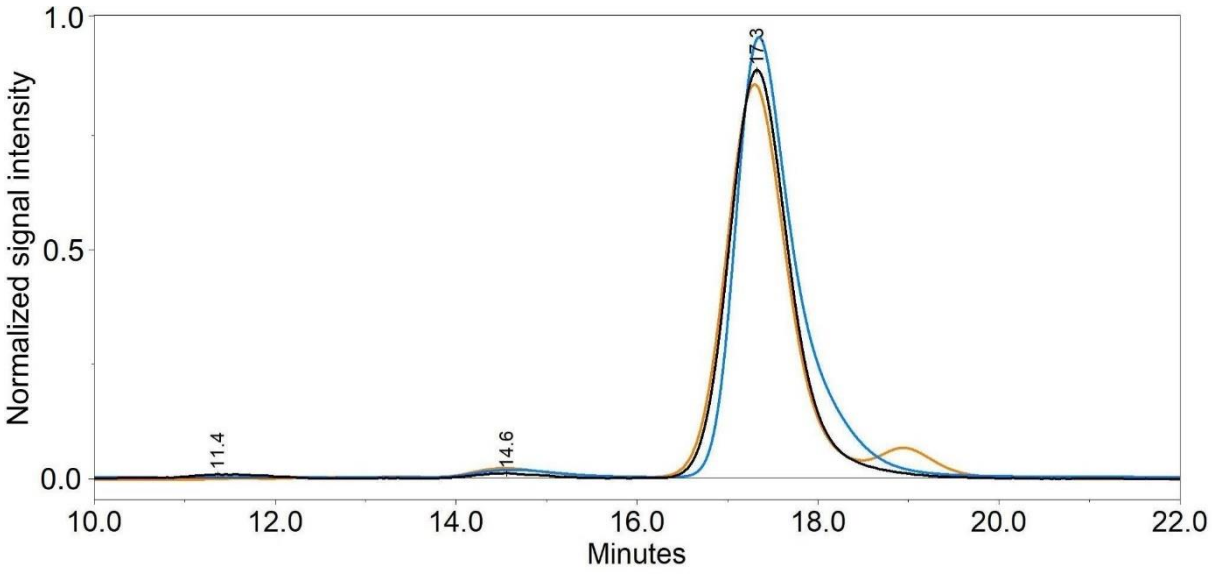

Supplementary Fig. 2. Comparison of retention time of unlabeled mAb and labeled mAb by SEC. Unlabeled mAb at H0 (blue), AF-labeled mAb at H0 (black), and AF-labeled mAb at S0 (orange). Signal intensity was normalized to the peak at 17.3 min. Retention time of the monomer peak was measured at 17.4 min (blue), 17.3 min (black), and 17.3 min (orange). Fluorescence of AF-labeled mAbs was measured at 495/519 nm. UV of unlabeled mAb was measured at 210 nm. mAb6 is shown as a representative example.

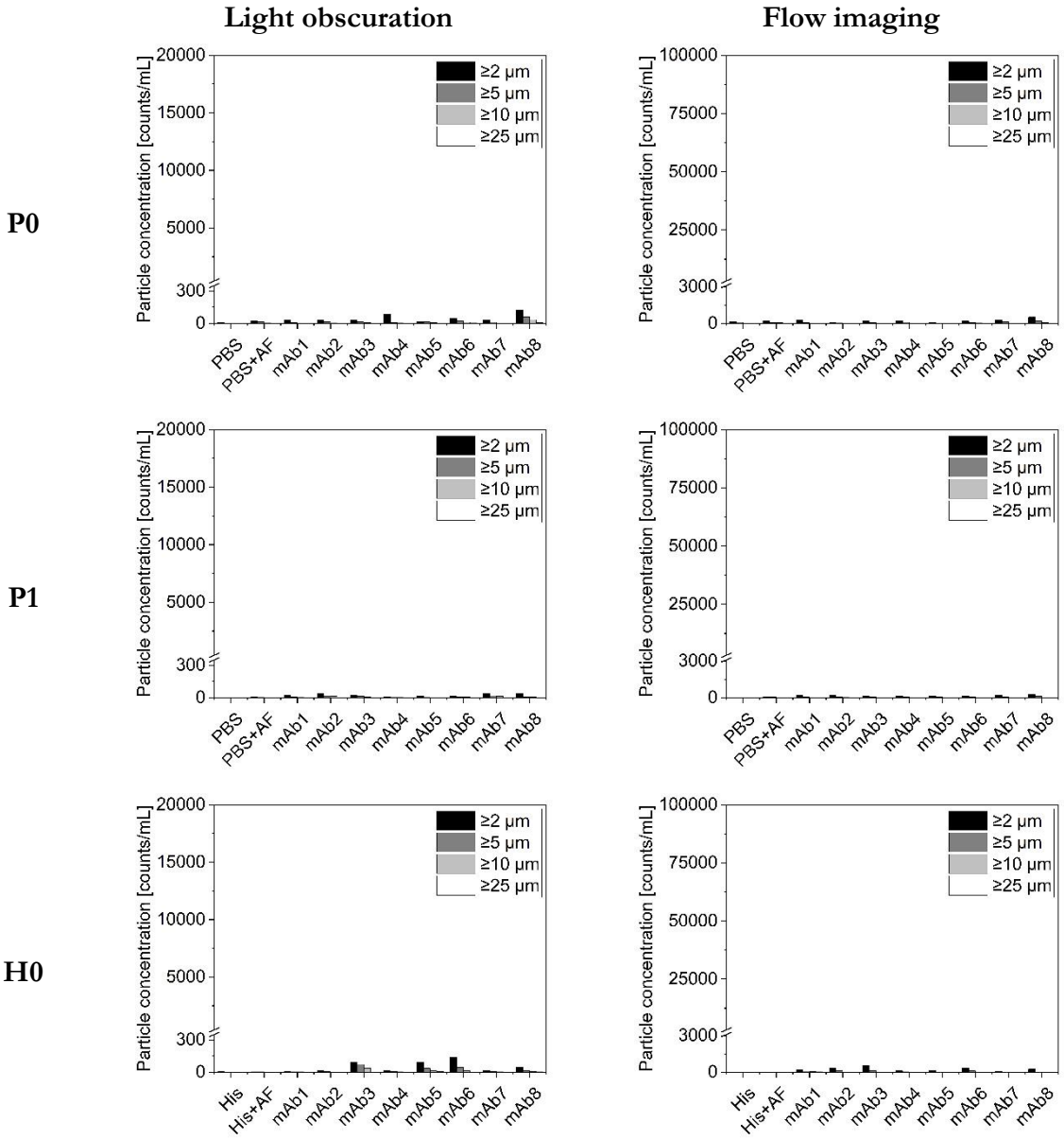

Supplementary Fig. 3. Subvisible particles. A: Analysis of PBS samples after preparation (P0), after incubation at 37°C for 5 days (P1) and after preparation in histidine-HCl (H0) using light obscuration (left column) and flow imaging (right column). Control sample without AF-labeled mAb, PBS and His; control sample spiked with AF, PBS+AF and His+AF. n=1.

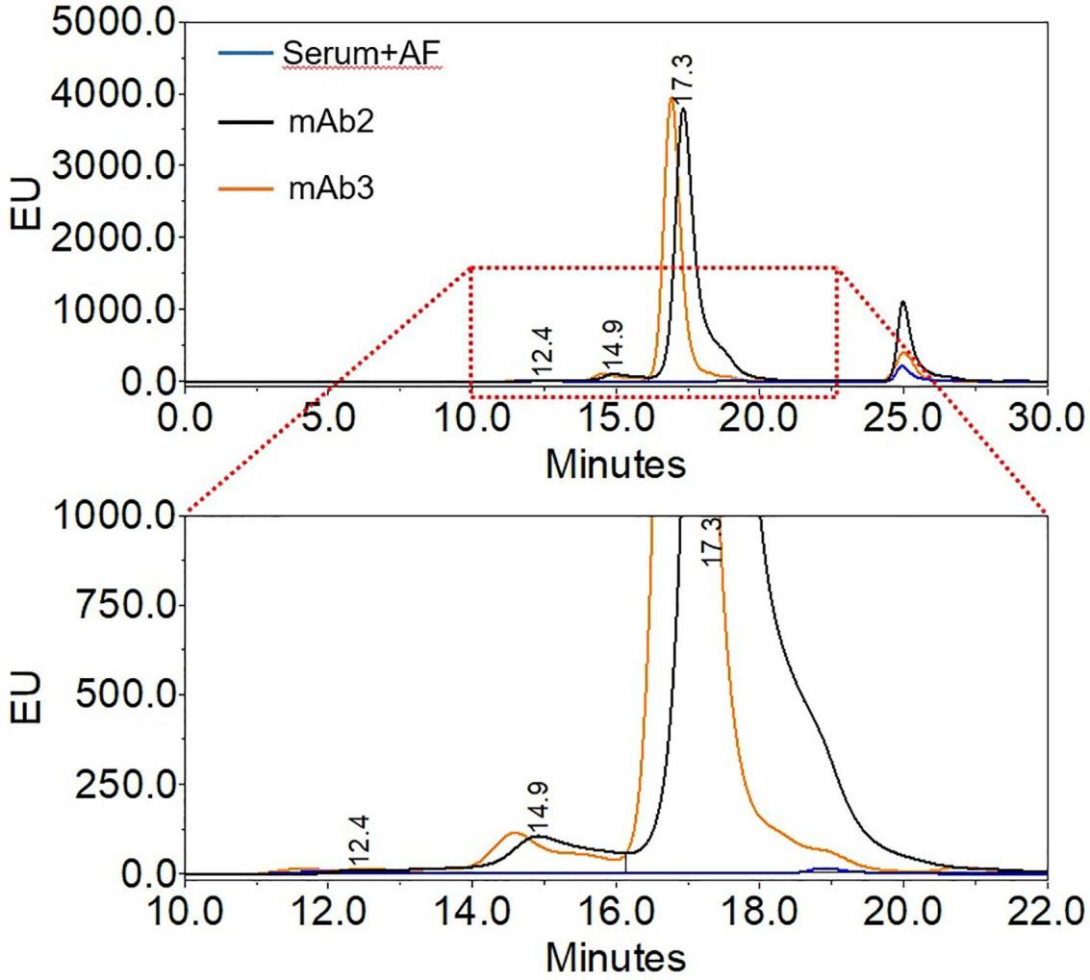

Supplementary Fig. 4. SEC-fluorescence of serum control, mAb2, and mAb3. Serum control sample spiked with AF (blue), mAb2 (black), and mAb3 (orange) each sample measured at S1. Fluorescence was measured at 495/519 nm. Emission units, EU.

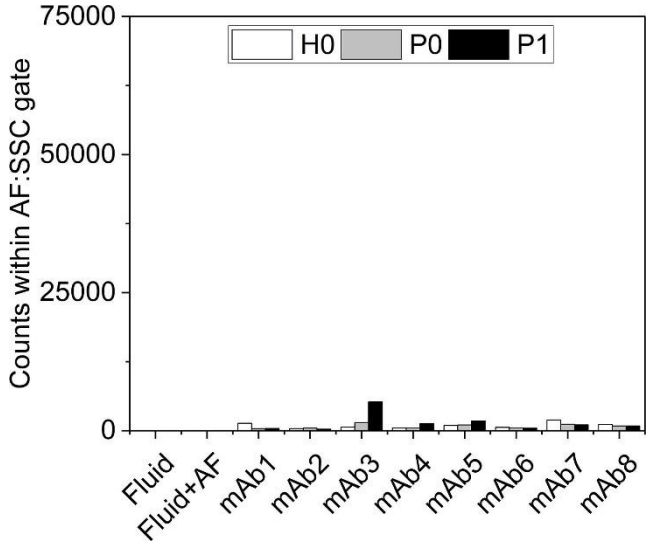

Supplementary Fig. 5. Flow Cytometry of mAbs in PBS and histidine-HCl. Counts of SSC1 gate after preparation in 20 mM histidine-HCl (H0), PBS (P0), and after incubation in PBS at 37°C for 5 days (P1). Control sample without AF-labeled mAb, Fluid; control sample spiked with AF, Fluid+AF.

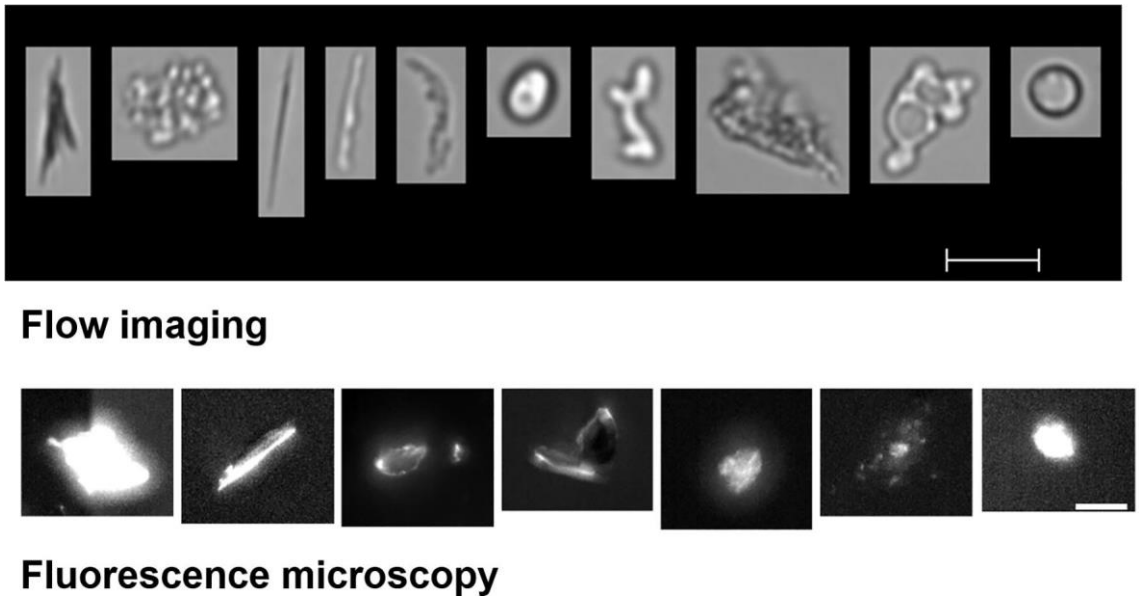

Supplementary Fig. 6. Representative particles of AF-labeled mAbs in serum. Upper row: particles analyzed by flow imaging. Lower row: particles analyzed by widefield fluorescence microscopy. Scale bar length: 25 µm.

Assessing Particle Formation of Biotherapeutics in Biological Fluids

The following chapter has been published as rapid communication in the Journal of Pharmaceutical Sciences.

Joachim Schuster, Christine E. Probst, Hanns-Christian Mahler, Susanne Joerg, Joerg Huwyler, and Roman Mathaes.
Assessing Particle Formation of Biotherapeutics in Biological Fluids
J Pharm Sci. 2021, 110(4), 1527-1532
doi: 10.1016/j.xphs.2020.12.038

The supplementary data was inserted into this chapter.

Journal of Pharmaceutical Sciences 110 (2021) 1527-1532

Contents lists available at ScienceDirect

Journal of Pharmaceutical Sciences

journal homepage: www.jpharmsci.org

Rapid Communication

Assessing Particle Formation of Biotherapeutics in Biological Fluids

Joachim Schuster [a, b], Christine E. Probst [c], Hanns-Christian Mahler [a], Susanne Joerg [a], Joerg Huwyler [b], Roman Mathaes [a, *]

[a] Lonza Pharma and Biotech, Drug Product Services, Basel, Switzerland
[b] Division of Pharmaceutical Technology, University of Basel, Pharmacenter, Basel, Switzerland
[c] Luminex Corporation, Seattle, WA, USA

ARTICLE INFO

Article history:
Received 13 August 2020
Revised 6 November 2020
Accepted 14 December 2020
Available online 7 January 2021

Keywords:
Protein aggregation
Serum
In vitro model
Subvisible particles
Antibody stability

ABSTRACT

The stability of therapeutic proteins can be impacted *in vivo* after administration, which may affect patient safety or treatment efficacy, or both. Stability testing of therapeutic proteins using models representing physiologic conditions may guide preclinical development strategy; however, to date only a few studies assessing the physical stability are available in the public domain. In this manuscript, the stability of seven fluorescently labeled monoclonal antibodies (mAbs) was evaluated in human serum and phosphate-buffered saline, two models often discussed to be representative of the situation in humans after intravenous administration. Subvisible particles were analyzed using light obscuration, flow imaging, and imaging flow cytometry. All methods showed that serum itself formed particles under *in vitro* conditions. Imaging flow cytometry demonstrated that mean particle size and counts of mAbs increased substantially in serum over five days; however, particle formation in phosphate-buffered saline was comparably low. Stability differences were observed across the mAbs evaluated, and imaging flow cytometry data indicated that fluorescently labeled mAbs primarily interacted with serum components. The results indicate that serum may be more suitable as *in vitro* model to simulate physiologic intravenous conditions in patients closely and evaluate the *in vivo* stability of therapeutic proteins. Fluorescence labeling and detection methods may be applied to differentiate particles containing therapeutic protein from high amounts of serum particles that form over time.

Introduction

Subvisible particles (SbVPs) are an obligatory critical quality attribute for therapeutic proteins and are rigorously monitored and controlled during the product life cycle. SbVPs in parenteral preparations are typically analyzed using light obscuration (LO). LO (or as alternative method, light microscopy) is currently the only SbVP method described in harmonized pharmacopeial monographs and remains the method of choice for drug product development and quality control testing. Additional characterization methods are often applied for more in-depth characterization, such as flow imaging (FI) testing.[1]

In addition to SbVPs being present or formed in the drug product prior to patient administration, it is possible that SbVPs may also form *in vivo*, i.e., after administration. SbVP formation may occur by aggregation of the therapeutic protein with endogenous biological components such as enzymes or other biological processes or due to conditions in the biological fluid driving self-aggregation.[2] To predict potential adverse effects in patients due to drug instability under physiologic conditions, stability of therapeutic proteins within the context of biological matrix is of increasing interest, especially during early stages of development and preferably prior clinical lead candidate selection.[2]

Evaluation of therapeutic protein stability in biological fluids has proven challenging. Conventional pharmaceutical methods for SbVP quantitation are unable to discriminate particles derived from therapeutic protein from other particles that may form in the biological fluid over incubation time.[2,3] Previous reports have indicated red blood cells undergo lysis and endogenous proteins can undergo aggregation and precipitation, i.e., forming proteinaceous particles, once isolated from animals/humans.[2–6] Fluorescence methods have been applied to enable the detection of therapeutic proteins in biological fluids[3,7–10]; however, analytical challenges remain due to the autofluorescence of biological fluid components.[3,11]

Abbreviations: AF, Alexa Fluor 488; BF, brightfield; FIL, flow imaging; IFC, imaging flow cytometry; LO, light obscuration; mAbs, monoclonal antibodies; PBS, phosphate-buffered saline; SbVP, subvisible particle; SSC, side scatter.

* Corresponding author.
E-mail address: roman.mathaes@lonza.com (R. Mathaes).

https://doi.org/10.1016/j.xphs.2020.12.038
0022-3549/

In this study, we investigated the stability of seven different monoclonal antibodies (mAbs) under simulated physiologic conditions (after potential intravenous administration) by mixing mAbs with human serum or phosphate-buffered saline (PBS) and tracking particle formation over a period of five days. To enable detection of the therapeutic protein within the serum matrix, mAbs were fluorescent-labeled by conjugation of Alexa Fluor 488 (AF) as described previously.[3] Particle quantitation was performed using LO and FI, analytical methods commonly applied for assessment of SbVPs. Because LO and FI lack fluorescence measurements, particles were additionally measured using imaging flow cytometry (IFC), which simultaneously collects brightfield (BF), side-scatter, and fluorescence images of particles in flow, thereby enabling differentiation of fluorescent and non-fluorescent particles.

Materials and Methods

All mAbs were manufactured by Lonza Biologics plc (Slough, UK) and provided in 20 mM histidine-HCl buffer (pH 6.0). Supplemental Table 1 summarizes isoelectric point and hydrophobicity of all mAbs used in this study. PBS pH 7.4, sodium azide, and AF NHS succinimidyl ester were purchased from Sigma-Aldrich (Buchs, Switzerland). Plasma-derived human male serum (type AB) was purchased from BioIVT (West Sussex, UK). Princeton pro spin columns were purchased from LubioScience (Zurich, Switzerland). PVDF 0.22 μm filter were purchased from Merck Millipore (Darmstadt, Germany).

Labeling of mAbs

Labeling of mAbs with AF was done as previously described by Schuster et al.[3] Briefly, all mAbs were covalently labeled at a four-fold molar excess of AF dye at 25 °C for 2 h. Excessive (unbound) dye was removed with Princeton pro spin columns hydrated with a 20 mM histidine-HCl buffer (pH 6.0).

In Vitro *Spiking and Incubation in Fluids*

Labeled mAbs and all fluids were prepared and handled under aseptic conditions (laminar flow) and filtered through a PVDF 0.22 μm filter. mAbs were mixed with 20 mM histidine-HCl buffer (pH 6.0) (control), PBS (pH 7.4), or human serum (pH 7.4) to reach a final concentration of 0.2 mg/mL. While the concentration of an administered therapeutic protein can vary substantially, the spiking concentration of 0.2 mg/mL is within the magnitude of concentrations that can be measured in patients.[12] Samples were analyzed immediately after mixing (T0d) and after an incubation at 37 °C for five days (T5d). PBS samples were incubated in a thermomixer (Eppendorf, Hamburg, Germany). Serum samples were incubated at 6.7% CO_2 to ensure maintaining the pH during storage time. All samples contained 0.1% (w/v) sodium azide. As additional control samples, PBS and serum were spiked with the equivalent volume of 20 mM histidine-HCl buffer without mAb. Additional controls were prepared by spiking PBS and serum with AF without mAb.

Light Obscuration

With the exception of using a smaller sample volume, LO was performed according to the pharmacoepeia (Ph Eur 2.9.19). A HIAC 9703+ equipped with a HRLD-150 detector (Beckman Coulter, Brea, CA) was used. Each sample was analyzed by four 0.2 mL injections. The average of the last three injections were reported. A 1 mL syringe and a flow rate of 10 mL/min was used. COUNT-CAL Count Precision Size Standard beads (Thermo Fisher Scientific, Waltham, MA) were used for the system suitability test.

Flow Imaging

FI measurements were collected using a FlowCAM VS1 (Fluid Imaging Technologies, Scarborough, ME) equipped with a 1 mL syringe, 80 μm flow cell, and a 10× (0.3 NA) objective (Olympus, Tokyo, Japan). A system suitability test for particle size (NIST traceable standards, Thermo Fisher Scientific) and particle count (COUNT-CAL Count Precision Size Standard) was performed using 5 μm beads. A volume of 0.3 mL was analyzed in each measurement at a flow rate of 0.1 mL/min. Data was acquired and processed using VisualSpreadsheet 4.2.52 (Fluid Imaging Technologies).

Imaging Flow Cytometry

Samples were analyzed using an Amnis® FlowSight® imaging flow cytometer (Luminex, Seattle, WA) equipped with a 20× magnification objective. Samples were acquired in a high-sensitivity mode with a flow rate of 1.22 μL/min. Images had a pixel resolution of 1 μm and a 60 μm (wide) field-of-view. BF images were acquired with channels 1 (457/45 nm) and channel 9 (582/25 nm). Side scatter (SSC) images were acquired in channel 6 (772/55); fluorescence images were acquired in channel 2 (532/55). SSC excitation laser (785 nm) and fluorescence excitation laser (488 nm) were set to 10 mW and 60 mW, respectively. A total sample volume of 50 μL was loaded into the instrument and each sample was measured for 2 min. PBS was used as sheath fluid. Data was analyzed using IDEAS® 6.2 image analysis software (Luminex, Seattle, WA). To discriminate fluorescently-labeled particles from unlabeled serum particles, we created gates in IFC scatter plots by using unlabeled serum controls i.e., serum not spiked with a mAb. As autofluorescence of serum particles increase as a function of particle size, gating enabled to select for fluorescently-labeled particles.

Results

Serum control samples measured in triplicate were monitored for particle formation over 5 days using LO (Table 1). Particles formed in serum over five day incubation, with absolute particle counts increasing. Particles were predominantly <10 μm. FI and IFC were used as additional characterization methods and confirmed an increase of particle counts over time (Supplemental Table 2).

BF images obtained by FI and IFC showed a wide range of particles in regards to size and morphology (Fig. 1). The majority of particles formed showed a circular morphology. Differences in terms of intensity, shape, and size were observed. Attempts to discriminate particles of the spiked therapeutic protein from particles formed in serum controls based on their morphological properties were unsuccessful (data not shown).

Fluorescently-labeled particles were differentiated from serum control particles using IFC. Serum control samples were compared to serum samples containing therapeutic mAb to identify autofluorescence events. Autofluorescence of serum control particles increased with particle SSC, and fluorescently-labeled particles containing therapeutic mAb were selected using high AF to SSC ratio (AF/SSC, Fig. 2a). SSC measures light scattered by the particle and is proportional to particle size and refractive index.[8,13] Interestingly, SSC and AF images obtained by IFC showed that fluorescently-labeled mAb particles in serum were dim and circular shaped, indicating an incorporation into serum particles forming over time (Fig. 2b). In contrast, AF-labeled particles in PBS were mostly bright and elongated, suggesting self-aggregation of mAbs. Moreover, many particles in serum showed a circular structure, which was not observed in PBS.

Table 1
SbVP Counts of Serum Control Samples.

Particles [Counts/mL]					
		T0d		T5d	
		Mean ± SD	RSD [%]	Mean ± SD	RSD [%]
LO	≥2 µm	258 ± 88	34.0	6431 ± 627	9.7
	≥5 µm	130 ± 25	19.0	1994 ± 481	24.1
	≥10 µm	55 ± 8	15.1	441 ± 214	48.6
	≥25 µm	6 ± 3	56.8	12 ± 9	73.6

Serum control samples at T0d (after preparation) and T5d (after incubation at 37 °C and pH 7.4 for five days) were measured by LO.
Of note, serum control samples were prepared independently. Particle counts are expressed as mean ± standard deviation. n = 3.

Fluorescent particle counts (measured within the AF/SSC gate) were substantially higher in serum samples (spiked with mAb) compared to PBS samples (spiked with mAb) (Fig. 3a and b). Moreover, the increase in counts from T0d to T5d was more pronounced in serum than in PBS. The mean particle size in serum increased over time (Fig. 3d and f), which was not observed in PBS (Fig. 3c and e). mAb3 and mAb7 showed a consistently stronger increase of particle counts in PBS; however, we also observed a smaller mean particle size of mAb3. Serum control samples (serum spiked with AF) demonstrated that the particles measured within the AF/SSC gate were in fact due to an interaction of AF-labeled mAbs with serum and not due to unbound AF. Fluorescent particle counts measured in control samples (i.e., Serum and Serum + AF) were negligible compared to those of mAbs. The unspiked PBS and serum controls (not containing a therapeutic protein or AF) showed no fluorescence signal confirming the specificity of the method to only detect labeled mAbs after adequate gating.

Fluorescence labeling may impact protein stability, therefore stability assessments of labeled samples may not directly apply to the unlabeled therapeutic counterpart. To evaluate the impact of fluorescence labeling on protein stability, we compared total particle counts of labeled mAbs to those of unlabeled mAbs in histidine-HCl, PBS, and human serum. Our results showed similar total particle counts and size in each fluid (Supplemental Fig. 1).

Discussion

Analyzing particle formation of therapeutic proteins in biological fluids is receiving increasing attention, in order to understand the fate and stability of drugs after administration. Due to the complexity of biological fluids, labeling of the therapeutic protein of interest is necessary to enable detection. For example, Filipe et al. used nanoparticle tracking analysis, fluorescence single particle tracking, flow cytometry, and confocal laser scanning microscopy to monitor particle formation in serum.[8,9] Other methods previously employed to track the physical stability of biotherapeutics in serum included asymmetrical flow field-flow fractionation[7] and widefield fluorescence microscopy.[3] Limitations of such methods may include small analysis volumes (e.g., fluorescence microscopy) or lack of particle images (e.g., flow cytometry).

In this study, we showed that SbVPs formed in serum over time. BF images obtained by FI and IFC revealed a circular structure of serum particles, of unknown nature, which may formed through aggregation and precipitation of endogenous proteins and/or cell-derived vesicles.[14] In previous studies, Luo et al. argued that endogenous proteins may undergo isoelectric precipitation after spiking of a therapeutic mAb formulation.[15,16] Endogenous proteins analyzed were classified as abundant serum/plasma proteins such as apolipoprotein, complement proteins, or immunoglobulin Gs. Using IFC, we could demonstrate that AF-labeled mAbs interacted with serum particles. Our BF and AF images revealed that the mean

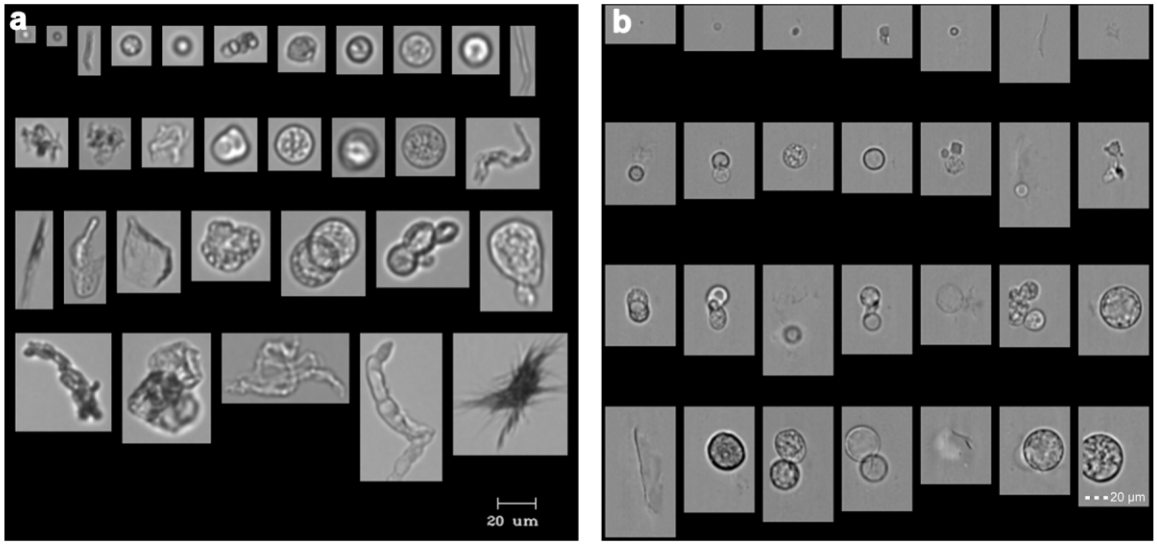

Fig. 1. Representative brightfield images of particles in serum controls. Serum controls, i.e., serum not spiked with a mAb, were measured after incubation at 37 °C for five days (T5d) by FI (a) and IFC (b).

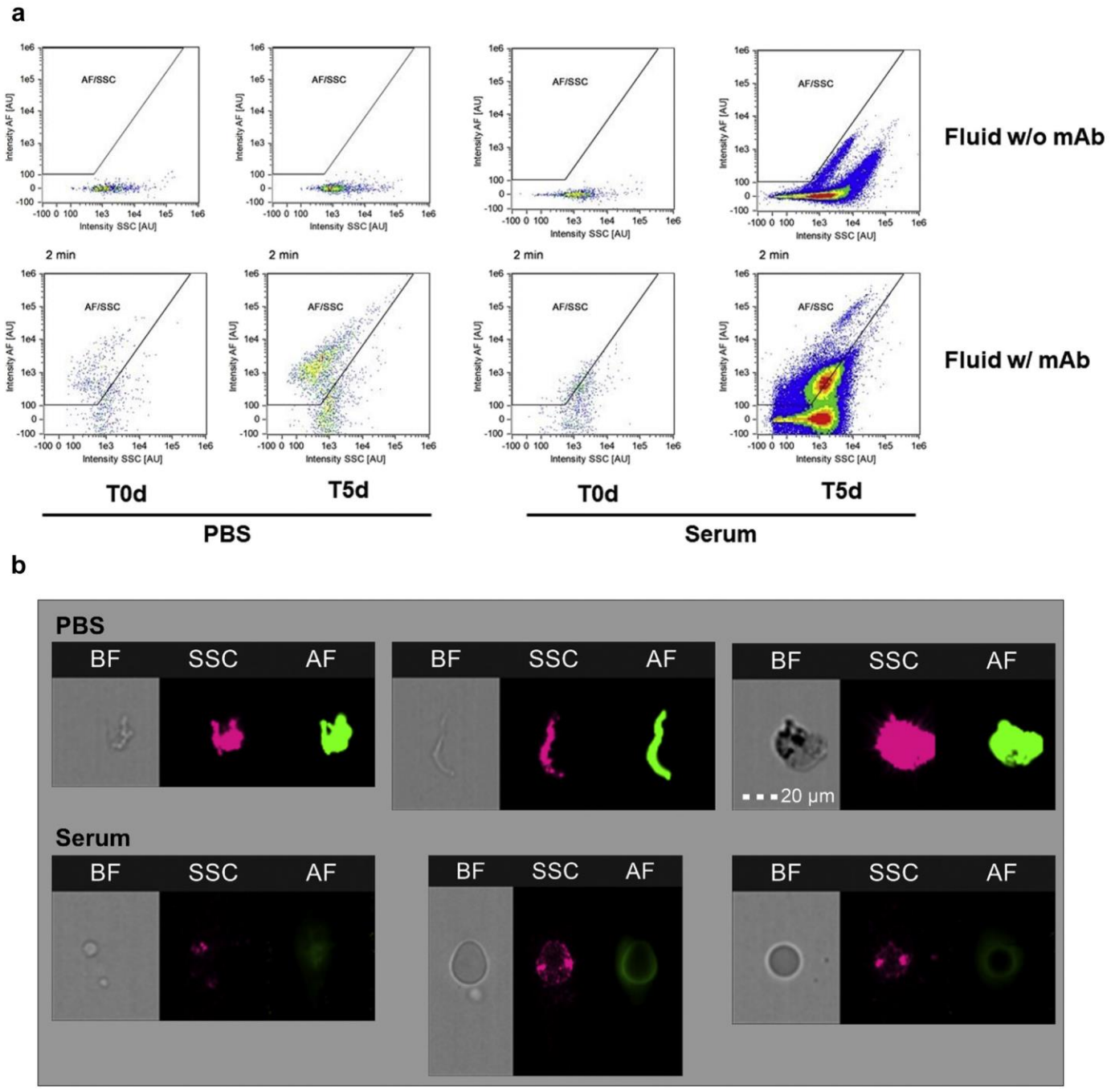

Fig. 2. Imaging flow cytometry analysis. (a): Fluorescence vs. side scatter IFC plots. The upper row shows the control samples, i.e., PBS or serum without a therapeutic protein or AF at T0d and T5d. The lower row shows a representative mAb in PBS or serum at T0d and T5d. The color density shown goes from low counts (blue) to high counts (red). (b): Representative images of AF-labeled protein particles in PBS or serum of mAb3. Images show examples of an AF-labeled mAb spiked in PBS (upper row) and serum (lower row), each measured at T5d using IFC. BF, brightfield; SSC, side scatter; AF, Alexa Fluor 488.

particle diameter decreased slightly in PBS over time, whereas increased markedly in serum as a function of time. Depending on the composition of newly formed particles (e.g., mostly non-labeled serum particles) the fluorescence intensity can decrease. This is in agreement with previous observations that protein aggregates in serum are less fluorescent compared to particles in formulation buffer.[8] This is most likely contributed due to interactions between the spiked fluorescent labeled-protein and non-fluorescent serum proteins. Solely based on the protein concentration, an interaction between AF-labeled mAbs (0.2 mg/mL) with endogenous serum proteins (51 mg/mL) is far more likely to occur than AF-labeled mAbs self-interaction. Comparing SbVP counts of mAbs in serum is impacted by the varying counts of serum particles forming *in vitro*. In general, particle counts measured by LO, FI, and IFC are not expected to match as each method features different measurement and calibration principles as well as measure particles in varying size ranges.[17]

As an alternative to serum, several studies used PBS due to its buffering capacity at pH 7.4, similar ionic strength as blood, and significantly less complex matrix to circumvent analytical

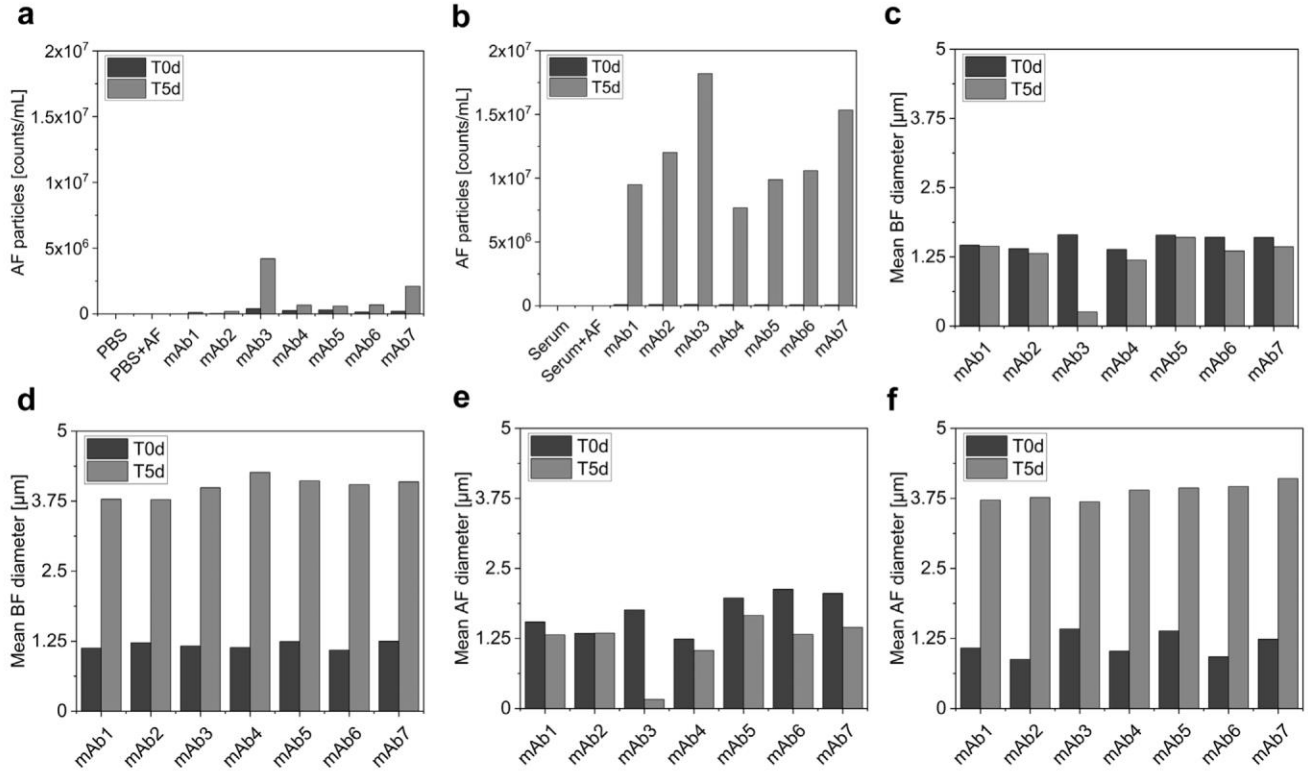

Fig. 3. SbVP count analysis by imaging flow cytometry. Total fluorescence particle counts measured within the fluorescence gate (AF/SSC) in PBS (a) and serum (b). Mean diameter of particles of brightfield images in PBS (c) and serum (d) as well as mean AF diameter in PBS (e) and serum (f). Samples were analyzed after preparation (T0d) and after five days of incubation at 37 °C (T5d). PBS + AF, PBS spiked with AF; Serum + AF, serum spiked with AF.

challenges encountered with biological fluids.[2,5,18] While certain chemical modifications showed similar results in PBS and serum, few studies have compared physical stability in PBS to serum.[6,18] Our results provide further evidence that mAbs are less stable in serum compared to PBS in regards to protein aggregation. Thus, PBSmay not be considered a suitable *in vitro* model to assess protein liabilities as the stability may not be impacted to an extent that enables to benchmark molecule candidates. Moreover, the conditions encountered in biological fluids differ from those in PBS. Particularly, the absence of serum matrix components such as macromolecules, steric exclusion effect, and electrostatic interactions may restrict the physiologic relevance of PBS.[2]

Conclusion

Analytical methods capable of measuring SbVP fluorescence facilitate an assessment of the stability of a therapeutic protein in biological fluids. We showed that our labeling protocol did not impact protein stability, and that IFC was able to discriminate between serum particles and mAb particles based on their visual appearance. This enabled characterizing the formation of SbVPs of seven different mAbs in serum, over an incubation time of five days. Further, we showed that using PBS may not be an adequate surrogate to assess mAb stability in serum due to differences in protein stability observed between the two matrices. Overall, assessing the physical stability of therapeutic proteins in biological fluids is of high importance, particularly prior clinical candidate selection and early pharmaceutical developability studies, as such studies can support the selection of better lead candidates.

Appendix A. Supplementary Data

Supplementary data to this article can be found online at https://doi.org/10.1016/j.xphs.2020.12.038.

References

1. Mahler HC, Friess W, Grauschopf U, Kiese S. Protein aggregation: pathways, induction factors and analysis. *J Pharm Sci*. 2009;98(9):2909-2934.
2. Schuster J, Koulov A, Mahler HC, et al. In vivo stability of therapeutic proteins. *Pharm Res*. 2020;37:23.
3. Schuster J, Koulov A, Mahler HC, et al. Particle analysis of biotherapeutics in human serum using machine learning. *J Pharm Sci*. 2020;109(5):1827-1832.
4. Dillon TM, Ricci MS, Vezina C, et al. Structural and functional characterization of disulfide isoforms of the human IgG2 subclass. *J Biol Chem*. 2008;283(23):16206-16215.
5. Yin S, Pastuskovas CV, Khawli LA, Stults JT. Characterization of therapeutic monoclonal antibodies reveals differences between in vitro and in vivo time-course studies. *Pharm Res*. 2013;30(1):167-178.
6. Schuster J, Mahler HC, Koulov A, et al. Tracking the physical stability of fluorescent-labeled mAbs under physiologic in vitro conditions in human serum and PBS. *Eur J Pharm Biopharm*. 2020;152:193-201.
7. Leeman M, Choi J, Hansson S, Storm MU, Nilsson L. Proteins and antibodies in serum, plasma, and whole blood-size characterization using asymmetrical flow field-flow fractionation (AF4). *Anal Bioanal Chem*. 2018;410(20):4867-4873.
8. Filipe V, Poole R, Oladunjoye O, Braeckmans K, Jiskoot W. Detection and characterization of subvisible aggregates of monoclonal IgG in serum. *Pharm Res*. 2012;29(8):2202-2212.
9. Filipe V, Poole R, Kutscher M, Forier K, Braeckmans K, Jiskoot W. Fluorescence single particle tracking for the characterization of submicron protein aggregates in biological fluids and complex formulations. *Pharm Res*. 2011;28(5):1112-1120.
10. Demeule B, Shire SJ, Liu J. A therapeutic antibody and its antigen form different complexes in serum than in phosphate-buffered saline: a study by analytical ultracentrifugation. *Anal Biochem*. 2009;388(2):279-287.
11. Wolfbeis OS, Leiner M. Mapping of the total fluorescence of human blood serum as a new method for its characterization. *Anal Chim Acta*. 1985;167:203-215.
12. Yang N, Tang Q, Hu P, Lewis MJ. Use of in vitro systems to model in vivo degradation of therapeutic monoclonal antibodies. *Anal Chem*. 2018;90(13):7896-7902.

13. Nishi H, Mathas R, Furst R, Winter G. Label-free flow cytometry analysis of subvisible aggregates in liquid IgG1 antibody formulations. *J Pharm Sci*. 2014;103(1):90-99.
14. van der Pol E, Boing AN, Harrison P, Sturk A, Nieuwland R. Classification, functions, and clinical relevance of extracellular vesicles. *Pharmacol Rev*. 2012;64(3):676-705.
15. Luo S, McSweeney KM, Wang T, Bacot SM, Feldman GM, Zhang B. Defining the right diluent for intravenous infusion of therapeutic antibodies. *MAbs*. 2020;12(1):1685814.
16. Luo S, Zhang B. Dextrose-mediated aggregation of therapeutic monoclonal antibodies in human plasma: implication of isoelectric precipitation of complement proteins. *MAbs*. 2015;7(6):1094-1103.
17. Probst C, Zeng Y, Zhu RR. Characterization of protein particles in therapeutic formulations using imaging flow cytometry. *J Pharm Sci*. 2017;106(8):1952-1960.
18. Schmid I, Bonnington L, Gerl M, et al. Assessment of susceptible chemical modification sites of trastuzumab and endogenous human immunoglobulins at physiological conditions. *Nat Commun Biol*. 2018;1:28.

Stability of Monoclonal Antibodies after Simulated Subcutaneous Administration

The following chapter is intended to be published as research article in the Journal of Pharmaceutical Sciences..

Joachim Schuster, Hanns-Christian Mahler, Susanne Joerg, Vinay Kamuju, Joerg Huwyler, and Roman Mathaes.
Stability of Monoclonal Antibodies after Simulated Subcutaneous Administration
J Pharm Sci. 2021, 110(6), 2386-2394
doi: 10.1016/j.xphs.2021.03.007

The supplementary data was inserted into this chapter.

Journal of Pharmaceutical Sciences 110 (2021) 2386–2394

Contents lists available at ScienceDirect

Journal of Pharmaceutical Sciences

journal homepage: www.jpharmsci.org

Pharmaceutical Biotechnology

Stability of monoclonal antibodies after simulated subcutaneous administration

Joachim Schuster[a,b], Hanns-Christian Mahler[a], Susanne Joerg[a], Vinay Kamuju[a], Joerg Huwyler[b], Roman Mathaes[a,*]

[a] Lonza Pharma and Biotech, Drug Product Services, Hochbergerstr. 60A, 4057 Basel, Switzerland
[b] Division of Pharmaceutical Technology, University of Basel, Pharmacenter, Basel, Switzerland

ARTICLE INFO

Article history:
Available online 12 March 2021

Keywords:
In vivo protein stability
In vitro model
Pre-clinical model
Physiologic conditions
Developability

ABSTRACT

Changes in the environment from the drug product to the human physiology might lead to physical and/or chemical modifications of the protein drug, such as *in vivo* aggregation and fragmentation. Although subcutaneous (SC) injection is a common route of administration for therapeutic proteins, knowledge on *in vivo* stability in the SC tissue is limited. In this study, we developed a physiologic *in vitro* model simulating the SC environment in patients. We assessed the stability of two monoclonal antibodies (mAbs) in four different protein-free fluids under physiologic conditions. We monitored protein stability over two weeks using a range of analytical methods, in analogy to testing purposes of a drug product. Both mAbs showed an increase of protein aggregates, fragments, and acidic species. mAb1 was consistently more stable in this *in vitro* model than mAb2, highlighting the importance of comparing the stability of different mAbs under physiologic conditions. Throughout the study, both mAbs were substantially less stable in bicarbonate buffers as compared to phosphate-buffered saline. In summary, our developed model was able to differentiate stability between molecules. Bicarbonate buffers were more suitable compared to phosphate-buffered saline in regards to simulating the *in vivo* conditions and evaluating protein liabilities.

Introduction

Subcutaneous (SC) injection is a common route of administration for therapeutic proteins, enabling self-administration of drug products, which is especially appealing to patients requiring frequent and/or long-term treatment.[1,2] Despite the increasing number of therapeutic proteins being delivered subcutaneously,[2] knowledge on the stability of proteins after administration is limited,[3] beyond pharmacokinetic considerations including distribution, metabolism, and elimination. Monoclonal antibodies (mAbs) typically have a SC bioavailability of 50 to 80%,[4] however, in certain cases considerably lower values have been reported.[5]

Incomplete bioavailability may be caused by pre-systemic degradation at the injection site and/or in the lymphatic system,[2] for example by *in vivo* precipitation. Such an event may not translate into variable bioavailability but may cause safety challenges *in vivo*. *In vivo* protein precipitation is particularly concerning, as e.g., protein aggregates forming at the SC injection site can impair treatment efficacy by altering pharmacokinetics/pharmacodynamics and/or may impact patient safety by promoting an immune response.[6] Thus, assessing *in vivo* protein stability (post-administration modifications) and understanding physiologic factors that may adversely impact the protein is fundamental in the development of therapeutic proteins.[3]

The *in vivo* protein stability is; however, not routinely analyzed with samples from clinical studies, due to a variety of challenges, including being able to obtain samples, ethical concerns, and analytical challenges. Thus, a number of groups developed *in vitro* models simulating human *in vivo* conditions. For example using the desired biological fluid such as serum/plasma[7–9] (related to intravenous administration), vitreous humor[7,10,11] (related to intravitreal injections), artificial SC fluid,[12–15] or SC tissue homogenate[16] (related to SC administration). Simulating the SC tissue is particularly challenging as the SC interstitial fluid is not readily accessible.[14,17,18]

Despite extensive efforts, analytical challenges persist as biological fluids contain a complex matrix and are inherently less stable

Abbreviation: AF, artificial fluid; AF+HA, artificial fluid + hyaluronan; BY, brown-yellow; CE-SDS, capillary electrophoresis - sodium dodecyl sulfate; cIEF, capillary isoelectric focusing; CO_2, carbon dioxide; FAL, Float-A-Lyzer; HA, hyaluronan; HMWS, high-molecular weight species; HP-SEC, high performance - size-exclusion chromatography; LMWS, low-molecular weight species; LO, light obscuration; mAb, monoclonal antibody; NTU, nephelometric turbidity units; PBS, phosphate-buffered saline; pI, isoelectric point; RM, reference material; SAL, Slide-A-Lyzer; SbVP, subvisible particle; SC, subcutaneous.

* Corresponding author.
E-mail address: roman.mathaes@lonza.com (R. Mathaes).

https://doi.org/10.1016/j.xphs.2021.03.007
0022-3549/

under *in vitro/ex vivo* conditions compared to *in vivo*. Approaches to circumvent analytical interference include labeling (e.g., via fluorescent dye) or purification (e.g., biotinylation) of the protein of interest. However, these approaches may change the biophysical properties and intrinsic protein stability and thus the physiologic relevance of an *in vitro* study. Reliable and representative *in silico, in vitro*, and animal *in vivo* models predicting the *in vivo* stability in patients are strongly needed as these can help to better understand the *in vivo* stability of therapeutic proteins and support drug product development.

In this study, we developed an *in vitro* model by assessing the stability of two mAbs in four different fluids aiming to simulate physiologic conditions. Parameters of the *in vitro* model were selected to resemble the composition and conditions of the SC tissue such as 34° C[19] and a pH of 7.4.[3] The average hypodermic temperature is slightly lower than the core body temperature[19] and has been used in previous SC *in vitro* models.[12,13] In addition, the study design considered relevant injection volumes and residence time of therapeutic proteins in the SC tissue (Table 1). The four protein-free fluids used in this study allowed tracking the stability over time without sample manipulation such as labeling or purification techniques. Samples were analyzed by turbidity, colorimetry, light obscuration (LO), flow imaging, high performance - size-exclusion chromatography (HP-SEC), capillary isoelectric focusing (cIEF), and capillary electrophoresis - sodium dodecyl sulfate (CE-SDS).

Material and methods

Material

Two different proprietary mAbs formulated in 20 mM histidine buffer (pH 6.0) were used in this study (Lonza Biologics, Slough, UK). Table 2 summarizes biophysical properties of both mAbs. Buffers for experiments and equipment were prepared using calcium chloride, L-histidine monohydrochloride monohydrate, histidine, magnesium chloride hexahydrate, potassium chloride, sodium bicarbonate, sodium phosphate, 1x phosphate-buffered saline (pH 7.4; PBS), and sodium diphosphate, all purchased from Sigma-Aldrich (St. Louis, MO). Ready to use artificial buffer Aqix® biopreservation medium was purchased from Life Science Production (Bedford, UK). Table 3 summarizes the composition of each fluid compared to the human SC interstitial fluid. Hyaluronan (HA) sodium salt, biosynthesized by *Streptococcus* species (molecular weight of 1.3 to 1.8 MDa) was purchased from Solabia (Pantin, France). A 27G 40 mm needle and silicone oil free Injekt® Solo syringe were purchased from B. Braun Medical AG (Melsungen, Germany). H_2O was obtained from a Milli-Q H_2O purification system (Millipore, Bedford, MA). Protein Clear™ HR Reagent kit for capillary electrophoresis - sodium dodecyl sulfate (CE-SDS) was acquired from PerkinElmer (Waltham, MA). Slide-A-Lyzer® G2, 2 kDa molecular weight cutoff and 5 to 15 mL capacity was purchased from Thermo Fisher Scientific (Waltham, MA). Spectra/Por® Float-A-Lyzer® G2, 0.5 to 1 kDa molecular weight cutoff and 2 to 5 mL capacity was purchased from Spectrum (Waltham, MA). All fluids and samples were prepared and incubated in sterile Nalgene cryoware (10 mL PETG media bottles, Sigma-Aldrich).

Table 2
Properties of mAbs investigated in this study.

	mAb1	mAb2
Isoform	IgG1λ	IgG1κ
Mass extinction coefficient [L $g^{-1}cm^{-1}$]	1.52	1.45
Concentration [mg/mL]	30	30
HIC [retention time]	12.3	17.7
measured pI[a]	9.1	8.1
calculated pI[a]	8.6	9.2
Theoretical charge at pH 7.4	6.6	14.6
k_D [mL/g][b]	6.5	20.5
A_2 x10^{-4} [mol mL/g^2][c]	1.03	1.55
Viscosity at 30 mg/mL [mPa s][d]	1.16	1.24

Both molecules were formulated and analyzed in 20 mM histidine buffer (pH 6.0).
[a] pI was measured by capillary isoelectric focusing and calculated using pKa values from EMBOSS.[28]
[b] k_D was measured by dynamic light scattering.
[c] A_2 was determined using static light scattering.
[d] Viscosity was measured at 25°C using an automatic shear rate. mAbs showed Newtonian behavior.
IgG: immunoglobulin G; pI: isoelectric point.

Preparation of artificial subcutaneous fluids

Four fluids were used in this study, namely, Aqix®, an artificial fluid (AF),[13] AF+hyaluronan (AF+HA), and PBS. Aqix and PBS are commercial ready-to-use (1x) bicarbonate and phosphate buffer-based

Table 1
Key factors for the development of a physiologic *in vitro* model simulating SC administration of mAbs. Summary of parameters that were selected for the development of a human-based physiologic *in vitro* model to simulate the SC space.

Drug delivery / pharmacokinetic parameters	Human SC Tissue	*In vitro* model
Residence time of mAbs at the SC injection site	1.7-13.5 days[20]; on average: 6-8 days[21]	Sampling time points: T0 days T7 days T14 days
Injection volume of commercialized mAbs	Majority of commercialized SC products: <1.5 mL[1]	550 μL
SC interstitial fluid volume	SC interstitial fluid volume: 2.28 mL/g dry tissue weight[22] Total SC tissue H_2O 4.47 mL/g dry tissue weight[22a]	4.95 mL artificial SC fluid
Volume ratio	3.0-8.9[b] e.g., 4.47 mL/g dry tissue weight and 0.5-1.5 mL SC injection volume	9.0 4.95 mL artificial SC fluid and 0.550 mL mAb
Protein concentration / dose	typically, 80 - 1000 mg of a mAb are delivered to patients[1] Concentration measurements within the SC tissue are challenging[14,17]	3 mg/mL
Fate of excipients following SC administration	Largely unknown; however, rapid distribution and dissociation of excipients is likely to occur *in vivo*[3,23]	Mixing of fluid and mAbs without excipients. Evaluation of dialysis membranes to simulate limited diffusion.
SC administration to patients	21-27G needle[24]; majority of SC products use 27G needle	27G needle

[a] Values measured in rats.
[b] Volume ratios for the human SC tissue are estimated as the exact composition such as tissue water is unknown. Moreover, the occupied area of an injected mAb can vary.[28]

Table 3
Composition of the human subcutaneous interstitial fluid/tissue and fluids used in this study.

Component	Human subcutaneous interstitial fluid[3]	1xAqix®	AF[13]	AF+HA	1xPBS
Sodium [mM]	134.6	135	134.5	134.5	157.0
Potassium [mM]	3.17	5	5.4	5.4	1.1
Chloride [mM]	111	119	119.5	119.5	154.0
Calcium [mM]	1.551	1.25	1.8	1.8	
Magnesium [mM]	0.66	0.45	0.4	0.4	
Bicarbonate [mM]	31	25	25	25	
Phosphate [mM]	0.610	-	-	-	4.0
Glucose [mM]	3.1-3.3	10	-	-	-
Glycerol [mM]	<0.2[29]	0.11	-	-	-
BES [mM]	N/A	5	-	-	-
L-Glutamate [mM]	0.035-0.051[30]	0.30	-	-	-
L-Glutamine [mM]	0.473- 0.585[30]	0.40	-	-	-
L-Aspartate [mM]	0.056-0.068[30]	0.02	-	-	-
L-Carnitine [mM]	-	0.05	-	-	-
Choline chloride [mM]	-	0.01	-	-	-
Thiamine pyrophosphate [nM]	-	40	-	-	-
Recombinant human insulin [mIU]	2-20 (blood)[31]	28	-	-	-
Hyaluronan [mg/mL]	3.6[22,25,a]	-	-	3.6	-
pH at 34°C[b]	7.4–7.6[32]	7.4	7.4	7.4	7.4
Osmolality [mOsm/kg H_2O][b]	300.8 mOsm/L H_2O[33, c]	303	295	-	290
Conductivity [mS/cm]	plasma: 11.7-12.3[34,d]	13.36	-	-	-

[a] measured in female Wistar-Møller rats[22]
[b] measured after preparation
[c] osmolarity was measured in mice
[d] measured at 25°C
Unless otherwise stated, values were provided by the vendor.
Importantly, SC tissue values can differ substantially depending on factors such as sampling technique, donor, and body location.
AF: artificial fluid; AF+HA: artificial fluids+hyaluronan.

solutions, respectively. AF and AF+HA were prepared, as described by Kinnunen et al.,[13] with AF+HA containing a physiologic HA concentration of 3.6 mg/mL.[22,25] Tab. 3 shows the composition and measured values for all four fluids. Aqix, AF, and AF+HA were equilibrated at 34°C and 7% carbon dioxide (CO_2) to reach the desired pH of 7.4. To avoid calcium phosphate or calcium carbonate precipitates in AF and AF+HA, calcium chloride was added once a stable pH was obtained as previously described.[26] The resulting solution was filtered through a 0.22 μm Stericup® filter (Merck Millipore, Darmstadt, Germany).

Development of a physiologic in vitro *model*

Previous studies developed models using a dialysis membrane.[10,11,13,27] We evaluated the applicability of dialysis cassettes compared to conventional 10 mL Nalgene bottles, in regards to assessing subvisible particle (SbVP) formation. Triplicates of Nalgene bottles, Slide-A-Lyzer, and Float-A-Lyzer cassettes were filled with 5 mL of AF. As an additional control, each container was filled with Milli-Q H_2O. Dialysis cassettes were placed in beakers filled with Milli-Q H_2O or AF. The solution in the beaker was mixed continuously on a magnetic stirring plate. Each container was incubated in the CO_2 incubator at 34°C and 7% CO_2. Solution pH and SbVPs were measured by LO at T0d, T7d, and T14d. Different volumes of 20 mM histidine buffer (pH 6.0) were mixed with AF (pH 7.4) to determine the maximum volume of histidine buffer that can be spiked in AF, whilst still maintaining the pH in a physiologic range. The pH was measured after mixing. To determine the buffering capacity of bicarbonate buffers (i.e., Aqix, AF, and AF+HA) in absence of CO_2 (i.e., after incubation), the pH of Aqix and AF (each 5 mL; pH 7.4) was monitored under ambient conditions in closed and open Nalgene bottles. Solution pH and SbVPs using LO were measured after T0min, T15 min, T30 min, T45 min,T60 min, T75 min, and T90 min pH.

Physiologic in vitro *model*

A total of 550 μL of stock mAb (30 mg/mL) was spiked in 4.95 mL of each fluid using a 40 mm 27 G hypodermic needle and 1 mL syringe to obtain a final concentration of 3 mg/mL. This resulted in a volume ratio of 10% drug product and 90% SC fluid. Samples in Aqix, AF, and AF+HA were incubated at 34°C and 7% CO_2 to maintain the physiologic pH of 7.4. PBS was incubated in a thermomixer C (Eppendorf, Hamburg, Germany) at 34°C in absence of CO_2. Aliquots of 1.6 mL were withdrawn at the desired time points of 30 min (T0d), 7 days (T7d), and 14 days (T14d). As control samples, each fluid was spiked with 550 μL of 20 mM histidine buffer (pH 6.0) without a mAb. Samples and controls were prepared independently and identically in triplicates and analyzed each by single measurement. Values were compared to drug substance reference material (RM) of mAb1 and mAb2, stored in 20 mM histidine buffer (pH 6.0) at 5°C. All samples and controls were analyzed at the desired time point in regards to pH, visible particles, colorimetry, turbidimetry, LO, protein concentration, and HP-SEC. For cIEF and CE-SDS samples were -80°C frozen until analysis. Aliquots were thawed at room temperature.

pH and conductivity

pH and conductivity was measured by a SevenExcellence pH and conductivity meter (Mettler Toledo, Columbus, OH).

Osmolality

Osmolality of each fluid was measured on the principle of freezing point depression by OsmoPRO micro-osmometer (Advanced instruments, Norwood, MA). Osmolality of each fluid (20 μL) was reported as mOsm/kg.

Colorimetry

The degree of coloration of liquids was measured according to the European Pharmacopeia 2.2.2. Samples were measured using Lico 690 spectrophotometer (Hach, Loveland, CO) and 10 mm plastic cuvette. The instrument was calibrated with Milli-Q H_2O. The spectral data of sample absorbance between 380 and 720 nm in 10 nm increments was transformed into Lab-values as described in European Pharmacopeia color code for brown-yellow (BY) units.

Opalescence / turbidity

The degree of opalescence of liquids was measured according to the European Pharmacopeia 2.2.1, using a 2100AN EPA 230Vac laboratory turbidimeter (Hach, Colorado, US). Light scattering intensity was converted to nephelometric turbidity units (NTU). The instrument was calibrated using Gelex secondary turbidity standards (Hach) in the range of 0 to 100 NTU. Samples (0.8 mL) were transferred and measured in 8 mm glass tubes (Hach Lange GmbH, Düsseldorf, Germany). For each sample at the same time point (n=3), the lowest value of three measurements was expressed as mean and standard deviation.

Protein concentration

The protein concentration was measured using the SoloVPE instrument, C Technologies (Bridgewater, NJ) mounted onto an Agilent Cary 60 UV-Vis spectrometer (Santa Clara, CA). SoloVPE fibrettes and single use polymer cuvettes were purchased from C Technologies. Samples of 100 μL were transferred to cuvettes and measured at 280 nm. System sustainability was tested using a CHE013 VPE 1 MM standard dye (C Technologies). Data was acquired by Cary WinUV software 5.0.0.1008 (Agilent Technologies, Santa Clara, CA).

Visible particles

Each sample and control was inspected for visible particles according to the method described in the European Pharmacopoeia (2.9.20).

Light obscuration

HIAC 9703+ equipped with a HRLD-150 detector (Beckman Coulter, Brea, CA) was used for LO measurements. SbVPs in the solution (≥2, ≥5, ≥10, ≥25 μm/mL) were characterized using the LO method described in the European Pharmacopoeia (2.9.19); however, with modified volumes. For sample measurements, a pre-run of 0.2mL was followed by three runs of 0.2 mL each. The average of the last three runs was reported. The system was set up with a 1 mL Hamilton syringe and a drawing speed of 10 mL/min. System suitability test was done using 5 μm COUNT-CAL Count Precision Size Standard beads (Thermo Fisher Scientific).

Flow imaging

SbVPs were measured using a FlowCam VS1 (Fluid Imaging Technologies, Scarborough, ME) set up with a 1 mL syringe, 10x NA/0.3 UPLFLN objective (Olympus, Tokyo, Japan), and an 80 μm field of view flow cell. Samples and controls (0.3 mL each) were analyzed at a flow rate of 0.1 mL/min. System suitability test was done by COUNT-CAL count precision size standards and 5 μm NIST traceable standards (Thermo Fisher Scientific). Data was acquired and processed by VisualSpreadsheet software 4.2.52 (Fluid Imaging Technologies).

High performance size-exclusion chromatography

The samples were analyzed using a TSKgel GS3000SWXL column (Tosoh Biosciences, Griesheim, Germany) and a Waters Alliance e2695 HPLC system with a UV/Vis detector. Mobile phase consisted of a 0.2 M sodium phosphate buffer (pH 7.0). The flow rate was maintained at 0.5 mL/min and 10 μL of sample at 0.75 mg/mL was injected. The column was maintained at a temperature of 25°C and UV absorbance measured at 210 nm. Chromatograms were processed with Empower3 software (Waters, Milford, MA).

Capillary electrophoresis

Fragmentation and aggregation of mAbs were studied by microfluid chip CE-SDS. All experiments were carried out using Protein Clear™ HR Reagent kit and LabChip GXII (Caliper Life Sciences, Hopkinton, MA). Samples were diluted in 20 mM sodium phosphate buffer (pH 6.0) to a concentration of 0.5 mg/mL. Reducing sample buffer was prepared by mixing 24.5 μL of 1 M dichlorodiphenyltrichloroethane with 700 μL of Protein Clear HR sample buffer, while non-reducing buffer consisted of only Protein Clear HR sample buffer. A total of 2.5 μL sample (0.5 mg/mL) was mixed with 18 μL of reducing or non-reducing buffer and heated at 70°C for 10 min. Following equilibration at room temperature the denatured samples were centrifuged at 2000 rpm for 2 min. After adding Milli-Q H_2O (35 μL), samples were analyzed. Electropherograms were processed using the Empower3 software (Waters).

Capillary isoelectric focusing

cIEF was carried out using iCE3 (Protein simple, San Jose, CA). mAb samples were diluted in a master mix containing 0.35% methyl cellulose solution, 4% carrier ampholyte (pH 8.5 to 10.5), 0.5% low pI marker (7.65), and 0.5% high pI marker (9.46) to reach a final protein concentration of 0.25 mg/mL. Samples were focused for 1 min at 1500 V and 8 min at 3000 V. Phosphoric acid (80 mM) and sodium hydroxide (100 mM) were used as anolyte and catholyte. Isoelectric pH and peak area were estimated using Empower3 software. All concentration were expressed as % v/v.

Data analysis

Unless otherwise stated all results are presented as mean and standard deviation of three independently prepared samples, each measured once. Data were plotted using Origin version 9.7.0.185 (OriginLab, Northampton, MA).

Results

Development of a physiologic in vitro *model*

In a first step, dialysis cassettes were evaluated versus a static model in Nalgene bottles. Slide-A-Lyzer and Float-A-Lyzer cassettes as well as conventional Nalgene bottles were tested for SbVPs upon incubation with AF and Milli-Q H_2O over 14 days. SbVP shedding by the container would create an measurement artifact and compromise the study read out.

LO data showed that AF-incubated in Nalgene bottles and Float-A-Lyzer dialysis cassettes formed no substantial SbVP counts (<100 particles/mL), whereas ca. 3800±2220 counts/mL of SbVPs ≥2 μm were measured in AF-incubated Slide-A-Lyzer dialysis cassettes at T14d (Fig. 1A). To exclude that SbVPs originated from the dialysis cassette or formed due to contamination, we incubated both dialysis cassettes and Nalgene bottles with Milli-Q H_2O (data not shown). At T14d, less than 300 counts/mL of SbVPs ≥2 μm were measured in each

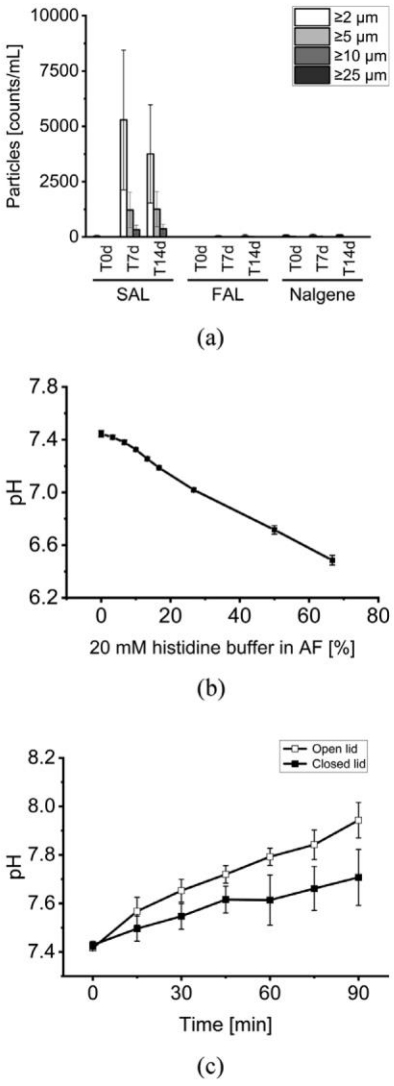

Fig. 1. Particles and pH analysis in different *in vitro* models. A: SbVP characterization of AF in Slide-A-Lyzer (SAL), Float-A-Lyzer (FAL), and Nalgene bottle (Nalgene), measured by LO. B: Determinion of the maximum volume ratio of 20 mM histidine buffer (pH 6.0) and AF while maintaining pH 7.4. C: pH monitoring of AF after incubation, i.e., in absence of CO_2 under ambient conditions (25°C, 0.04% CO_2 in air) with an open and closed lid. n=3.

container. The nature of SbVPs formed in Slide-A-Lyzer dialysis cassettes were not further investigated and out of scope of this study.

To determine if the buffering capacity of a bicarbonate buffer (without dialysis) was sufficient to maintain the desired physiologic pH of 7.4, we measured the pH of different volume ratios of 20 mM histidine buffer (pH 6.0) and AF (Fig. 1B). We confirmed that the pH remained at 7.4 after spiking a volume of 10% 20 mm histidine buffer (drug product formulation) to AF. Moreover, we showed that after incubation in a CO_2 incubator, the pH increased under ambient conditions (in absence of CO_2), however, the increase was negligible as samples were analyzed within 90 min (Fig. 1C).

Considering the low particle formation of the fluids and sufficient buffering capacity, the dialysis cassettes did not offer any benefits compared to the conventional Nalgene bottle. In fact, the dialysis cassettes added unnecessary complexity to the *in vitro* models including the risk of SbVP shedding, leaching of other contaminations, and adsorption of any components. As a result, all follow-up experiments were done in Nalgene bottles without dialysis cassettes.

Table 4
Turbidity analysis. Nephelometric turbidity units (NTU) of controls and samples at T0d, T7d, and T14d. n=3.

		Turbidity [NTU] Control	mAb1	mAb2
Aqix	T0d	0.7 ± 0.3	2.9 ± 0.6	2.0 ± 0.2
	T7d	0.8 ± 0.7	1.9 ± 0.2	2.3 ± 0.3
	T14d	0.2 ± 0.2	2.1 ± 0.4	2.5 ± 0.5
AF	T0d	1.3 ± 0.5	2.9 ± 0.4	2.4 ± 1.1
	T7d	1.2 ± 0.3	2.6 ± 0.4	3.0 ± 0.4
	T14d	0.7 ± 0.4	2.6 ± 0.7	4.3 ± 0.3
AF+HA	T0d	0.7 ± 0.6	3.1 ± 0.7	2.3 ± 0.6
	T7d	1.5 ± 0.4	3.0 ± 0.3	3.1 ± 0.0
	T14d	1.1 ± 0.2	2.9 ± 0.5	2.7 ± 0.0
PBS	T0d	0.3 ± 0.3	2.8 ± 0.9	2.4 ± 0.7
	T7d	0.5 ± 0.4	2.4 ± 0.9	2.2 ± 0.1
	T14d	0.2 ± 0.2	1.6 ± 0.2	2.9 ± 1.2

Visible and subvisible particle analysis, turbidity, and colorimetry

No particles were observed by visual inspection directly after mixing of mAb1 and mAb2 with each fluid nor after incubation. Table 4 shows that turbidity of all fluids mixed with mAbs were consistently higher than their controls. With the exception of mAb2 in AF at T14d, turbidity remained consistent over all time points with no substantial increases observed. Likewise, no substantial differences in turbidity between mAb1 and mAb2 were observed. Colorimetric data showed no differences between mAb1 and mAb2 (<BY7 at each time point in all fluids). Controls were colorless at each time point.

Fig. 2 shows SbVP counts of mAb1 and mAb2 in all fluids measured by LO. High SbVP counts were measured for mAb1 and mAb2 in all three bicarbonate buffers, which increased over time. Interestingly, neither mAb formed only minimal SbVP counts in PBS. The vast majority of SbVP forming in all fluids were <5 μm in size. mAb1 showed higher counts for SbVP ≥5 μm in Aqix compared to mAb2. With the exception of AF+HA samples, protein concentration was consistent among all samples, ranging from 3.0 to 3.5 mg/mL (data

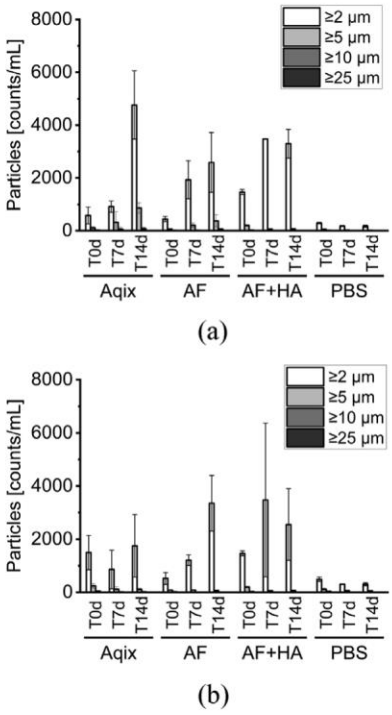

Fig. 2. SbVP analysis. LO data of mAb1 (A) and mAb2 (B). Each sample was prepared in triplicates and measured once at each time point. n=3.

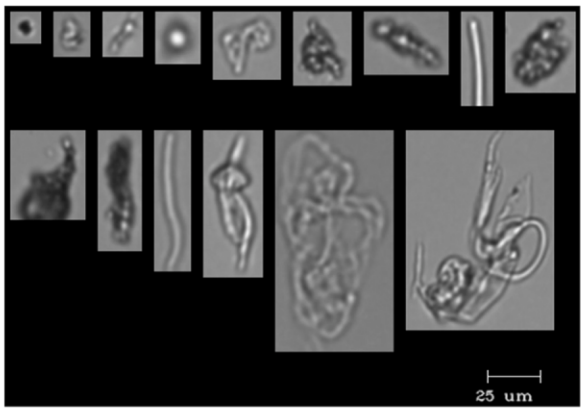

Fig. 3. Representative images of SbVPs. Images show SbVPs of mAb2 in AF+HA measured at T14d by flow imaging.

not shown). AF+HA samples showed slightly higher values of 3.8 mg/mL, presumably due to HA. SbVP counts of all fluid controls were comparable to Milli-Q H_2O, confirming cleanliness of the containers and stability of the fluids over T14d (Supplementary Figure 1).

Flow imaging data confirmed the trend observed by LO (data not shown). All fluid controls showed substantially lower counts compared to the respective sample. Both mAbs showed lower counts in PBS compared to bicarbonate buffers at each time point. The vast majority of particles were <5 μm. No substantial differences between mAb1 and mAb2 were measured by flow imaging. Fig. 3 shows representative images of SbVPs ≥10 μm of mAb2 in AF+HA at T14d. Most SbVPs showed an appearance consistent with proteinaceous materials.

Assessing soluble aggregates and fragments by HP-SEC

High-molecular weight species (HMWS) of mAb1 were virtually unaltered in all fluids (Fig. 4). However, HMWS of mAb2 increased consistently in all fluids by ca. twofold. Low-molecular weight species (LMWS) of both mAbs increased in all fluids over time. mAb1 contained LMWS in the RM and all four fluids at T0d, whereas mAb2 showed no LMWS at the initial time point. The increase of LMWS over time for mAb1 was less pronounced compared to mAb2. Interestingly, the relative abundance of LMWS in PBS was lower compared to bicarbonate buffers. Both mAbs showed the most pronounced increase of LMWS in AF+HA. Overall, the HP-SEC method showed adequate performance. The variability of monomer, HMWS, and LMWS of the independent preparations was low (Fig. 4; small error bars). In addition, the results followed a clear stability trend over time without any outlier. These observations confirmed that the HP-SEC method is stability indicating. Supplementary Figure 2 provides an estimation of HMWS and LMWS observed, which were at 300 to 400 kDa and ca. 50 kDa.

Characterization of protein fragmentation by CE-SDS

Fig. 5A and B shows non-reduced CE-SDS. Fragments consistently increased in all fluids, with mAb2 showing a more pronounced increase compared to mAb1. Moreover, post peaks consistently increased in all fluids over time, whereas remained unaltered for mAb1. For both mAbs, the increase of fragments was less pronounced in PBS as compared to bicarbonate buffers. Fig. 5C and D show reduced CE-SDS. As observed under non-reduced conditions, mAb2 showed consistently higher fragmentation as compared to mAb1. Moreover, both mAbs were more stable in PBS compared to bicarbonate buffers. AF+HA showed the most pronounced increase of

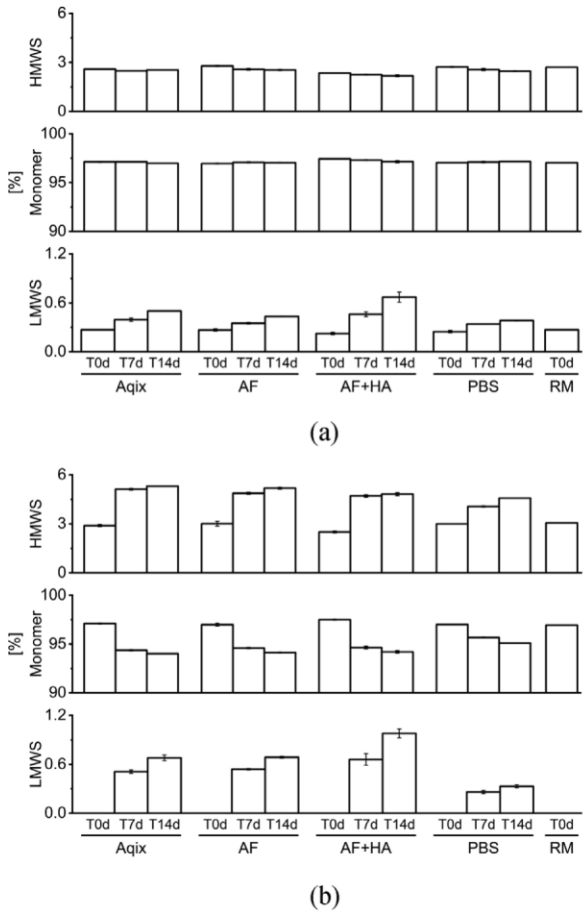

Fig. 4. HP-SEC analysis: mAb1 (A) and mAb2 (B) were measured in four fluids at each three time points. Data are expressed as percentage of total peak area. With the exception of the reference material (RM) measured at T0d, all results are expressed as mean with error bars denoting the standard deviation.

fragmentation in both mAbs under reduced and non-reduced conditions, confirming our HP-SEC data.

Charge variants

The abundance of acidic species consistently increased for both mAbs in each fluid over time. mAb1 and mAb2 differed in their initial charge heterogeneity, with mAb1 containing 58% acidic and 2.5% basic species in the RM, whereas mAb2 contained 23% acidic and 10% basic species in the RM (Fig. 6). Acidic species of mAb1 and mAb2 increased after mixing with each fluid over time. For both mAbs, the increase in acidic species was less pronounced in PBS compared to bicarbonate buffers. Basic species of mAb1 remained almost unchanged, whereas decreased over time for mAb2 in all fluids. The main isoform of mAb1 shifted from 9.1 in RM to 8.9 in bicarbonate fluids, whereas no changes were observed in mAb2.

Discussion

Different *in vitro* models developed elsewhere, used static incubation[8,9,35-37] or a dialysis setup.[7,10,11,13,27,38] Dialysis simulates a slow influx of the SC interstitial fluid[13,27] and allows to diffuse small molecules (excipients) across the membrane, whilst retaining the therapeutic protein locally. Such events have been argued to occur after SC administration.[23] Moreover, dialysis and buffer exchange help to overcome the low buffering capacity of biological fluids under *in vitro/ex vivo* conditions.[3]

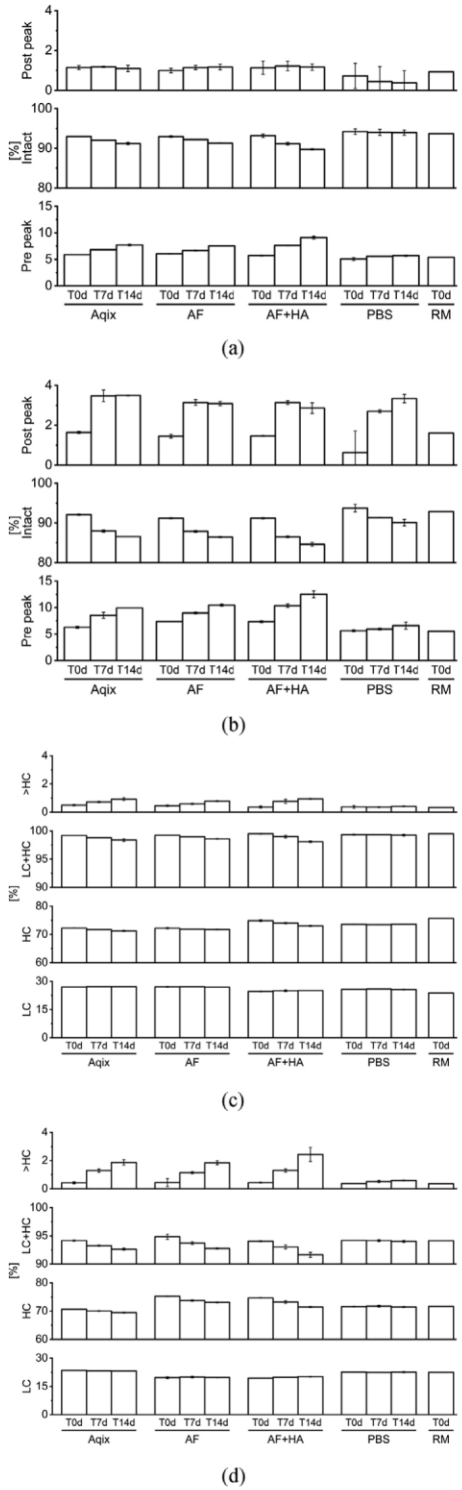

Fig. 5. CE-SDS analysis. Non-reduced CE-SDS of mAb1 (A) and mAb2 (B) as well as reduced CE-SDS of mAb1 (C) and mAb2 (D) reference material (RM).

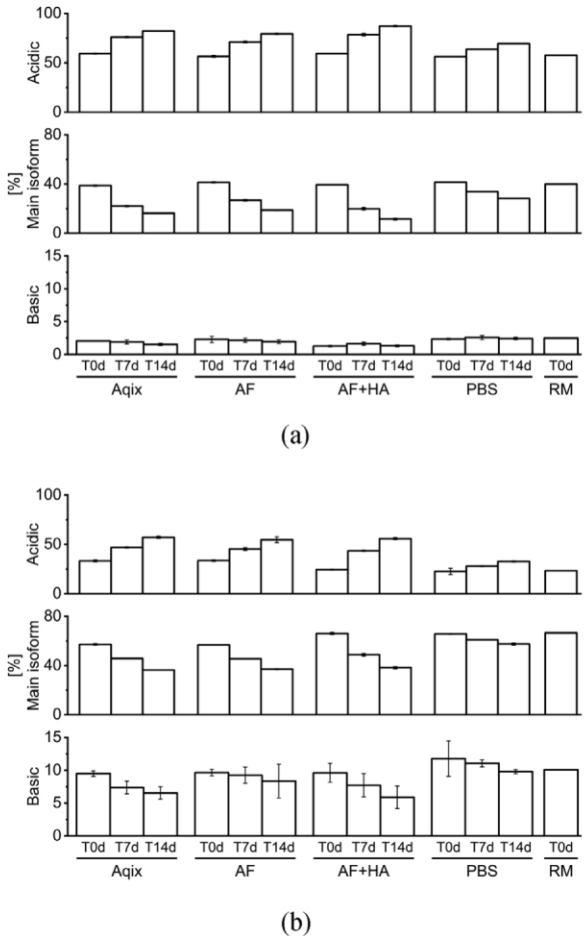

Fig. 6. Charge heterogeneity. cIEF data of mAb1 (A) and mAb2 (B). Except for the reference material (RM), each time point shown is expressed as mean with the error bars representing the standard deviation from three independently prepared samples.

Firstly, we compared different model systems in regards to SbVP counts and established conventional Nalgene bottles without a dialysis cassette as appropriate. We found that, despite the low buffering capacity of bicarbonate buffers *in vitro*, the physiologic pH was sufficiently maintained at pH 7.4 without dialysis. Moreover, our results showed that due to SbVP formation inside the Slide-A-Lyzer dialysis cassette, this setup was poorly suitable when assessing SbVPs of proteins. Only minimal SbVP formation was measured inside Float-A-Lyzer dialysis cassette and Nalgene bottle. Separation of excipients from the therapeutic protein is assumed to occur rather quickly *in vivo*, solely based on diffusion and different route of elimination.[3,39] Thus, we spiked mAbs in four fluids without excipients and selected Nalgene bottles instead of a dialysis setup as *in vitro* model.

The developed analytical methods in this study were stability indicating, showing a distinct stability trend over time as well as small variability within independently prepared samples. Our data showed that mAb1 was consistently more stable in the *in vitro* model than mAb2. Both mAbs formed SbVPs in all three bicarbonate buffers, while only minimal SbVP formation was observed in PBS. HP-SEC and CE-SDS data confirmed that mAb2 fragmented to a higher extent than mAb1 in all fluids. Moreover, HMWS of mAb2 increased over time, whereas HMWS of mAb1 remained virtually unaltered. cIEF showed that for mAb1 basic isoforms remained constant and the increase of acidic species coincided with a decrease of the main isoform. Contrary for mAb2 the increase in acidic species coincided with a decrease of basic and the main isoform. The increase of acidic species observed in both mAbs can presumably be attributed to deamidation, which is known to commonly occur *in vivo*.[40]

As a next step we compared the impact of different fluids on protein stability. All fluids used in this study had a similar osmolality (ca. 290 mOsm/kg) and were incubated under the same conditions (34°C; pH 7.4). Throughout the study both mAbs were consistently less stable in all three bicarbonate buffers compared to PBS. Thus, differences in protein stability observed between PBS and bicarbonate buffers are expected to be caused by their electrolyte composition and/or

different buffering mechanisms (phosphate buffer vs. bicarbonate buffer[41]). Such factors were postulated to cause *in vivo* protein modifications[3]. These results are in agreement with our recent study, in which eight different fluorescent-labeled mAbs were considerably less stable in serum compared to PBS, indicating that other factors than temperature, pH, and osmolality impact *in vivo* protein stability[8]. However, comparisons between these studies are difficult due to different analytical approaches (labeled vs. unlabeled), different fluids (serum vs. protein-free artificial fluids), and a protein's propensity to aggregate/fragment.

Although it remains unknown which fluid would be predictive of events in patients, solely based on a physiologic point of view, the composition and conditions in the bicarbonate buffers are more representative of the *in vivo* environment than PBS. Furthermore, we have shown that certain protein degradation events such as aggregation and fragmentation were more pronounced in bicarbonate buffers compared to PBS. Thus, bicarbonate buffers are more suitable to evaluate protein liabilities and differences in stability among several protein candidates than PBS.

While physiologic parameters such as temperature, pH, ionic composition, and osmolality in our *in vitro* model were similar to those found in the human SC tissue, other components such as cells and proteins (SC protein concentration: ca. 20 mg/mL[42]) were not simulated. Although the basal proteolytic activity in the SC tissue is low, administration of a therapeutic protein can enhance enzymatic activity.[43] This is particularly important when assessing enzymatically-driven degradation events such as fragmentation. Cells are fundamental modulators from a PK/PD perspective (e.g., potency), however, previous studies have shown limited stability of fluids due to cell lysis *in vitro*[44] and potential clogging of analytical instruments.[45] With an increasing complexity of fluids (e.g., neat biological fluid or spiking endogenous proteins to fluids), analytical challenges arise, which can cause matrix interference.[43] More complex *in vitro* models, require additional analytical procedures such as fluorescence labeling or purification (e.g., biotinylation) of the protein of interest to enable detectability. However, altering the protein of interest may create measurement artifacts and limit the possibility to investigate certain degradation products. For example, some protein fragments forming in biological fluids may not contain the fluorophore or binding site for the desired target and would consequently remain undetected. Therefore, we used protein-free fluids, which allowed a direct analysis in the fluids without sample manipulation such as fluorescence labeling.

Although artificial fluids are missing matrix components of biological fluids (e.g., proteases, cells) the model can be readily adopted to track additional protein modifications. For example, adding cysteine and cystine to simulate *in vivo* redox conditions[38,44] and to investigate thioether or trisulfide bond formation[3]. Conditions that have also been argued to cause fragmentation.[46]

Amongst the fluids used in this study, Aqix contained the most complex composition (e.g., containing glucose), which enables assessing protein glycation.[47] HA was added to AF+HA due to its pivotal role in the SC tissue controlling hydraulic conductivity,[48] regulating interstitial fluid volume,[49] excluding proteins from the interstitial space,[22] contributing negative charge,[25] and previous use in artificial biological fluids.[11,13] With most commercial mAbs exhibiting a pI>8,[50] interactions between positively charged mAbs and negatively charged SC tissue components (i.e., HA and chondroitin sulfate) are likely to occur and may compromise protein stability *in vivo*. Although AF+HA showed a slightly more pronounced increase in regards to protein degradation throughout the study, we did not observe substantial differences between the bicarbonate buffers used. Aqix and AF+HA were slightly more complex in their composition than AF, however, appeared to impact protein stability to the same extent. Ultimately, AF appears as a promising fluid to simulate SC administration, as it remained stable over the incubation period and enabled to detect differences in protein stability among the tested mAbs.

Monitoring the pH during analysis time was particularly important as the absence of CO_2 after incubation leads to an alkaline pH shift over time as reported for biological fluids (e.g., serum).[8] A pH increase may restrict the physiologic relevance and can lead to salt precipitates of artificial fluids.[26] Modifications in the biological fluid may increase over time or reverse due to an increase of pH.

Conclusion

The development of a reliable *in vitro* model, simulating physiologic conditions is receiving increasing attention. We developed a model enabling insight on protein aggregation, fragmentation, and charge heterogeneity under simulated physiologic conditions, without altering the protein of interest. Due to biological fluids forming SbVPs under *ex vivo* conditions, artificial fluids and/or models maintaining the fluid stability are needed, particularly when assessing the physical stability of therapeutic proteins. PBS was regarded as less suitable to model physiologic conditions as the physiologic ionic composition and buffering mechanism seem to impact *in vivo* stability. Thus, certain protein liabilities may not be detected when using PBS.

Studies accurately modelling physiologic parameters after simulated administration can improve knowledge on *in vivo* stability of therapeutic proteins. Understanding physiologic factors and sequence hotspots of proteins impacting the stability of therapeutic proteins and incorporating these into a suitable *in vitro* model is instrumental in the development of therapeutic proteins. Although it remains unknown how these findings correlate to *in vivo* data in humans, such studies are particularly appealing as they can be used as a screening tool before entering resource-demanding clinical studies.

Further studies are required to understand which physiologic factors impact the *in vivo* stability of proteins. Ideally, comparing the *in vivo* stability of mAb molecules which differ only slightly in their variable domains can give insight on the impact of certain biophysical properties and/or sequence hot-spots. Lastly, studies could aim to evaluate different *in vitro* models to further improve knowledge in the field of *in vivo* protein stability.

Supplementary materials

Supplementary material associated with this article can be found, in the online version, at doi:10.1016/j.xphs.2021.03.007.

References

1. Mathaes R, Koulov A, Joerg S, Mahler HC. Subcutaneous injection volume of biopharmaceuticals-pushing the boundaries. *J Pharm Sci*. 2016;105(8):2255–2259.
2. Sanchez-Felix M, Burke M, Chen HH, Patterson C, Mittal S. Predicting bioavailability of monoclonal antibodies after subcutaneous administration: Open innovation challenge. *Adv Drug Deliv Rev*. 2020.
3. Schuster J, Koulov A, Mahler HC, Detampel P, Huwyler J, Singh S, Mathaes R. In vivo stability of therapeutic proteins. *Pharm Res*. 2020;37:23.
4. Richter WF, Christianson GJ, Frances N, Grimm HP, Proetzel G, Roopenian DC. Hematopoietic cells as site of first-pass catabolism after subcutaneous dosing and contributors to systemic clearance of a monoclonal antibody in mice. *MAbs*. 2018;10(5):803–813.
5. McDonald TA, Zepeda ML, Tomlinson MJ, Bee WH, Ivens IA. Subcutaneous administration of biotherapeutics: Current experience in animal models. *Curr Opin Mol Ther*. 2010;12(4):461–470.
6. Rosenberg AS. Effects of protein aggregates: an immunologic perspective. *AAPS J*. 2006;8(3):E501–E507.
7. Liu YD, Chen Y, Tsui G, Wei B, Yang F, Yu C, Cornell C. *Predictive In Vitro Vitreous and Serum Models and Methods to Assess Thiol-related Quality Attributes in Protein Therapeutics*. Anal Chem; 2020.

8. Schuster J, Mahler HC, Koulov A, Joerg S, Racher AJ, Huwyler J, Detampel P, Mathaes R. Tracking the physical stability of fluorescent-labeled mAbs under physiologic in vitro conditions in human serum and PBS. *Eur J Pharm Biopharm*. 2020;152:193–201.
9. Schuster J, Koulov A, Mahler HC, Joerg S, Huwyler J, Schleicher K, Detampel P, Mathaes R. Particle analysis of biotherapeutics in human serum using machine learning. *J Pharm Sci*. 2020;109(5):1827–1832.
10. Patel S, Stracke JO, Altenburger U, Mahler HC, Metzger P, Shende P, Jere D. Prediction of intraocular antibody drug stability using ex-vivo ocular model. *Eur J Pharm Biopharm*. 2017;112:177–186.
11. Awwad S, Lockwood A, Brocchini S, Khaw PT. The PK-Eye: A novel in vitro ocular flow model for use in preclinical drug development. *J Pharm Sci*. 2015;104 (10):3330–3342.
12. Bown HK, Bonn C, Yohe S, Yadav DB, Patapoff TW, Daugherty A, Mrsny RJ. In vitro model for predicting bioavailability of subcutaneously injected monoclonal antibodies. *J Control Release*. 2018;273:13–20.
13. Kinnunen HM, Sharma V, Contreras-Rojas LR, Yu Y, Alleman C, Sreedhara A, Fischer S, Khawli L, Yohe ST, Bumbaca D, Patapoff TW, Daugherty AL, Mrsny RJ. A novel in vitro method to model the fate of subcutaneously administered biopharmaceuticals and associated formulation components. *J Control Release*. 2015;214:94–102.
14. Doell A, Schmitz OJ, Hollmann M. Shedding light into the subcutis: A mass spectrometry based immunocapture assay enabling full characterization of therapeutic antibodies after injection in vivo. *Anal Chem*. 2019;91(15):9490–9499.
15. Thati S, McCallum M, Xu Y, Zheng M, Chen Z, Dai J, Pan D, Dalpathado D, Mathias N. Novel applications of an in vitro injection model system to study bioperformance: Case studies with different drug modalities. *J Pharm Innov*. 2020;15:268–280.
16. Mach H, Gregory SM, Mackiewicz A, Mittal S, Lalloo A, Kirchmeier M, Shameem M. Electrostatic interactions of monoclonal antibodies with subcutaneous tissue. *Ther Deliv*. 2011;2(6):727–736.
17. Wiig H, Swartz MA. Interstitial fluid and lymph formation and transport: physiological regulation and roles in inflammation and cancer. *Physiol Rev*. 2012;92 (3):1005–1060.
18. Schaupp L, Ellmerer M, Brunner GA, Wutte A, Sendlhofer G, Trajanoski Z, Skrabal F, Pieber TR, Wach P. Direct access to interstitial fluid in adipose tissue in humans by use of open-flow microperfusion. *Am J Physiol*. 1999;276(2):E401–E408.
19. Webb P. Temperatures of skin, subcutaneous tissue, muscle and core in resting men in cold, comfortable and hot conditions. *Eur J Appl Physiol Occup Physiol*. 1992;64(5):471–476.
20. Zhao L, Ji P, Li Z, Roy P, Sahajwalla CG. The antibody drug absorption following subcutaneous or intramuscular administration and its mathematical description by coupling physiologically based absorption process with the conventional compartment pharmacokinetic model. *J Clin Pharmacol*. 2013;53(3):314–325.
21. Ryman JT, Meibohm B. Pharmacokinetics of monoclonal antibodies. *CPT Pharmacometrics Syst Pharmacol*. 2017;6(9):576–588.
22. Reed RK, Lepsoe S, Wiig H. Interstitial exclusion of albumin in rat dermis and subcutis in over- and dehydration. *Am J Physiol*. 1989;257(6 Pt 2):H1819–H1827.
23. Kinnunen HM, Mrsny RJ. Improving the outcomes of biopharmaceutical delivery via the subcutaneous route by understanding the chemical, physical and physiological properties of the subcutaneous injection site. *J Control Release*. 2014;182:22–32.
24. Duems-Noriega O, Arino-Blasco S. Subcutaneous fluid and drug delivery: safe, efficient and inexpensive. *Rev Clin Gerontol*. 2015;25:117–146.
25. Aukland K, Reed RK. Interstitial-lymphatic mechanisms in the control of extracellular fluid volume. *Physiol Rev*. 1993;73(1):1–78.
26. Bretag AH. Synthetic interstitial fluid for isolated mammalian tissue. *Life Sci*. 1969;8(5):319–329.
27. Lobo B, Lo S, Wang YJ, Wong RL. *Method and Formulation for Reducing Aggregation of a Macromolecule Under Physiological Conditions*. Google Patents; 2014. In Genentech I, editor, ed..
28. Rice P, Longden I, Bleasby A. EMBOSS: the European molecular biology open software suite. *Trends Genet*. 2000;16(6):276–277.
29. Ilias I, Tzanela M, Nikitas N, Vassiliadi DA, Theodorakopoulou M, Apollonatou S, Tsagarakis S, Dimopoulou I. Evidence of subcutaneous tissue lipolysis enhancement by endogenous cortisol in critically Ill patients without shock. *In Vivo*. 2015;29(4):497–499.
30. Maggs DG, Jacob R, Rife F, Lange R, Leone P, During MJ, Tamborlane WV, Sherwin RS. Interstitial fluid concentrations of glycerol, glucose, and amino acids in human quadricep muscle and adipose tissue. Evidence for significant lipolysis in skeletal muscle. *J Clin Invest*. 1995;96(1):370–377.
31. Kratz A, Ferraro M, Sluss PM, Lewandrowski KB. Case records of the Massachusetts General Hospital. Weekly clinicopathological exercises. Laboratory reference values. *N Engl J Med*. 2004;351(15):1548–1563.
32. Wike-Hooley JL, Van der Zee J, van Rhoon GC, Van den Berg AP, Reinhold HS. Human tumour pH changes following hyperthermia and radiation therapy. *Eur J Cancer Clin Oncol*. 1984;20(5):619–623.
33. Guyton AC, Hall JE. *Textbook of Medical Physiology*. 11th ed. Philadelphia: Elsevier Inc; 2006.
34. Turitto V, Slack SM. Blood and Related Fluids. editors. In: Murphy W, Black J, Hastings G, eds. *Handbook of Biomaterial Properties*. New York: Springer; 2016:115–124. ed..
35. Schmid I, Bonnington L, Gerl M, Bomans K, Thaller AL, Wagner K, Schlothauer T, Falkenstein R, Zimmermann B, Kopitz J, Hasmann M, Bauss F, Haberger M, Reusch D, Bulau P. Assessment of susceptible chemical modification sites of trastuzumab and endogenous human immunoglobulins at physiological conditions. *Nat Commun Biol*. 2018;1(28).
36. Yang N, Tang Q, Hu P, Lewis MJ. Use of in vitro systems to model in vivo degradation of therapeutic monoclonal antibodies. *Anal Chem*. 2018;90(13):7896–7902.
37. Yin S, Pastuskovas CV, Khawli LA, Stults JT. Characterization of therapeutic monoclonal antibodies reveals differences between in vitro and in vivo time-course studies. *Pharm Res*. 2013;30(1):167–178.
38. Jiang XG, Wang T, Kaltenbrunner O, Chen K, Flynn GC, Huang G. Evaluation of protein disulfide conversion in vitro using a continuous flow dialysis system. *Anal Biochem*. 2013;432(2):142–154.
39. Del Amo EM, Rimpela AK, Heikkinen E, Kari OK, Ramsay E, Lajunen T, Schmitt M, Pelkonen L, Bhattacharya M, Richardson D, Subrizi A, Turunen T, Reinisalo M, Itkonen J, Toropainen E, Casteleijn M, Kidron H, Antopolsky M, Vellonen KS, Ruponen M, Urtti A. Pharmacokinetic aspects of retinal drug delivery. *Prog Retin Eye Res*. 2017;57:134–185.
40. Liu H, Nowak C, Patel R. Modifications of recombinant monoclonal antibodies in vivo. *Biologicals*. 2019;59:1–5.
41. Linthwaite VL, Janus JM, Brown AP, Wong-Pascua D, O'Donoghue AC, Porter A, Treumann A, Hodgson DRW, Cann MJ. The identification of carbon dioxide mediated protein post-translational modifications. *Nat Commun*. 2018;9 (1):3092.
42. Haaverstad R, Romslo I, Larsen S, HO Myhre. Protein concentration of subcutaneous interstitial fluid in the human leg. A comparison between the wick technique and the blister suction technique. *Int J Microcirc Clin Exp*. 1996;16 (3):111–117.
43. Varkhede N, Bommana R, Schoneich C, Forrest ML. Proteolysis and oxidation of therapeutic proteins after intradermal or subcutaneous administration. *J Pharm Sci*. 2020;109(1):191–205.
44. Dillon TM, Ricci MS, Vezina C, Flynn GC, Liu YD, Rehder DS, Plant M, Henkle B, Li Y, Deechongkit S, Varnum B, Wypych J, Balland A, Bondarenko PV. Structural and functional characterization of disulfide isoforms of the human IgG2 subclass. *J Biol Chem*. 2008;283(23):16206–16215.
45. Leeman M, Choi J, Hansson S, Storm MU, Nilsson L. Proteins and antibodies in serum, plasma, and whole blood-size characterization using asymmetrical flow field-flow fractionation (AF4). *Anal Bioanal Chem*. 2018;410(20):4867–4873.
46. Vlasak J, Ionescu R. Fragmentation of monoclonal antibodies. *MAbs*. 2011;3 (3):253–263.
47. Goetze AM, Liu YD, Arroll T, Chu L, Flynn GC. Rates and impact of human antibody glycation in vivo. *Glycobiology*. 2012;22(2):221–234.
48. Richter WF, Jacobsen B. Subcutaneous absorption of biotherapeutics: knowns and unknowns. *Drug Metab Dispos*. 2014;42(11):1881–1889.
49. Wiig H, Reed RK, Tenstad O. Interstitial fluid pressure, composition of interstitium, and interstitial exclusion of albumin in hypothyroid rats. *Am J Physiol Heart Circ Physiol*. 2000;278(5):H1627–H1639.
50. Hotzel I, Theil FP, Bernstein LJ, Prabhu S, Deng R, Quintana L, Lutman J, Sibia R, Chan P, Bumbaca D, Fielder P, Carter PJ, Kelley RF. A strategy for risk mitigation of antibodies with fast clearance. *MAbs*. 2012;4(6):753–760.

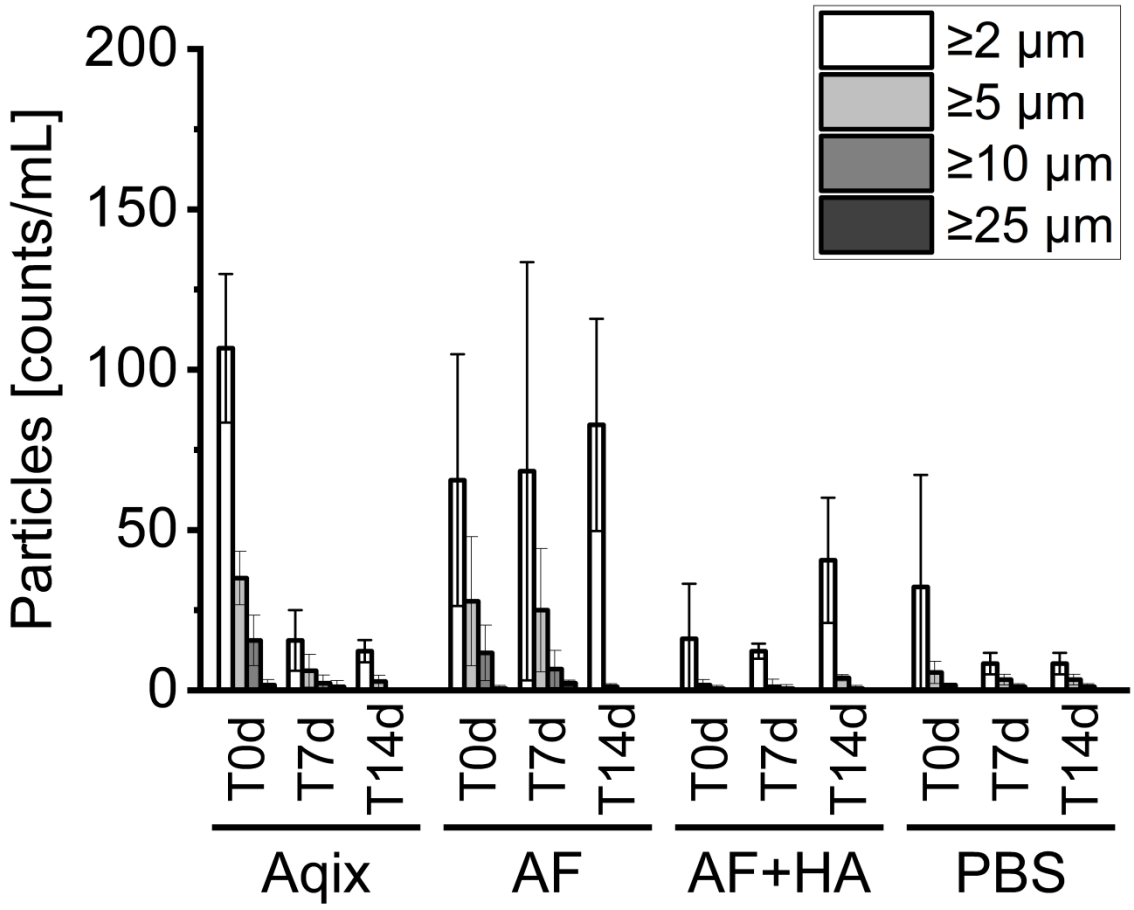

Supplementary Figure 1: SbVP analysis. LO analysis of fluid controls, i.e., spiked with histidine buffer. Each control was prepared in triplicates and measured once at each time point. n=3

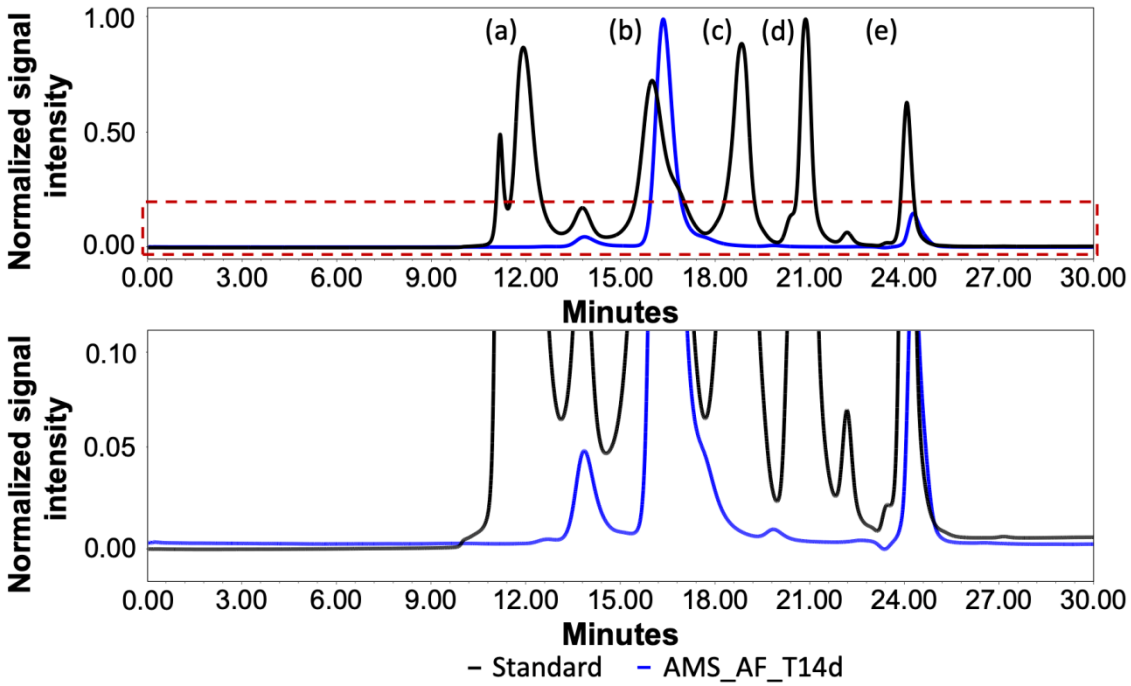

Supplementary Figure 2: HP-SEC chromatogram. Overlay of a HPLC size standard (black line) with mAb in AF after 14d of incubation (blue line). Molecular weight of the standard peaks: (a) 670 kDa, (b) 158 kDa, (c) 44 kDa, (d) 17 kDa, (e) 1.35 kDa. MW of mAb2 monomer: 147 kDa. Signal intensity of the standard and mAb were normalized.

Discussion

Analytical Challenges Assessing the *In Vivo* Protein Stability

Assessing the *in vivo* stability of therapeutic proteins is evolving. However, due to the complexity of biological fluids, analyzing the stability of therapeutic proteins under physiologic conditions remains challenging. To date, the majority of studies simulate the *in vivo* fate of therapeutic proteins under *in vitro* conditions. In such studies, the protein of interest is mixed with a representative human body fluid and incubated under simulated physiologic condition. Regardless of the route of administration, once injected or infused, therapeutic proteins are immersed in a complex biological fluid, containing hundreds to thousands of molecules. For example, the endogenous protein concentration in whole blood ranges from 55 to 80 mg/mL[59]. In the event that a mAb is the therapeutic protein of interest, the main analytical challenge is to detect the therapeutic IgG without interference from endogenous IgGs found in biological fluids (e.g., 6.1 to 13.0 mg/mL in blood[59]). In addition to endogenous IgGs, other proteins may also interfere with the detection[60].

To circumvent matrix interference of biological fluids, analytical approaches can be subdivided into three strategies. Firstly, labeling the protein of interest (e.g., via fluorescence dye). Secondly, purifying the protein of interest (e.g., via protein A). Thirdly, modifying or substituting human biological fluids (e.g., using other fluids such as PBS). Each of these analytical strategies leads to a trade-off between the physiologic relevance of a given fluid and enabling analysis without matrix interference. For example, analysis in PBS is uncomplicated due to the absence of proteins, which presumably led to its usage to simulate physiologic conditions. However, its composition deviates profoundly from that found in human biological fluids and thus it has been questioned whether PBS is representative of *in vivo* conditions. On the other hand, analysis in complex biological fluids such as human serum/plasma requires sample manipulation such as labeling or purification techniques. These sample workup procedures may impact the stability of a therapeutic protein. Due to the unique composition of biological fluids, simulating a specific route of administration requires unique *in vitro* models.

Development of an *In Vitro* Intravenous Model

The human body continuously adjusts to internal and external changes to maintain physiologic conditions such as osmo-, thermo-, and chemical- regulation. As an example, the blood pH is primarily regulated by the bicarbonate buffer between pH 7.35 to 7.45. Simulating the complex

homeostasis of the human body under *in vitro* conditions is therefore difficult. We demonstrated that if the conditions are not adjusted during the experimental setup (e.g., incubation under a carbon dioxide atmosphere), the pH of human serum increases rapidly to values of 8 or higher[61]. This was a key finding as pH changes may compromise the stability of a fluid, matrix compounds, and is ultimately not reflective of the physiologic conditions encountered in patients. Our developed *in vitro* model maintained the physiologic pH of the fluid by adjusting the carbon dioxide level to a desired concentration[61,62]. To simulate the conditions after IV administration we selected human serum as biological fluid. Whole blood or human plasma represent alternative options. However, previous reports stated that cell lysis occurred in blood under *in vitro* conditions[63] and plasma contains a higher protein concentration than serum, potentially causing matrix interference to an even higher extent[44].

Advances have been made in regards to the knowledge on the *in vivo* stability of therapeutic proteins, with the vast majority of studies focusing on chemical degradation, while knowledge on physical protein stability after administration is limited[44]. To the best of our knowledge there are no studies available assessing SbVP formation of therapeutic proteins in serum over time points beyond 24 h. Due to the long half-life of therapeutic proteins, shedding light on SbVP formation and protein aggregation after exposure to biological fluids was a main focus of our developed model.

We have shown that despite maintaining physiologic conditions (pH 7.4, 37°C) and handling samples aseptically, human serum itself formed SbVPs *in vitro*[61,64,65]. Therefore SbVP methods such as LO and FI were inapplicable as it was not possible to differentiate whether particles originated from the serum matrix or spiked mAb[61,64,65]. We chose to fluorescent-label mAbs prior to the exposure to human serum as it enabled to assess the stability of a protein directly in a neat biological fluids without requiring purification steps. This is particularly important when assessing SbVP formation in biological fluids. Purification techniques are less applicable, as insoluble aggregates may not be captured from the biological fluid.

Fluorescence labeling is debated as the conjugated fluorophore itself may compromise the intrinsic protein stability. Our accelerated stability study showed no difference in the stability between the labeled and unlabeled mAbs. [44]Another important aspect to consider during method development was the autofluorescence of human serum due to matrix components such as tryptophan, riboflavin, and bilirubin[66]. Although the fluorescence intensity of these compounds is typically negligible compared to that of fluorescent probes, autofluorescence can still interfere with analysis[67]. Depending upon the intensity of a fluorescent probe and the degree of labeling, a

sufficient signal to noise ratio is required[68]. We demonstrated that at the excitation and emission maxima of Alexa Fluor 488, the fluorescence intensity of serum was negligible.

The developed fluorescence methods, namely, HP-SEC-FLD, flow cytometry, imaging flow cytometry, and fluorescence microscopy, enabled to monitor SbVP formation, protein aggregation, and fragmentation in neat human serum. We observed substantial differences in regards to protein fragmentation as certain mAbs contained LMWS of up to 20%, while others remained stable over 5 days in serum. Interestingly, some mAbs fragmented upon exposure to serum. We also observed an increase of HMWS in all 8 mAbs in serum over time, which can most likely be attributed to an interaction with serum proteins. Solely based on the concentration of spiked therapeutic proteins (0.2 mg/mL) and that of serum (55 to 80 mg/mL) an interaction with serum proteins is far more likely to occur than self-aggregation of the mAbs. All developed fluorescence methods were stability indicating and allow to benchmark the stability of therapeutic proteins directly in unaltered biological fluids.

Despite the advantages to assess the stability in serum, the developed methods had certain limitations in regards to protein fragments and aggregates. For example, a mAb may cleave at a position that results in protein fragments without a fluorophore. Thus, only fragments containing a fluorophore were detected. Due to serum containing ca. 10,000 endogenous proteins over a wide molecular range[69], non-labeled fragments cannot be separated from the serum matrix. Such interreferences from endogenous proteins have been previously reported using CE-SDS[26]. Advances in intact MS coupled with CE[70] or LC[26,71] may offer a promising alternative to track protein fragmentation in biological fluids. However, these methods require purification steps prior to analysis. This causes limitations as the protein of interest may degrade upon exposure to a biological fluid and may not bind to the desired target. For example, deamidation can decrease binding affinity or a protein fragment may not contain the target-binding site[50]. Such degraded proteins would remain undetectable in the biological fluid. Combining two independent capturing techniques and adequate control experiments during sample work up can minimize the risk of a method bias towards certain modifications[72].

Our imaging flow cytometry data revealed that unlabeled particles forming in serum were interacting with those of spiked fluorescently-labeled particles[64]. Depending on the size and composition of newly formed particles (e.g., mostly non-labeled serum particles), the fluorescence intensity can decrease[64,73]. The fluorescence intensity of particles may fall under the limit of detection of the analytical method and remains undetected. We have shown that independently prepared control samples, i.e., serum without a therapeutic mAb, varied in particle counts. This

finding is particularly important to consider when comparing SbVP counts of mAbs spiked in a biological fluid. This confirmed also our HP-SEC-FLD results showing an increase of HMWS over time in serum.

To assess the impact of fluids on the stability of mAbs, we compared PBS to human serum *in vitro*. Throughout the study we observed that all mAbs remained stable in PBS, i.e., no relevant SbVP formation, protein aggregation, nor fragmentation was observed. This indicated that the serum matrix degraded mAbs as temperature, pH, and osmolality were virtually identical to that in PBS.

While it is known that protein properties such as pI impact PK, e.g., pI values lower than the physiologic pH lead to a longer half-life[27], studies aiming to correlate the *in vivo* stability to protein properties are missing. We selected eight mAbs based on their pI and hydrophobicity as these aspects are known to impact protein aggregation. While most commercial mAbs have an pI of >8[74], pI values ranging from 6.1 to 9.4 have been reported[75]. Whether positive or negative charged mAbs differ in their stability *in vivo* is unknown. Particularly, a mAb with an pI close to the physiologic pH is expected to have low colloidal stability. The stability among the tested mAbs differed markedly in serum, however, our results showed no correlation between *in vivo* protein stability and their pI and hydrophobicity. It may be argued that due to the sequence differences between the mAbs used in our studies, it is possible that other factors than pI and hydrophobicity impacted the *in vivo* stability. For example, hydrophobic patches may impact *in vivo* aggregation. Further studies are required to assess the impact of protein properties on their stability *in vivo*. Ideally, mAbs with slight differences in their CDR and/or framework region, yet remaining a high sequence similarity overall, can give further insight into which biophysical properties impact *in vivo* protein stability[45]. Knowledge on the impact of protein properties on *in vivo* stability during the pre-clinical development would be instrumental for the selection of clinical candidates.

Development of an *In Vitro* Subcutaneous Model

The human SC tissue is complex as it hypothesized to contain a heterogenous network comrpising a stationary "water-poor, colloid-rich" and mobile "water-rich, colloid-poor" phase within the interstitium[76,77]. Based on this hypothesis, the phases are in a functional equlibirium and alternating regions of low and high negative charge densities exist[78,79]. The compisition of the human SC interstitial fluid is not precisely known as it is not readily accessible and most sampling methods are invasive causing leakage of other fluid compartments[80-82]. Due to the constraint on human SC tissue availability, we prepared protein-free artificial physiologic fluids.

We showed that all developed artificial fluids remained stable over extended periods of time, i.e., no relevant SbVP formation was observed. This is important, as contrary to biological fluids forming SbVPs within days, it enables to monitor SbVPs over periods of time relevant to therapeutic proteins (e.g., 21 days half-life of mAbs)[62]. The high stability of artificial fluids may be due to the absence of matrix compounds such as lipids and proteins.

To investigate our previous findings about the impact of different fluids on the *in vivo* protein stability further, three protein-free physiologic fluids were compared to PBS. Throughout the study both tested mAbs were substantially more stable in PBS compared to all bicarbonate buffers. Although the developed *in vitro* model simulated SC administration as compared to our previous IV *in vitro* model, our results confirmed our earlier observation that the tested mAbs were substantially more stable in PBS. Interestingly, PBS and the bicarbonate buffer AF differed only in electrolyte composition and buffering mechanism, however, showed considerable differences in their impact on protein stability. For example, for both mAbs substantial SbVP counts were measured in AF, whereas minimal SbVP counts were measured in PBS. While it remains unknown whether data obtained in PBS or bicarbonate buffers translate more accurately to events occurring in patients, solely based on the composition, the developed bicarbonate buffers resemble the *in vivo* conditions more closely than PBS. Linthwaite *et al.* showed that carbon dioxide can bind to proteins reversibly and cause protein carbamylation, which is thought to be linked to protein function[83]. Carbon dioxide-dependent modifications may be more common than previously appreciated. In addition to the higher physiologic resemblance, benchmarking the stability of different mAbs in PBS may be challenging as the conditions were not impacting the stability to an extent that allows to detect protein liabilities in our study.

Our HP-SEC results showed a consistent increase in fragments over time. Compared to our previous studies in serum, fragmentation was substantially lower in bicarbonate fluids with values of up to 1%. Comparing these studies is challenging as the study in serum involved fluorescence labeling, whereas no labeling was used in the SC model. Furthermore, fragmentation may be enzymatically driven by the serum matrix, which is lacking in protein-free bicarbonate fluids. Another consideration is a protein's propensity to fragment.

Our studies challenged the "doctrine" of using PBS to simulate *in vivo* conditions and demonstrated that PBS is poorly suitable to evaluate *in vivo* protein aggregation and fragmentation. All bicarbonate buffers were suitable to assess protein liabilities under physiologic conditions, with no substantial differences among the fluids. Hyaluronan appeared to have no impact on protein stability. Thus, a solution containing the main cations and anions of extracellular fluids, i.e., AF, as used in previous studies[84] appeared to be sufficient to detect stability differences among the tested mAbs. The developed SC *in vitro* model simulated the pH, electrolyte composition, osmolality, and bicarbonate buffer found in the human SC tissue. The absence of proteins enabled to assess the stability of a therapeutic protein without sample manipulation such as purification/labeling and thus resembles the clinical setting more closely. Not relying on fluorescence detection allowed to apply additional methods such as CE-SDS and iCE.

Overall, the developed SC model was reliable enabling even longer incubation times (e.g., 1 month) without labeling and purification techniques and could be implemented as an early screening tool to evaluate the *in vivo* stability of therapeutic proteins.

Outlook

Selection of a Biological Fluid

The selection of a representative fluid to simulate the conditions encountered in patients is fundamental in the development of reliable *in vitro* models. While there are no commercial fluids available to simulate SC administration, human whole blood, serum, and plasma are available to simulate IV administration. Due to the limited stability of whole blood *in vitro*, studies used serum or plasma. Whether serum or plasma impact the stability of a protein differently and which fluid may be better suitable to simulate IV administration remains unknown. Previous preliminary studies reported no differences between serum and plasma[60,85], however, studies specifically comparing the impact of these fluids on protein stability remain largely missing. While the composition between serum and plasma is nearly identical, i.e., serum contains 3 to 5 g/L less protein than plasma, these fluids are prepared differently. Plasma is prepared by adding an anticoagulant (e.g., ethylenediaminetetraacetic acid) to prevent clotting of whole blood. Serum can prepared by defibrinating plasma (plasma-derived serum) or by allowing whole blood to clot naturally and then using the supernatant after centrifugation (off-clot serum). Future studies should also compare pooled serum/plasma to that of individual donors as well as biological fluids from healthy subjects to that of patients. Another aspect to consider is a comparison of different species. For example, Arvinte *et al.* reported a spiked therapeutic protein aggregated in animal plasma but not in human plasma *in vitro*[86,87]. Furthermore, patient related aspects such as immune status and genotypes could be considered.

Despite advances in fluorescence labeling and purification techniques as well as different analytical approaches to reduce the complexity of biological fluids, each method leads to a compromise between the physiologic relevance of a fluid and the ability to detect the protein of interest[88]. Although we have shown the advantage of preparing artificial protein-free physiologic buffers[62], the protein composition in biological fluids such as serum/plasma may offer an alternative approach.

Serum/plasma contains approximately 10,000 endogenous proteins[69] of which merely 22 proteins constitute to 99% of the protein concentration[89]. The vast majority of these proteins are larger than 50 kDa. Thus, depleting these proteins by size (e.g., ultrafiltration) allows to substantially decrease the protein concentration while maintaining the majority of the original composition, including many peptides/proteins. Theoretically, a serum ultrafiltrate exhibits a relevant electrolyte composition, osmolality, pH, thiol concentration, and even remains peptidases/proteases having a lower molecular weight than the desired molecular weight cut-off (e.g., <50 kDa). Depending on

the selected size cut-off, matrix interference may still occur and requires adequate control experiments[90,91]. Theoretically, 50 kDa appears as an adequate cut-off as it removes endogenous albumin (66 kDa) and IgGs (150 kDa), which contribute to more than 50% of the total protein concentration in most biological fluids. Future studies could aim to reduce the complexity of biological fluids by stripping endogenous serum/plasma proteins using tangential flow filtration or centrifugal ultrafiltration. This reduces the matrix complexity to an extent that enables direct analysis in the fluid without sample manipulation such as labeling, while maintaining the majority of the composition of a biological fluid.

Ultimately, it is not known how protein stability under *in vitro* models translate to clinical results. While further studies are warranted to assess how translatable *in vitro* findings are to an *in vivo* setting, one study by Yang *et al.* compared the chemical stability of a mAb *in vitro* to that of healthy humans and reported promising findings[48]. The PBS *in vitro* model showed good correlation to *in vivo* data, however, a human serum *in vitro* model showed an even higher correlation, highlighting the importance of a biological fluid.

Advanced *In Vitro* Models

The aim to reduce animal experiments during pre-clinical development stages due to an ethical and resource perspective has long been discussed; making *in vitro* models an attractive alternative[92]. For example, Sánchez-Félix *et al.* discussed the advantage of reliable *in vitro* models during pre-clinical stages to predict the bioavailability of therapeutic proteins after SC administration[3]. Animal models show poor correlation to clinical data of therapeutic proteins[93]. Several research groups developed *in vitro* models, which simulated and maintained the physiologic conditions over extended periods of time to mimic the fate of therapeutic proteins after different routes of administration[93-97]. In that regard, *in vitro* models are advantageous as they can accelerate the selection of safe and effective candidate molecules and potentially bridge the gap to clinical studies.

In vitro models can differ in their study design as certain models used static incubation[26,43,48,60-62,64,65,73,98,99] or a dialysis setup[55,93-97,100-102]. As these study designs are fundamentally different, future studies could aim at evaluating the impact of either study design on the stability of therapeutic proteins. We showed that certain dialysis cassettes led to particle shedding and were thus poorly applicable when assessing SbVP counts of therapeutic proteins[62]. However, dialysis chambers are argued to emulate the fate after SC injection more closely, as the biological fluid and DP are mixed slowly and dialysis allows diffusion of excipients from the therapeutic protein. Thus, such advanced *in vitro* models may offer an attractive alternative and should be further evaluated in future studies. Further improvements of *in vitro* models such as controlled flow rate may extend the stability of

biological fluids and thus resemble physiologic conditions more accurately and for longer durations.

Besides the importance of studies investigating the impact the biological fluids on unstressed therapeutic proteins, another research question is related to the fate of stressed proteins. A DP may degrade prior to administration, e.g., during storage or clinical preparation, it remains unknown if a stressed protein would degrade further *in vivo* or if the environment may function as a repair system. As an example, protein dimers generated before administration may reverse back to a monomer or continue to degrade *in vivo*[46]. Further investigations in this field will have significant implications for future model developments and contribute knowledge about the relationship between physiologic conditions and *in vivo* stability of proteins.

Conclusion

Therapeutic proteins can degrade upon exposure to physiologic conditions. Human-based *in vitro* models are a promising alternative to animal models to evaluate the *in vivo* stability of therapeutic proteins. PBS appeared not suitable to simulate physiologic conditions, particularly, in regards to physical protein stability and protein fragmentation. Fluorescence labeling is a reliable technique to track protein stability in unaltered biological fluids, showed however limited applicability in regards to SbVPs due to the instability of human serum *in vitro*.

The developed SC model is promising as physiologic conditions and fluids remain stable over several weeks, enabling to simulate the *in vivo* environment closely. Artificial fluids can be modified to resemble other relevant extracellular fluids and simulate different routes of administration (e.g., vitreous humor for intravitreal injection). The matrix composition enables to apply a wide range of analytical methods typically used for DP characterization.

Such *in vitro* models are strongly needed as they allow for a faster evaluation and may be better suitable to translate to clinical data. Collectively, correlating *in silico* and *in vitro* data to those found in patients is instrumental in the development of such models and can contribute significant knowledge to the *in vivo* stability of therapeutic proteins. Such strategies should be implemented as an early risk assessment of molecules before entering resource demanding clinical trials as this can accelerate pre-clinical development. This allows to re-engineer therapeutic protein candidates during pre-clinical stages and ultimately improve their stability *in vivo* in patients.

References

1. Urquhart L 2020. Top companies and drugs by sales in 2019. Nat Rev Drug Discov 19(4):228.
2. Kaplon H, Reichert JM 2019. Antibodies to watch in 2019. MAbs 11(2):219-238.
3. Sanchez-Felix M, Burke M, Chen HH, Patterson C, Mittal S 2020. Predicting bioavailability of monoclonal antibodies after subcutaneous administration: Open innovation challenge. Adv Drug Deliv Rev.
4. Hamuro L, Kijanka G, Kinderman F, Kropshofer H, Bu DX, Zepeda M, Jawa V 2017. Perspectives on Subcutaneous Route of Administration as an Immunogenicity Risk Factor for Therapeutic Proteins. J Pharm Sci 106(10):2946-2954.
5. Manning MC, Chou DK, Murphy BM, Payne RW, Katayama DS 2010. Stability of protein pharmaceuticals: an update. Pharm Res 27(4):544-575.
6. Hawe A, Wiggenhorn M, van de Weert M, Garbe JH, Mahler HC, Jiskoot W 2012. Forced degradation of therapeutic proteins. J Pharm Sci 101(3):895-913.
7. Chi EY, Krishnan S, Randolph TW, Carpenter JF 2003. Physical stability of proteins in aqueous solution: mechanism and driving forces in nonnative protein aggregation. Pharm Res 20(9):1325-1336.
8. Gao J, Yin DH, Yao Y, Sun H, Qin Z, Schoneich C, Williams TD, Squier TC 1998. Loss of conformational stability in calmodulin upon methionine oxidation. Biophys J 74(3):1115-1134.
9. Falconer RJ 2019. Advances in liquid formulations of parenteral therapeutic proteins. Biotechnol Adv 37(7):107412.
10. Mahler HC, Borchard G, Luessen H. 2010. Protein Pharmaceuticals: Formulation, Analytics and Delivery. ed., Aulendorf: ECV, Editio-Cantor-Verlag.
11. Wang W 1999. Instability, stabilization, and formulation of liquid protein pharmaceuticals. Int J Pharm 185(2):129-188.
12. Thiagarajan G, Semple A, James JK, Cheung JK, Shameem M 2016. A comparison of biophysical characterization techniques in predicting monoclonal antibody stability. MAbs 8(6):1088-1097.
13. Marti DN 2005. Apparent pKa shifts of titratable residues at high denaturant concentration and the impact on protein stability. Biophys Chem 118(2-3):88-92.
14. Mahler HC, Friess W, Grauschopf U, Kiese S 2009. Protein aggregation: pathways, induction factors and analysis. J Pharm Sci 98(9):2909-2934.
15. Rosenberg AS 2006. Effects of protein aggregates: an immunologic perspective. AAPS J 8(3):E501-507.
16. Carpenter JF, Randolph TW, Jiskoot W, Crommelin DJ, Middaugh CR, Winter G, Fan YX, Kirshner S, Verthelyi D, Kozlowski S, Clouse KA, Swann PG, Rosenberg A, Cherney B 2009. Overlooking subvisible particles in therapeutic protein products: gaps that may compromise product quality. J Pharm Sci 98(4):1201-1205.
17. Mahler HC, Jiskoot W. 2012. Analysis of Aggregates and Particles in Protein Pharmaceuticals. ed., Hoboken, NJ: John Wiley & Sons.
18. Manning MC, Patel K, Borchardt RT 1989. Stability of protein pharmaceuticals. Pharm Res 6(11):903-918.
19. Doessegger L, Mahler HC, Szczesny P, Rockstroh H, Kallmeyer G, Langenkamp A, Herrmann J, Famulare J 2012. The potential clinical relevance of visible particles in parenteral drugs. J Pharm Sci 101(8):2635-2644.
20. Mathaes R, Mahler HC 2018. Next Generation Biopharmaceuticals: Product Development. Adv Biochem Eng Biotechnol 165:253-276.
21. Norde W. 2000. Proteins at solid surfaces. In Baszkin A, Norde W, editors. Physical and Chemistry of Biological Interfaces, ed., Basel: Marcel Dekker p115-135.

22. Chi EY, Weickmann J, Carpenter JF, Manning MC, Randolph TW 2005. Heterogeneous nucleation-controlled particulate formation of recombinant human platelet-activating factor acetylhydrolase in pharmaceutical formulation. J Pharm Sci 94(2):256-274.
23. Vermeer AW, Bremer MG, Norde W 1998. Structural changes of IgG induced by heat treatment and by adsorption onto a hydrophobic Teflon surface studied by circular dichroism spectroscopy. Biochim Biophys Acta 1425(1):1-12.
24. Brynda E, Houska M, Kalal J, Cepalova NA 1980. Adsorption of human fibrinogen and human serum albumin onto polyethylene. Ann Biomed Eng 8(3):245-252.
25. Rabe M, Verdes D, Rankl M, Artus GR, Seeger S 2007. A comprehensive study of concepts and phenomena of the nonspecific adsorption of beta-lactoglobulin. Chemphyschem 8(6):862-872.
26. Yin S, Pastuskovas CV, Khawli LA, Stults JT 2013. Characterization of therapeutic monoclonal antibodies reveals differences between in vitro and in vivo time-course studies. Pharm Res 30(1):167-178.
27. Chiu ML, Goulet DR, Teplyakov A, Gilliland GL 2019. Antibody Structure and Function: The Basis for Engineering Therapeutics. Antibodies (Basel) 8(4).
28. Wang W 2005. Protein aggregation and its inhibition in biopharmaceutics. Int J Pharm 289(1-2):1-30.
29. Wang W, Singh S, Zeng DL, King K, Nema S 2007. Antibody structure, instability, and formulation. J Pharm Sci 96(1):1-26.
30. Kabat EA. 1991. Sequences of Proteins of Immunological Interest: Tabulation and Analysis of Amino Acid and Nucleic Acid Sequences of Precursors, V-Regions, C-Regions, J-Chain, T-Cell Receptors for Antigen T-Cell Surface Antigens, [Beta]2-Microglobulins, Major Histocompatibility Antigens, Thy-1, Complement, C-Reactive Protein, Thymopoietin, Integrins, PostGamma Globulin, [Alpha]2-Macroglobulins, and Other Related Proteins. ed.: National Institutes of Health.
31. Pan H, Chen K, Chu L, Kinderman F, Apostol I, Huang G 2009. Methionine oxidation in human IgG2 Fc decreases binding affinities to protein A and FcRn. Protein Sci 18(2):424-433.
32. Wang W, Vlasak J, Li Y, Pristatsky P, Fang Y, Pittman T, Roman J, Wang Y, Prueksaritanont T, Ionescu R 2011. Impact of methionine oxidation in human IgG1 Fc on serum half-life of monoclonal antibodies. Mol Immunol 48(6-7):860-866.
33. Bertolotti-Ciarlet A, Wang W, Lownes R, Pristatsky P, Fang Y, McKelvey T, Li Y, Li Y, Drummond J, Prueksaritanont T, Vlasak J 2009. Impact of methionine oxidation on the binding of human IgG1 to Fc Rn and Fc gamma receptors. Mol Immunol 46(8-9):1878-1882.
34. Vlasak J, Ionescu R 2011. Fragmentation of monoclonal antibodies. MAbs 3(3):253-263.
35. Mills BJ, Moussa EM, Jameel F. 2020. Monoclonal Antibodies: Structure, Physicochemical Stability, and Protein Engineering. In Jameel F, Skoug JW, Nesbitt RR, editors. Development of Biopharmaceutical Drug-Device Products, ed., Cham, Switzerland: Springer International Publishing. p 3-26.
36. Powell MF. 1994. Peptide Stability in Aqueous Parenteral Formulation. In Cleland JL, Langer R, editors. Formulation and Delivery of Proteins and Peptides, ed., Washington DC: American Chemical Society. p 100-117.
37. Powell MF. 1996. A Compendium and Hydropathy/Flexibility Analysis of Common Reactive Sites in Proteins: Reactivity at Asn, Asp, Gln, and Met Motifs in Neutral pH Solution. In Pearlman R, Wang JY, editors. Formulation, Characterization, and Stability of Protein Drugs, ed., New York: Plenum Press. p 1-140.
38. Liu H, Gaza-Bulseco G, Sun J 2006. Characterization of the stability of a fully human monoclonal IgG after prolonged incubation at elevated temperature. J Chromatogr B Analyt Technol Biomed Life Sci 837(1-2):35-43.
39. Moritz B, Stracke JO 2017. Assessment of disulfide and hinge modifications in monoclonal antibodies. Electrophoresis 38(6):769-785.

40. Cordoba AJ, Shyong BJ, Breen D, Harris RJ 2005. Non-enzymatic hinge region fragmentation of antibodies in solution. J Chromatogr B Analyt Technol Biomed Life Sci 818(2):115-121.
41. Moorthy BS, Xie B, Moussa EM, Iyer LK, Chandrasekhar S, Panchal JP, Topp EM. 2015. Effect of Hydrolytic Degradation on the In Vivo Properties of Monoclonal Antibodies. In Rosenberg AS, Demeule B, editors. Biobetters - Protein Engineering to Approach the Curative, ed., New York: Springer. p 105-135.
42. Gaza-Bulseco G, Liu H 2008. Fragmentation of a recombinant monoclonal antibody at various pH. Pharm Res 25(8):1881-1890.
43. Schmid I, Bonnington L, Gerl M, Bomans K, Thaller AL, Wagner K, Schlothauer T, Falkenstein R, Zimmermann B, Kopitz J, Hasmann M, Bauss F, Haberger M, Reusch D, Bulau P 2018. Assessment of susceptible chemical modification sites of trastuzumab and endogenous human immunoglobulins at physiological conditions. Nature Communications Biology 1(28).
44. Schuster J, Koulov A, Mahler HC, Detampel P, Huwyler J, Singh S, Mathaes R 2020. In Vivo Stability of Therapeutic Proteins. Pharm Res 37(2):1-17.
45. Goulet DR, Atkins WM 2020. Considerations for the Design of Antibody-Based Therapeutics. J Pharm Sci 109(1):74-103.
46. Wang W, Singh SK, Li N, Toler MR, King KR, Nema S 2012. Immunogenicity of protein aggregates--concerns and realities. Int J Pharm 431(1-2):1-11.
47. Liu H, Nowak C, Patel R 2019. Modifications of recombinant monoclonal antibodies in vivo. Biologicals 59:1-5.
48. Yang N, Tang Q, Hu P, Lewis MJ 2018. Use of In Vitro Systems To Model In Vivo Degradation of Therapeutic Monoclonal Antibodies. Anal Chem 90(13):7896-7902.
49. Bults P, Bischoff R, Bakker H, Gietema JA, van de Merbel NC 2016. LC-MS/MS-Based Monitoring of In Vivo Protein Biotransformation: Quantitative Determination of Trastuzumab and Its Deamidation Products in Human Plasma. Anal Chem 88(3):1871-1877.
50. Huang L, Lu J, Wroblewski VJ, Beals JM, Riggin RM 2005. In vivo deamidation characterization of monoclonal antibody by LC/MS/MS. Anal Chem 77(5):1432-1439.
51. Tran JC, Tran D, Hilderbrand A, Andersen N, Huang T, Reif K, Hotzel I, Stefanich EG, Liu Y, Wang J 2016. Automated Affinity Capture and On-Tip Digestion to Accurately Quantitate in Vivo Deamidation of Therapeutic Antibodies. Anal Chem 88(23):11521-11526.
52. Mehl JT, Sleczka BG, Ciccimaro EF, Kozhich AT, Gilbertson DG, Vuppugalla R, Huang CS, Stevens B, Mo J, Deyanova EG, Wang Y, Huang RY, Chen G, Olah TV 2016. Quantification of in vivo site-specific Asp isomerization and Asn deamidation of mAbs in animal serum using IP-LC-MS. Bioanalysis 8(15):1611-1622.
53. Liu H, Ponniah G, Zhang HM, Nowak C, Neill A, Gonzalez-Lopez N, Patel R, Cheng G, Kita AZ, Andrien B 2014. In vitro and in vivo modifications of recombinant and human IgG antibodies. MAbs 6(5):1145-1154.
54. Goetze AM, Liu YD, Arroll T, Chu L, Flynn GC 2012. Rates and impact of human antibody glycation in vivo. Glycobiology 22(2):221-234.
55. Lobo B, Lo S, Wakankar A, Wang YJ, Wong RL, Goldbach P, Mahler HC. 2010. Method and formulation for reducing aggregation of a macromolecule under physiological conditions. In Genentech I, F. Hoffmann-La Roche Ag, editor, ed.: Google Patents.
56. Jiskoot W, Beuvery EC, de Koning AA, Herron JN, Crommelin DJ 1990. Analytical approaches to the study of monoclonal antibody stability. Pharm Res 7(12):1234-1241.
57. Kinderman F, Yerby B, Jawa V, Joubert MK, Joh NH, Malella J, Herskovitz J, Xie J, Ferbas J, McBride HJ 2019. Impact of Precipitation of Antibody Therapeutics following Subcutaneous Injection on Pharmacokinetics and Immunogenicity. J Pharm Sci 108(6):1953-1963.
58. Richter WF, Christianson GJ, Frances N, Grimm HP, Proetzel G, Roopenian DC 2018. Hematopoietic cells as site of first-pass catabolism after subcutaneous dosing and contributors to systemic clearance of a monoclonal antibody in mice. MAbs 10(5):803-813.

59. Kratz A, Ferraro M, Sluss PM, Lewandrowski KB 2004. Case records of the Massachusetts General Hospital. Weekly clinicopathological exercises. Laboratory reference values. N Engl J Med 351(15):1548-1563.
60. Demeule B, Shire SJ, Liu J 2009. A therapeutic antibody and its antigen form different complexes in serum than in phosphate-buffered saline: a study by analytical ultracentrifugation. Anal Biochem 388(2):279-287.
61. Schuster J, Mahler HC, Koulov A, Joerg S, Racher AJ, Huwyler J, Detampel P, Mathaes R 2020. Tracking the physical stability of fluorescent-labeled mAbs under physiologic in vitro conditions in human serum and PBS. Eur J Pharm Biopharm 152:193-201.
62. Schuster J, Mahler HC, Joerg S, Kamuju V, Huwyler J, Mathaes R 2021. Stability of Monoclonal Antibodies after Simulated Subcutaneous Administration. J Pharm Sci 110(6):2386-2394.
63. Dillon TM, Ricci MS, Vezina C, Flynn GC, Liu YD, Rehder DS, Plant M, Henkle B, Li Y, Deechongkit S, Varnum B, Wypych J, Balland A, Bondarenko PV 2008. Structural and functional characterization of disulfide isoforms of the human IgG2 subclass. J Biol Chem 283(23):16206-16215.
64. Schuster J, Probst C, Mahler HC, Joerg S, Huwyler J, Mathaes R 2021. Assessing Particle Formation of Biotherapeutics in Biological Fluids. J Pharm Sci 110(4):1527-1532.
65. Schuster J, Koulov A, Mahler HC, Joerg S, Huwyler J, Schleicher K, Detampel P, Mathaes R 2020. Particle Analysis of Biotherapeutics in Human Serum using Machine Learning. J Pharm Sci 109(5):1827–1832.
66. Wolfbeis OS, Leiner M 1985. Mapping of the total fluorescence of human blood serum as a new method for its characterization. Analytica Chimica Acta 167:203-215.
67. Leblond F, Davis SC, Valdes PA, Pogue BW 2010. Pre-clinical whole-body fluorescence imaging: Review of instruments, methods and applications. J Photochem Photobiol B 98(1):77-94.
68. Cilliers C, Nessler I, Christodolu N, Thurber GM 2017. Tracking Antibody Distribution with Near-Infrared Fluorescent Dyes: Impact of Dye Structure and Degree of Labeling on Plasma Clearance. Mol Pharm 14(5):1623-1633.
69. Adkins JN, Varnum SM, Auberry KJ, Moore RJ, Angell NH, Smith RD, Springer DL, Pounds JG 2002. Toward a human blood serum proteome: analysis by multidimensional separation coupled with mass spectrometry. Mol Cell Proteomics 1(12):947-955.
70. Han M, Pearson JT, Wang Y, Winters D, Soto M, Rock DA, Rock BM 2017. Immunoaffinity capture coupled with capillary electrophoresis - mass spectrometry to study therapeutic protein stability in vivo. Anal Biochem 539:118-126.
71. Li F, Weng Y, Zhang G, Han X, Li D, Neubert H 2019. Characterization and Quantification of an Fc-FGF21 Fusion Protein in Rat Serum Using Immunoaffinity LC-MS. AAPS J 21(5):84.
72. Li Y, Huang Y, Ferrant J, Lyubarskaya Y, Zhang YE, Li SP, Wu SL 2016. Assessing in vivo dynamics of multiple quality attributes from a therapeutic IgG4 monoclonal antibody circulating in cynomolgus monkey. MAbs 8(5):961-968.
73. Filipe V, Poole R, Oladunjoye O, Braeckmans K, Jiskoot W 2012. Detection and characterization of subvisible aggregates of monoclonal IgG in serum. Pharm Res 29(8):2202-2212.
74. Hotzel I, Theil FP, Bernstein LJ, Prabhu S, Deng R, Quintana L, Lutman J, Sibia R, Chan P, Bumbaca D, Fielder P, Carter PJ, Kelley RF 2012. A strategy for risk mitigation of antibodies with fast clearance. MAbs 4(6):753-760.
75. Goyon A, Excoffier M, Janin-Bussat MC, Bobaly B, Fekete S, Guillarme D, Beck A 2017. Determination of isoelectric points and relative charge variants of 23 therapeutic monoclonal antibodies. J Chromatogr B Analyt Technol Biomed Life Sci 1065-1066:119-128.
76. Gersh I, Catchpole HR 1960. The nature of ground substance of connective tissue. Perspect Biol Med 3:282-319.

77. Gilanyi M, Ikrenyi C, Fekete J, Ikrenyi K, Kovach AG 1988. Ion concentrations in subcutaneous interstitial fluid: measured versus expected values. Am J Physiol 255(3 Pt 2):F513-519.
78. Haljamae H, Linde A, Amundson B 1974. Comparative analyses of capsular fluid and interstitial fluid. Am J Physiol 227(5):1199-1205.
79. Haljamae H 1978. Anatomy of the interstitial tissue. Lymphology 11(4):128-132.
80. Wiig H, Swartz MA 2012. Interstitial fluid and lymph formation and transport: physiological regulation and roles in inflammation and cancer. Physiol Rev 92(3):1005-1060.
81. Doell A, Schmitz OJ, Hollmann M 2019. Shedding Light into the Subcutis: A Mass Spectrometry Based Immunocapture Assay Enabling Full Characterization of Therapeutic Antibodies after Injection in Vivo. Anal Chem 91(15):9490-9499.
82. Schaupp L, Ellmerer M, Brunner GA, Wutte A, Sendlhofer G, Trajanoski Z, Skrabal F, Pieber TR, Wach P 1999. Direct access to interstitial fluid in adipose tissue in humans by use of open-flow microperfusion. Am J Physiol 276(2):E401-408.
83. Linthwaite VL, Janus JM, Brown AP, Wong-Pascua D, O'Donoghue AC, Porter A, Treumann A, Hodgson DRW, Cann MJ 2018. The identification of carbon dioxide mediated protein post-translational modifications. Nat Commun 9(1):3092.
84. Kinnunen HM, Mrsny RJ 2014. Improving the outcomes of biopharmaceutical delivery via the subcutaneous route by understanding the chemical, physical and physiological properties of the subcutaneous injection site. J Control Release 182:22-32.
85. Luo S, McSweeney KM, Wang T, Bacot SM, Feldman GM, Zhang B 2020. Defining the right diluent for intravenous infusion of therapeutic antibodies. MAbs 12(1):1685814.
86. Arvinte T, Cudd A, Palais C, Poirier E. 2018. The Formulation of Biological Molecules. In Tovey GD, editor Pharmaceutical Formulation - The Science and Technology of Dosage Forms, ed., Croydon, UK: The Royal Society of Chemistry. p 288-316.
87. Arvinte T, Poirier E, Palais C. 2015. Prediction of Aggregation In Vivo by Studies of Therapeutic Proteins in Human Plasma. In Rosenberg AS, Demeule B, editors. Biobetters - Protein Engineering to Approach the Curative, ed., New York: Springer. p 91-104.
88. Schuster J, Mahler HC, Joerg S, Huwyler J, Mathaes R 2021. Analytical challenges assessing aggregation and fragmentation of therapeutic proteins in biological fluids. J Pharm Sci 110(9):3103-3110.
89. Tirumalai RS, Chan KC, Prieto DA, Issaq HJ, Conrads TP, Veenstra TD 2003. Characterization of the low molecular weight human serum proteome. Mol Cell Proteomics 2(10):1096-1103.
90. Cheon DH, Nam EJ, Park KH, Woo SJ, Lee HJ, Kim HC, Yang EG, Lee C, Lee JE 2016. Comprehensive Analysis of Low-Molecular-Weight Human Plasma Proteome Using Top-Down Mass Spectrometry. J Proteome Res 15(1):229-244.
91. Merrell K, Southwick K, Graves SW, Esplin MS, Lewis NE, Thulin CD 2004. Analysis of low-abundance, low-molecular-weight serum proteins using mass spectrometry. J Biomol Tech 15(4):238-248.
92. Awwad S, Henein C, Ibeanu N, Khaw PT, Brocchini S 2020. Preclinical challenges for developing long acting intravitreal medicines. Eur J Pharm Biopharm 153:130-149.
93. Bown HK, Bonn C, Yohe S, Yadav DB, Patapoff TW, Daugherty A, Mrsny RJ 2018. In vitro model for predicting bioavailability of subcutaneously injected monoclonal antibodies. J Control Release 273:13-20.
94. Kinnunen HM, Sharma V, Contreras-Rojas LR, Yu Y, Alleman C, Sreedhara A, Fischer S, Khawli L, Yohe ST, Bumbaca D, Patapoff TW, Daugherty AL, Mrsny RJ 2015. A novel in vitro method to model the fate of subcutaneously administered biopharmaceuticals and associated formulation components. J Control Release 214:94-102.
95. Awwad S, Lockwood A, Brocchini S, Khaw PT 2015. The PK-Eye: A Novel In Vitro Ocular Flow Model for Use in Preclinical Drug Development. J Pharm Sci 104(10):3330-3342.

96. Patel S, Muller G, Stracke JO, Altenburger U, Mahler HC, Jere D 2015. Evaluation of protein drug stability with vitreous humor in a novel ex-vivo intraocular model. Eur J Pharm Biopharm 95(Pt B):407-417.
97. Patel S, Stracke JO, Altenburger U, Mahler HC, Metzger P, Shende P, Jere D 2017. Prediction of intraocular antibody drug stability using ex-vivo ocular model. Eur J Pharm Biopharm 112:177-186.
98. Liu YD, Goetze AM, Bass RB, Flynn GC 2011. N-terminal glutamate to pyroglutamate conversion in vivo for human IgG2 antibodies. J Biol Chem 286(13):11211-11217.
99. Liu YD, van Enk JZ, Flynn GC 2009. Human antibody Fc deamidation in vivo. Biologicals 37(5):313-322.
100. Lobo B, Lo S, Wang YJ, Wong RL. 2014. Method and formulation for reducing aggregation of a macromolecule under physiological conditions. In Genentech I, editor, ed.: Google Patents.
101. Liu YD, Chen Y, Tsui G, Wei B, Yang F, Yu C, Cornell C 2020. Predictive In Vitro Vitreous and Serum Models and Methods to Assess Thiol-related Quality Attributes in Protein Therapeutics. Anal Chem.
102. Jiang XG, Wang T, Kaltenbrunner O, Chen K, Flynn GC, Huang G 2013. Evaluation of protein disulfide conversion in vitro using a continuous flow dialysis system. Anal Biochem 432(2):142-154.

Appendix

Publications Included in This Thesis

Schuster J, Koulov A, Mahler HC, Detampel P, Huwyler J, Singh S, Mathaes R 2020. In Vivo Stability of Therapeutic Proteins. Pharm Res 37(2):1-17.

Schuster J, Mahler HC, Joerg S, Huwyler J, Mathaes R 2021. Analytical challenges assessing aggregation and fragmentation of therapeutic proteins in biological fluids. J Pharm Sci 110(9):3103-3110.

Schuster J, Koulov A, Mahler HC, Joerg S, Huwyler J, Schleicher K, Detampel P, Mathaes R 2020. Particle Analysis of Biotherapeutics in Human Serum using Machine Learning. J Pharm Sci 109(5):1827–1832.

Schuster J, Mahler HC, Koulov A, Joerg S, Racher AJ, Huwyler J, Detampel P, Mathaes R 2020. Tracking the physical stability of fluorescent-labeled mAbs under physiologic in vitro conditions in human serum and PBS. Eur J Pharm Biopharm 152:193-201.

Schuster J, Probst C, Mahler HC, Joerg S, Huwyler J, Mathaes R 2021. Assessing Particle Formation of Biotherapeutics in Biological Fluids. J Pharm Sci 110(4):1527-1532.

Schuster J, Mahler HC, Joerg S, Kamuju V, Huwyler J, Mathaes R 2021. Stability of Monoclonal Antibodies after Simulated Subcutaneous Administration. J Pharm Sci 110(6):2386-2394.

Additional Publications Written During the Research Period (not included in this thesis)

Schuster J, Kamuju V, Mathaes R 2021. Assessment of Antibody Stability in a Novel Protein-Free Serum Model. Pharmaceutics 13(6).

Schuster J, Kamuju V, Mathaes R 2021. Fate of Antibody and Polysorbate Particles in a Human Serum Model. Eur J Pharm Biopharm. *under revision*